PHYSIOLOGICAL REGULATION OF CALCIUM AND PHOSPHORUS HOMEOSTASIS IN COMMERCIAL LAYING HENS DURING THE DAILY LAY CYCLE FROM EARLY THROUGH EXTENDED PRODUCTION

by

MICAELA SINCLAIR-BLACK

(Under the Direction of Laura E. Ellestad)

ABSTRACT

Modern laying hens have been selected for sustained production at older ages and produce an egg every 24 hours. Egg formation utilizes calcium and phosphorus from dietary and skeletal origins; however, as hens age, mineral imbalances occur, leading to poor-quality eggshells and osteoporosis. These challenges pose economic and welfare concerns, and a deeper understanding of mineral homeostasis in older hens is essential. Therefore, the objectives of this study were to (1) identify the intestinal distribution of transcripts regulating calcium and phosphorus uptake, (2) investigate the circadian regulation of calcium and phosphorus uptake and utilization, and (3) evaluate the physiological control of calcium and phosphorus homeostasis during the daily lay cycle through an extended production period. In the first study, expression of genes regulating mineral absorption in the small intestine and ceca was analyzed. The subsequent two studies investigated expression of similar genes in liver, kidney, ileum, and shell gland during the daily oviposition cycle (Studies 2 and 3) and across extended production up to 95 weeks (Study 3). Circulating vitamin D_3 metabolites were measured in the second and third studies, while dry matter

digestibility and eggshell characteristics were evaluated in the third study only. The ileum and ceca were identified as potentially important sites for calcium and phosphorus uptake. Furthermore, the ileum, kidney, and shell gland may be capable of 1α-, 25- and 24-hydroxylation of vitamin D_3 to regulate local mineral utilization within tissues. Aged hens likely transition into and out of eggshell calcification less efficiently than younger hens, reducing eggshell thickness and breaking strength. Termination of eggshell calcification appears to be mediated by reductions in bicarbonate availability coupled with elevated phosphorus delivery to the shell gland. Reductions in circulating $1,25(OH)_2D_3$ with age likely reduced mineral transporter expression in the shell gland, ileum, and kidney, potentially impacting bone mineralization and eggshell calcification. Collectively, these data identified key hormonal signaling pathways and mineral transporters involved in eggshell calcification and bone mineralization during the daily lay cycle and how they become dysregulated with age. These data are essential for developing solutions to address poor eggshell quality and compromised skeletal structure in aged hens.

INDEX WORDS: Laying hen, calcium, phosphorus, vitamin D_3, oviposition cycle, extended production

PHYSIOLOGICAL REGULATION OF CALCIUM AND PHOSPHORUS HOMEOSTASIS IN COMMERCIAL LAYING HENS DURING THE DAILY LAY CYCLE FROM EARLY THROUGH EXTENDED PRODUCTION

by

MICAELA SINCALIR-BLACK

BS, Animal Science, University of Pretoria, South Africa, 2017

MS, Animal Science, University of Pretoria, South Africa, 2019

A Dissertation Submitted to the Graduate Faculty of The University of Georgia in Partial Fulfillment of the Requirements for the Degree

DOCTOR OF PHILOSOPHY

ATHENS, GEORGIA

2024

PHYSIOLOGICAL REGULATION OF CALCIUM AND PHOSPHORUS HOMEOSTASIS IN COMMERCIAL LAYING HENS DURING THE DAILY LAY CYCLE FROM EARLY THROUGH EXTENDED PRODUCTION

by

MICAELA SINCLAIR-BLACK

Major Professor:	Laura E. Ellestad
Committee:	Roselina Angel
	Jenny Nicholds
	Brian Fairchild
	Prafulla Regmi

Electronic Version Approved:

Ron Walcott
Vice Provost for Graduate Education and Dean of the Graduate School
The University of Georgia
December 2024

DEDICATION

Granny and Grandpa, I love and miss you both deeply. I will always cherish our time spent together, and I know that you are smiling down from heaven. I hope I can make you proud.

Maria Johanna Sinclair-Black
July 13, 1940 – May 28, 2023

Robert William Sinclair-Black
June 27, 1937 – October 21, 2023

Your unconditional love will never be forgotten. There will always be two paw-sized holes in my heart, and I am sorry I couldn't be there for one last walk together.

Hazel & Zeus

ACKNOWLEDGEMENTS

To Dr. Laura Ellestad, thank you for granting me this opportunity to pursue my dreams and for deepening my passion for science and innovation. I am immensely grateful for the skills and life lessons I have gained under your mentorship and how you have grown me into the scientist I am today. Your patience, compassion, and fairness are a testament to your great leadership, and I am honored to be a part of the Ellestad lab.

To Dr. Roselina Angel, thank you for believing in me and providing me the opportunity to chase my dreams across the world. You have been an inspiration throughout my journey, and I always appreciate your motivation and support.

To Dr. Peter Plumstead, thank you for introducing me to the world of poultry and for always being someone I can look to for advice and support. You changed the trajectory of my career and gave me the confidence to reach for the stars. I hope that someday I can be the guiding light you were to me, and I will forever be grateful.

To Dr. Prafulla Regmi, Dr. Brian Fairchild, and Dr. Jenny Nicholds, thank you for serving on my committee and for your guidance and advice throughout my Ph.D.

To Xabier Arbe and David Cavero, I am sincerely appreciative of the funding provided during my studies and for your continued input.

To the past and present members of the Ellestad lab, thank you for your assistance and friendship throughout my time at UGA.

To Brett, thank you for being the best office partner and friend. I will miss the laughter and fun times, and I don't think I would have made it this far without the many gallons of coffee we shared.

To Alejandra & Manuel, thank you for being there for both Ayrton and I more times than I can count. Your kindness and friendship have kept us afloat through the rough times, and you were always there to celebrate alongside us during the great times.

To my family, your unwavering love and encouragement gave me the strength and determination to pursue my passions. We may have been oceans apart, but not a day went by that I didn't feel your love and support.

To Ayrton, thank you for being my rock; words cannot describe how much you mean to me and how much I love you. Your support and love have always been a constant. Thank you for always believing in me when I didn't believe in myself, and I will always be grateful for the sacrifices you made to accompany me on this adventure.

TABLE OF CONTENTS

Page

LIST OF TABLES

Page

LIST OF FIGURES

Page

CHAPTER 1

INTRODUCTION

To meet the demands of an increasing global population, the production of high-quality and affordable animal proteins, such as table eggs, must be prioritized. Consequently, the number of eggs produced per hen has been increased through genetic selection for longer clutch lengths and improved management (Thiruvenkadan et al., 2010; Pelletier, 2018). In previous years laying hens were maintained in production through 70 weeks of age due to declines in production noted at later ages (Martin, 1984). Modern commercial layers, however, can maintain higher hen-day egg production rates at older ages, such that management guides anticipate 80% production at 80 weeks (H&N International, 2020), allowing for the extension of egg production cycles to upwards of 100 weeks in modern systems. This is a 57% increase in the number of weeks hens spend in a productive state, and as a result, fewer replacement hens are needed to maintain the global number of laying hens (Bain et al., 2016). The reduction in replacement hen numbers also has impacted the number of breeding stock required, resulting in fewer resources utilized to produce the same amount of eggs. Consequently, extending laying production up to 100 weeks has considerable economic and environmental benefits and is rapidly being adopted on a global scale.

Modern hens produce an egg approximately every 24 hours (Nys et al., 2011), using calcium and phosphorus derived from dietary and skeletal sources (Comar et al., 1949). Eggshell calcification initiates as the follicle enters the shell gland, between 5 to 7 hours post-oviposition, where it is calcified in distinct structural layers over the next 18 hours. The initial deposition of mamillary knobs occurs between 5-10 hours post-oviposition at a rate of 0.1 g calcium/ hour, while

the palisade layer, which provides structural strength, is calcified most rapidly at a rate of 0.33 g calcium/hour over 12 hours (Gautron et al., 2021). A considerable portion of palisade layer calcification occurs during the dark stage of the lighting cycle, when hens are unlikely to consume feed. Therefore, to meet these elevated calcium demands, labile medullary bone calcium stores are broken down to meet the requirements for eggshell calcification (Mueller et al., 1964). Following oviposition, these skeletal reserves are remineralized when eggshell calcification is not actively occurring (Wilson et al., 1990; Kerschnitzki et al., 2014). As such, a 24-hour cycle occurs wherein the medullary bone is mineralized following oviposition and resorbed during the dark phase to provide calcium for the subsequent eggshell. This cycle is regulated by calcium and phosphorus homeostasis, reviewed by Bar (2008), and an equilibrium must be maintained between bone deposition and bone breakdown each day. As such, factors reducing mineral availability would likely impair bone mineralization and eggshell quality, and a deeper knowledge of the physiological regulation of the daily lay cycle is essential.

Imbalances in the physiological regulation of calcium and phosphorus homeostasis are also increasingly likely to occur as hens age. Older hens in extended production systems exhibit higher prevalences of eggs with thin eggshells and altered eggshell ultrastructure (Radwan, 2015; Benavides-Reyes et al., 2021) that are prone to breakage and bacterial contamination, leading to economic and food safety concerns. Eggshell calcification is influenced by hormonal systems such as parathyroid hormone, calcitonin, and vitamin D_3, which regulate the expression of mineral transporters and subsequent mineral availability from the intestine and skeletal reserves (Bar, 2008; Bar, 2009; Dacke et al., 2015). As such, disturbances to these hormonal systems in aged hens likely reduce mineral availability for eggshell formation and may contribute to the reduced eggshell quality observed during extended egg production. Therefore, investigations into the

physiological regulation of mineral homeostasis across ages is essential to maintaining eggshell quality.

In addition to poor-quality eggshells, older hens exhibit a higher prevalence of osteoporotic bones (Yamada et al., 2021) which are more likely to fracture due to their fragile and brittle nature. Fractures are considered a significant animal welfare concern in laying hens (FAWC, 2010), and solutions must be developed to limit their occurrence. During eggshell calcification, labile medullary bone is broken down by osteoclasts; however, over time, imbalances in calcium and phosphorus homeostasis result in osteoclasts also resorbing structural cortical bone (Wilson et al., 1992). Unlike medullary bone, cortical bone cannot be replaced unless egg production halts (Hudson et al., 1993). Consequently, aged hens exhibit bones with reduced calcified tissue and cortical thickness; however, total bone porosity and medullary bone tissue volume increase (Yamada et al., 2021). Since medullary bone exhibits a greater degree of disorganization than cortical bone (Dacke et al., 1993), reductions in cortical thickness and increases in medullary bone volume (Fleming et al., 2010) ultimately decrease the breaking strength of bones, resulting in an elevated risk of fracture in older hens. The extent to which cortical bone is broken down can likely be limited by ensuring sufficient remineralization of medullary bone following oviposition; however, a deeper understanding of the physiological regulation of calcium and phosphorus homeostasis is required to achieve this.

Ultimately, as hens are maintained in production for extended periods, poor-quality eggshells and skeletal fractures will continue to rise, generating economic and welfare concerns unless effective solutions are developed. The development of these solutions demands a deeper understanding of the systems that govern calcium and phosphorus uptake and utilization during stages of bone mineralization and eggshell calcification, as well as how these systems become

dysregulated with age. As such, a study was initially conducted to investigate the distribution of transcripts regulating mineral uptake from the small intestine and ceca. Subsequent studies then evaluated the physiological regulation of calcium and phosphorus homeostasis across tissues during the daily lay cycle and across a 95-week extended egg production cycle.

CHAPTER 2

LITERATURE REVIEW

Overview of commercial table egg production

The global population is expected to grow by approximately 2 billion individuals over the next 30 years (United Nations, 2015), increasing demand for affordable, high-quality, and sustainable animal protein sources such as table eggs. As such, there is heightened pressure on egg producers to keep up with future demand while using increasingly limited resources. The number of laying hens in the United States is maintained between approximately 312 million to 315 million (United States Department of Agriculture, 2024), an increase of over 19 million hens from 2014 (United States Department of Agriculture, 2014). Additionally, the efficiency of egg production within these systems has improved year by year. Studies conducted by Pelletier et al. (2014) and Pelletier (2018) investigated changes to the environmental footprint of conventional caged egg production systems in Canada and the United States over 50 years and found that, even though egg production has increased between 30 to 50%, the amount of greenhouse gases, land use, and water consumption was reduced by approximately 57%, 71%, and 53% respectively. These improvements are due to enhancements in feed formulation, manure management, and genetic selection. Combined advances in nutritional and environmental management and genetic selection have resulted in modern laying hens maintaining a greater persistency of lay at older ages, thereby allowing for the extension of production cycles to later ages.

Commercial laying hens have traditionally been kept in production until around 70 weeks of age; however, improvements in the persistency of lay have allowed modern hens to sustain

clutch lengths of over 119 eggs (Cabezas-Garcia et al., 2022), often resulting in upwards of 80% production at 80 weeks (H&N International, 2020). As such, modern laying hens are being maintained in production systems for up to 100 weeks of age. One significant advantage of retaining hens through 100 weeks is that the proportion of time spent in a productive state is increased relative to the rearing period (Bain et al., 2016). Furthermore, extended cycles require hens to be replaced at a slower rate, consequently reducing the number of breeders needed to sustain egg-laying flocks. The reduction in breeding hens would be accompanied by reduced feed requirements and lower environmental impacts for those flocks as well (Bain et al., 2016). As such, maintaining layers through 100 weeks has both environmental and economic benefits.

Oviposition cycle and egg formation

Commercial laying hens produce an egg approximately every 24 hours (Nys et al., 2011) and must efficiently utilize calcium and phosphorus for eggshell calcification and cuticle formation, respectively (Cusack et al., 2003). The maintenance of this 24-hour cycle is mediated by the hypothalamic-pituitary-ovarian axis (Zhao et al., 2024b). Initially, gonadotrophin-releasing hormone 1 (GnRH-1) is released from the hypothalamus and regulates luteinizing hormone (LH) production from the anterior pituitary gland. Within the daily lay cycle, LH concentration in circulation peaks approximately 4-8 hours before ovulation (Heald et al., 1967), and this surge stimulates ovulation. During the same time as the LH surge, progesterone levels are also at their highest (Kappauf et al., 1972) and, based upon the presence of both LH and progesterone receptors in the stigma of the F1 follicle, these hormones may also contribute to ovulation. Each successive ovulation occurs slightly later each day, resulting in a gradual shift in individual oviposition times; however, the LH surge is limited to a 4 to 11 hour period after the initiation of the dark phase of the lighting cycle (Fraps, 1964). Consequently, if the LH surge does not occur by 11 hours after

the onset of darkness, the LH surge will not occur and will instead start the following dark period, resulting in a pause day between clutches. Genetic selection for reduced oviposition intervals has resulted in longer clutch lengths, fewer pause days, and a greater proportion of hens laying eggs within the first 3 hours of the light phase (McClung et al., 1975; Gow et al., 1984).

As recently reviewed by Sinclair-Black et al. (2023): “Ovulation occurs 15-75 minutes after oviposition (Sturkie et al., 1976), and the follicle resides in the infundibulum for under 30 minutes (Sah et al., 2018). It continues into the magnum, where albumen is added over the next 3.25-3.5 hours (Nys et al., 2011), then enters the isthmus, where inner and outer shell membranes are deposited around the albumen (Warren et al., 1935). Calcium carbonate is deposited onto the outer shell membrane (Hincke et al., 2010) in the shell gland, and the eggshell develops over the final 19-20 hours (Nys et al., 2011; Gautron et al., 2021). As previously described (Nys et al., 2011; Gautron et al., 2021), the eggshell develops as distinct mamillary, palisade, and cuticle layers that are deposited from interior to exterior. During the mineralization of the mammillary and palisade layers, the deposition of amorphous calcium carbonate is followed by its transformation into calcite crystals (Rodriguez-Navarro et al., 2015). Initially, the mamillary layer forms at nucleation sites laid on the outer shell membrane between 5-6 hours post-oviposition (HPOP), and the mamillary core develops between 7-10 HPOP. Large calcite crystal units form the columnar palisade layer between 10-22 HPOP, and two hours before oviposition, eggshell calcification subsides, and the cuticle layer forms an organic film preventing bacterial penetration of the egg (Board et al., 1973; Chen et al., 2019). Between the calcified shell and cuticle lies a calcium and phosphorus-rich hydroxyapatite [$Ca_{10}(PO_4)_6(OH)_2$] crystal layer (Wedral et al., 1974; Cusack et al., 2003). Since phosphorus is a potent inhibitor of calcite formation (Bachra et al., 1963; Simkiss, 1964), some authors speculate that these crystals (Dennis et al., 1996) or the secretion of

phosphate-containing organic eggshell constituents towards the end of shell formation (Nys et al., 1991) may be involved in terminating calcification."

The organic matrix of the shell also plays a significant role in eggshell crystal morphology and ultrastructure (Gautron et al., 1996) and is comprised of proteins, glycoproteins, and proteoglycans (Arias et al., 1991). The first eggshell-specific soluble matrix protein to be identified was ovocleidin-17 (Hincke et al., 1995), and numerous others including ovocleidin-116 (Hincke et al., 1999), ovocalixyn-36 (Gautron et al., 2007), and ovocalixyn-32 (Gautron et al., 2001) have subsequently been identified and characterized. Furthermore, several more ubiquitous proteins, including ovalbumin and lysozyme-C, have also been linked to changes in eggshell structure (Zhao et al., 2024a). Each of these proteins is secreted into the shell gland lumen during different phases of the oviposition cycle (Marie et al., 2015), and they are linked to the following stages of eggshell production and morphology. Ovocleidin-17 has been associated with stabilization and initial formation of the mamillary knobs (Marie et al., 2015), while ovocleidin-116 is primarily located in the palisade layer of the eggshell and one of the most abundant eggshell matrix proteins (Hincke et al., 1999). Similarly, ovocalyxin-36 has also been found within the palisade layer and is likely involved in the rapid phases of eggshell calcification (Gautron et al., 2007). Lastly, ovocalyxin-32 localizes to the outer palisade layer and vertical hydroxyapatite layer during the final phases of eggshell calcification (Hincke et al., 2003; Miksik et al., 2007). In order to sustain eggshell quality through extended lay, both the organic and inorganic fractions of the eggshell must be maintained.

Bone development and remodeling for egg production

During embryonic and juvenile development, cortical and trabecular bone consisting of highly organized hydroxyapatite crystals is formed. These bone types provide structural support to the skeleton and continue to develop up until the onset of sexual maturity when structural bone

deposition then subsides (Hudson et al., 1993). At the onset of egg-laying, calcium requirements substantially increase to meet the demands for rapid eggshell calcification. Since eggshell calcification occurs primarily during the dark phase when dietary calcium is largely unavailable, hens mobilize approximately 20-40% of the calcium required for eggshell formation from labile calcium stores in the bone (Comar et al., 1949). These labile stores are present as medullary bone, and its development in pneumatic and long bones is initiated by increased circulating estrogen at the onset of sexual maturity (Whitehead, 2004). The mechanism by which estrogen stimulates medullary bone development is likely through estrogen receptors (ER) located in osteogenic cells (Ohashi et al., 1991a; Ohashi et al., 1991b), and in laying hens, ERα but not ERβ appears to facilitate the formation of medullary bone (Imamura et al., 2006; Hiyama et al., 2009). Medullary bone formation initiates on the endosteal surface of long bones and continues to form inwards towards the center of the marrow cavity. Interestingly, the occurrence of medullary bone in the humerus, a pneumatic bone, varies between 7% and 83% in different flocks of the same genetic line (Fleming et al., 1998). Medullary bone has a greater degree of non-collagenous proteins, proteoglycans, and a higher degree of calcification than cortical bone. Furthermore, it is highly vascularized with randomly orientated hydroxyapatite crystals (Ascenzi et al., 1963; Dacke et al., 1993), which allows for rapid anabolism and catabolism of hydroxyapatite during egg formation (Bonucci et al., 1975). Since hydroxyapatite is composed of calcium and phosphorus, bone resorption releases both minerals into circulation as ionized calcium (iCa^{2+}) and inorganic phosphate (PO_4^{3-}) that must be utilized for shell formation or excreted.

Medullary bone undergoes remineralization when eggshell calcification is not occurring (Wilson et al., 1990; Kerschnitzki et al., 2014) and is resorbed during eggshell calcification (Van de Velde et al., 1984b) through increased osteoclast activity driven by parathyroid hormone (PTH)

and the bioactive form of vitamin D_3, 1,25-dihydroxycholecalciferol [$1,25(OH)_2D_3$] (Taylor et al., 1969). When PTH binds PTH receptor 1 (PTH1R) on osteocytes (Silve et al., 1982; Zhao et al., 2002), the receptor activator of nuclear factor-kappa B ligand (RANKL) is secreted and interacts with the receptor activator of nuclear factor-kappa B (RANK) on osteoclast surfaces, stimulating bone resorption. Additionally, PTH increases osteoclast vacuolar-type adenosine triphosphatase (V-ATPase) activity, causing intracellular acidification required for bone breakdown (Liu et al., 2016). Osteoclast activity increases nine-fold during shell calcification (Van de Velde et al., 1984b), and osteoclast activity is not limited to medullary bone, resulting in osteoclasts resorbing structural bone once medullary bone is depleted. As structural bone is resorbed, medullary bone is deposited in its place, often resulting in bone volume and bone ash remaining constant or increasing throughout the production cycle (Whitehead, 2004). This shift in bone composition, despite a constant bone volume and ash, results in reduced bone-breaking strength due to the irregularly woven structure of medullary bone. It should be noted that while the structural contribution of medullary bone is low, its presence in the humerus positively impacts humeral breaking strength (Fleming et al., 1998). Together, laying hen bone functions as a dynamic reservoir of minerals needed for eggshell calcification. Sustaining an equilibrium of medullary bone accretion and breakdown during egg laying is vital to maintaining this reservoir and the skeletal integrity of the hen.

Vitamin D_3 metabolism and mechanism of action

Vitamin D_3 is integral for regulating calcium and phosphorus homeostasis and, therefore, skeletal integrity and eggshell quality. However, before vitamin D_3 can influence calcium and phosphorus homeostasis, it must first be converted into its biologically active metabolite, $1,25(OH)_2D_3$. The formation of $1,25(OH)_2D_3$ requires sequential hydroxylations of dietary vitamin D_3 absorbed from

the small intestine. Upon entry into the bloodstream, vitamin D_3 is initially bound to chylomicrons and transported to the liver (Haddad et al., 1993). The first hydroxylation takes place in the liver by a 25-hydroxylase enzyme encoded by *CYP2R1* or *CYP27A1* genes (Watanabe et al., 2013; Shang et al., 2023), with >90% of dietary vitamin D_3 converted into 25(OH)D_3 (Heaney et al., 2008; San Martin Diaz, 2018).

Following 25-hydroxylation, 25(OH)D_3 re-enters circulation and is bound to a chaperone protein known as vitamin D binding protein [DBP] (Bouillon et al., 1980). Hepatic expression of DBP and its levels in circulation increase rapidly at the onset of lay (Nys et al., 1985; Kuwata et al., 2024), and it exhibits differential binding affinities for each of the vitamin D_3 metabolites, having the greatest affinity for 25(OH)D_3 (Bouillon et al., 1980). This DBP-25(OH)D_3 complex is transported to the proximal renal tubules of the kidney. In mammals, it has been shown that 25(OH)D_3 is absorbed via receptor-mediated endocytosis by megalin and cubilin in the proximal renal tubules (Nykjaer et al., 2001; Kaseda et al., 2011). In chickens, megalin was also found to localize to the apical surface of the proximal tubules (Plieschnig et al., 2012), and renal cubilin mRNA expression is significantly decreased in aged hens (Kuwata et al., 2024). Once within renal epithelial cells, 25(OH)D_3 undergoes a second, more tightly regulated hydroxylation at the 1α-carbon to form 1,25$(OH)_2D_3$ (Jones et al., 1998). In mammals and fish, this is carried out by an enzyme encoded by *CYP27B1* (Monkawa et al., 1997; Shinki et al., 1997; Chun et al., 2014); however, this gene has not been identified in chickens, and the enzyme responsible is currently unknown despite recent publications that have reported measuring expression of *CYP27B1* mRNA or an equivalent in chickens (Shanmugasundaram et al., 2012; Gloux et al., 2020a; Gloux et al., 2020b; Yan et al., 2022). Investigation into transcripts amplified reveals these are not likely the correct candidate genes but rather an enzyme involved in retinoic acid metabolism (*CYP27C1*) or

one identified as vitamin D_3 hydroxylase-associated protein (Ettinger et al., 1994; Ettinger et al., 1995), neither of which have demonstrable 1α-hydroxylase activity.

The 1α-hydroxylation of $25(OH)D_3$ is stimulated by PTH when circulating iCa^{2+} and $1,25(OH)_2D_3$ are low; however, the efficiency of this may decrease with age (Abe et al., 1982; Gloux et al., 2020b). During periods of elevated circulating $1,25(OH)_2D_3$, 1α-hydroxylase is inhibited, and 24-hydroxylase encoded by *CYP24A1* is upregulated. The 24-hydroxylase enzyme inactivates $25(OH)D_3$ by producing biologically inert $24,25(OH)_2D_3$ or $1,24,25(OH)_3D_3$ (Holick et al., 1973; Omdahl et al., 2002), thereby preventing excessive bone resorption and intestinal calcium absorption. Hydroxylation of $25(OH)D_3$ into either active or inactive metabolites provides an additional level of control by fine-tuning the availability of this hormone.

Vitamin D_3 affects calcium and phosphorus homeostasis by influencing the expression and activity of transport and chaperone molecules for these minerals. When bound by $1,25(OH)_2D_3$, vitamin D receptor (VDR) is a ligand-activated transcription factor that enters the nucleus and forms a heterodimeric complex with retinoid-X-receptor alpha (RXRA) or gamma (RXRG) and binds vitamin D_3 response elements (VDRE) in regulatory regions of vitamin D_3-responsive genes (Bikle, 2014). Not all tissues respond to $1,25(OH)_2D_3$ in the same way. For example, shell gland calbindin D-28k (*CALB1*) expression does not appear to be influenced by $1,25(OH)_2D_3$ (Bar et al., 1977), unlike that in the kidney and small intestine (Taylor et al., 1972), and may be under the control of estrogen (Nys et al., 1992b; Corradino et al., 1993), driven by half-palindromic estrogen response elements in the *CALB1* promoter, as has been shown in mice (Gill et al., 1995). Since CALB1 in shell gland, intestine, and kidney share the same electrophoretic mobility, amino acid composition, and immunoreactivity, it is likely the same protein (Fullmer et al., 1976); however, estrogen receptor rather than VDR is likely a key regulatory protein driving its expression in the

shell gland. Vitamin D_3 has extensive influence on calcium and phosphorus homeostasis across multiple tissues and is tightly regulated by its own concentrations as well as actions of other hormones. Regarding avian vitamin D_3 metabolism, several questions remain surrounding the identification of *CYP27B1* and the influence of fibroblast growth factor 23 (FGF23) and PTH on vitamin D_3 regulation.

Calcium homeostasis and transport

Daily egg production and bone remineralization exert significant physiological pressure upon calcium homeostasis. Within the 24-hour oviposition cycle, the highest demand for calcium occurs between 10 and 22 HPOP when the eggshell exhibits a rapid growth phase, depositing approximately 0.33g of calcite per hour (Gautron et al., 2021). Eggshell calcification readily utilizes iCa^{2+} in the blood, resulting in a steady decline in iCa^{2+} from approximately 8 to HPOP (Parsons et al., 1980; Sinclair-Black et al., 2024). This decline in iCa^{2+} is detected by a G-coupled protein receptor, calcium-sensing receptor [CASR] (Diaz et al., 1997), which is able to detect fluctuations in iCa^{2+} as small as 200μM (Hofer et al., 2003). The presence of CASR has been observed across various tissues in the chicken, including the parathyroid glands, kidney, small intestine, and oviduct (Deng et al., 2010; Hui et al., 2021). While all these tissues actively participate in calcium metabolism, the highest prevalence of CASR has been observed in the parathyroid gland (Deng et al., 2010) due to its role in regulating PTH release.

Secretion of PTH from chief cells of the parathyroid gland increases as circulating iCa^{2+} is depleted from the blood during eggshell calcification (Van de Velde et al., 1984a; Singh et al., 1986). The primary function of PTH is to increase iCa^{2+} levels back within the homeostatic range by stimulating bone resorption (Taylor et al., 1969) and elevating $1,25(OH)_2D_3$ production in the kidney (Brenza et al., 2000) through the upregulation of renal 1α-hydroxylase activity (Fraser et

al., 1973). The subsequent increase in plasma $1,25(OH)_2D_3$ assists PTH in increasing circulating calcium by increasing dietary calcium absorption from the small intestine (Spencer et al., 1978; Chandra et al., 1990) and by increasing renal calcium reabsorption (Jande et al., 1981; Narbaitz et al., 1982).

Calcitonin (CALC), in birds, is produced within ultimobranchial bodies near the thyroid gland (Copp et al., 1967; Kraintz et al., 1969) and typically has a contrasting role to PTH such that it serves to decrease iCa^{2+} levels. In mammals, this is achieved by inhibiting bone resorption (Baylink et al., 1968) and renal calcium reabsorption (Cochran et al., 1970). Under normocalcemic conditions in rats, CALC was shown to stimulate the expression of *CYP27B1* and increase circulating $1,25(OH)_2D_3$ (Shinki et al., 1999); however, other authors observed modest impacts of CALC on calcium homeostasis under normocalcemic conditions (Davey et al., 2008). In contrast to the well-defined role of CALC in mammals, its role in avian species is less clear. In parathyroidectimized starlings, CALC administration resulted in elevated renal calcium excretion; however, no differences in renal calcium excretion were observed for non-parathyroidectomized starlings receiving CALC, suggesting that parathyroid hormone may counteract the effects of CALC in avian species (Clark et al., 1980). In laying hens, CALC decreased plasma iCa^{2+} levels in non egg-producing hens, but no differences were noted in productive egg-forming hens (Luck et al., 1979). The receptor for CALC has been identified in the shell gland, kidney, and bone of mature laying hens (Yasuoka et al., 1998; Ieda et al., 2001; Garcia-Mejia et al., 2024; Sinclair-Black et al., 2024), suggesting that this hormone may play a role in regulating calcium homeostasis during egg production. However, unlike in mammals, CALC does not influence avian osteoclast activity under normal physiological conditions (Nicholson et al., 1987; Eliam et al., 1988), nor does it appear to affect renal cyclic adenosine monophosphate formation in chickens or pigeons

(Dousa, 1974). This implies that avian CALCR could use alternative intracellular signaling pathways or that CALC does not have the same effect on bone as it does in mammals. Currently, there is limited evidence that CALC strongly influences calcium homeostasis in birds, and its importance is still unknown.

Calcium absorption from the small intestine appears to fluctuate throughout the daily egg formation cycle (Hurwitz et al., 1969; Hurwitz et al., 1973) and is thought to occur primarily in the duodenum and jejunum, with smaller amounts absorbed in the ileum (Hurwitz et al., 1965; Hurwitz et al., 1968). Intestinal calcium uptake occurs through active transcellular and passive paracellular pathways. Active transcellular absorption accounts for most calcium uptake and involves ATPase plasma membrane calcium transporting 1 (ATP2B1), 2 (ATP2B2), and 4 (ATP2B4), sodium-calcium exchanger 1 (NCX1), transient receptor potential cation channel subfamilies C member 1 (TRPC1), M member 7 (TRPM7), and V member 2 ((TRPV2), and CALB1 (Bar, 2009; Gloux et al., 2019). Passive paracellular calcium absorption likely takes place via tight junction proteins 1 (TJP1), 2 (TJP2), and 3 (TJP3), claudin 2 (CLDN2) and 12 (CLDN12), and occludin (OCLN) (Gloux et al., 2019; Gloux et al., 2020b). Findings suggest that intestinal capacity for calcium absorption could change with age, as expression of some transcellular (*ATP2B4*, *TRPV2*) and paracellular (*TJP3*, *CLDN2*, *OCLN*) transporters decreased in older hens (Gloux et al., 2020b). Calcium transport in the shell gland (Brionne et al., 2014) and kidney occurs through many of these same proteins, with the addition of transient receptor potential cation channel subfamily V member 6 (TRPV6) in the kidney (Proszkowiec-Weglarz et al., 2013; Gautron et al., 2021; Wang et al., 2022). This has been shown to decrease with age in hens (Gloux et al., 2020b), indicating that the calcium-handling capacity of the kidney is perturbed in older layers. In addition to the above-listed transporters, recent findings suggest vesicular transport

systems may export calcium into the shell gland lumen (Stapane et al., 2020). Given that the maintenance of eggshell strength and bone quality throughout the production cycle depends on efficient hormonal regulation and transport of calcium, a deeper comprehension of these systems is required to sustain robust eggshell quality during extended production cycles.

Phosphorus homeostasis and transport

Phosphorus is an essential component of hydroxyapatite, the primary mineral component of bone, and as such, 80% of total body phosphorus is stored in the skeleton. Bone resorption during periods of eggshell calcification releases calcium and phosphorus into circulation, and while the shell gland utilizes the majority of calcium for the developing eggshell, the amount of phosphorus required for the eggshell is considerably less. Consequently, during rapid eggshell formation, the concentration of phosphorus increases in the blood (Nys et al., 1986; Frost et al., 1990) and must be excreted to negate the toxic effects of hyperphosphatemia. Regulation of circulating phosphorus occurs in the kidney, small intestine, and bone (Michigami et al., 2018) and is primarily regulated by FGF23.

Bone-derived FGF23 was first implicated in mammalian calcium and phosphorus metabolism by Shimada et al. (2004) after observing the phosphaturic effects of FGF23 in autosomal-dominant hypophosphatemic rickets and osteomalacia (Shimada et al., 2000). Further investigations using mice (Perwad et al., 2005) and laying hens (Ren et al., 2017; Wang et al., 2018; Gloux et al., 2020a; Ren et al., 2020) later confirmed that hyperphosphatemia increases FGF23 production in bone. It has been shown to bind to one of four FGF receptors (FGFR1-4) that use the co-receptor klotho (KL) in mammals (Razzaque, 2009). The nature of the effect of FGF23 in mammals depends upon the tissue and the availability of KL. Cells involved in the regulation of phosphorus levels, such as the chief cells of the parathyroid gland and renal epithelial cells,

require KL for FGF23 actions. In contrast, cell types unrelated to phosphorus homeostasis, such as macrophages, lymphocytes, and hepatocytes, are influenced by FGF23 in a KL-independent manner Richter et al. (2018).

In chickens, the effects of FGF23 on calcium and phosphorus homeostasis are less extensively studied; however, several similarities between avian and mammalian species have been identified. Laying hens express *FGF23* mRNA in both medullary and structural bone (Hadley et al., 2016; Wang et al., 2018), and increases in *FGF23* expression in medullary bone occur as they age (Gloux et al., 2020b). Furthermore, *FGFR1-4* and *KL* mRNA have been observed in the kidney, intestine, bones, and shell gland of hens (Ren et al., 2020; Garcia-Mejia et al., 2024; Sinclair-Black et al., 2024). Immunoneutralization of FGF23 in laying hens led to increased plasma P_i and bone ash under phosphorus-deficient conditions (Bobeck et al., 2012; Ren et al., 2017), and limiting dietary P_i in laying hens reduced circulating P_i, suppressed bone *FGF23* mRNA, circulating FGF23, and renal sodium-dependent P_i transporter IIa (*NaP$_i$IIa*) expression, and induced duodenal sodium-dependent P_i transporter IIb (*NaP$_i$IIb*) expression (Ren et al., 2020). These changes corresponded with reduced phosphorus excretion and increased calcium excretion.

Studies conducted in mammals have found that FGF23 directly inhibited PTH secretion (Ben-Dov et al., 2007), decreased renal P_i transporter 2 (*P$_i$T*-2) expression (Tomoe et al., 2009), and limited $1,25(OH)_2D_3$ production in the kidney, in part through upregulation of 24-hydroxylase (Perwad et al., 2007). In hens, similarities potentially exist since elevated medullary *FGF23* mRNA during eggshell calcification was followed by periods of increased renal *CYP24A1* expression post-oviposition, which may, in turn, have led to observed reductions in $1,25(OH)_2D_3$ (Gloux et al., 2020a).

In addition to FGF23, PTH is an inhibitor of renal phosphorus resorption. Since PTH induces bone breakdown, the simultaneous downregulation of renal phosphorus uptake and subsequent increase in excretion is beneficial in preventing hyperphosphatemia. In chickens, Wideman et al. (1981) demonstrated that administered PTH both increased tubular secretion of phosphorus as well as inhibited its uptake, resulting in the efficient elimination of phosphorus from the kidney tubules. The capacity of the kidney to regulate phosphorus balance could change with age, as expression of *NaP$_i$IIa* and phosphorus transporter 1 (*P$_i$T-1*) in the kidney decreases in older hens (Gloux et al., 2020b). Since PTH stimulates 1,25$(OH)_2D_3$ production, it also indirectly increases phosphorus absorption from the intestine (Liao et al., 2017). However, in the kidney, 1,25$(OH)_2D_3$ appears to directly stimulate renal phosphorus reabsorption in the short-term and inhibit it in the long-term (Liang et al., 1982; Liang et al., 1984). Intestinal phosphorus uptake in chickens is thought to be mediated by P_iT-1, P_iT-2, NaP$_i$IIa, and NaP$_i$IIb (Yan et al., 2007; Huber et al., 2015; Li et al., 2018), with NaP$_i$IIb as the primary transporter in the duodenum, jejunum, and ileum and P_iT-1 as the primary transporter in the ileum (Gloux et al., 2019; Garcia-Mejia et al., 2024). With the identification of FGF23 in recent years and its role in mammalian phosphorus homeostasis, a new outlook on mineral homeostasis has emerged; however, many questions still exist about its role in avian species and its influence on vitamin D_3 metabolism. Opportunities exist to explore the profile and actions of FGF23 in birds and its impacts on bone mineralization and eggshell calcification.

Acid-base balance

The blood's acid-base balance substantially affects calcium and phosphorus homeostasis through its impacts on calcium-protein binding to vitellogenin and albumin (Loken et al., 1960; Guyer et al., 1980) and the availability of bicarbonate ions (Mongin, 1968). In chickens, blood pH values

are tightly regulated between 7.3 and 7.69 (Ding et al., 2021). Factors influencing blood pH are numerous and include temperature, partial pressure of oxygen (pO_2), partial pressure of carbon dioxide (pCO_2), bicarbonate (HCO_3^-), and presence of electrolytes such as Na^+, K^+, and Cl^- (Richards, 1970; Cohen et al., 1971; Cohen et al., 1974). As such, blood pH is controlled by both pulmonary and renal activities. Environmental factors influencing either respiratory rate or kidney function have the potential to influence calcium and phosphorus availability for bone mineralization and eggshell calcification. The commonly observed acid-base disturbances in chickens are acidosis or alkalosis of the respiratory or metabolic category (Craan et al., 1982; El Hadi et al., 1982).

Respiratory alkalosis is often a result of acute heat stress in laying hens (El Hadi et al., 1982), during which hens increase their respiratory rate to dissipate excess body heat (Randall et al., 1939). This hyperventilation leads to increased exhalation of CO_2 and decreases pCO_2; at the same time, blood oxygenation increases alongside pO_2 (Cieplnego, 2011). Since pCO_2 is a weak acid, reductions in its levels during heat stress tend to increase blood pH (Toyomizu et al., 2005), which can negatively affect the availability of calcium for bone mineralization and eggshell calcification (Odom et al., 1984) because more calcium is bound to vitellogenin and albumin in plasma (Loken et al., 1960).

Similarly, during states of metabolic acidosis, eggshell quality and bone mineralization are also impaired (Keshavarz et al., 1990). Metabolic acidosis in chickens is often induced by ingesting excess organic acids or ammonium chloride (Cohen et al., 1971). However, it may also arise due to impaired renal function (Kraut et al., 2010). The kidney is responsible for resorbing bicarbonate and excreting ammonium ions to neutralize the net endogenous acid load (Uribarri et al., 1995). Therefore, impairments to kidney function can lead to increased bicarbonate loss and ammonium

buildup, resulting in metabolic acidosis over time (Kraut et al., 2016). The increased loss of bicarbonate may impact the availability of this ion to form calcium carbonate in the eggshell (Mongin, 1978). In the rachitic chick, metabolic acidosis impaired the renal conversion of $25(OH)D_3$ into $1,25(OH)_2D_3$ by up to 40% *in vitro* and induced hyperphosphatemia (Sauveur, 1977). Rats placed into an acidotic state share similar increases in blood phosphorus, and it has been hypothesized that metabolic acidosis may limit the responsiveness of the kidney to the phosphaturic actions of PTH (Beck et al., 1975). Since $1,25(OH)_2D_3$ is crucial for calcium absorption, metabolic acidosis likely limits calcium uptake and utilization and may also explain the decreases in shell quality observed by Keshavarz et al. (1990). In mammals, metabolic acidosis has also been observed to impair bone formation and increase bone breakdown (Kraut et al., 1986), which is also an important area that should be investigated in avian species. Overall, it is clear that the acid-base balance of the chicken has a wide-ranging influence on calcium and phosphorus homeostasis and should be considered when inferring conclusions from data.

Dietary impacts on calcium and phosphorus homeostasis

Meeting the nutritional requirements for egg laying is critical for maintaining the homeostatic balance of calcium and phosphorus throughout the productive lifecycle of laying hens. The most commonly used calcium source in the laying hen diet is fine and coarse particle limestone grit (Saunders-Blades et al., 2009), though other alternatives, such as oyster shell, are considered equally effective (Roland, 1986). The ratio of fine-to-coarse limestone varies between 60:40 and 75:25 depending on the age of the flock, with older flocks usually having a higher level of coarse limestone included in the laying ration (Hervo et al., 2022). Limestone typically contains between 33.3% and 39.7% calcium, depending on its origin (Gilani et al., 2022), making it an excellent calcium source. Furthermore, limestone geological properties and particle size impact its

solubility, which is an important factor to consider when formulating laying hen diets (Zhang et al., 1997). Since eggshell calcification occurs during the dark period of the lighting cycle, feed intake is limited, and laying hens must rely upon the steady dissolution of large particle limestone to provide dietary calcium (Zhang et al., 1997). During this time, hens reduce intestinal pH by stimulating H^+/K^+-ATPase activity in the proventriculus (Guinotte et al., 1995), resulting in subsequent secretion of hydrochloric acid (Guinotte et al., 1993). Together, these actions increase the solubilization of large particle calcium retained in the gizzard (Scanes et al., 1987). As such, coarse particle limestone should be of adequate particle size to solubilize at a rate that is slow enough to continue providing calcium several hours after the intake of feed has ceased during the dark phase of the lighting program, which is necessary for optimal shell quality (Cheng et al., 1990). The fine limestone portion of the diet should solubilize faster than the coarse limestone to provide minerals for bone remineralization; however, it should not solubilize instantaneously due to the potential negative interactions with phytate and other divalent minerals in the digestive tract of the laying hen (Kim et al., 2018).

Phytate is the primary storage form of plant-based phosphorus, with 50 to 80% of plant phosphorus occurring in this form (Sun, 2018). At pH levels above 5, phytate rapidly binds monovalent and divalent cations (Martin et al., 1986). As such, calcium sources with high solubility, due to small particle size or high porosity (Shi et al., 2000), rapidly react with phytate in the small intestine to form insoluble phytate-calcium complexes that are resistant to degradation by phytase enzymes (Taylor, 1965). Higher limestone levels in the diet or inclusion of highly soluble limestone sources also increase the pH of the digesta (Kim et al., 2018), which favors calcium-phytate binding. Consequently, the formation of these insoluble complexes reduces intestinal absorption of both calcium and phosphorus (Kim et al., 2018) and may contribute to

imbalances in calcium and phosphorus homeostasis that interfere with eggshell and bone mineralization. In addition to interactions with phytate, high levels of dietary calcium may also hinder the absorption of other divalent minerals such as iron, copper, manganese, and zinc due to competition for intestinal transport and chelation with other minerals (Smith et al., 1984). As such, poultry diets are typically formulated with a ratio of calcium to available phosphorus in mind. In broilers, a ratio of between 2.22 to 2.67 of calcium to available phosphorus is recommended to optimize performance and bone health (National Research Council, 1994); however, in mature laying hens, this ratio can be as high as 12:1 due to elevated demands for eggshell calcification and medullary bone remineralization (Pastore et al., 2012) .

Another factor to consider when formulating laying hen diets is the dietary electrolyte balance (dEB). The dEB (meq/kg) can be calculated as ($[Na^+] + [K^+]$) - $[Cl^-]$. These ions are critical for tissue accretion, maintenance of the cellular electrochemical gradient, enzymatic reactions, osmotic pressure of cells, and acid-base balance. Since calcium and phosphorus transport relies upon cellular electrochemical gradients and the acid-base balance influences calcium and bicarbonate availability, dEB can affect eggshell quality (Gezen et al., 2005) and bone integrity (Araujo et al., 2022). During periods of heat stress, considerable reduction in circulating ion levels occur through hyperventilation and elevated fluid intake, which can be corrected by including sodium bicarbonate, potassium carbonate, and ammonium chloride; however, care should be taken not to alter the dEB too drastically to avoid imbalances in mineral homeostasis. In laying hens at peak production under thermoneutral conditions, dEB values ranging between 176 and 242 mEq/kg showed no adverse effects on egg weight, eggshell thickness, or number of cracked eggs (Senkoylu et al., 2005); however, diets provided with dEB outside that range (80 mEq/Kg and 330 mEq/kg) resulted in eggshells with lower breaking strength and consequently an increased

percentage of cracked eggs (Gezen et al., 2005). Taken together, laying hen rations must be carefully balanced to ensure optimal dietary calcium and phosphorus delivery.

Challenges associated with extended egg production

Although extended egg production has economic and environmental benefits (Bain et al., 2016; Pelletier, 2018), it is also accompanied by several challenges. Aged laying hens produce heavier eggs with eggshells that are thinner (Al-Batshan et al., 1994; Tumova et al., 2012; Padhi et al., 2013) and of poorer quality. Early studies by Roland (1977) found that 73-week-old hens produced unsaleable shell-less eggs or eggs with ultrathin shells at a rate of approximately 10%. These losses are further compounded when considering the percentage of eggs broken during washing and packaging (3.7%) and transport (1.1% -3%), as reviewed by Hamilton et al. (1979). Poor-quality eggshells may also increase the risk of bacterial spoilage and contamination (Edema et al., 2006), which poses serious food safety concerns.

Alterations to eggshell ultrastructure, such as the thickness of the palisade layer (Radwan, 2015; Benavides-Reyes et al., 2021) and the organization of calcite crystals and the mammillary layer (Bain, 1992; Dunn et al., 2011), likely contribute to reduced breaking strength observed in older laying hens. Interestingly, Feng et al. (2020) found no differences in mammillary density in 72-week-old hens compared to 42-week-old hens; however, later fusion of calcite crystals and reduced palisade layer thickness were observed alongside reduced breaking strength. Transcriptome analysis of genes in the shell gland influencing eggshell quality identified 183 differentially expressed genes in older hens, with 8.51% of those genes related to post-translational modification of proteins and 6.38% of genes related to mineral transport and metabolism (Feng et al., 2020). These findings demonstrate how hen age dysregulates gene expression involved in eggshell mineralization and potentially reduces protein functionality. Further proteomic evaluation

of eggshells in laying hens from 38 to 108 weeks of age also revealed lower levels of ovocleidin-116, osteopontin, calcium transport proteins, and higher levels of ovalbumin and lysozyme C, which likely influence the structural integrity of the eggshell (Zhao et al., 2024a). Overall, reduced eggshell quality in aged hens is likely a consequence of imbalances at both the genomic and protein levels, leading to irregular calcium and phosphorus deposition during eggshell calcification. Therefore, solutions to inferior eggshell quality must be found as production systems continue to extend past 100 weeks.

In addition to reductions in eggshell quality, skeletal integrity is negatively impacted by hen age. Aged hens exhibit tibiae with lower calcified tissue and cortical thickness; however, tibia total bone porosity and medullary bone volume are greater (Yamada et al., 2021). Since medullary bone exhibits a greater degree of disorganization than cortical bone (Dacke et al., 1993), reductions in cortical thickness and increase in medullary bone volume ultimately decrease the breaking strength of bones, resulting in an elevated risk of fracture in aged hens. Furthermore, altered expression of bone resorption markers carbonic anhydrase 2 and *VDR*, as well as reduced expression of accretion proteins such as collagen type 1 alpha 1 (*COL1A1*) in older hens (Gloux et al., 2020b), likely leads to irregular remodeling of medullary bone. Studies have shown that the percentage of caged hens experiencing at least one fracture in their lifetime ranges between 10% and 24% (Gregory et al., 1989). It is also worth noting that there is an increasing shift towards cage-free production systems. Within these systems, hens are allowed a greater degree of movement that results in increased potential for collisions with barn structures and a subsequently greater incidence of fracture (Sandilands et al., 2009; Baker et al., 2020). Therefore, it is even more essential to maintain calcium and phosphorus homeostasis in alternative housing systems and to develop solutions to improve skeletal strength in high-producing hens.

Rationale and objectives

Genetic selection for longer clutch sequences and fewer pause days in laying hens requires a strict balance of mineral uptake and utilization; however, as hens are maintained in production for extended periods of up to 100 weeks, dysregulation of calcium and phosphorus homeostasis is becoming an increasing challenge. As hens age, eggshell quality rapidly decreases, resulting in an increased number of eggs with thin and brittle shells (Al-Batshan et al., 1994). These eggs are prone to breakage and bacterial contamination during collection, packaging, and transport, leading to economic losses for egg producers and food safety concerns. Furthermore, older hens experience a higher prevalence of osteoporosis, resulting in fragile and brittle bones with an increased occurrence of fractures. These fractures are likely a source of considerable pain (Nasr et al., 2012), and their increased prevalence poses significant concerns about animal welfare that need to be addressed.

Eggshell calcification and bone mineralization are both under the hormonal influence of PTH, CALC, $1,25(OH)_2D_3$, and FGF23, which in turn alter the uptake, utilization, and excretion of calcium and phosphorus for these processes as well as overall mineral balance. While a deeper understanding of calcium and phosphorus homeostasis and the mechanisms by which it is hormonally regulated has developed in recent years, much of our knowledge of mechanisms involved is largely derived from mammalian research. Laying hens undergo additional biological processes, such as the development and maintenance of medullary bone and eggshell calcification, so direct inferences from mammals to birds may be flawed, and critical knowledge gaps exist. Therefore, the overarching objective of this project was to gain a comprehensive understanding of the physiological regulation of calcium and phosphorus homeostasis in laying hens during daily egg formation and across a 95-week egg production cycle.

We hypothesize that the stage of egg formation and hen age will significantly affect the physiological regulation of calcium and phosphorus homeostasis within key tissues through differences in the expression of enzymes involved in vitamin D_3 metabolism, hormone receptors, and mineral transporters. Altered mineral homeostasis will result in changes to circulating hormones, vitamin D_3 metabolites, egg quality, and skeletal integrity.

Therefore, the specific objectives of this research were as follows:

1. Determine the distribution of transcripts regulating calcium and phosphorus uptake in the intestinal tract of laying hens.
2. Investigate changes in the physiological regulation and utilization of calcium and phosphorus within the 24-hour egg formation cycle in laying hens.
    a. Evaluate changes in whole blood chemical profile and blood gases during the daily egg formation cycle.
    b. Quantify changes in circulating plasma hormone & vitamin D_3 metabolites during the daily egg formation cycle.
    c. Quantify changes in expression levels of key genes involved in calcium and phosphorus metabolism in kidney, liver, and shell gland tissue during the daily egg formation cycle.
3. Evaluate changes in the physiological regulation and utilization of calcium and phosphorus during egg formation from early through extended lay.
    a. Evaluate changes in the whole blood chemical profile and blood gases during egg formation during early, peak, late, and extended production.
    b. Quantify fluctuations in vitamin D_3 metabolites during egg formation during early, peak, late, and extended production.

c. Identify the expression patterns of genes involved in the regulation and utilization of calcium and phosphorus during egg formation during early, peak, late, and extended production.
d. Track changes in dry matter digestibility during egg formation during early, peak, late, and extended production.

CHAPTER 3

INTESTINAL DISTRIBUTION OF TRANSCRIPTS REGULATING CALCIUM AND PHOSPHORUS UPTAKE IN COMMERCIAL LAYING HENS [1]

[1]Sinclair-Black, M., Garcia, R.A., Evans, C., Angel, R., Arbe, X., Cavero, D., Ellestad L.E. 2024. To be submitted to *Poultry Science*

Abstract

Intestinal supply of calcium and phosphorus is crucial for the maintenance of eggshell quality and skeletal integrity in laying hens; however, the hormones and transporters that govern mineral uptake and homeostasis within the small intestine and ceca have not been fully elucidated. To investigate intestinal distribution of transcripts for genes involved in the regulation of calcium and phosphorus homeostasis, the duodenum, jejunum, ileum, and ceca were collected from 21-week-old commercial laying hens with a hard-shelled egg in the shell gland (n=7/tissue), and mRNA expression was evaluated using RT-qPCR. Genes encoding 24-hydroxylase and 25-hydroxylase were identified in all tissues, with higher levels noted in the ileum and ceca, suggesting these tissues may contribute to local vitamin D_3 availability. Expression of receptors involved in the hormonal regulation of calcium and phosphorus transport, such as calcium-sensing receptor, parathyroid hormone receptor 1, and fibroblast growth factor receptors 1, 2, 3, and 4, tended to increase in expression from the duodenum through the ileum, potentially demonstrating increased hormonal sensitivity within the distal small intestine. Similar distal increases in expression within the small intestine were observed for calcium transporters sodium-calcium exchanger 1 (*NCX1*), plasma membrane ATPase 2 and 4, transient receptor potential cation channels C1, V2, and M7, and inorganic phosphorus transporter 1 (*P_iT-1*) and 2, thereby suggesting an increased absorptive capacity by the jejunum and ileum compared to the duodenum. Interestingly, cecal expression of *NCX1* and *P_iT-1* was substantially higher than any location within the small intestine, identifying the ceca as a novel tissue that could be contributing to calcium and phosphorus uptake in laying hens. Together, these results highlight the importance of the distal small intestine and ceca in maintaining the homeostatic balance of calcium and phosphorus in laying hens and provide

information that can be used to optimize dietary mineral delivery for robust skeletal mineralization and eggshell quality.

Introduction

Egg formation occurs approximately every 24 hours in commercial laying hens (Bell, 2002; Nys et al., 2011) and requires calcium and phosphorus derived from intestinal uptake and bone resorption. Eggshell mineralization primarily occurs during the nocturnal fast, limiting intestinal mineral supply during this process. To compensate, medullary bone is broken down to support calcium and phosphorus demands associated with shell formation (Dacke et al., 1993). As the nocturnal fast ends, dietary calcium and phosphorus are utilized to restore medullary bone reserves that can be used for future eggshell formation (Kerschnitzki et al., 2014). In this way, intestinal mineral supply influences bone and eggshell mineralization, and understanding intestinal regulation of calcium and phosphorus uptake is necessary to ensure an adequate supply of minerals for optimal eggshell quality and skeletal integrity.

The transport of minerals from the intestinal lumen into circulation is achieved through both transcellular and paracellular routes. Transcellular mineral transport relies upon the presence of protein channels through the cell membrane and is, therefore, a saturable and rate-limiting method of mineral uptake. Transcellular diffusion channels that move ions with the electrochemical concentration gradient include calcium transporters such as transient receptor potential cation channels C1, V2, and M7 (TRPC1, TRPV2, and TRPM7) and inorganic phosphorus transporters 1 and 2 (P_iT-1 and P_iT-2) (Gloux et al., 2019). Alternatively, transcellular mineral transport can occur against the electrochemical concentration gradient via mineral antiporters, symporters, or ATP-dependent active transporters. Examples of these include sodium-calcium exchanger 1 (NCX1) (Liao et al., 2019), sodium-dependent phosphorus transporter 2b

(NaP$_i$IIb) (Hu et al., 2018), and plasma membrane calcium ATPases 1, 2, and 4 (PMCA1, PMCA2, PMCA4) (Hoenderop et al., 2005), respectively. Paracellular influx of minerals in the intestine is controlled by tight junctions, composed of tight junction proteins and claudins, whose abundance influences mineral and water permeability between cells in a passive and unsaturable manner and has been reviewed by Alexander et al. (2014). Paracellular transport primarily takes place when the concentration of luminal calcium is greater than circulating calcium levels (Areco et al., 2020). Until recently, the contribution of paracellular transport to calcium and phosphorus uptake in chickens has remained undocumented; however, Gloux et al. (2019) identified paracellular transport genes potentially involved in intestinal mineral absorption in laying hens, including candidates such as tight junction proteins 1, 2, and 3 (*TJP1, TJP2, TJP3*) and claudin 2 (*CLDN2*).

One factor influencing intestinal calcium and phosphorus uptake is hormonally active 1α,25-dihydroxycholecalciferol [1α,25(OH)$_2$D$_3$] that is synthesized following two consecutive hydroxylations of vitamin D$_3$ in the liver and the kidney (Bikle, 2018). The initial hydroxylation is thought to be primarily facilitated by hepatic 25-hydroxylase, encoded by the cytochrome P450 2R1 (*CYP2R1*) gene (Cheng et al., 2003; Watanabe et al., 2013). The second hydroxylation is modulated by renal 1α-hydroxylase, encoded by cytochrome P450 27B1 (*CYP27B1*) (Monkawa et al., 1997; Chun et al., 2014); however, this gene has not yet been identified in avian species (Sinclair-Black et al., 2023). Alternatively, 25-dihydroxycholecalciferol [25(OH)$_2$D$_3$] can undergo renal 24-hydroxylation by cytochrome P450 24 A1 (CYP24A1) to form 24,25-dihydroxycholecalciferol [24,25(OH)$_2$D$_3$], an inactive vitamin D$_3$ metabolite that is excreted by the kidney (Omdahl et al., 2002). Hormonally active 1α,25(OH)$_2$D$_3$ binds to vitamin D$_3$ receptor (VDR), which forms a complex with its heterodimeric partners, retinoid receptors alpha (RXRA) and gamma (RXRG) (Carlberg et al., 1998; Haussler et al., 2011). Together, these heterodimers

function as transcriptional regulators of genes mediating calcium and phosphorus uptake and utilization across tissues, including the intestine (King et al., 1986) and kidney (Hall et al., 1990). While there is evidence that $1\alpha,25(OH)_2D_3$ regulates transcellular mineral transport (Pansu et al., 1981), the extent to which this hormone acts on the paracellular pathways is unclear.

Further regulation of intestinal mineral transport is achieved through hormonal signaling pathways, many of which are conserved between mammalian and avian species, as reviewed by Sinclair-Black et al. (2023). Intestinal calcium absorption is stimulated by low ionized calcium (iCa^{2+}), as a result of the secretion of parathyroid hormone (PTH) that binds parathyroid hormone receptor 1 (PTH1R). Elevated PTH may upregulate $1\alpha,25(OH)_2D_3$ production (Liao et al., 2017) or directly upregulate calcium transporters (Nemere et al., 1986). In contrast, high iCa^{2+} can lead to calcitonin secretion from ultimobranchial glands and subsequent binding with calcitonin receptor (CALCR) in target tissues. In chickens, the influence of calcitonin upon calcium and phosphorus uptake from the intestine remains unclear, and further investigation into the role of calcitonin on dietary mineral absorption is necessary.

During periods of elevated circulating phosphorus, bone-derived fibroblast growth factor 23 (FGF23) is released (Poorhemati et al., 2023) and binds to FGF receptors (FGFR1, 2, 3, or 4) alongside co-receptor klotho (KL) (Razzaque, 2009). This complex induces the expression of phosphorus transporters, resulting in phosphaturic effects (Tomoe et al., 2009). Furthermore, FGF23 signaling may inhibit the 1α-hydroxylation of vitamin D_3 and inhibit PTH secretion (Ben-Dov et al., 2007), thereby influencing calcium and phosphorus homeostasis. A review by Erben (2018) highlighted bone and kidney as the primary target tissues for the physiological actions of FGF23 in mammalian species. Some of these effects appear to be conserved between mammalian and avian species (Bobeck et al., 2012; Ren et al., 2017; Ren et al., 2020); however, the effects of

FGF23 on mineral homeostasis in tissues other than bone and kidney have yet to be described in birds.

Together, the intestinal uptake of minerals is a function of transcellular and paracellular processes that are likely influenced by hormonal signaling pathways involving $1\alpha,25(OH)_2D_3$, FGF23, PTH, and calcitonin. Elucidating how these hormones influence the expression of intestinal calcium and phosphorus transporters is crucial for evaluating regional absorptive capacity and may provide valuable insights for optimizing mineral delivery to enhance uptake and utilization during periods of bone mineralization and eggshell calcification. Thus, the objective of this study was to investigate the distribution of factors regulating calcium and phosphorus uptake within the small intestine and ceca of commercial laying hens.

Materials and methods

Animals & tissue collection

Individually-caged Hy-line-W36 hens in early production (21-weeks-of-age) were housed in an environmentally controlled room with a lighting schedule of 16H light:8H dark. Hens were given free access to water and a commercially available pelleted diet [Country Feeds®, Layer Feed 16%, Nutrena] with the guaranteed analysis of 16% crude protein (minimum), 2.5% crude fat (minimum), 8% crude fiber (maximum), 0.45% available phosphorus (maximum), 3.4 to 3.9% calcium, 0.15 to 0.23% sodium, 0.7% lysine (minimum), and 0.3% methionine (minimum). All animal procedures were approved by The Institutional Animal Care and Use Committee of the University of Georgia.

Immediately prior to sampling, hens were palpated to confirm the presence of a hard-shelled egg in the shell gland, and those with an egg present were selected for sampling (n = 7). This was done to ensure the hens were actively producing eggs during the time of sampling and minimize

variation in mineral intestinal absorption believed to occur across different stages of eggshell calcification (Hurwitz et al., 1965). Each hen was considered an experimental unit. Hens were euthanized by injection of 1 mL sodium pentobarbital (390 mg/mL) and phenytoin sodium (50 mgl/mL) (Euthasol®, Virbac, Westlake, TX) into the brachial wing vein. From each hen, the distal two inches of the duodenum, middle two inches of the jejunum, and proximal two inches of the ileum were removed and the right ceca was collected. Intestinal contents were flushed from each section using 0.9% saline solution. Following this, collected sections were cut longitudinally, placed onto an ice-cold marble surface, and approximately 30 mg of mucosa was collected following scraping and homogenization. Samples were immediately snap-frozen in liquid nitrogen and stored at -80°C until total RNA was extracted.

RNA extraction and reverse transcription-quantitative PCR (RT-qPCR)

Total RNA was isolated from all tissues using QIAzol lysis buffer (Qiagen, Germantown, MD) according to the protocol outlined by the manufacturer. To each sample, 1 mL of QIAzol was added, and it was subsequently homogenized using a Mini-Bead Beater (Biospec Products, Bartlesville, OK). Homogenization occurred over three 45-second bursts separated by a 1-minute on-ice cooling step between bursts. Chloroform was added to the homogenate, and samples were centrifuged at 12,000 relative centrifugal force (RCF) at 4 °C for 15 minutes. The aqueous layer was transferred and combined with an equal volume of isopropanol, allowing total RNA to precipitate on ice for 10 minutes. Following precipitation, samples were centrifuged at 12,000 RCF and 4 °C for 10 minutes. The resulting total RNA pellets were rinsed twice with 75% ethanol, separated by centrifugation at 7,500 RCF and 4 °C for 5 minutes. Lastly, total RNA pellets were allowed to dry and reconstituted with 300 µL RNase-free water. Quantification of total RNA was conducted using a NanoDrop-1000 spectrophotometer (Thermo Scientific, Waltham, MA).

Thereafter, 1 µg total RNA was analyzed on a 1% agarose gel and visualized using a UV imaging system (BioSpectrum, Upland, CA) in conjunction with Visionworks LS software (Wasserburg, Germany) to verify the integrity of the RNA.

Reverse transcription reactions (20 µL) consisted of 1 µg total RNA, 5 µM random hexamers (Invitrogen, Carlsbad, CA), 5 µM anchored-dT primer (Integrated DNA Technologies, Coralville, IA), 0.5 mM dNTPs (Thermo Scientific), 200 U M-MuLV reverse transcriptase (New England Biolabs, Ipswich, MA), 2 µL 10X M-MuLV buffer (New England Biolabs), and 8 U of RNaseOUT (Invitrogen). Total RNA, primers, and dNTPs were combined and heated at 65 °C for 5 minutes. Samples were then placed on ice for at least one minute before the addition of the M-MuLV enzyme, M-MuLV buffer, and RNaseOUT. Following this, further incubations took place at 25 °C for 5 minutes, 42 °C for 60 minutes, and finally 65 °C for 20 minutes. A negative control to assess for genomic DNA contamination consisted of pooled RNA from all samples; however, the reverse transcriptase enzyme was not included. All reactions were diluted 1:10 with nuclease-free water prior to quantitative PCR (qPCR).

Primers (Table 1) used for qPCR analysis were designed using Primer3 Plus software (Untergasser et al., 2012). Each primer was constructed to span introns with the following characteristics: amplicon length of 100 to 125 base pairs, primer length between 18 and 30 nucleotides, primer melting temperature between 58 to 60 °C, and GC content between 40 to 60%. Expression of mRNA for the indicated genes was measured using duplicate 10 µL reactions that consisted of 2 µL diluted cDNA, 5 µL PowerUp™ SYBR Green Master Mix (Applied Biosystems, Foster City, CA), and 400 nM of each forward and reverse primer. Thermal cycling was conducted on a QuantStudio3 real-time PCR instrument (Applied Biosystems), with the following cycling conditions: 95 °C for 5 minutes, 40 cycles of 95 °C for 15 seconds, 58 °C for 30 seconds, 72 °C

for 30 seconds, and a post-amplification dissociation curve to confirm that a single product was amplified.

Levels of target mRNA expression were normalized to glyceraldehyde-3-phosphate dehydrogenase (*GAPDH*) using the equation: $\Delta CT = CT_{\text{Target gene}} - CT_{GAPDH}$, followed by a transformation as $2^{-\Delta CT}$. To express these data relative to levels in the duodenum, each transformed value was divided by the average transformed value for the duodenum using the following equation: [($2^{-\Delta CT}$) Sample] / [Average ($2^{-\Delta CT}$) duodenum]. As a result, the value for duodenal expression for each gene is equal to one in all cases.

Statistical Analysis

Each hen was considered an experimental unit. Data were analyzed with JMP Pro 16 software (SAS Institute, Inc, Cary, NC) using a one-way analysis of variance (ANOVA), with intestinal location as the model effect. *Post hoc* comparison of means was conducted using Fisher's test of least significant difference. Differences were considered significant at $P \leq 0.05$.

Results

Vitamin D_3 metabolism and signaling

To establish the extent of local vitamin D_3 25- and 24-hydroxylation within intestinal tissues and its influence on associated genomic signaling, mRNA expression of vitamin D_3 hydroxylase enzymes, *VDR*, and heterodimeric transcriptional partners of VDR were measured (Figure 3.1). Expression of neither *CYP2R1* nor *CYP24A1* differed across the duodenal and jejunal segments of the intestine, whereas ileal expression was at least 2-fold greater for both genes (Figure 3.1A, B; $P \leq 0.05$). Cecal expression of *CYP2R1* was intermediate compared to the ileum and other small intestine regions, while cecal *CYP24A1* did not differ from the ileum ($P > 0.05$) but was higher than duodenum and jejunum (Figure 3.1A, B; $P \leq 0.05$). Levels of *VDR* were consistent throughout the

small intestine (P>0.05) but lower in the ceca (Figure 3.1C; P≤0.05). In contrast, expression of both *RXRA* and *RXRG* increased distally from the duodenum through the ileum, with *RXRA* maintaining elevated expression in the ceca (Figure 3.1D; P≤0.05) and *RXRG* showing decreased cecal expression (Figure 3.1E; P≤0.05).

Mineral homeostasis

Hormonal signaling. In order to evaluate the intestinal distribution of hormonal signaling pathways contributing to mineral uptake, expression of calcium-sensing receptor (*CASR*), *PTH1R*, *CALCR*, *FGFR1 – 4*, and *KL* was measured in the small intestine and ceca (Figure 3.2). Levels of *CASR* were 4-fold higher in the jejunum and 10-fold greater in the ileum than either duodenum or ceca (Figure 3.2A; P≤0.05). Ileal *PTH1R* was 10-fold greater than duodenum and jejunum and more than 3.5-fold that of the ceca (Figure 3.2B; P≤0.05). Furthermore, *PTH1R* levels were higher in the ceca than those observed in the proximal two sections of the small intestine (Figure 3.2B; P≤0.05). Expression of *CALCR* was notably higher in the ceca, exhibiting levels more than 4-fold greater than that in all segments of the small intestine, which increased distally from the duodenum through ceca (Figure 3.2C; P≤0.05). Unlike other hormonal receptors, *KL* mRNA was distinctly elevated in the jejunum at levels 22-fold higher than the duodenum and 7-fold higher than the ileum and ceca (Figure 3.2D; P≤0.05). All receptors for FGF23 shared similar expression patterns, wherein mRNA levels increased distally between the duodenum and ileum, with ceca exhibiting similar levels to those in the ileum (Figure 3.2E-H; P≤0.05). Jejunal levels of these individual receptors differed in that they were similar to the duodenum (*FGFR2*, *FGFR4*), similar to the ileum (*FGFR1*), or intermediate in expression between the two (*FGFR3*) [Figure 3.2E-H; P≤0.05].

Calcium uptake. Calcium absorption along the intestinal tract is essential for the maintenance of calcium homeostasis in laying hens. Therefore, to evaluate the regional absorptive capacity of the

small intestine and ceca, mRNA expression of calcium transporters was analyzed (Figure 3.3). The calcium chaperone calbindin (*CALB1*) exhibited similar levels across the small intestine (P>0.05) and lower expression in the ceca (Figure 3.3A; P≤0.05).

Contrastingly, *NCX1* and *TRPM7* mRNA were 37-fold and 4-fold higher in the ceca, respectively, than any section of the small intestine (Figure 3.3B, H; P≤0.05). Expression of *PMCA1* generally declined distally along the intestine except for the ileum, which showed similar levels to the duodenum (Figure 3.3C; P≤0.05). Ileal *PMCA2* levels were twice that of other segments of the small intestine and ceca (Figure 3.3D, H; P≤0.05). Most calcium transporters examined, including *NCX1*, *PMCA4*, *TRPC1*, *TRPV2*, and *TRPM7*, increased in expression as intestinal location became more distal (Figure 3.3 B, E, F, G, H; P≤0.05).

Phosphorus absorption. Absorption of phosphorus that is utilized during bone mineralization and eggshell formation is concurrently regulated alongside calcium in the small intestine. Thus, mRNA expression of intestinal transporters facilitating dietary phosphorus uptake was measured (Figure 3.4). Expression of *P_iT-1* increased gradually from the duodenum to the ileum; however, cecal mRNA levels of this gene were almost 15-fold greater than that of the duodenum (Figure 3.4A; P≤0.05). Similar to *P_iT-1*, *P_iT-2* also tended to increase distally; however, cecal levels were not elevated above those in the small intestine (Figure 3.4B; P≤0.05). Unlike other phosphorus transporters, *NaP_iIIb* decreased in a stepwise manner from the duodenum through the ileum (Figure 3.4C; P≤0.05). Cecal levels of *NaP_iIIb* were generally higher than those in the small intestine; however, expression of this gene was only detected in cecal tissue in two out of the seven hens, leading to considerable hen-to-hen variation. Consequently, no significant differences in expression between duodenum and ceca were observed (Figure 3.4C; ≤0.05). Lastly, no differences were observed in xenotropic and polytropic retrovirus receptor 1 (*XPR1*) mRNA between all

segments of the small intestine and ceca (Figure 3.4D; P>0.05). Expression of *NaP$_i$IIa* was not detected in any of the intestinal segments.

Tight junction mineral transport. In order to evaluate the potential contribution of paracellular transport to intestinal mineral uptake, mRNA expression of TJPs and CLDN2 was measured in the small intestine and ceca (Figure 3.5). Together, *TJP1*, *TJP2,* and *TJP3* exhibited similar expression patterns, wherein levels increased gradually from the duodenum to the ceca (Figure 3.5 A, B, C; P≥0.05). Contrastingly, *CLDN2* was highest in the duodenum and jejunum, followed by a steady decrease in mRNA abundance through to the ceca, which had significantly lower levels (Figure 3.5 D; P≤0.05).

Discussion

Laying hens rely upon intestinal calcium and phosphorus absorption to sustain daily egg formation and bone mineralization. As such, this study set out to investigate the intestinal distribution of transcripts related to mineral uptake to evaluate the relative contributions of each location to calcium and phosphorus utilization. Differences in transcript abundance were measured without further investigation into whether the protein associated with the mRNA differed. Since differences in mRNA expression may not reflect functional modifications at a cellular level in all cases, caution should be used when interpreting these results. Nonetheless, these data help identify systems and processes potentially involved in regulating intestinal mineral uptake. Our findings suggest that both the small intestine and ceca may be capable of local 25- and 24-hydroxylation of vitamin D_3. Moreover, the ileum appears to be an important site for calcium and phosphorus uptake, which could be regulated by hormonal signaling pathways that include the genomic actions of vitamin D_3. Furthermore, significantly elevated levels of select calcium (*NCX1*) and phosphorus (*P$_i$T-1*)

transporters in the ceca suggest that this tissue may be a novel site for calcium and phosphorus absorption.

Biologically active 1α,25$(OH)_2D_3$ is a crucial factor involved in maintaining the homeostatic balance of calcium and phosphorus in laying hens through its transcriptional regulation of genes involved in mineral uptake and utilization. Production of this metabolite canonically occurs via sequential hydroxylation reactions, beginning with hepatic 25-hydroxylation of vitamin D_3 and followed by renal 1α-hydroxylation of 25(OH)D_3 (Jones et al., 1998). Alternatively, 25(OH)D_3 may undergo renal 24-hydroxylation to form 24,25$(OH)_2D_3$ as part of a negative feedback loop to prevent the overproduction of 1α,25$(OH)_2D_3$ (Omdahl et al., 2002). Interestingly, results from this study identified the expression of two enzymes capable of vitamin D_3 hydroxylation, *CYP2R1* and *CYP24A1* (Omdahl et al., 2002), within the duodenum, jejunum, ileum, and ceca, none of which are traditionally associated with that function. Since the small intestine is a site of vitamin D_3 absorption (Bar et al., 1980), the expression of enzymatic regulators of vitamin D_3 availability may improve the local utilization of vitamin D_3 present in the diet, reducing the reliance upon hepatic and renal vitamin D_3 enzymatic conversion. If such mechanisms exist within enterocytes, they may also partially account for the lack of a direct relationship between circulating 1α,25$(OH)_2D_3$ and intestinal expression of *CYP24A1* observed in mice, which is used as a marker for local transcriptional activity of 1α,25$(OH)_2D_3$ (Reynolds et al., 2018). In avian species, correlations between circulating 1α,25$(OH)_2D_3$ and differences in intestinal mineral transporter expression are not well established. Previous studies in chickens have identified the expression of *CYP24A1* in the duodenum of broilers (Hsiao et al., 2018) and jejunal expression of *CYP2R1* in laying hens (Guo et al., 2022). Furthermore, in rats, *in vitro* intestinal 24-hydroxylation of vitamin D_3 has been shown by Kumar et al. (1977). Curiously, our results showed significantly

greater expression of *CYP2R1* and *CYP24A1* in the ileum relative to both the duodenum and jejunum. These enzymes, in conjunction with the expression of vitamin D_3 transcriptional regulatory proteins, *VDR*, *RXRA*, and *RXRG*, in the present study suggest that the small intestine participates in local vitamin D_3 availability, with the ileum likely having the greatest impact.

The retention time within the small intestine and ceca is often correlated with increased absorption of minerals such as calcium. In dogs (Cramer, 1965) and rats (Cramer et al., 1959; Marcus et al., 1962), the ileum is considered a major site of calcium absorption due, in part, to increased retention time of digestive contents. Similarly, in chickens, total ileal retention of digesta also represents a substantial period (47 – 64% of total small intestine retention time) compared to that of the duodenum (2 – 5%) and jejunum (31 – 48%) (Shires et al., 1986; Van der Klis et al., 1990; Rougiere et al., 2010). As such, it is likely that the ileum contributes to mineral uptake and homeostasis; however, previous literature investigating calcium absorption in laying hens has identified the duodenum and jejunum as the primary sites of uptake (Hurwitz et al., 1965; Hurwitz et al., 1973). These studies utilized isotopes such as the reference marker yttrium-91 to measure the relative disappearance of calcium and phosphorus (Hurwitz et al., 1965) or measured the uptake of ^{45}Ca and ^{32}P from ligated intestinal segments *in situ* (Hurwitz et al., 1973). Findings from our research identified considerable upregulation of *CASR* and *PTH1R* in the ileum relative to duodenal expression, both of which are involved in the hormonal regulation of calcium and phosphorus homeostasis. Information regarding the role of intestinal CASR in regulating calcium and phosphorus uptake is scant; however, a review by Chanpaisaeng et al. (2021) proposes that CASR may regulate calcium entry into the enterocyte through calcium transporters such as transient receptor potential vanilloid subfamily member 6 (TRPV6) (Lee et al., 2019). Findings from the present study did not detect the intestinal expression of *TRPV6*, which is in line with

observations by others (Proszkowiec-Weglarz et al., 2013; Proszkowiec-Weglarz et al., 2019; Hu et al., 2022; Garcia-Mejia et al., 2024; Sinclair-Black et al., 2024); however, immunohistochemical analysis by Yang et al. (2011) suggests that TRPV6 may be localized to the brush-border membrane of intestinal cells of laying hens. Nonetheless, similar regulation of calcium entry may take place via other transient receptor potential subfamilies such as *TRPC1*, *TRPV2*, or *TRPM7*, which increased their expression distally in the small intestine, similar to *CASR*. Elevated levels of ileal *CASR* compared to the duodenum were also detected by Hui et al. (2021). Additionally, CASR may regulate phosphate metabolism through interactions with FGF23 (Wongdee et al., 2018). Results from our study demonstrated significant increases in the levels of *FGFR1, 2, 3,* and *4* from the duodenum through the ileum. In mice, FGF23 signaling via its receptors has been shown to reduce intestinal phosphorus absorption via NaP_iIIb (Gattineni et al., 2009; Tomoe et al., 2009). Findings from the current study demonstrated similar inverse relationships between the expression of the *FGFR1*, *2*, *3,* and *4* and *NaPiIIb* in the small intestine but not in the ceca, suggesting that cecal phosphorus transport may not be as tightly controlled or that it is regulated in a different manner to the small intestine. Interestingly, *KL*, the co-receptor required for high-affinity binding of FGF23 to its receptors, was substantially elevated in the jejunum compared to other regions in the small intestine and ceca. It should be noted, however, that *KL* is capable of interacting with receptors for several members of the FGF family, including FGF19 that is secreted by the intestine in response to feeding and strongly dependent on the presence of KL to exert its effects (Sun et al., 2023). As such, the dramatically higher levels of jejunal *KL* in the current study may not be directly related to FGF23-mediated phosphorus regulation.

Further regulation of intestinal calcium and phosphorus uptake and utilization may also take place via the actions of PTH binding PTH1R. Potential effects of this have been noted in

chickens, wherein significant increases in calcium and phosphorus uptake from the chick duodenum were observed upon perfusion with bovine-PTH (Nemere et al., 1986; Nemere, 1996). As such, elevated *PTH1R* expression in the ileum may indicate regional sensitivity to PTH. This sensitivity may drive expression of calcium transporters *PMCA2*, *PMCA4*, *TRPC1*, *TRPV2*, and *TRPM7*, along with phosphorus transporters *P_iT-1* and *P_iT-2*, all of which were significantly higher in the ileum compared to the duodenum in our findings. Likewise, PTH signaling via PTH1R may also regulate paracellular calcium transport by inhibiting claudin 14 expression, as previously demonstrated in the kidneys of mice (Sato et al., 2017). Our results demonstrated an inverse relationship between ileal *PTH1R* and *CLDN2* levels, suggesting that similar negative feedback between PTH and CLDN2 may exist in the ileum. A previous study conducted in laying hens investigated the intestinal expression profile of genes related to mineral transport and identified distinct intestinal distribution patterns for calcium transporters (*TRPC1*, *PMCA1*, and *PMCA4*), tight junction proteins (*TJP2* and *TJP3*), and *VDR* (Gloux et al., 2020a). The findings showed significantly higher expression in the jejunum than the duodenum for all genes except *PMCA1*. Previous research has highlighted the efficacy of duodenal and jejunal calcium and phosphorus absorption in chickens (Hurwitz et al., 1965; Hurwitz et al., 1973), often resulting in the exclusion of ileum from experimental designs in more recent publications. Findings presented here, however, demonstrated higher levels of hormone receptors, vitamin D_3 hydroxylases, and mineral transporters in the proximal ileum, indicating that this portion of the small intestine may play a larger role in the regulation of calcium and phosphorus uptake and utilization than previously considered.

Findings from our study also yielded several unexpected results pertaining to potential mineral transport occurring in the ceca of laying hens. Avian ceca play important roles in water

absorption, carbohydrate fermentation (Sergeant et al., 2014; Polansky et al., 2016), and nitrogen recycling (Karasawa, 1999); however, their role in mineral uptake is poorly understood. Results herein demonstrated considerable upregulation of cecal *NCX1,* a calcium transporter, with levels that were 30-fold greater than duodenal and jejunal levels and 18-fold greater than ileal levels. Other calcium transport and paracellular transport genes, including *PMCA4*, *TRPC1*, *TRPV2*, *TRPM7*, *TJP1*, *TJP2*, and *TJP 3,* also tended to be greatest in the ceca, with *PMCA4* and *TRPM7* exhibiting expression that was significantly higher than any location within the small intestine and double that observed in the ileum. Moreover, in the ceca, the phosphorus transporter *P_iT-1* was more than 15-fold greater than in the duodenum, and *NaPiIIb* levels were 20-fold higher those in the ileum. Together, these data strongly suggest that the ceca may indeed play a role in the mineral homeostasis of laying hens. Further evidence that the ceca may participate in mineral uptake has been demonstrated by immunohistochemical studies conducted in owls that identified the presence of VDR, CALB1, and a voltage-gated calcium channel (Meyer et al., 2009) in the ceca, as well as in rats, where high rates of cecal calcium absorption driven by $1\alpha,25(OH)_2D_3$ signaling have been observed (Karbach et al., 1993). Physical characteristics of ceca may also contribute to this tissue's role as a promising location for further investigation into the utilization of calcium and phosphorus in chickens. The length of the ceca in laying hens represents approximately 25% of the entire small intestine (Herrera et al., 2017), and the retention time of cecal digestive contents can range from 70 minutes to over 16 hours (Shires et al., 1986; Garcon et al., 2023). Furthermore, microvilli in the proximal region of the ceca have been identified and show similar structural characteristics to microvilli observed in the small intestine (Ferrer et al., 1991), suggesting similar absorptive capabilities. Overall, our findings highlight a potentially novel role of the ceca in mediating laying hen intestinal calcium and phosphorus transport. Elucidating the extent to which this tissue

contributes to mineral homeostasis is crucial to improving our understanding of calcium and phosphorus dynamics in laying hens.

In conclusion, this study identified key transporters and hormonal signaling pathways involved in intestinal calcium and phosphorus absorption and utilization by laying hens. The expression of vitamin D_3 hydroxylase enzymes and associated vitamin D_3 transcriptional regulatory proteins were found in all segments of the small intestine and ceca, demonstrating a capacity for intestinal regulation of vitamin D_3 metabolite production and subsequent transcriptional regulation at the local level. Moreover, the ileum and the ceca were highlighted as important tissues involved in maintaining the homeostatic balance of calcium and phosphorus, suggesting that the role of the distal intestine in mineral uptake should be reconsidered in laying hens. Together, these findings can be used to optimize nutritional strategies geared towards delivering minerals to intestinal locations where absorption would be most effective during periods of bone mineralization and eggshell calcification, ultimately resulting in improvements in skeletal integrity and eggshell quality.

Table 3.1. Primers used for reverse transcription-quantitative PCR.

Target	Forward Primer (5'-3')	Reverse Primer (5'-3')	Transcript ID
Vitamin D_3 metabolism and action			
CYP2R1	GGACAGCAATGGACAGTTTG	AGGAAAACGCAGGTGAAATC	09745[1]
CYP24A1	TGGTGACACCTGTGGAACTT	CTCCTGAGGGTTTGCAGAGT	59161[1]
VDR	CTGCAAAATCACCAAGGACA	CATCTCACGCTTCCTCTGC	96121[1]
RXRA	ACTGCCGCTACCAGAAGTGT	GACTCCACCTCGTTCTCGTT	59924[1]
RXRG	GAAGCCTACACGAAGCAGAA	CCGATCAGCTTGAAGAAGAA	49224[1]
Calcium homeostasis			
CASR	CTGCTTCGAGTGTGTGGACT	GATGCAGGATGTGTGGTTCT	55986[1]
PTH1R	CCAAGCTACGGGAAACAAAT	ATGGCATAGCCATGAAAACA	08796[1]
CALCR	GCAGTTGCAAGAGCCAAATA	AGCTTTGTCACCAACACTCG	15478[1]
CALB1	AAGCAGATTGAAGACTCAAAGC	CTGGCCAGTTCAGTAAGCTC	74265[1]
NCX1	TCACTGCAGTCGTGTTTGTG	AAGAAAACGTTCACGGCATT	13920[1]
PMCA1	TTAATGCCCGGAAAATTCAC	TCCACCAAACTGCACGATAA	80355[1]
PMCA2	CCAGTTTGGAGGAAAACCAT	GATGGTTGCAATGACCTGAC	66024[2]
PMCA4	GTGCGGGAGAAGGAGATGAG	TAAGGCCACACCATCCTGAG	66603[2]
TRPC1	TGCATTTGCTAATGTGCTGA	TTCCAAAATCTTGCAGCATC	04155[1]
TRPV2	TGCTTGATGTCAGTGGGTCT	ATTGGTGTTTCCAGGCTCTT	71938[2]
TRPM7	AACTTCAGAGCGAAGCATCA	TTAGCTCAGGGGAATCATCC	41724[2]
Phosphorus homeostasis			
P_it-1	TATCCTCCTCATTTCGGCGG	CTCTTCTCCATCAGCGGACT	94781[1]
P_it-2	CCATCCCCGTGTACCTTATG	AGACATGGCCATCACTCCTC	51992[1]
NaP_iIIa	ATCGGCTTGGGGGTGATC	GAGGGCGATCTGGAAGGAG	58978[1]
XPR1	GTGACATTTGCAGCCCTCTA	GGTCCCAGATGAGGGTGTAG	23428[2]
Paracellular mineral transport			
TJP2	ATGCTGTCCCTGTCAAAACA	CACGATCCTCCAGGTAAGGT	40767[2]
TJP3	CGAGCTCTTTGAGATTGCAC	GTGCTTGTCCTTTTCAGCAA	68103[2]
Normalization Gene			
GAPDH	AGCCATTCCTCCACCTTTGAT	AGTCCACAACACGGTTGCTGTAT	23323[1]

[1]Transcript identification from Ensembl chicken genome assembly (GRCg6a; (http://www.ensembl.org/Gallus_gallus/Info/Index) preceded by ENSGALT000000
[2]Transcript identification from Ensembl chicken genome assembly (GRCg7b; (http://www.ensembl.org/Gallus_gallus/Info/Index) preceded by ENSGALT000100

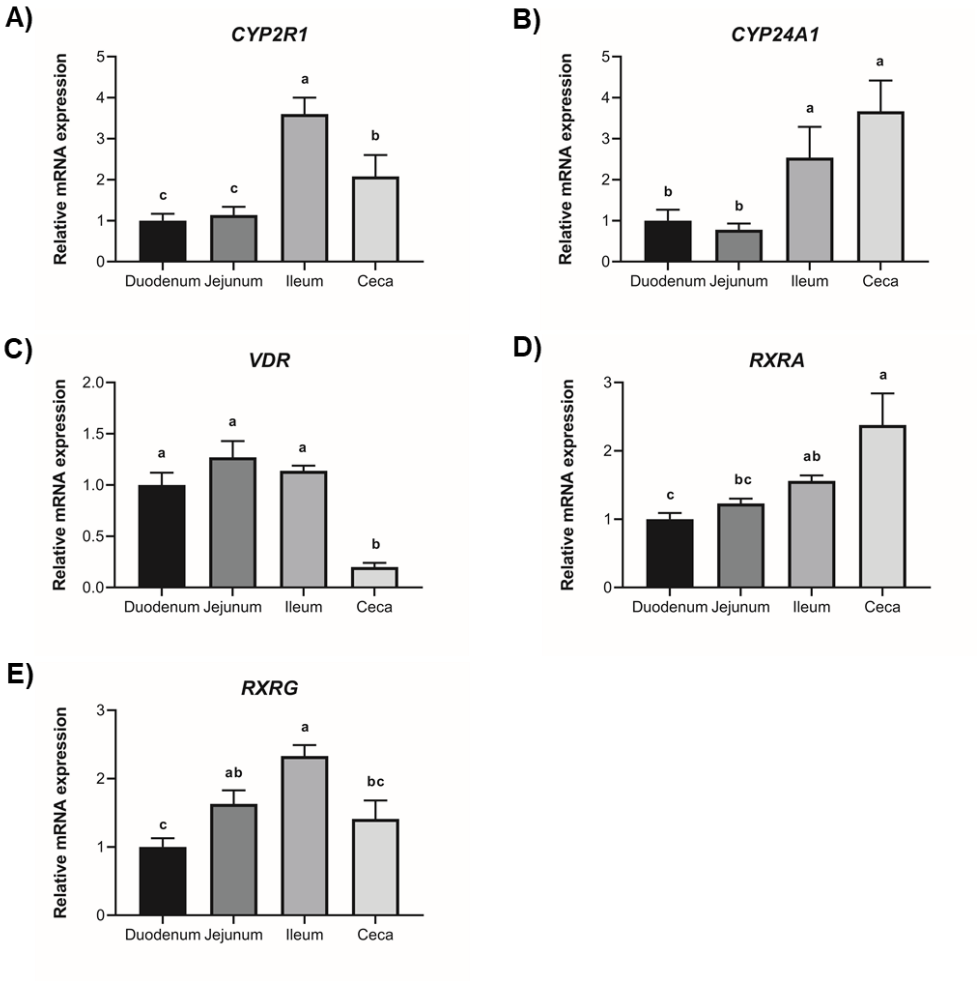

Figure 3.1. Expression of genes involved in vitamin D_3 metabolism and signaling.
Relative levels of mRNA were measured within the small intestine and ceca for (A) *CYP2R1*, (B) *CYP24A1*, (C) *VDR, (D) RXRA*, and (E) *RXRG*. Expression of target genes was determined by RT-qPCR and normalized to *GAPDH* mRNA. All values (mean+SEM; n=7 hens) are expressed relative to the duodenum (equivalent to 1). Data were analyzed by one-way ANOVA followed by Fisher's test of least significant difference when ANOVA indicated significance, and bars not sharing a common letter differ significantly ($P \leq 0.05$). Expression of *CYP27B1* was not measured, as the gene has not been identified in chickens.

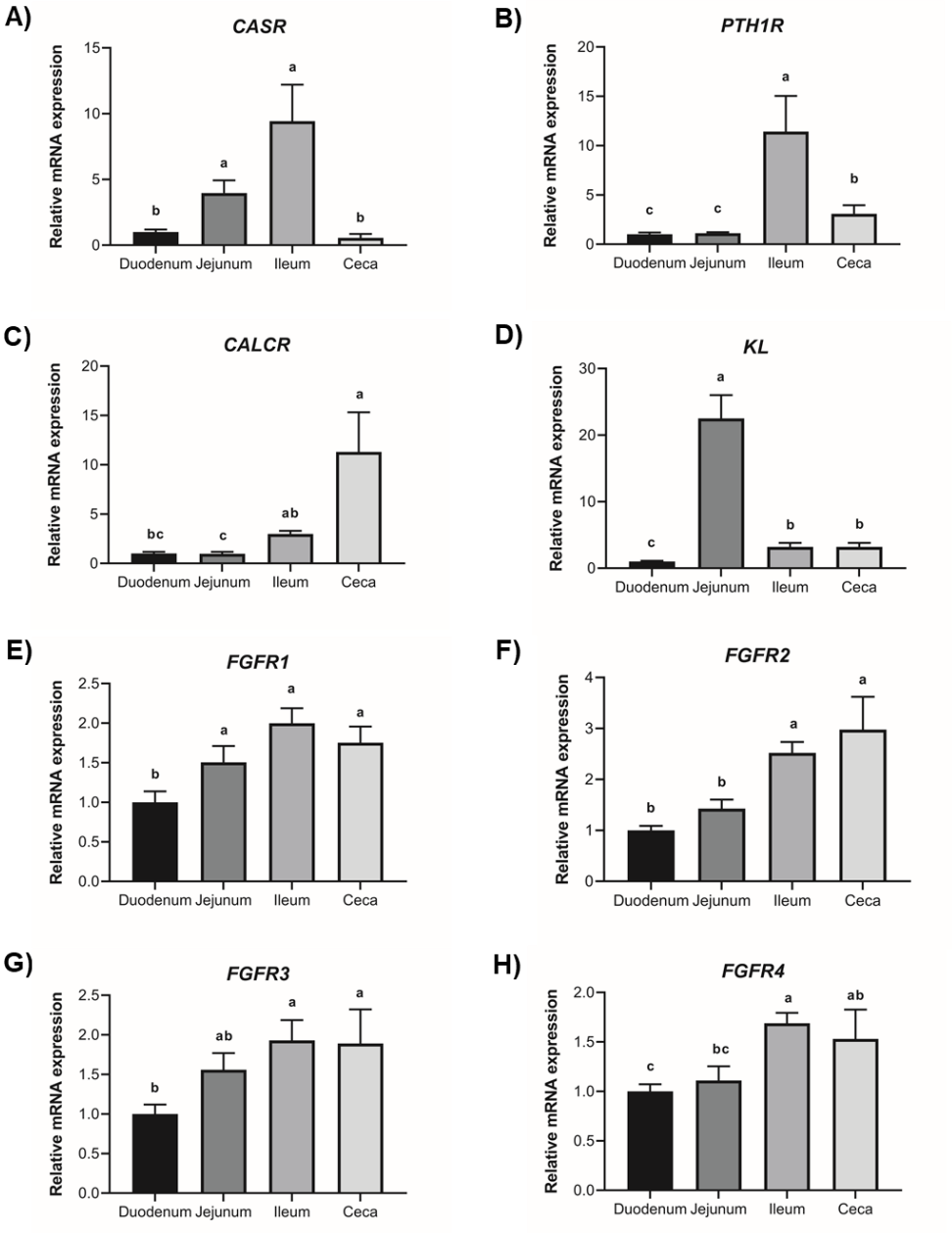

Figure 3.2. Expression of receptors for hormones mediating mineral homeostasis.
Relative levels of mRNA were measured within small intestine and ceca for (A) *CASR*, (B) *PTH1R*, (C) *CALCR*, (D) *KL*, (E) *FGFR1*, (F) *FGFR2*, (G) *FGFR3*, and (H) *FGFR4*. Expression of target genes was determined by RT-qPCR and normalized to *GAPDH* mRNA. All values (mean+SEM; n=7 hens) are expressed relative to the duodenum (equivalent to 1). Data were analyzed by one-way ANOVA followed by Fisher's test of least significant difference when ANOVA indicated significance, and bars not sharing a common letter differ significantly ($P \leq 0.05$).

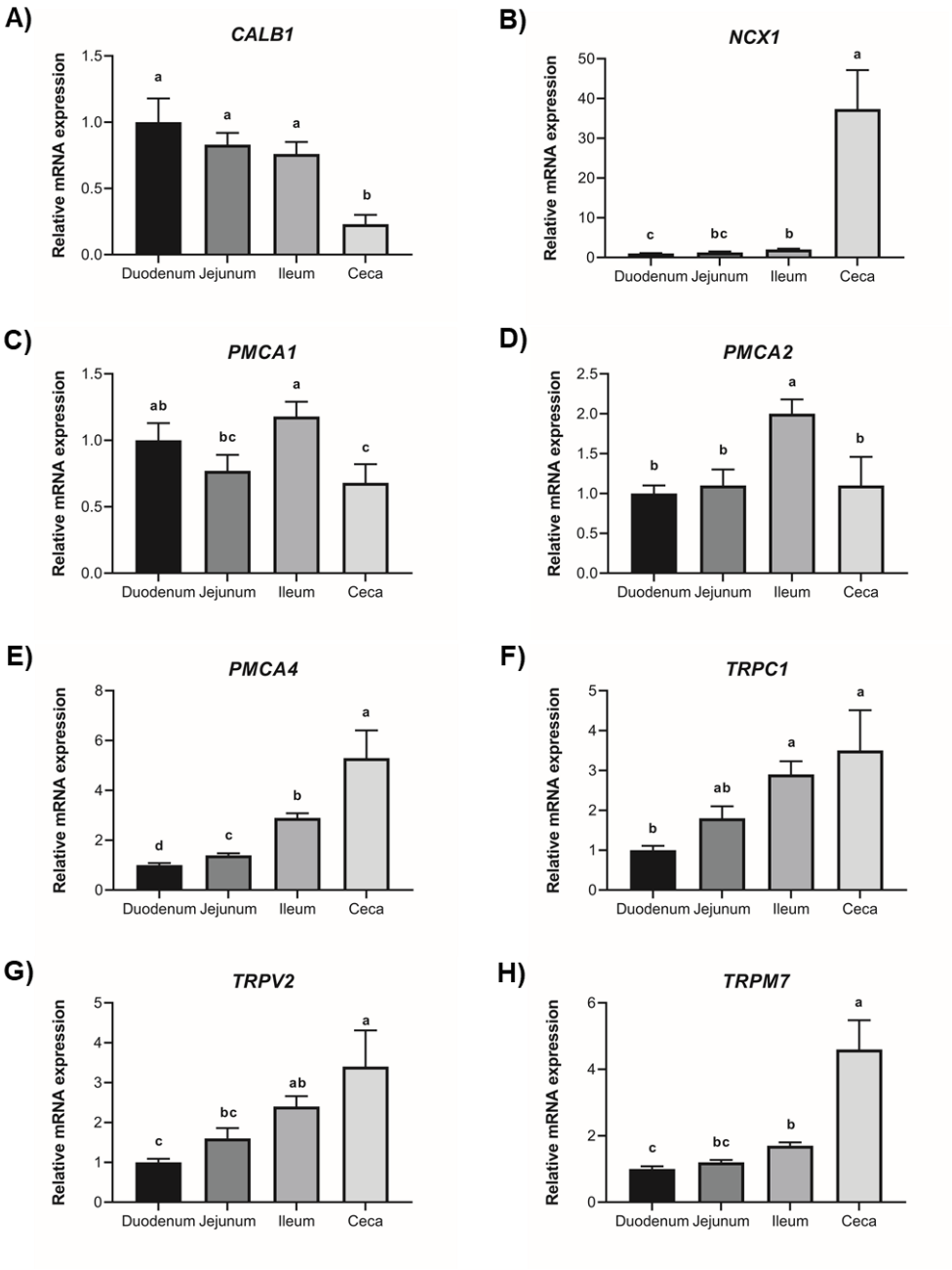

Figure 3.3. Expression of genes involved in calcium transport.
Relative levels of mRNA were measured within the small intestine and ceca for (A) *CALB1*, (B) *NCX1*, (C) *PMCA1*, (D) *PMCA2*, (E) *PMCA4*, (F) *TRPC1*, (G) *TRPV2*, and (H) *TRPM7*. Expression of target genes was determined by RT-qPCR and normalized to *GAPDH* mRNA. All values (mean+SEM; n=7 hens) are expressed relative to the duodenum (equivalent to 1). Data were analyzed by one-way ANOVA followed by Fisher's test of least significant difference when ANOVA indicated significance, and bars not sharing a common letter differ significantly ($P \leq 0.05$).

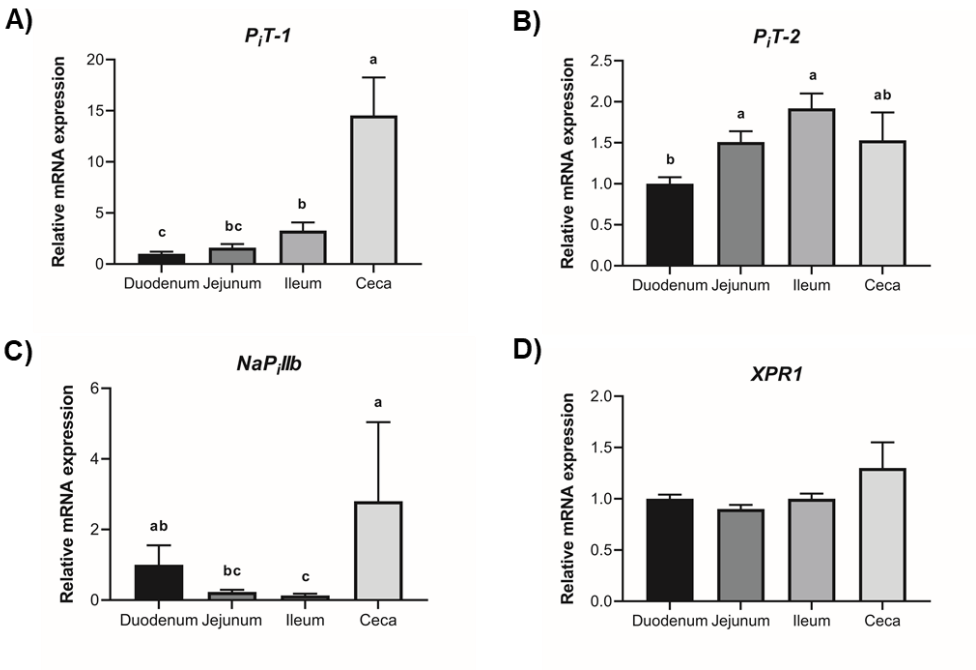

Figure 3.4. Expression of genes involved in phosphorus transport.
Relative levels of mRNA were measured within the small intestine and ceca for (A) *PiT-1*, (B) *PiT-2*, (C) *NaPiIIb*, and (D) *XPR1*. Expression of target genes was determined by RT-qPCR and normalized to *GAPDH* mRNA. All values (mean+SEM; n=7 hens) are expressed relative to the duodenum (equivalent to 1). Data were analyzed by one-way ANOVA followed by Fisher's test of least significant difference when ANOVA indicated significance, and bars not sharing a common letter differ significantly ($P \leq 0.05$).

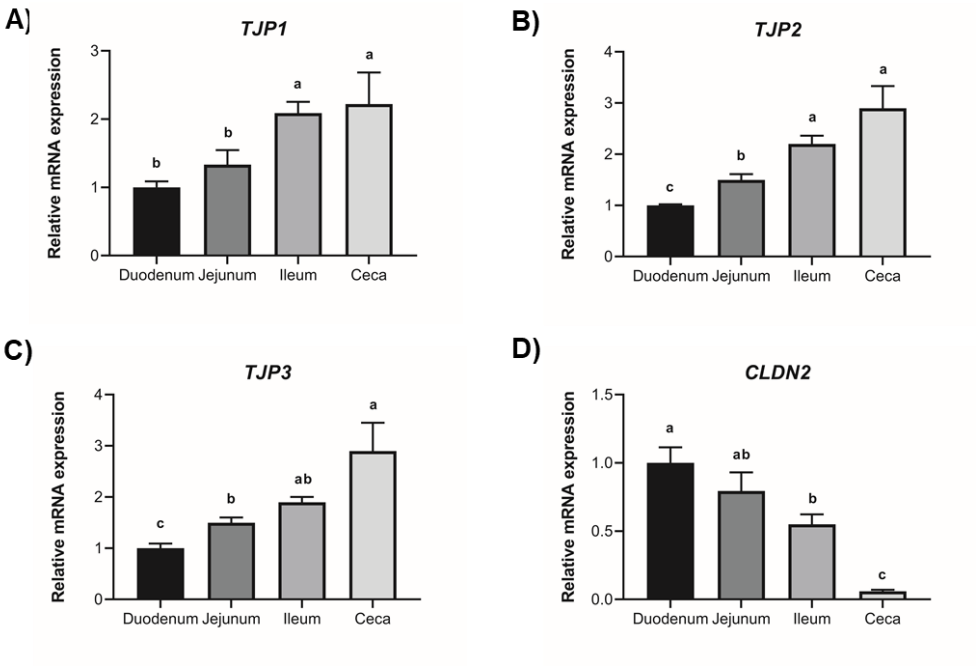

Figure 3.5. Expression of genes involved in paracellular mineral transport.
Relative levels of mRNA were measured within the small intestine and ceca for (A) *TJP1*, (B) *TJP2*, (C) *TJP3*, (D) *CLDN2*. Expression of target genes was determined by RT-qPCR and normalized to *GAPDH* mRNA. All values (mean+SEM; n=7 hens) are expressed relative to the duodenum (equivalent to 1). Data were analyzed by one-way ANOVA followed by Fisher's test of least significant difference when ANOVA indicated significance, and bars not sharing a common letter differ significantly ($P \leq 0.05$).

CHAPTER 4

CIRCADIAN REGULATION OF CALCIUM AND PHOSPHORUS HOMEOSTASIS DURING THE OVIPOSITION CYCLE IN LAYING HENS[2]

[2]Sinclair-Black, M., Garcia, R.A., Blair, L.R., Angel, R., Arbe, X., Cavero, D., Ellestad L.E. 2024. *Poultry Science***.** 103:1-11. doi: 10.1016/j.psj.2023.103209
Reprinted here with the permission of the publisher

Abstract

Maintenance of calcium and phosphorus homeostasis in laying hens is crucial for preservation of skeletal integrity and eggshell quality, though physiological regulation of these systems is incompletely defined. To investigate changes in mineral and vitamin D_3 homeostasis during the 24-hour egg formation cycle, 32-week-old commercial laying hens were sampled at 1, 3, 4, 6, 7, 8, 12, 15, 18, 21, 23, and 24 hours post-oviposition (HPOP; $n \geq 4$). Ovum location and egg calcification stage were recorded, and blood chemistry, plasma vitamin D_3 metabolites, circulating parathyroid hormone (PTH), and expression of genes mediating uptake and utilization of calcium and phosphorus were evaluated. Elevated levels of renal 25-hydroxylase from 12–23 HPOP suggest this tissue might play a role in vitamin D_3 25-hydroxylation during eggshell calcification. In shell gland, retinoid-x-receptor gamma upregulation between 6 to 8 HPOP followed by subsequently increased vitamin D receptor indicate that vitamin D_3 signaling is important for eggshell calcification. Increased expression of PTH, calcitonin, and fibroblast growth factor 23 (FGF23) receptors in the shell gland between 18–24 HPOP suggest elevated sensitivity to these hormones towards the end of eggshell calcification. Shell gland sodium-calcium exchanger 1 was upregulated between 4 and 7 HPOP and plasma membrane calcium ATPase 1 increased throughout eggshell calcification, suggesting the primary calcium transporter may differ according to eggshell calcification stage. Expression in shell gland further indicated that bicarbonate synthesis precedes transport, where genes peaked at 6–7 and 12–18 HPOP, respectively. Inorganic phosphorus transporter 1 (*P_iT-1*) expression peaked in kidney between 12–15 HPOP, likely to excrete excess circulating phosphorus, and in shell gland between 18–21 HPOP. Upregulation of FGF23 receptors and *PiT-1* during late eggshell calcification suggest shell gland phosphorus uptake is important at this time. Together, these findings identified potentially novel hormonal pathways involved in

calcium and phosphorus homeostasis along with associated circadian patterns in gene expression that can be used to devise strategies aimed at improving eggshell and skeletal strength in laying hens.

Introduction

Eggs produced by commercial laying hens are a source of affordable, high-quality protein. Modern layers produce an egg approximately every 24 hours (Bell, 2002), and during this process, there is a continuous and substantial demand for calcium and phosphorus for eggshell calcification and bone remodeling. In recent decades, the number of eggs produced per hen housed has substantially increased. These increases in egg number are largely due to lengthened production cycles that have been achieved through both genetic selection and improved management practices (Bain et al., 2016). As hens age, a disequilibrium often occurs in which calcium and phosphorus uptake and utilization becomes disrupted, leading to a reduction in bone integrity and eggshell quality (Al-Batshan et al., 1994; Alfonso-Carrillo et al., 2021; Benavides-Reyes et al., 2021). However, the physiological pathways that become perturbed are incompletely defined. This makes a deeper understanding of processes regulating calcium and phosphorus homeostasis during the 24-hour oviposition cycle in peak production essential in order to facilitate effective investigation into how they change in older hens.

Regulation of calcium and phosphorus metabolism is influenced by hormonally active 1α,25-dihydroxycholecalciferol [1α,25$(OH)_2D_3$], which undergoes two sequential hydroxylation reactions in the liver and kidney before becoming biologically active (Ponchon et al., 1969a; Fraser et al., 1970). In both mammalian (Cheng et al., 2003) and avian species (Watanabe et al., 2013), hepatic formation of 25-hydroxycholecalciferol [25$(OH)D_3$] is modulated by 25-hydroxylase that is encoded by the gene cytochrome P450 2R1 (*CYP2R1*). In mammals, the second 1α-hydroxylation is catalyzed by cytochrome P450 27 B1 (*CYP27B1*) (Meyer et al., 2020); however, this gene has not been identified in avian species (Sinclair-Black et al., 2023). Alternatively, 25$(OH)D_3$ may undergo renal 24-hydroxylation that is modulated by the gene cytochrome P450

24 A1 (*CYP24A1*), to form inactive 24,25-dihydroxycholecalciferol [24,25$(OH)_2D_3$]. The impact of 1α,25$(OH)_2D_3$ on calcium and phosphorus homeostasis occurs primarily through its genomic actions on vitamin D_3 responsive genes such as calbindin (*CALB1*), an intracellular calcium chaperone (Jande et al., 1981) that facilitates its cytosolic movement following cellular uptake via transporters such as transient receptor potential cation channel subfamily V member 6 (TRPV6), sodium-calcium exchanger 1 (NCX1), and ATPase plasma membrane calcium transporting 1 (PMCA1) (Bar, 2009; Gloux et al., 2019). A study conducted in broilers (Han et al., 2023) suggests that 1α,25$(OH)_2D_3$ may influence expression of *NCX1* and *PMCA1*, while findings in mice also indicate that *TRPV6* may be regulated by 1α,25$(OH)_2D_3$ (Nijenhuis et al., 2003). As such, increases in 1α,25$(OH)_2D_3$ can enhance calcium uptake in the laying hen at tissues such as intestine and kidney and influence ionized calcium (iCa^{2+}) levels.

Circulating iCa^{2+} concentrations are monitored by calcium-sensing receptor (CASR) (Diaz et al., 1997), and high levels lead to production of calcitonin (CALC) from the ultimobranchial glands in chickens (Ziegler et al., 1969). In mammals, the secretion of CALC serves to decrease iCa^{2+} by increasing renal calcium excretion; however, the overall impact of CALC on plasma iCa^{2+} in poultry is negligible (Sommerville et al., 1987), and its influence on avian calcium and phosphorus homeostasis remains unclear. Periods of low iCa^{2+} stimulate parathyroid hormone (PTH) excretion by the parathyroid glands (Singh et al., 1986). Circulating PTH binds parathyroid 1 receptor (PTH1R) in tissues such as the small intestine and kidney to enhance calcium uptake and reabsorption both in chickens (Pinheiro et al., 2012) and mammals (Sato et al., 2017). Further influences of PTH in chickens are elevated bone remodeling through increased osteoclast activity (Taylor et al., 1969; Miller, 1978), increased 1α,25$(OH)_2D_3$ formation, and enhanced renal phosphorus excretion (Sommerville et al., 1987).

Further regulation of renal phosphorus homeostasis is mediated by bone-derived fibroblast growth factor 23 (FGF23) signaling through fibroblast growth factor receptors 1 (FGFR1), 2 (FGFR2), 3 (FGFR3), and 4 (FGFR4) and their co-receptor klotho (KL). It is released in response to elevated circulating phosphorus, and studies in mammals show that FGF23 increases renal phosphorus elimination (Shimada et al., 2004), decreases production of $1\alpha,25(OH)_2D_3$ (Bai et al., 2003), and inhibits PTH secretion (Ben-Dov et al., 2007; Carpenter et al., 2020). In laying hens, hyperphosphatemia elevates expression of *FGF23* mRNA in bone (Hadley et al., 2016; Wang et al., 2018; Ren et al., 2020). A study by Ren et al. (2017) demonstrated that immunoneutralization of FGF23 decreased phosphorus excretion in laying hens, which suggests that FGF23 may play a similar phosphaturic role to that observed in mammals; however, the mechanisms through which FGF23 alters avian phosphorus homeostasis is not fully characterized, and its effects on vitamin D_3 metabolism and PTH production are unclear (Ren et al., 2017; Ren et al., 2020).

Several tissues are involved in regulating calcium and phosphorus homeostasis in laying hens, such as the small intestine, bone, and kidney (Bar, 2009). Hormonal action at bone and small intestine elicits similar changes in circulating calcium and phosphorus levels due to increased or decreased uptake of both minerals simultaneously. In contrast, the kidney is able to independently regulate calcium and phosphorus reabsorption and excretion so that levels in the blood can be differentially regulated. Differential excretion of calcium and phosphorus in the chicken kidney is regulated by the actions of PTH, $1\alpha,25(OH)_2D_3$, and FGF23 (Wideman, 1986; Wang et al., 2018). In this way, the kidney is a key tissue mediating dynamic changes in mineral homeostasis during the oviposition cycle.

An additional tissue that places a high demand upon calcium and phosphorus utilization in laying hens is the shell gland. During the oviposition cycle, this tissue rapidly delivers minerals

and bicarbonate ions into the shell gland lumen for deposition onto the developing eggshell. The eggshell is composed of 96% calcium carbonate (Hincke et al., 2012), and the calcium required for its formation originates from circulation and is transported across shell gland epithelial cells into the lumen (Nys et al., 1999). Circulating calcium is either obtained from medullary bone that serves as a labile calcium source or the diet (Dacke et al., 1993). As the bulk of eggshell calcification takes place during the dark phase (Hertelendy et al., 1960; Nys et al., 2011), bone-derived calcium may contribute up to 40% of that in the eggshell (Comar et al., 1949). The developing eggshell also requires bicarbonate ions, which precipitate with calcium in the shell gland lumen to form the calcium carbonate (Nys et al., 1999). Bicarbonate is formed by the intracellular hydration of carbon dioxide by carbonic anhydrase 2 (CA2) and transported into the shell gland lumen by solute carrier family 26 member 9 (SLC26A9) (Hodges et al., 1967; Nys et al., 2018). Low amounts of phosphorus (0.1 – 0.4%) are incorporated into the eggshell at increasing levels towards the outer layers of the inorganic component and into the cuticle (Cusack et al., 2003) that prevents microbial contamination.

As the length of commercial egg production cycles continues to increase, close attention must be paid to the physiological systems that govern calcium and phosphorus utilization in modern laying hens. However, limited knowledge pertaining to the influence of $1\alpha,25(OH)_2D_3$, CALC, PTH, and FGF23 on local and systemic calcium and phosphorus homeostasis exists in avian species, particularly in relation to calcium and phosphorus transporter expression in shell gland and kidney. Furthermore, physiological changes that occur during the daily oviposition cycle are not well understood. Therefore, the objective of this study was to investigate the dynamic nature of calcium and phosphorus homeostasis during the 24-hour oviposition cycle in laying hens in order to identify systems and transporters that may regulate key processes in calcium and

phosphorus utilization during stages of eggshell calcification, medullary bone repletion, and transition between the two.

Materials and methods

Animals & tissue collection

A total of 80 Hyline W36 hens (32 weeks-of-age) were housed in an environmentally controlled room under a 16H light:8H dark lighting program in individual cages so oviposition time of each hen could be monitored. Hens had free access to water and were fed a commercially available pelleted diet [Country Feeds®, Layer Feed 16%, Nutrena] with the guaranteed analysis listed in Table 4.1. All animal procedures used in this study were approved by The Institutional Animal Care and Use Committee of the University of Georgia.

During the experiment, hens monitored and subsequently selected for sampling were laying at 92.3% (±2.8 % SEM) hen day egg production. Individual oviposition times of each hen were determined for 3 days, and they were allocated into 12 groups that were sampled at the following hours post-oviposition (HPOP): 1, 3, 4, 6, 7, 8, 12, 15, 18, 21, 23, and 24. These time points were selected to investigate in detail the dynamics of calcium and phosphorus utilization related to bone remodeling and eggshell calcification in order to define physiological signatures associated with mineral homeostasis during periods of bone deposition, shell deposition, and transitions between these states (Etches, 1986; Wilson et al., 1990; Sugiyama et al., 1993; Clunies et al., 1995; Kebreab et al., 2009; Rodriguez-Navarro et al., 2015). At the allocated HPOP, 4 mL of blood were collected from the brachial wing vein into a lithium heparinized syringe. Whole blood (100 µL) was immediately analyzed using the iSTAT hand-held blood analyzer with CG8+ cartridges (Zoetis, Parsippany-Troy Hills, NJ), and remaining blood was centrifuged at 1,500 relative centrifugal force at 4 °C for 10 minutes for plasma collection. Plasma was stored at -20 °C until analysis of

circulating vitamin D_3 metabolites, total phosphorus (tP), and PTH was conducted as described below. Following blood collection, hens were euthanized by injection of 1 mL sodium pentobarbital (Euthasol®, Virbac, Westlake, TX) into the alternate brachial wing vein. The following tissues were collected from each hen (approximately 500 mg each): right lobe of the liver, caudal lobe of the right kidney, and central shell gland. Tissues were immediately snap-frozen in liquid nitrogen and stored at -80°C until RNA extraction and reverse transcription reactions were conducted.

The location of the ovum within the reproductive tract and calcification stage of those in the shell gland were recorded following tissue collection (Figure 4.1). Eggshell calcification progress was described as early, mid, or late using the following parameters. Early calcification was described as the presence of a weak, thin eggshell with a rough texture, mid-calcification was delineated by a thick eggshell with a rough texture that crackled when mild pressure was applied by hand, and late eggshell calcification was used to describe a smooth, thick-shelled egg similar to a fully formed egg that cracked only after strong pressure was applied by hand. Hens that had not ovulated or exhibited an ovum that was located at an unexpected location for the time point at which they were sampled were excluded from further analysis. As a result, the number of hens that were utilized for further analysis were as follows (Figure 4.1): n=6 hens at 3, 4, 6, 7, 23, and 24 HPOP; n=5 hens at 8, 12, and 21 HPOP; n=4 hens at 1, 15, and 18 HPOP.

RNA extraction & reverse transcription-quantitative PCR (RT-qPCR)

Total RNA isolation was completed using QIAzol lysis reagent (Qiagen, Germantown, MD) according to the manufacturer's protocol. In brief, 1 mL of QIAzol was added to the sample tubes followed by homogenization using a Mini-Bead Beater (Biospec Products, Bartlesville, OK). Tissues were homogenized over three 45-second bursts and allowed to cool on ice for 1 minute

between bursts. Homogenate was extracted with chloroform, and total RNA was precipitated with isopropanol at 4 °C for 10 minutes. Pellets were washed twice with 70% ethanol, allowed to dry, and reconstituted with 200 µL RNase-free water. Total RNA concentration was quantified using a NanoDrop-1000 spectrophotometer (Thermo Scientific, Waltham, MA). Following quantification, 1 µg total RNA was analyzed on a 1% agarose gel and visualized using a UV imaging system (BioSpectrum, Upland, CA) in conjunction with Visionworks LS software (Wasserburg, Germany) to verify the integrity of the RNA.

One µg of total RNA was reverse transcribed into cDNA in 20 µL reactions. Each reaction contained 4 µL of total RNA (250 ng/µL), 5 µM random hexamers (Invitrogen, Carlsbad, CA), 5 µM anchored-dT primer (Integrated DNA Technologies, Coralville, IA), 0.5 mM dNTPs (Thermo Scientific), 200 U M-MuLV reverse transcriptase (New England Biolabs, Ipswich, MA), 2 µL 10X M-MuLV buffer (New England Biolabs), and 8 U of RNaseOUT (Invitrogen). Initially, total RNA, primers, and dNTPs were combined and incubated at 65 °C for 5 minutes. Following this, samples were placed on ice for at least one minute before the addition of the M-MuLV enzyme, M-MuLV buffer, and RNaseOUT. The samples were then further incubated at 25 °C for 5 minutes, 42 °C for 60 minutes, and finally 65 °C for 20 minutes. A negative no RT reaction to control for genomic DNA contamination was created using an RNA pool from all samples but the reverse transcriptase enzyme was not included. All reactions were diluted 1:10 with nuclease-free water, with the exception of cDNA used for 18s ribosomal RNA (*18s*) amplification, which was diluted 1:500. Primers (Table 2) for measuring levels of each transcript were designed using Primer3 Plus software (Untergasser et al., 2012) to span introns with the following characteristics: amplicon length of 100 to 125 base pairs, primer length between 18 and 30 nucleotides, primer melting temperature between 58 to 60 °C, and GC content between 40 to 60%. Expression of mRNA was

evaluated for the indicated genes using duplicate 10 µL reactions that consisted of 2 µL diluted cDNA, 5 µL PowerUp™ SYBR Green Master Mix (Applied Biosystems, Foster City, CA), and 400 nM of each forward and reverse primer. Thermal cycling was conducted on a StepOnePlus real-time PCR instrument (Applied Biosystems), with cycling conditions as follows: 95 °C for 5 minutes, 40 cycles of 95 °C for 15 seconds, 58 °C for 30 seconds, 72 °C for 30 seconds, and a post-amplification dissociation curve to ensure that a single product was amplified. Levels of target mRNA expression for the kidney were normalized to glyceraldehyde-3-phosphate (*GAPDH*) mRNA, and expression of target genes in the liver and shell gland were normalized to *18s* ribosomal RNA (*18s*). Levels of mRNA were normalized using the following equation: $\Delta CT = CT_{\text{Target gene}} - (CT_{18s} \text{ or } CT_{GAPDH})$ and then transformed as $2^{-\Delta CT}$. To express these data relative to 1 HPOP, each transformed value was divided by the average transformed value at 1 HPOP using the following equation [$(2^{-\Delta CT})$ Sample] / [Average $(2^{-\Delta CT})$ 1 HPOP]. As a result, the value for 1 HPOP is equal 1 in all cases.

Vitamin D_3 metabolites

Plasma was analyzed for $25(OH)D_3$, $1\alpha,25(OH)_2D_3$, and $24,25(OH)_2D_3$ levels. Analysis was completed by liquid chromatography-tandem mass spectrometry (Heartland Assays, Ames, IA) with the following lower limits of detection (LLD) and lower limits of quantification (LLQ): $25(OH)_2D_3$ – 0.5 ng/mL (LLD) and 1.5 ng/mL (LLQ); $24,25(OH)_2D_3$ – 0.1 ng/mL (LLD) and 0.3 ng/mL (LLQ); and $1\alpha,25(OH)_2D_3$ – 5.0 pg/mL (LLD) and 10 pg/mL (LLQ).

Parathyroid hormone

A competitive enzyme-linked immunosorbent assay (ELISA) for chicken PTH (CUSABIO, Wuhan, China) was utilized according to a modified version of the manufacturer's instructions. In brief, plasma samples were added to the ELISA plate in 50 µL duplicates along with PTH standards

(0, 6.25, 12.5, 25, 50, and 100 pg/mL) in 50 µL triplicates. After addition of the samples and standards, biotin-conjugated PTH was added, followed by overnight incubation at 4 °C for 18 hours. After incubation, the plate was rinsed using wash buffer, followed by the addition of horseradish peroxidase-avidin, and a second incubation at 37 °C for 30 minutes was conducted. The plate was washed a final time, followed by the addition of enzyme substrate, and incubated at 37 °C for 15 minutes. Finally, the stop solution was applied, and the optical density of each well was read at a 450 nm wavelength using a Victor Nivo Multimode microplate reader (Perkin Elmer, Waltham, MA). This assay has been previously validated for parallelism and sensitivity using a series of four two-fold dilutions of five independent laying hen plasma samples with starting concentrations of 40 – 60 pg/mL. All samples exhibited parallelism at least through the manufacturer's reported sensitivity of 6.25 pg/mL. Intra- and inter-assay coefficient of variations (CVs) for the ELISA were determined to be 9.9% and 12.4%, respectively, and fall under the manufacturer's value of <15% for each measurement of precision.

Blood Chemistry

Immediately following collection, 100 µL of whole blood was analyzed using an iSTAT hand-held blood analyzer with CG8+ cartridges (Zoetis). Additionally, 100 µL of plasma was analyzed using a VetScan2 equipped with Avian/Reptilian Profile Plus cartridges (Zoetis). Parameters measured by CG8+ cartridges included pH, partial pressure of carbon dioxide (pCO_2), partial pressure of oxygen (pO_2), base excess (BEecf), bicarbonate, total carbon dioxide (TCO_2), oxygen saturation (sO_2), sodium (Na^+), potassium (K^+), iCa^{2+}, glucose (GLU), haematocrit (Hct), and haemoglobin (Hb) (Supplementary Table S1). Parameters measured using the Avian/Reptilian Profile Plus cartridges included aspartate amino transferase (AST), creatinine kinase (CK), uric acid (UA), GLU, tP, total protein (tPr), albumin (ALB), globulin (GLOB), K^+, and Na^+

(Supplementary Table S2). Values for bile acid and total calcium were also measured using VetScan2 device but fell outside the upper detection limit.

Statistical Analysis

Each hen was considered the experimental unit, and the level of replication for each parameter is indicated in the appropriate figure legend. All data were analyzed with JMP Pro 16 software (SAS Institute, Inc, Cary, NC) using a one-way analysis of variance (ANOVA), with HPOP as the model effect. Fishers' test of least significant difference was utilized to separate means. All differences were considered significant at $P \leq 0.05$. Normalized CT values (ΔCT) were analyzed for gene expression data to correct for non-normality of transformed and relative data. Absolute concentration of other parameters followed a normal distribution, and these values were directly analyzed.

Results

Ovum location

Following ovulation, progression of the ovum through the reproductive tract ensures the sequential development of the follicle into a calcified egg over approximately 24-hours. Establishing the times in which the ovum resides at each location within the oviduct and evaluating eggshell calcification state once it reaches the shell gland is crucial for understanding stages of mineral utilization for bone or shell formation during the daily oviposition cycle. As such, prior to analysis, both ovum location and stage of eggshell calcification were recorded for all hens used in further analysis is shown in Figure 4.1. One hour following oviposition, all hens that had ovulated were found to have the ovum present in the magnum. The ovum then transitioned into the isthmus between 3 and 4 HPOP, where the eggshell membrane was added to the follicle. Entry of the developing egg into the shell gland took place between 4 and 6 HPOP, and from this point onwards

calcification on the shell membranes took place. Early calcification of the eggshell occurred between 6 and 12 HPOP, while mid-calcification was observed between 12 and 18 HPOP, and finally, late eggshell calcification took place between 18 to 24 HPOP. Together, this information was used to ensure that ovum location and stage of calcification was as expected for all hens used for physiological analyses.

Vitamin D_3 metabolism and action

Enzymatic conversion. Vitamin D_3 is a crucial regulatory component of calcium and phosphorus homeostasis; however, dietary vitamin D_3 must undergo a series of hydroxylation reactions in the liver and kidney before biologically active $1\alpha,25(OH)_2D_3$ is formed. As such, relative mRNA expression of vitamin D_3 hydroxylase enzymes were measured in the liver and kidney in conjunction with circulating vitamin D_3 metabolites throughout the oviposition cycle. Hepatic expression of the vitamin D_3 25-hydroxylase enzyme *CYP2R1* initially exhibited a decrease between 3 and 6 HPOP before levels were re-established at 7 HPOP. Thereafter, hepatic *CYP2R1* remained relatively stable through 24 HPOP (Figure 4.2A; $P \leq 0.05$) and, overall, it did not exhibit consistent changes throughout the egg-laying cycle. Renal expression of *CYP2R1* was lowest between 1 and 8 HPOP and again at 24 HPOP when compared to expression between 12 and 23 HPOP (Figure 4.2B; $P \leq 0.05$), a period of high calcium demand. Levels of renal *CYP24A1* that catabolizes bioactive metabolites decreased considerably between 1 and 7 HPOP, including a transient reduction that occurred at 3 HPOP. Levels then remained low between 7 and 12 HPOP, followed by heightened expression between 15 to 24 HPOP (Figure 4.2C; $P \leq 0.05$). While differences in renal and hepatic mRNA expression of *CYP2R1* were observed across different HPOP, circulating levels of plasma $25(OH)D_3$ were not influenced by time post-oviposition (Figure 4.2D; $P > 0.05$). However, bioactive $1\alpha,25(OH)_2D_3$ concentrations were elevated between

1 and 6 HPOP, and decreased between 7 and 21 HPOP, except for peaks occurring at 12 and 18 HPOP. Finally, 1α,25$(OH)_2D_3$ increased between 21 and 24 HPOP (Figure 4.2E; P≤0.05). Levels of 24,25$(OH)_2D_3$ in the plasma did not change significantly over time (Figure 4.2F; P>0.05), which was in contrast to observed changes in *CYP24A1* mRNA expression. Given the expression patterns of renal *CYP2R1* and the lack of changes in circulating 25$(OH)_2D_3$, it is possible that kidney could play a role in local production of this metabolite to facilitate renal mineral homeostasis during eggshell calcification

1α,25(OH)$_2$D$_3$ signaling. Hormonally active 1α,25$(OH)_2D_3$ affects calcium and phosphorus metabolism through transcriptional regulation of vitamin D_3-responsive genes in tissues that participate in mineral uptake and utilization. Expression of vitamin D receptor (*VDR*) and its associated heterodimeric partners, retinoid-X-receptors alpha (*RXRA*) and gamma (*RXRG*), were measured in the shell gland and kidney to evaluate 1α,25$(OH)_2D_3$ responsiveness in these tissues. Renal expression of *VDR* exhibited minimal variation across the 24h period, except for a peak that occurred at 1 HPOP (Figure 4.3A; P≤0.05). Levels of renal *RXRA* remained consistent between 1 and 12 HPOP, then declined gradually between 12 and 21 HPOP before increasing again between 21 and 24 HPOP (Figure 4.3B; P≤0.05). Expression of *RXRG* in the kidney was unaltered across time points (Figure 4.3C; P>0.05). Shell gland *VDR* increased between 1 and 12 HPOP before gradually declining again between 15 and 24 HPOP (Figure 4.3D; P≤0.05). Though mRNA expression of *RXRA* in shell gland followed a similar pattern to that of renal *RXRA*, differences were not statistically significant (Figure 4.3E; P>0.05). Lastly, levels of *RXRG* in the shell gland increased 6-fold between 1 and 6 HPOP, and this upregulated expression was maintained through 8 HPOP before substantially declining again at 12 HPOP and remaining low through 24 HPOP (Figure 4.3F; P≤0.05). These results demonstrate the dynamic responsiveness of these tissues,

particularly the shell gland, during the oviposition cycle and indicate that sensitivity of the shell gland to $1\alpha,25(OH)_2D_3$ could increase as the eggshell enters the shell gland.

Circulating factors associated with calcium and phosphorus homeostasis

Measuring fluctuations in circulating calcium, phosphorus, and factors that influence their homeostasis and utilization for eggshell and bone formation is integral for understanding both mineral status and metabolic responses of layers. To evaluate this, circulating levels of iCa^{2+}, bicarbonate, PTH, and tP were measured. Circulating iCa^{2+} was not significantly influenced by HPOP (Figure 4.4A; $P>0.05$); however, a transient reduction was noted at 3 HPOP, as well as a notable decrease that occurred between 8 and 15 HPOP. Circulating bicarbonate levels tended to increase between 3 and 7 HPOP and remained high until 18 HPOP before declining again at 21 HPOP (Figure 4.4B; $P=0.0752$). Plasma PTH concentrations remained relatively stable throughout the oviposition cycle, except for significant decreases between 21 and 23 HPOP, after which levels increased again at 24 HPOP (Figure 4.4C; $P\leq0.05$). Lastly, tP was initially low between 1 and 8 HPOP before increasing significantly at 12 HPOP. It remained elevated through 21 HPOP and then declined at 23 and 24 HPOP to levels similar to those observed between 1 and 8 HPOP (Figure 4D; $P\leq0.05$). This pattern in tP is likely reflective of medullary bone resorption that occurs to provide calcium necessary for rapid eggshell formation between 12 and 18 HPOP. Additional whole blood parameters measured (PH, pCO_2, pO_2, TCO_2, K^+, Glu, Hct, and Hb) did not significantly differ across time points (Supplementary Table S1; $P>0.05$); however, BEecf generally increased between 1 and 12 HPOP before gradually declining at subsequent time points. Levels of sO_2 were stable between 1 and 7 HPOP before gradually declining through 18 HPOP and remained low thereafter (Supplementary Table S1; $P\leq0.05$). Whole blood Na^+ decreased between 6 and 12 HPOP and exhibited a transient increase at 15 HPOP. Thereafter, Na^+

concentrations increased between 18 and 23 HPOP (Supplementary Table S1; P≤0.05). Several plasma parameters exhibited no significant differences across time points such as AST, CK, tPr, ALB, GLOB, K^+, and Na^+ (Supplementary Table S2; P>0.05). Contrastingly, UA and GLU exhibited differences across time points wherein both showed similar reductions in concentration between 8 and 15 HPOP; however, prior to this decrease, GLU significantly increased between 3 and 7 HPOP (Supplementary Table S2; ≤0.05).

Calcium homeostasis

Hormonal signaling. Calcium homeostasis is modulated, in large part, by the hormonal actions of PTH and CALC at tissues that express their receptors in response to CASR. Therefore, expression of *CASR*, *PTH1R*, and *CALCR* were measured in the kidney and shell gland. Though renal expression of *CASR* and *CALCR* were not significantly influenced by time post-oviposition (Figure 4.5A, C; P>0.05), changes in *CALCR* approached significance (P=0.0596). Levels of renal *CALCR* remained stable between 1 and 8 HPOP, increased gradually through 15 HPOP, and then decreased at 18 HPOP and remained low for the remaining time points. Expression of *PTH1R* in the kidney was impacted by time within the oviposition cycle, wherein levels were lowest between 15 and 23 HPOP (Figure 4.5B; P≤0.05). While expression of *CASR* in the shell gland was not significantly altered by time post-oviposition (Figure 4.5D; P>0.05), significant changes in *PTH1R* (Figure 4.5E; P≤0.05) and *CALCR* (Figure 4.5F; P≤0.05) were observed, though differences were more apparent for *PTH1R*. Both genes exhibited similar patterns, wherein their expression decreased from intermediate levels at 1 HPOP to low levels between 3 and 18 (*PTH1R*) or 21 (*CALCR*) HPOP before markedly increasing again through 24 HPOP. These results suggest that both CALC and PTH are important mediators of mineral homeostasis during the oviposition cycle, particularly within the shell gland.

Calcium transport and utilization. In order to determine which transporters are important for mediating calcium movement in the kidney and shell gland throughout the oviposition cycle, expression of *CALB1*, *NCX1*, *PMCA1*, and *TRPV6* were evaluated. Levels of renal *PMCA1* remained consistent between 1 and 8 HPOP, elevated at 12 HPOP, and then gradually declined until 18 HPOP (Figure 4.6C; $P \leq 0.05$). Unlike *PMCA1*, renal *CALB1* (Figure 4.6A; $P > 0.05$), *NCX1* (Figure 4.6B; $P > 0.05$), and *TRPV6* (Figure 4.6D; $P > 0.05$) expression was not significantly influenced by time post-oviposition; however, they all showed similar patterns, with the highest levels around 12 and 15 HPOP during peak eggshell calcification.

Eggshell is primarily composed of calcium carbonate crystals, requiring both calcium and bicarbonate ions for its formation. To investigate changes in the shell gland associated with eggshell calcification, levels of *CALB1*, *NCX1*, *PMCA1*, *CA2*, and *SLC26A9* were evaluated. The calcium chaperone *CALB1* exhibited considerable differences in expression throughout the 24-hour egg formation cycle, wherein low levels between 1 and 6 HPOP were followed by a 14-fold increase between 6 and 15 HPOP and a subsequent steady decline through 24 HPOP (Figure 4.7A; $P \leq 0.05$). Shell gland *NCX1* also showed significant effects of HPOP, with levels rising between 1 to 8 HPOP before gradually declining until 24 HPOP (Figure 4.7B; $P \leq 0.05$). Expression of *PMCA1* was found to be low from 1 to 4 HPOP, after which it steadily increased through 24 HPOP (Figure 7C; $P \leq 0.05$). Expression of another membrane calcium transporter, *TRPV6*, was not detected in this tissue. Levels of *CA2* increased gradually between 1 and 8 HPOP and declined thereafter (Figure 4.7D; $P \leq 0.05$), while the bicarbonate transporter *SLC26A9* exhibited a 10-fold increase in expression between 1 and 12 HPOP before declining between 12 and 24 HPOP (Figure 4.7E; $P \leq 0.05$). Overall, findings from the kidney and shell gland indicate which transporters play

important roles in retaining calcium at the kidney and utilizing it for eggshell formation during times of peak mineralization, as well as define the timing of bicarbonate synthesis and transport.

Phosphorus homeostasis

Hormonal signaling. Phosphorus homeostasis is mediated by the interactions of FGF23 with its receptors; therefore, kidney and shell gland were evaluated as potential targets of FGF23 signaling by measuring mRNA expression of *FGFR1–4* and *KL* throughout the oviposition cycle. Renal expression of *FGFR1* (Figure 4.8A; $P>0.05$) and *KL* (Figure 4.8E; $P>0.05$) were not significantly influenced by time post-oviposition. Contrastingly, other FGFRs did change in the kidney throughout the oviposition cycle. Levels of *FGFR2* exhibited a peak in expression at 12 HPOP (Figure 4.8B; $P\leq0.05$), *FGFR3* declined towards the end of eggshell calcification at 21 and 24 HPOP (Figure 4.8C; $P\leq0.05$), *FGFR4* increased gradually between 6 and 15 HPOP before declining again at subsequent time points (Figure 4.8D; $P\leq0.05$). Changes in expression of *FGFR2* and *FGFR4* suggest these receptors could be important for increasing renal sensitivity to FGF23 during periods of elevated bone breakdown to support rapid eggshell calcification.

Phosphorus within the eggshell is primarily deposited as a hydroxyapatite layer beneath the cuticle and in phosphate-containing organic compounds within the cuticle. As such, temporal regulation of *FGFR1 – 4* and *KL* expression was examined in the shell gland. As seen in the kidney, *FGFR1* expression in the shell gland was not significantly influenced by time post-oviposition (Figure 4.9A; $P>0.05$), though mRNA for other FGF23 receptors did vary in this tissue. Levels of shell gland *FGFR2* (Figure 4.9B; $P\leq0.05$) and *FGFR3* (Figure 4.9C; $P\leq0.05$) exhibited similar patterns, where expression remained low until 18 HPOP and then increased sharply between 18 and 24 HPOP, as eggshell calcification was concluding. Additionally, *FGFR2* exhibited a gradual decline between 8 and 15 HPOP, when the eggshell begins rapidly calcifying. Expression of

FGFR4 in the shell gland gradually declined between 7 and 18 HPOP before re-establishing expression levels between 21 and 24 HPOP (Figure 4.9D; P≤0.05). Unlike renal expression of *KL*, shell gland *KL* showed significant changes in expression across time points. Levels were highest between 1 and 3 HPOP, then reduced through 15 HPOP and increased again between 18 and 24 HPOP (Figure 4.9E; P≤0.05). Dynamic changes observed in the expression of FGF23 receptors in the shell gland indicate that this tissue could be a novel target for FGF23 signaling, which likely increases in sensitivity towards the end of eggshell calcification.

Phosphorus transport and utilization. Phosphorus transporters are crucial for modulating renal uptake and excretion of this mineral during the oviposition cycle. Renal expression of inorganic phosphorus transporter 1 (*P_iT-1*) remained very low from 1 to 8 HPOP, and this was followed by a stark almost 30-fold increase between 8 and 15 HPOP before levels reduced to intermediate values thereafter (Figure 4.10A; P≤0.05). Renal inorganic phosphorus transporter 2 (*P_iT-2*) also remained relatively low between 1 and 8 HPOP, increased at 12 and 15 HPOP, and then declined to intermediate levels between 18 and 24 HPOP (Figure 4.10B; P≤0.05), though the fold changes were not as large. Renal sodium-dependent phosphate transporter IIa (*NaP_iIIa*) expression was not affected by time post-oviposition (Figure 4.10C; P>0.05), and kidney expression of sodium-dependent phosphate transporter IIb (*NaP_iIIb*) was not detected. These results highlight the need for renal excretion of excess phosphorus resulting from medullary bone break down necessary to support eggshell calcification and identify *P_iT-1*, and to a lesser extent *P_iT-2*, as key transporters involved in this process.

Expression patterns of the phosphorus transporters *PiT-1*, *PiT-2*, and *NaP_iIIa* were examined in the shell gland to evaluate if they changed throughout the daily oviposition cycle Expression of *P_iT-1* remained low from 1 to 8 HPOP, and then it steadily increased over 10-fold

by 21 HPOP before declining at 23 and 24 HPOP (Figure 4.10D; P≤0.05). In contrast, expression of *P_iT-2* in the shell gland was not significantly impacted by time post-oviposition (Figure 4.10E; P>0.05). As in kidney, expression of *NaP_iIIb* was not detected in the shell gland, nor was *NaP_iIIa*. As in the kidney, *P_iT-1* likely plays a major role in transporting phosphorus within the shell gland during late eggshell calcification and cuticle formation.

Discussion

Modern laying hens develop an egg approximately every 24 hours (Nys et al., 2011), during which calcium and phosphorus homeostasis is influenced by bone remodeling and eggshell calcification. This study set out to identify circadian fluctuations in pathways that mediate regulation of calcium and phosphorus utilization during the 24-hour oviposition cycle. Findings suggest a possible role of the kidney in 25-hydroxylation of vitamin D_3 and highlighted key transporters involved in mineral utilization during egg formation in both shell gland and kidney. Additionally, the shell gland was identified as a novel target for FGF23 signaling, and expression patterns suggest that the shell gland may be responsive to other hormonal regulators of calcium and phosphorus homeostasis such as $1\alpha,25(OH)_2D_3$, PTH, and CALC.

Canonically, vitamin D_3 undergoes two independent hydroxylation reactions in the liver and kidney, respectively, before it can be transformed into biologically active $1\alpha,25(OH)_2D_3$ (Bikle, 2018). In mammalian (Ponchon et al., 1969a; Ponchon et al., 1969b) and avian species (Watanabe et al., 2013), the first reaction occurs in the liver wherein 25-hydroxylase, encoded by the *CYP2R1* gene, converts vitamin D_3 into $25(OH)D_3$. Under physiological conditions, this process occurs in an unregulated and constitutive fashion (Tucker et al., 1972b; Heaney et al., 2008). Interestingly, findings by Tucker et al. (1972b) identified 25-hydroxylase in the kidney of white leghorn chicks that was capable of forming $25(OH)D_3$ when vitamin D_3 was added *in vitro*.

Results from our study showed that hepatic expression of *CYP2R1* exhibited minor changes during the oviposition cycle; however, renal mRNA expression of *CYP2R1* was generally upregulated between 12 and 23 HPOP, which coincides with observed stages of mid and late eggshell calcification. In contrast, circulating levels of $1\alpha,25(OH)_2D_3$ were generally lower during these time points, suggesting its rapid utilization by the kidney, shell gland, and small intestine to facilitate eggshell calcification. Together, these results suggest that the kidney may play a supporting role in the 25-hydroxylation of vitamin D_3, particularly during periods of high calcium demand when the eggshell is most rapidly calcifying. This $25(OH)D_3$ may be utilized locally to enhance the efficacy of conversion of dietary vitamin D_3 into $1\alpha,25(OH)_2D_3$ and may not contribute to circulating levels of $25(OH)D_3$. Since $1\alpha,25(OH)_2D_3$ is involved in regulating calcium and phosphorus uptake and excretion in the kidney of chickens (Taylor et al., 1972), the presence of both 25-hydroxylase and 1α-hydroxylase enzymes in the kidney would likely improve efficiency of renal calcium and phosphorus handling.

When $1\alpha,25(OH)_2D_3$ binds VDR, it functions as a ligand-activated transcription factor that binds with its heterodimeric partners RXRA and RXRG (Kliewer et al., 1992). Together, this complex binds vitamin D_3 response elements (VDRE) in the promotor regions of vitamin D_3 responsive genes to regulate their transcription. Studies conducted in chickens show that *CALB1* is transcriptionally upregulated by VDR/RXR complexes in both kidney and small intestine (Bar et al., 1990a; Norman, 1990; Nys et al., 1992a). However, evidence that *CALB1* is similarly responsive in the shell gland is limited (Bar et al., 1977; Bar et al., 1984). Despite this, Yoshimura et al. (1997) showed strong immunohistochemical staining of VDR in the shell gland of egg-producing hens, and RT-qPCR results from this study confirm the presence of *VDR* mRNA in this tissue. In the current study, expression of shell gland *VDR* gradually increased from the time of

oviposition through 12 HPOP, when peak eggshell calcification begins, before gradually declining through 24 HPOP as calcification slowed. Additionally, *RXRG* levels increased 6-fold from 6 to 8 HPOP and rapidly decreased thereafter, which coincided with observed early stages of eggshell calcification. Contrastingly, *RXRA* exhibited minimal variation across time points. Together, these results suggest that the shell gland is a likely target tissue for $1\alpha,25(OH)_2D_3$ and that RXRG may be of greater importance in eliciting dynamic genomic responses to this hormone than RXRA during the oviposition cycle. Furthermore, differences in the availability of RXRG may alter the hormonal responsiveness of the shell gland. These temporal changes in the transcriptional machinery during eggshell calcification indicate that $1\alpha,25(OH)_2D_3$ plays a role in facilitating eggshell development.

In addition to potentially mediating uptake and utilization of calcium by the shell gland, $1\alpha,25(OH)_2D_3$ may also regulate bicarbonate production in shell gland epithelial cells. Bicarbonate formation by CA2 is crucial for precipitation of calcium carbonate crystals that form the bulk of the eggshell (Gutowska et al., 1945; Robinson et al., 1963), and a functional VDRE has been identified in the promotor region of chicken CA2 (Quelo et al., 1994; Quelo et al., 1998). Additionally, studies conducted by Narbaitz et al. (1981) and Grunder et al. (1990) demonstrated that differences in $1\alpha,25(OH)_2D_3$ supply influence CA2 activity in chickens. In the current study, expression of *CA2* mRNA in shell gland tissue increased four-fold from oviposition through early eggshell calcification and remained elevated until 8 HPOP. This closely mirrors expression of *RXRG*, suggesting that differences in *CA2* expression may be modulated by RXRG availability to dimerize with existing VDR in the shell gland. Bicarbonate ions are transferred into the shell gland lumen by the SLC26A9 transporter (Nys et al., 2018). Our findings demonstrated a considerable 10-fold increase in expression of this transporter between 1 and 12 HPOP before levels declined

from 15 to 21 HPOP, as eggshell calcification slowed. Interestingly, the expression profile of *SLC26A9* also closely resembled that of *VDR*, thereby illustrating a further mechanism by which $1\alpha,25(OH)_2D_3$ genomic actions may regulate bicarbonate production and transport in the shell gland. Additional bicarbonate for eggshell calcification is also supplied from circulation (Nys et al., 2018) and results from this study show that circulating bicarbonate levels were generally higher during the periods of eggshell calcification, between 7 and 18 HPOP. In this way, both local and systemic bicarbonate formation is increased to support eggshell calcification.

Calcium levels in both circulation and tissues are closely monitored by CASR, which can influence the expression of calcium and phosphorus transporters, either directly (Kantham et al., 2009; Loupy et al., 2012) or indirectly through its stimulatory influence on PTH secretion (Ba et al., 2003). Circulating PTH binds PTH1R located in the plasma membrane of target tissues, invoking hormonal signaling that facilitates increases in circulating iCa^{2+} levels. In contrast, binding of CALC to its receptor, CALCR, generally serves to decrease blood iCa^{2+} levels. Together, these hormonal signaling pathways act upon tissues such as the kidney to facilitate changes in calcium and phosphorus transporter expression and mediate uptake or excretion of these minerals. Findings from our study showed that renal *CASR* expression increased numerically between 8 to 15 HPOP, which was inversely related to circulating iCa^{2+} during this time. The period of increased renal *CASR* also coincided with upregulated expression of the calcium transporters *NCX1*, *PMCA1*, *TRPV6*, as well as the chaperone protein *CALB1*. Upregulation of these renal calcium transporters likely served to increase calcium reabsorption necessary for eggshell calcification.

Renal *CALCR* expression was also increased from 8 to 15 HPOP, though the change only approached statistical significance. While this increase seems counterintuitive to calcium

reabsorption in the kidney, it is possible that CALC signaling is also involved in mediating the renal phosphaturic response, as levels of *P_iT-1*, *P_iT-2*, *FGFR2*, and *FGFR4* show similar increases. However, it should be noted the role of CALC signaling in avian renal function is incompletely understood. In chickens, CALC does not appear to stimulate the production of the intracellular second messenger, cyclic AMP, which is in contrast to the response noted in rats (Dousa, 1974). Additionally, administration of exogenous CALC to hens was shown to only alter renal function in the absence of PTH (Sommerville et al., 1987). Lastly, there is conflicting evidence as to whether CALC influences renal production of $1\alpha,25(OH)_2D_3$. *In vitro* findings by Rasmussen et al. (1972) suggest that CALC may inhibit $1\alpha,25(OH)_2D_3$ production in cultured chick renal cells, while a similar study conducted by Larkins et al. (1973) showed opposing results. Findings from the aforementioned studies suggest that avian CALC may utilize alternative cellular signaling pathways or function secondarily to PTH to alter renal vitamin D_3 metabolism. Since the role of CALC in avian species is not well defined, understanding how it mediates calcium and phosphorus homeostasis in the kidney and other organs is important to gain a holistic view of these physiological systems.

Results from the shell gland showed substantial increases in both *PTH1R* and *CALCR* as eggshell calcification slows and shortly after ovulation, thereby suggesting that the shell gland has increased hormonal sensitivity to PTH and CALC during these times. Interestingly, previous studies have also found an increased binding affinity of CALC to the plasma membrane fraction of shell gland mucosal tissue in chickens (Ieda et al., 2001) and guineafowl (Ogawa et al., 2003) during late shell calcification. The observed differences in binding affinity in these studies are likely a result of an increased number of receptors in the shell gland, which is supported by the RT-qPCR expression data from the present study. Furthermore, large differences in expression of

CALCR and *PTH1R* between stages of the oviposition cycle indicate that CALC and PTH may elicit greater dynamic effects in the shell gland than in other tissues examined. Upregulation of these receptors in the shell gland late in the oviposition cycle suggests that PTH and CALC hormonal signaling may contribute to processes involved in cessation of eggshell calcification.

Outside of periods when eggshell calcification is occurring, phosphorus in the blood is used to replenish hydroxyapatite crystals in medullary bone (Dacke et al., 2015). However, once eggshell calcification is initiated, calcium demands increase and medullary bone is resorbed to support eggshell calcification (Van de Velde et al., 1984b). As a result, phosphorus originating from this hydroxyapatite is released into the blood (Nys et al., 1986). Since elevated phosphorus levels in the blood can be toxic, it must be either eliminated at the kidney or utilized for physiological processes. One of the key hormones regulating phosphorus homeostasis is FGF23. It is released from bone in response to elevated circulating phosphorus and signals through one of four receptors in combination with their co-receptor, KL, to decrease circulating phosphorus. In mammals, it does so by inhibiting renal phosphorus absorption and decreasing 1α-hydroxylation of vitamin D_3 and PTH production (Razzaque, 2009; Donate-Correa et al., 2012); however, the extent of FGF23's effects in chickens has not been fully elucidated. In chickens, *FGF23* is expressed in both structural (Hadley et al., 2016; Lyu et al., 2023) and medullary (Hadley et al., 2016) bone, its expression in medullary bone increases with age (Gloux et al., 2020b), and its receptors have been identified in kidney, small intestine, and bone (Ren et al., 2020). Hyperphosphatemia has been shown to increase bone-derived *FGF23* expression (Wang et al., 2018), and immunoneutralization of FGF23 in chickens reduced phosphorus excretion (Bobeck et al., 2012; Ren et al., 2017). Functionally, it appears that avian FGF23 responds to high phosphorus levels and increases its excretion; however, effects on 1α-hydroxylation of vitamin D_3 and its influence on PTH activity

are unclear. It has been shown to either have no effect on levels of $1\alpha,25(OH)_2D_3$ and PTH (Ren et al., 2020) or increase PTH while reducing $1\alpha,25(OH)_2D_3$ (Ren et al., 2017).

Findings herein showed that circulating tP was highest from 12 to 21 HPOP, which corresponded with mid and late eggshell calcification stages in this study. As such, increases in blood phosphorus were likely due to medullary bone breakdown to support eggshell calcification. In a possible response to these elevated phosphorus levels, expression of renal *FGFR2* and *FGFR4* were upregulated at 12 and 15 HPOP, respectively, and they could be at least partially responsible for the considerable 20-to 30-fold increase in *P_iT-1* levels and 3-fold increase in *P_iT-2* at these same time points. Furthermore, while Ren et al. (2020) noted differences in renal expression of *NaP_iIIa* during phosphorus restriction, no notable differences were observed in the current study. Taken together, it appears that FGF23 signaling may influence renal phosphorus excretion by acting through select FGF23 receptors to modulate expression of phosphorus transporters during the oviposition cycle. Based on the fold-changes observed, *P_iT-1* appears to have the greatest influence on phosphorus dynamics in the kidney during egg formation.

Evidence from this study also revealed a potentially novel role for FGF23 in regulating phosphorus dynamics in the shell gland. Phosphorus concentrations increase in the outer quarter of the eggshell and the cuticle (Cusack et al., 2003), and it is thought that this may be involved in the cessation of eggshell calcification due to its inhibition of calcite formation (Bachra et al., 1963; Simkiss, 1964) or as a result of an increase in phosphate-containing organic components in the cuticle layers (Nys et al., 1991). Since FGF23 appears to alter phosphorus transporter expression in the kidney (Ren et al., 2020), it is possible that similar effects may occur in the shell gland. Findings from this study showed notable decreases in expression of shell gland *FGF2*, *FGF3*, *FGF4*, and *KL* between 8 and 15 HPOP, a period of rapid eggshell calcification, followed by

increases in expression of shell gland *FGFR2, FGFR3,* and *KL* between 18 and 24 HPOP, as eggshell calcification slows. Furthermore, levels of *PiT-1* increased approximately 10-fold between 8 and 21 HPOP. Together, it appears that sensitivity to FGF23 and levels of *P_iT-1* transporters remain low during active eggshell calcification, likely to prevent the premature termination of eggshell calcification. Following this, levels of both FGF23 receptors and P_it-1 rise, which may facilitate cessation of the eggshell mineralization process.

Together, it was shown that several genes exhibited dynamic changes in expression during the daily oviposition cycle in both the kidney (Figure 4.11 A) and shell gland (Figure 4.11B). Select renal plasma membrane calcium transporters and the intracellular calcium chaperone *CALB1* maintained intermediate levels prior to ovum entry into the shell gland and during early eggshell calcification stages; however, during rapid eggshell calcification, expression of these transporters in the kidney peaked. This peak in expression likely resulted in enhanced renal calcium reabsorption to supply the developing eggshell. Renal phosphorus transporters followed a similar pattern to that of calcium transporters; however, initial expression from 1 to 8 HPOP was substantially lower. Unlike elevated calcium transporters, which serve to retain calcium for eggshell formation, increased phosphorus transporter expression during mid eggshell calcification was likely a result of the need to excrete excess circulating phosphorus originating from medullary bone breakdown during this period. Shell gland plasma membrane calcium transporters were either increasingly upregulated for the duration that the eggshell was present in the shell gland (*PMCA1*) or peaked during early eggshell calcification (*NCX1*), while *CALB1* levels increased through mid calcification before rapidly declining. These results demonstrate how differences in expression of calcium transporters and *CALB1* may regulate the rate of calcium transfer to the developing eggshell. Bicarbonate formation in the shell gland epithelial cells appears to peak prior to its

transfer into the shell gland lumen during mid calcification, based on the expression patterns of *CA2* and *SLC26A9*. Lastly, as calcification of the eggshell slows, phosphorus transporter expression increases and likely influences the termination of eggshell calcification and facilitates cuticle formation.

In this study, hens were fed *ad libitum* and sampled during both the light (1, 3, 4, 6, 7, 8, 21, 23, and 24 HPOP) and dark (12, 15, and 18 HPOP) periods. Since there was not a period of feed withdrawal prior to euthanasia, timing of sample collection relative to the last meal and level of digesta within the intestinal tract could have influenced our findings. This effect would likely be greatest during the light period, as hen-to-hen variations in feeding patterns could affect the amount of dietary calcium and phosphorus that would be available for bone remodeling and eggshell calcification at the time of sampling. In contrast, there is a nocturnal fast during the dark period (Scanes et al., 1987), and hens sampled during this time should have a more consistent, albeit lower, level of feed within the intestinal tract that would reduce variability during the 12 – 18 HPOP timepoints. However, during these times the egg had entered the shell gland and was at varying levels of mineralization. As the gross level of eggshell calcification was determined by hand, more subtle differences in calcification state could not be determined and could have been an additional source of variation during these times.

In conclusion, this study investigated physiological processes regulating calcium and phosphorus homeostasis that occur during the daily oviposition cycle in commercial laying hens. In doing so, key genes that exhibited dynamic changes during the oviposition cycle were identified, and these likely play a key role in mediating mineral homeostasis by driving uptake or excretion in the kidney and utilization by the shell gland. In addition, a possible role for the kidney in local 25-hydroxylation of vitamin D_3 was uncovered. It was also shown that $1\alpha,25(OH)_2D_3$ could

facilitate the shell gland's ability to utilize calcium for eggshell formation through VDR/RXRG transcriptional regulation of select transport proteins. Furthermore, the shell gland appears to be a novel target for FGF23 signaling, and this hormone could regulate its ability to incorporate phosphorus into outer layers of the shell. Together, this new fundamental information can be used both to develop additional studies aimed at understanding dynamics of calcium and phosphorus homeostasis in layers and to identify disturbances in these processes that occur as hens age. This knowledge is crucial in the development of effective strategies aimed at improving the calcium and phosphorus balance in laying hens, which would ultimately improve egg quality and skeletal health.

Table 4.1. Guaranteed analysis for Country Feeds®, Layer Feed 16% Pellet, Nutrena.

Nutrient	Min %	Max %
Crude protein	16	
Crude fat	2.5	
Crude fiber		8
Calcium	3.4	3.9
Available phosphorus	0.45	
Sodium	0.15	0.23
Lysine	0.7	
Methionine	0.3	

Table 4.2. Primers used for reverse transcription-quantitative PCR.

Target	Forward Primer (5'-3')	Reverse Primer (5'-3')	Transcript ID[1]
Vitamin D_3 metabolism and action			
CYP2R1	GGACAGCAATGGACAGTTTG	AGGAAAACGCAGGTGAAATC	09745
CYP24A1	TGGTGACACCTGTGGAACTT	CTCCTGAGGGTTTGCAGAGT	59161
VDR	CTGCAAAATCACCAAGGACA	CATCTCACGCTTCCTCTGC	96121
RXRA	ACTGCCGCTACCAGAAGTGT	GACTCCACCTCGTTCTCGTT	59924
RXRG	GAAGCCTACACGAAGCAGAA	CCGATCAGCTTGAAGAAGAA	49224
Calcium homeostasis and eggshell calcification			
CASR	CTGCTTCGAGTGTGTGGACT	GATGCAGGATGTGTGGTTCT	55986
PTH1R	CCAAGCTACGGGAAACAAAT	ATGGCATAGCCATGAAAACA	08796
CALCR	GCAGTTGCAAGAGCCAAATA	AGCTTTGTCACCAACACTCG	15478
CALB1	AAGCAGATTGAAGACTCAAAGC	CTGGCCAGTTCAGTAAGCTC	74265
NCX1	TCACTGCAGTCGTGTTTGTG	AAGAAAACGTTCACGGCATT	13920
PMCA1	TTAATGCCCGGAAAATTCAC	TCCACCAAACTGCACGATAA	80355
TRPV6	TATGCTGGAACGAAAACTGC	TTGTGCTTGTTGGGATCAAT	23779
CA2	CCTGACTACTCCACCACTGC	TCTCAGCACTGAAGCAAAGG	52439
SLC26A9	TCCACGATGCTGTTTTGTTT	GAGCTGCTTTCATCCACAGA	01070
Phosphorus homeostasis			
FGFR1	GACAGACTTCAACAGCCAGC	CCAACATCACACCCGAGTTC	66938
FGFR2	CAGGGGTCTCGGAATATGAA	GCTTCAGCCATCACCACTT	38732
FGFR3	GGAGTACTTGGCGTCACAGA	TCTAGCAAGGCCAAAATCAG	01712
FGFR4	CTTGCCCGTCAAGTGGAT	TGAAGATCTCCCACATCAGAA	28231
KL	CCAAGAGAGATGATGCCAAA	CATCCAGAAGGGACCAGACT	15785[2]
P_it-1	TATCCTCCTCATTTCGGCGG	CTCTTCTCCATCAGCGGACT	94781
P_it-2	CCATCCCCGTGTACCTTATG	AGACATGGCCATCACTCCTC	51992
NaP_iIIa	ATCGGCTTGGGGGTGATC	GAGGGCGATCTGGAAGGAG	58978
Housekeeping Genes			
GAPDH	AGCCATTCCTCCACCTTTGAT	AGTCCACAACACGGTTGCTGTAT	23323
18s[3]	AGCCTGCGGCTTAATTTGAC	CAACTAAGAACGGCCATGCA	

[1]Transcript identification from Ensembl chicken genome assembly (GRCg6a; (http://www.ensembl.org/Gallus_gallus/Info/Index) preceded by ENSGALT000000
[2]Transcript identification from Ensembl chicken genome assembly (GRCg7b; (http://www.ensembl.org/Gallus_gallus/Info/Index) preceded by ENSGALT000100
[3]Sequence for 18S rRNA is not on the assembled chicken genome, and primers were designed based on the sequence in GenBank (accession numbers AF173612).

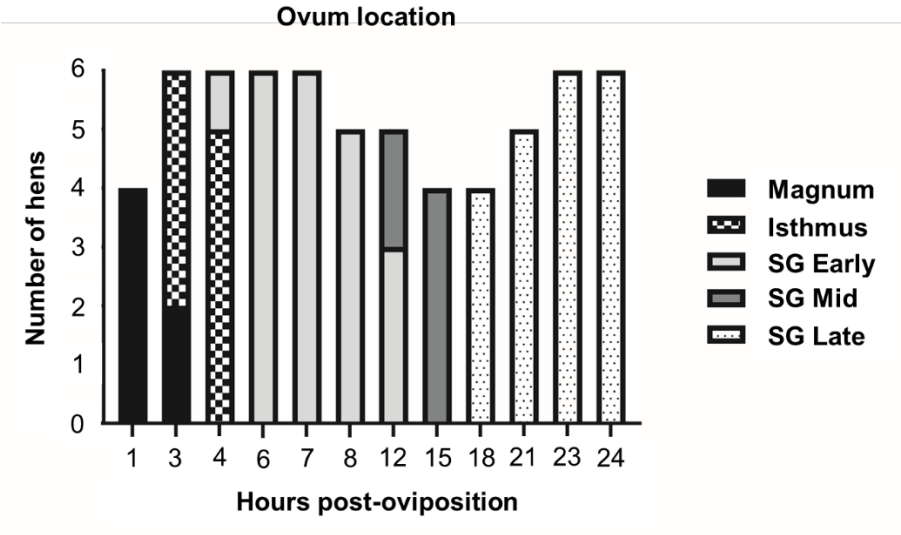

Figure 4.1. Ovum position and eggshell calcification stage across the 24-h oviposition cycle. Ovum location within the oviduct and state of eggshell calcification when the ovum was in the shell gland (SG) are shown for hens used at indicated hours post-oviposition.

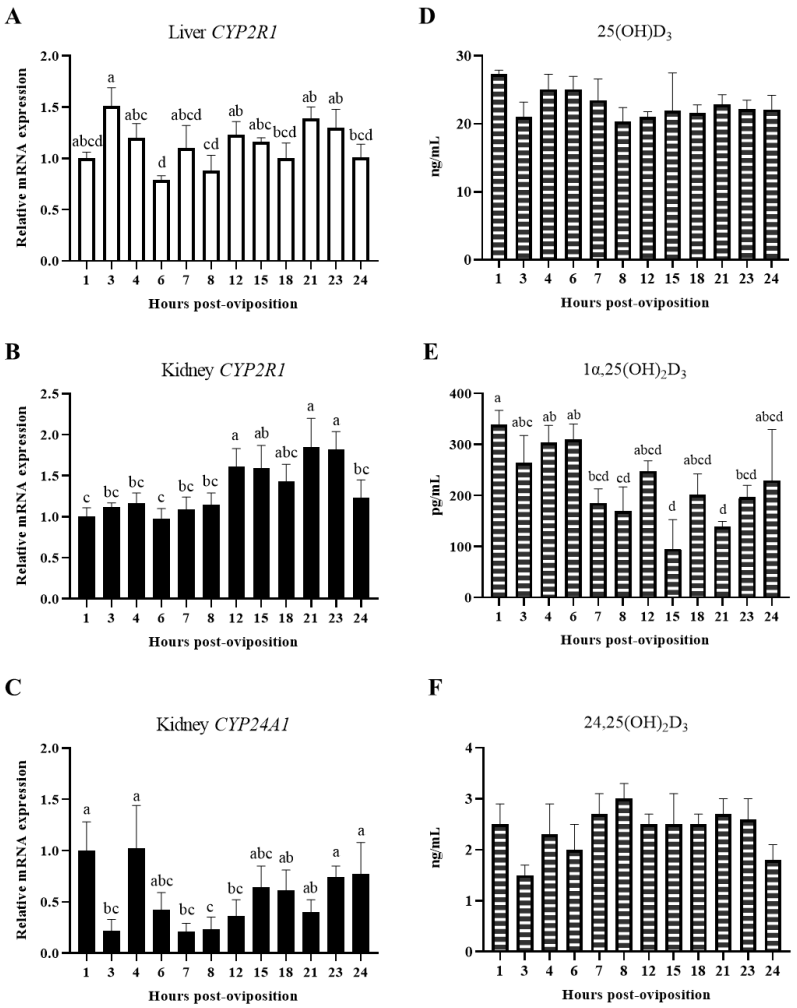

Figure 4.2. Expression of genes for enzymes that metabolize vitamin D_3 and levels of circulating vitamin D_3 metabolites.

Relative levels of mRNA were measured at indicated hours post-oviposition (HPOP) for (A) liver *CYP2R1*, (B) renal *CYP2R1*, and (C) renal *CYP24A1*. Expression of target genes was determined by RT-qPCR and normalized to *GAPDH* mRNA for kidney and liver. All values (mean+SEM; n=6 hens at 3, 4, 6, 7, 23, and 24 HPOP; n=5 hens at 8, 12, and 21 HPOP; n=4 hens at 1, 15, and 18 HPOP) are expressed relative to 1 HPOP (equivalent to 1). Circulating levels of (D) 25(OH) D_3, (E) 1α,25$(OH)_2D_3$, and (F) 24,25$(OH)_2D_3$ were analyzed by liquid chromatography-tandem mass spectrometry (mean+SEM; n=6 hens at 23 HPOP; n=5 hens at 3, 7, 8, 21, and 24 HPOP; n=4 hens at 4, 6, 12, and 18 HPOP; n=3 hens at 1 HPOP; n=2 hens at 15 HPOP). Differences in available plasma volumes resulted in fewer hens analyzed at some time points. Data were analyzed by one-way ANOVA followed by Fisher's test of least significant difference when ANOVA indicated significance, and bars not sharing a common letter differ significantly ($P \leq 0.05$). Expression of *CYP27B1* was not measured, as the gene has not been identified in chickens.

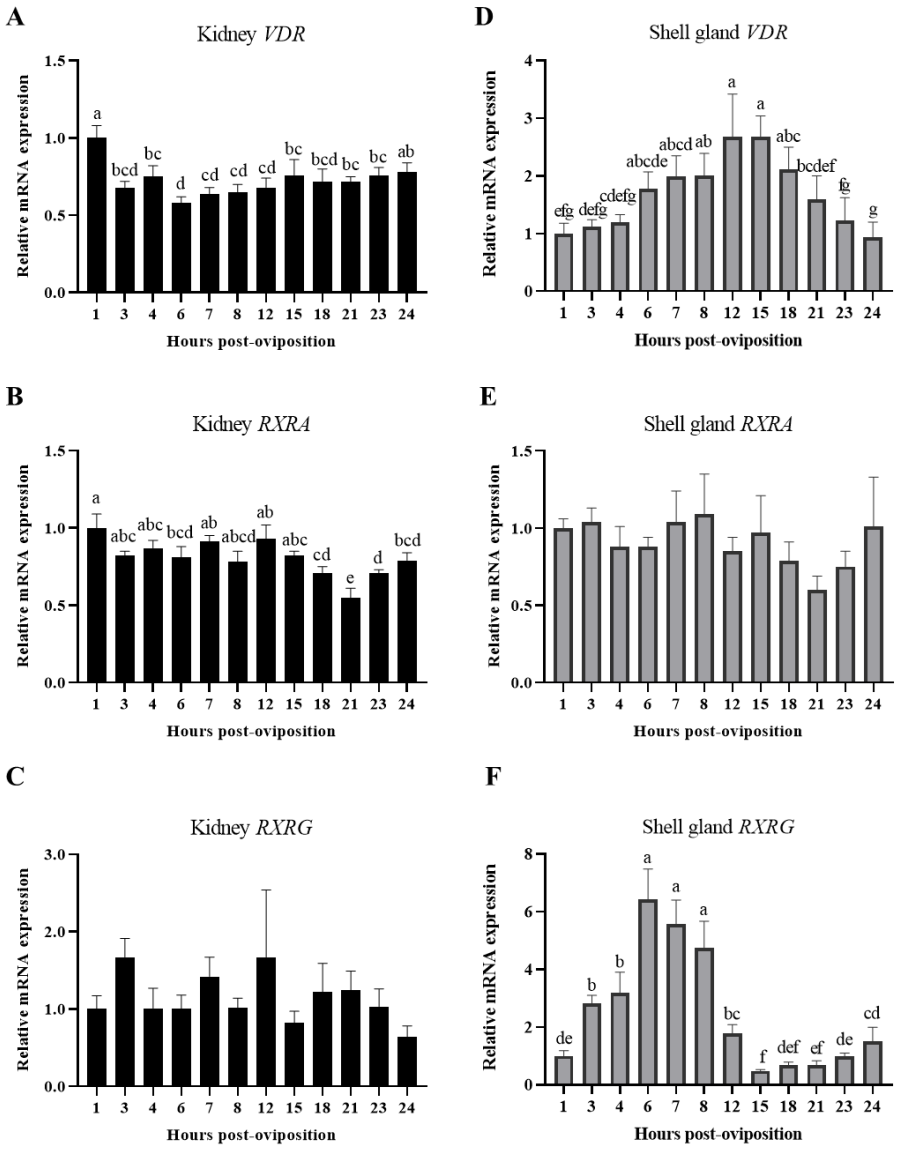

Figure 4.3. Expression of genes for vitamin D_3 receptor and its heterodimeric partners in kidney and shell gland.

Relative levels of mRNA were measured at indicated hours post-oviposition (HPOP) for renal (A) *VDR*, (B) *RXRA*, (C) *RXRG*, and shell gland (D) *VDR*, (E) *RXRA*, (F) *RXRG*. Expression of target genes was determined by RT-qPCR and normalized to *GAPDH* mRNA for the kidney and *18s* rRNA for shell gland. All values (mean+SEM; n=6 hens at 3, 4, 6, 7, 23, and 24 HPOP; n=5 hens at 8, 12, and 21 HPOP; n=4 hens at 1, 15, and 18 HPOP) are expressed relative to 1 HPOP (equivalent to 1). Data were analyzed by one-way ANOVA followed by Fisher's test of least significant difference when ANOVA indicated significance, and bars not sharing a common letter differ significantly ($P \leq 0.05$).

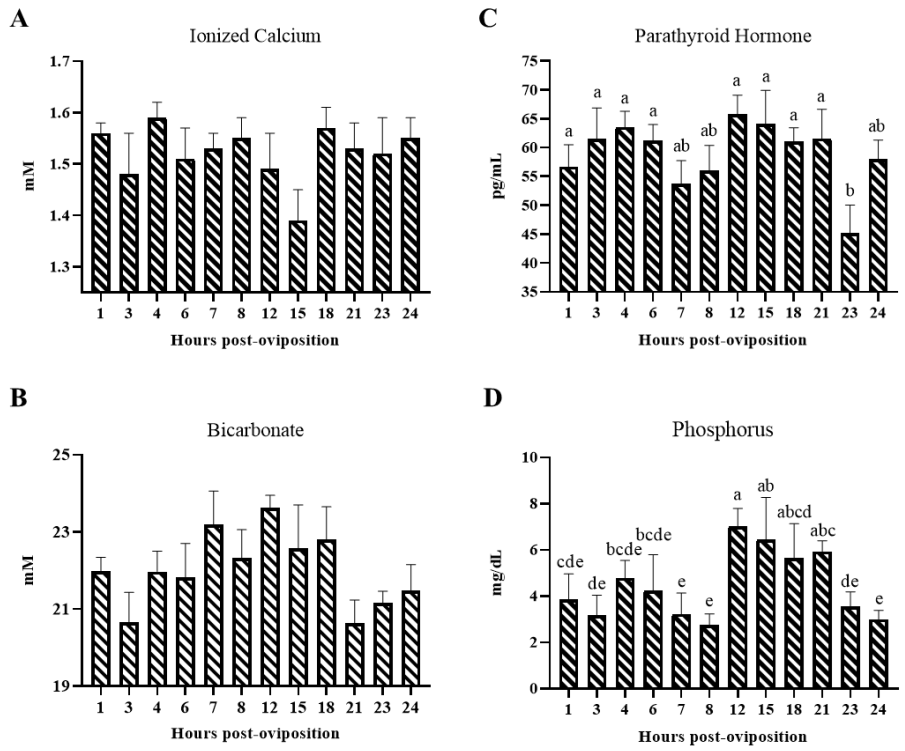

Figure 4.4. Circulating factors associated with mineral homeostasis.
Circulating (A) ionized calcium and (B) bicarbonate were measured using CG8+ cartridges and an iSTAT hand-held blood analyzer at indicated hours post-oviposition (HPOP) (mean+SEM; n=6 hens at 3, 4, 6, 7, 23, and 24 HPOP; n=5 hens at 8, 12, and 21 HPOP; n=4 hens at 1, 15, and 18 HPOP). (C) Plasma parathyroid hormone was measured using an ELISA (mean+SEM; n=6 hens at 3, 4, 6, and 23 HPOP; n=5 hens at 7, 8, 12, 21, and 24 HPOP; n=4 hens at 1, 15, and 18 HPOP). (D) Plasma phosphorus was measured using Avian/Reptile Profile Plus cartridges and a VetScan2 (mean+SEM; n=6 hens at 7, 23, and 24 HPOP; n=5 hens at 12 HPOP; n=4 hens at 1, 4, 8, 15, and 21 HPOP; n=3 hens at 3,6, and 18 HPOP). Differences in available plasma volumes resulted in fewer hens analyzed at some time points. Data were analyzed by one-way ANOVA followed by Fisher's test of least significant difference when ANOVA indicated significance, and bars not sharing a common letter differ significantly ($P \leq 0.05$).

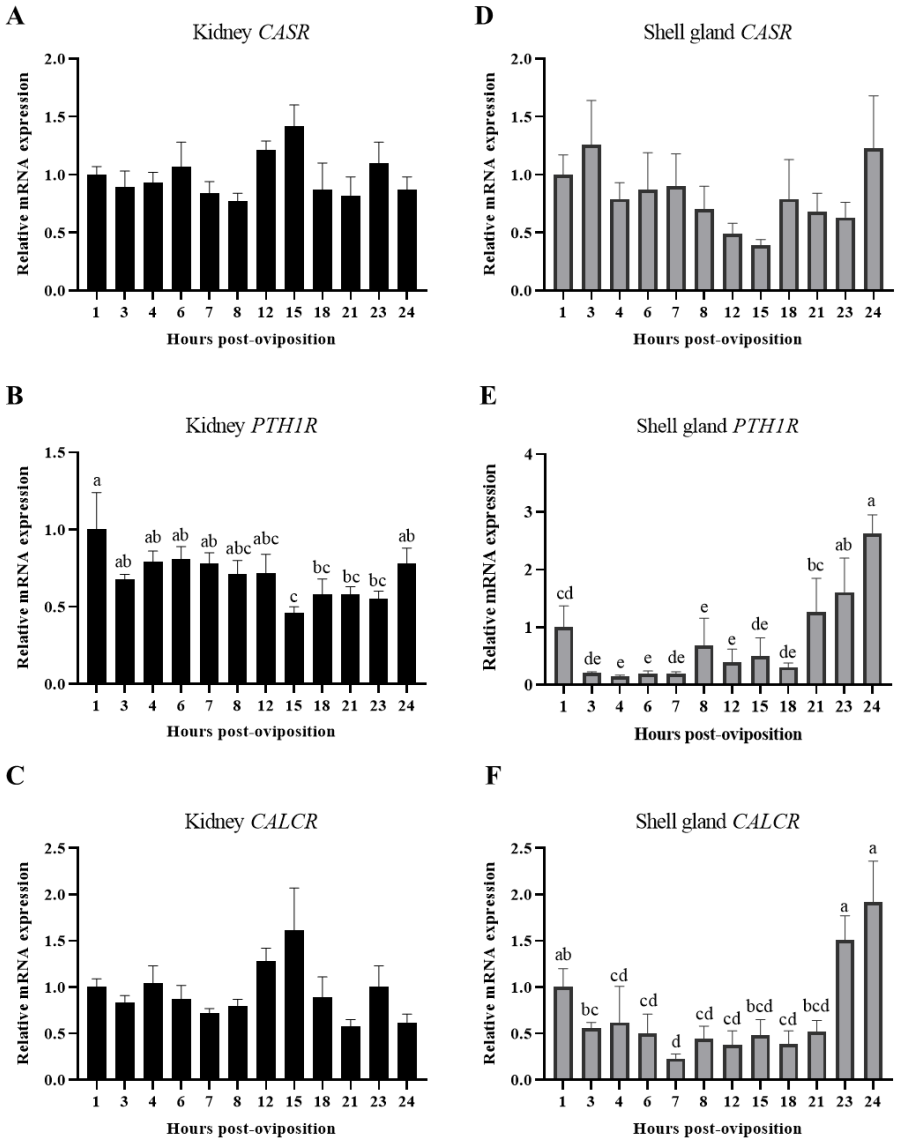

Figure 4.5. Expression of hormonal mediators of calcium homeostasis in kidney and shell gland.

Relative levels of mRNA were measured at indicated hours post-oviposition (HPOP) for kidney (A) *CASR*, (B) *PTH1R*, (C) *CALCR*, and shell gland (D) *CASR*, (E) *PTH1R*, and (F) *CALCR*. Expression of target genes was determined by RT-qPCR and normalized to *GAPDH* mRNA for the kidney and *18s* rRNA for shell gland. All values (mean+SEM; n=6 hens at 3, 4, 6, 7, 23, and 24 HPOP; n=5 hens at 8, 12, and 21 HPOP; n=4 hens at 1, 15, and 18 HPOP) are expressed relative to 1 HPOP (equivalent to 1). Data were analyzed by one-way ANOVA followed by Fisher's test of least significant difference when ANOVA indicated significance, and bars not sharing a common letter differ significantly ($P \leq 0.05$).

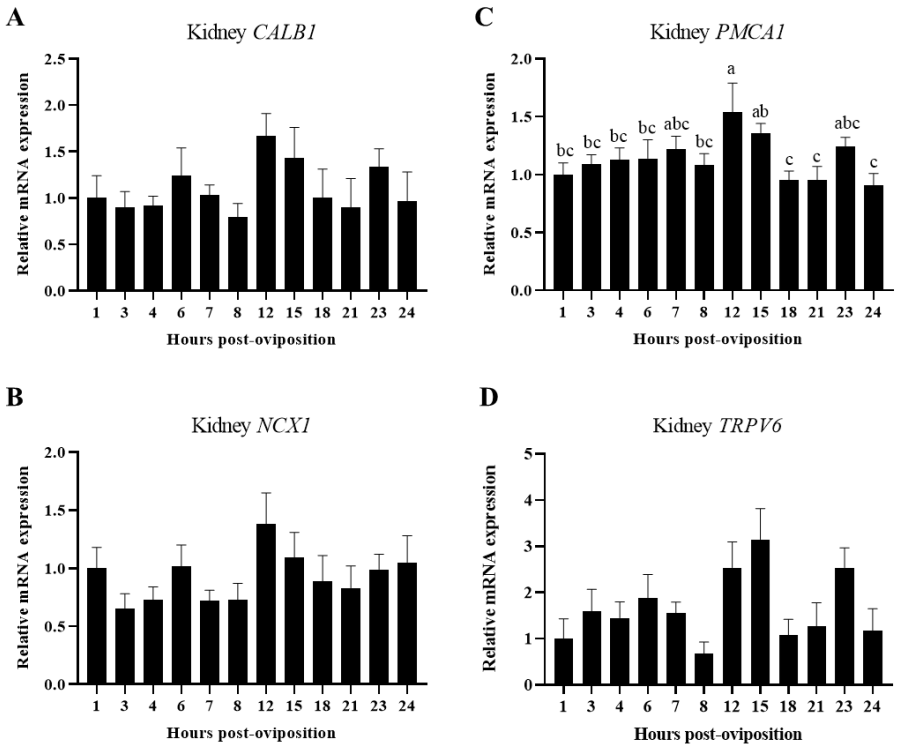

Figure 4.6. Expression of genes associated with calcium transport in kidney.
Relative levels of mRNA were measured at indicated hours post-oviposition (HPOP) for kidney (A) *CALB1*, (B) *NCX1*, (C) *PMCA1*, and (D) *TRPV6*. Expression of target genes was determined by RT-qPCR and normalized to *GAPDH* mRNA. All values (mean+SEM; n=6 hens at 3, 4, 6, 7, 23, and 24 HPOP; n=5 hens at 8, 12, and 21 HPOP; n=4 hens at 1, 15, and 18 HPOP) are expressed relative to 1 HPOP (equivalent to 1). Data were analyzed by one-way ANOVA followed by Fisher's test of least significant difference when ANOVA indicated significance, and bars not sharing a common letter differ significantly ($P \leq 0.05$).

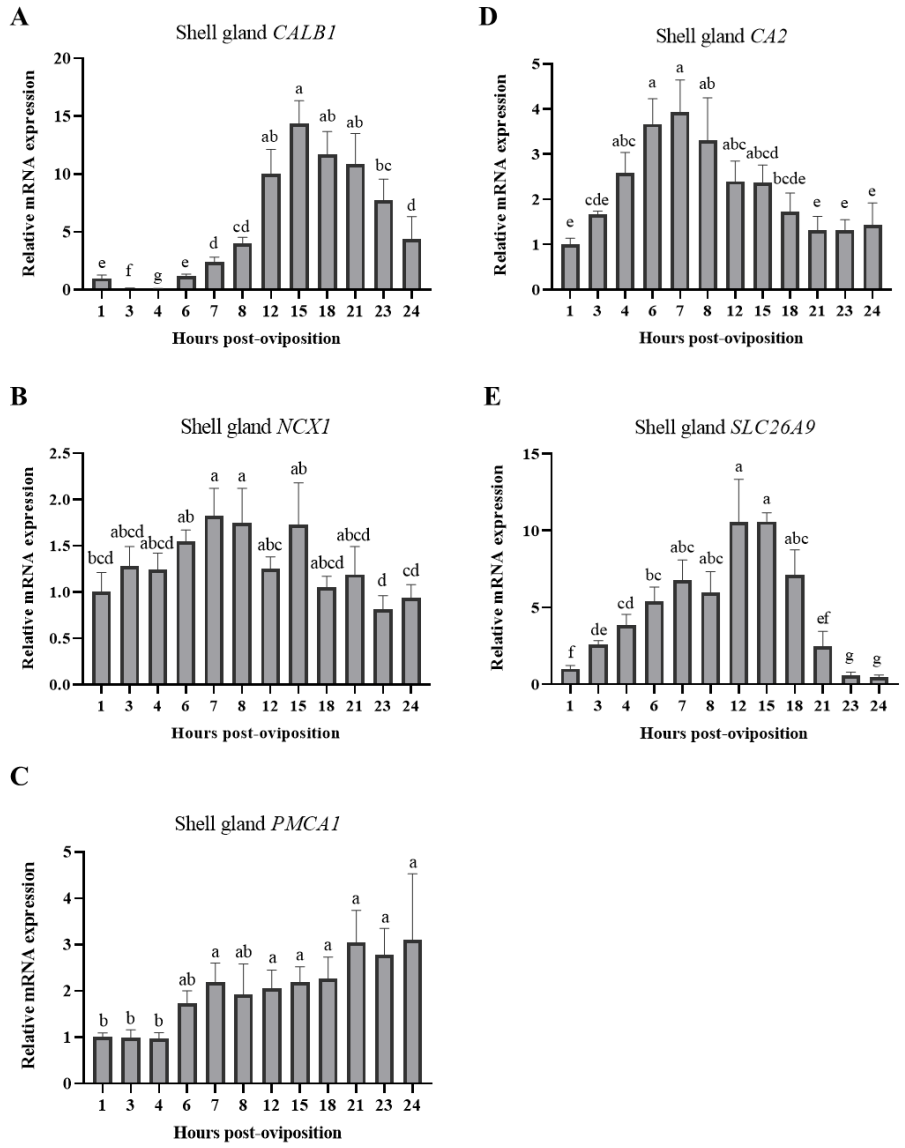

Figure 4.7. Expression of genes associated with eggshell calcification in shell gland.
Relative levels of mRNA were measured at indicated hours post-oviposition (HPOP) for shell gland (A) *CALB1*, (B) *NCX1*, (C) *PMCA1*, (D) *CA2*, (E) *SLC26A9*. Expression of target genes was determined by RT-qPCR and normalized to *18s* rRNA. All values (mean+SEM; n=6 hens at 3, 4, 6, 7, 23, and 24 HPOP; n=5 hens at 8, 12, and 21 HPOP; n=4 hens at 1, 15, and 18 HPOP) are expressed relative to 1 HPOP (equivalent to 1). Data were analyzed by one-way ANOVA followed by Fisher's test of least significant difference when ANOVA indicated significance, and bars not sharing a common letter differ significantly ($P \leq 0.05$).

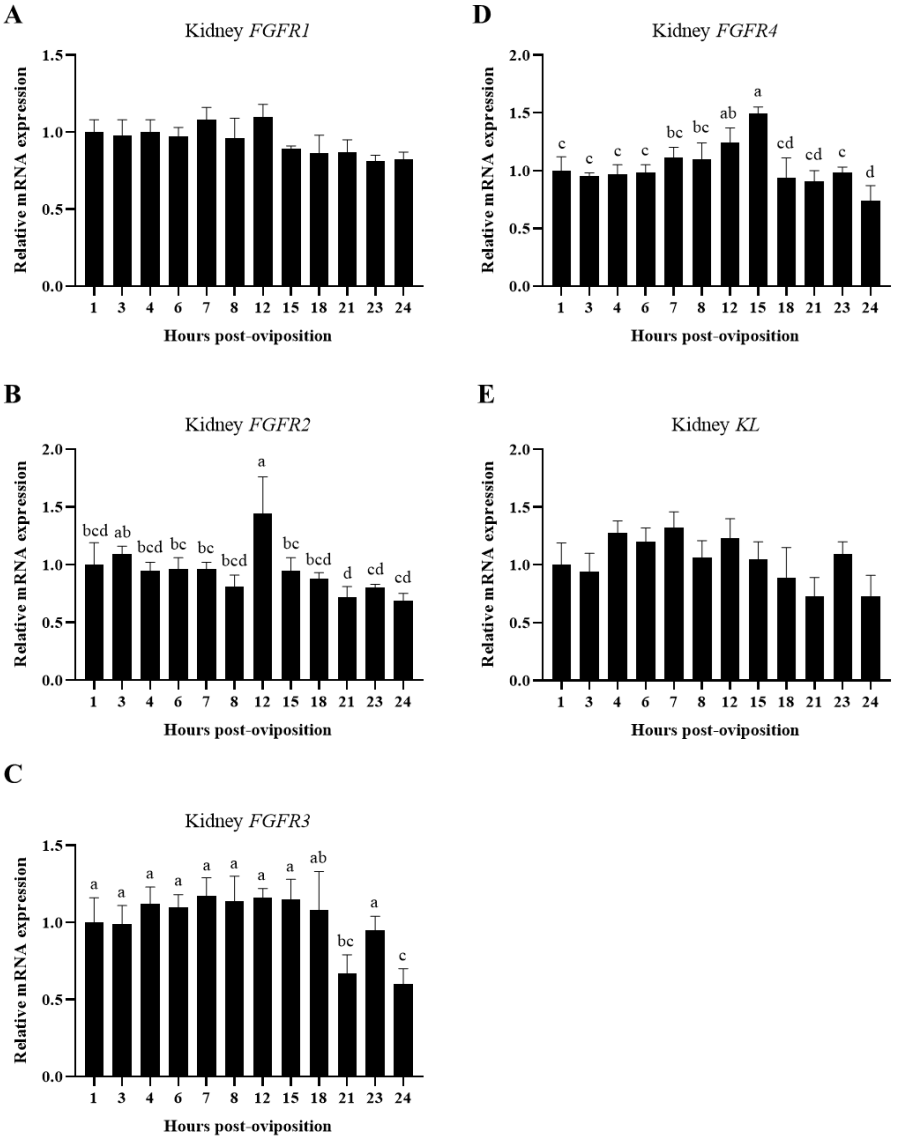

Figure 4.8. Expression of genes for FGF23 receptors in kidney.
Relative levels of mRNA were measured at indicated hours post-oviposition (HPOP) for kidney (A) *FGFR1*, (B) *FGFR2*, (C) *FGFR3*, and (D) *FGFR4*, and (E) *KL*. Expression of target genes was determined by RT-qPCR and normalized to *GAPDH* mRNA. All (mean+SEM; n=6 hens at 3, 4, 6, 7, 23, and 24 HPOP; n=5 hens at 8, 12, and 21 HPOP; n=4 hens at 1, 15, and 18 HPOP) are expressed relative to 1 HPOP (equivalent to 1). Data were analyzed by one-way ANOVA followed by Fisher's test of least significant difference when ANOVA indicated significance, and bars not sharing a common letter differ significantly ($P \leq 0.05$).

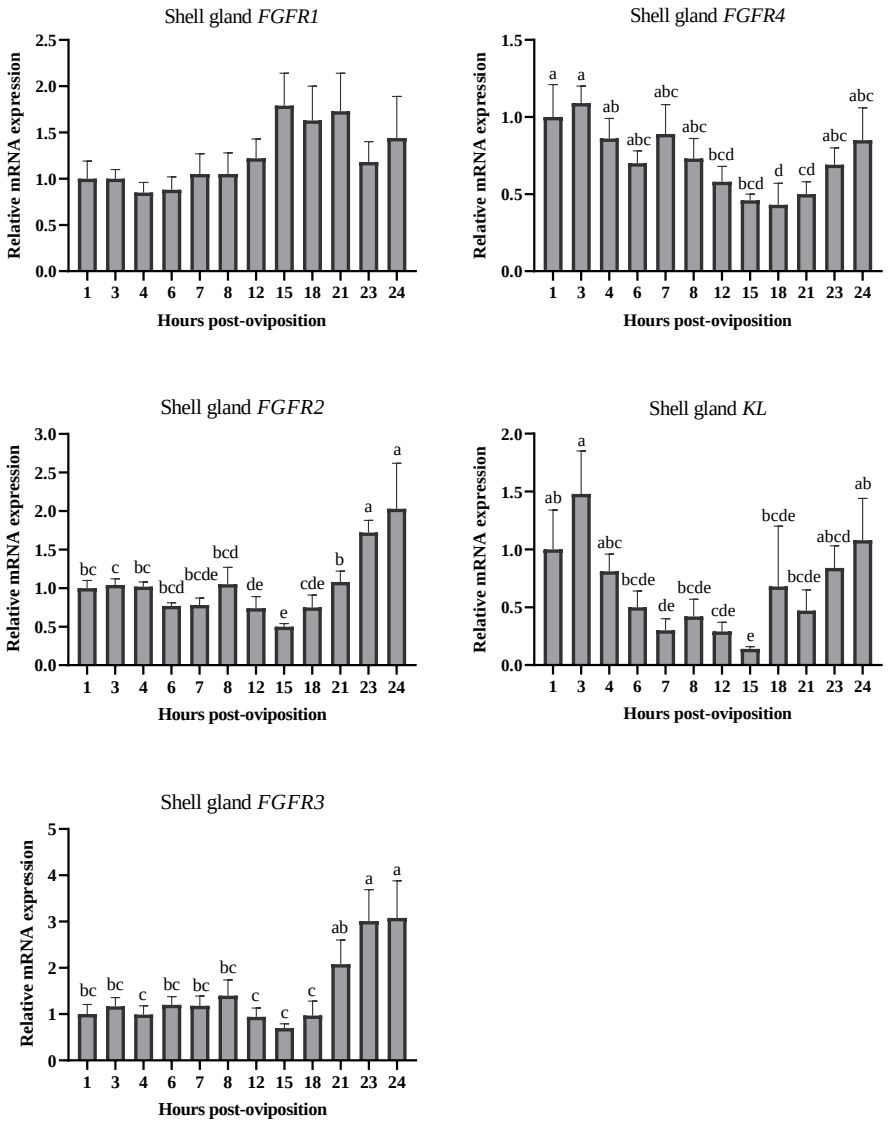

Figure 4.9. Expression of genes for FGF23 receptors in shell gland.
Relative levels of mRNA were measured at indicated hours post-oviposition (HPOP) for shell gland (A) *FGFR1*, (B) *FGFR2*, (C) *FGFR3*, and (D) *FGFR4*, and (E) *KL*. Expression of target genes was determined by RT-qPCR and normalized to *18s* rRNA. All values (mean+SEM; n=6 hens at 3, 4, 6, 7, 23, and 24 HPOP; n=5 hens at 8, 12, and 21 HPOP; n=4 hens at 1, 15, and 18 HPOP) are expressed relative to 1 HPOP (equivalent to 1). Data were analyzed by one-way ANOVA followed by Fisher's test of least significant difference when ANOVA indicated significance, and bars not sharing a common letter differ significantly ($P \leq 0.05$).

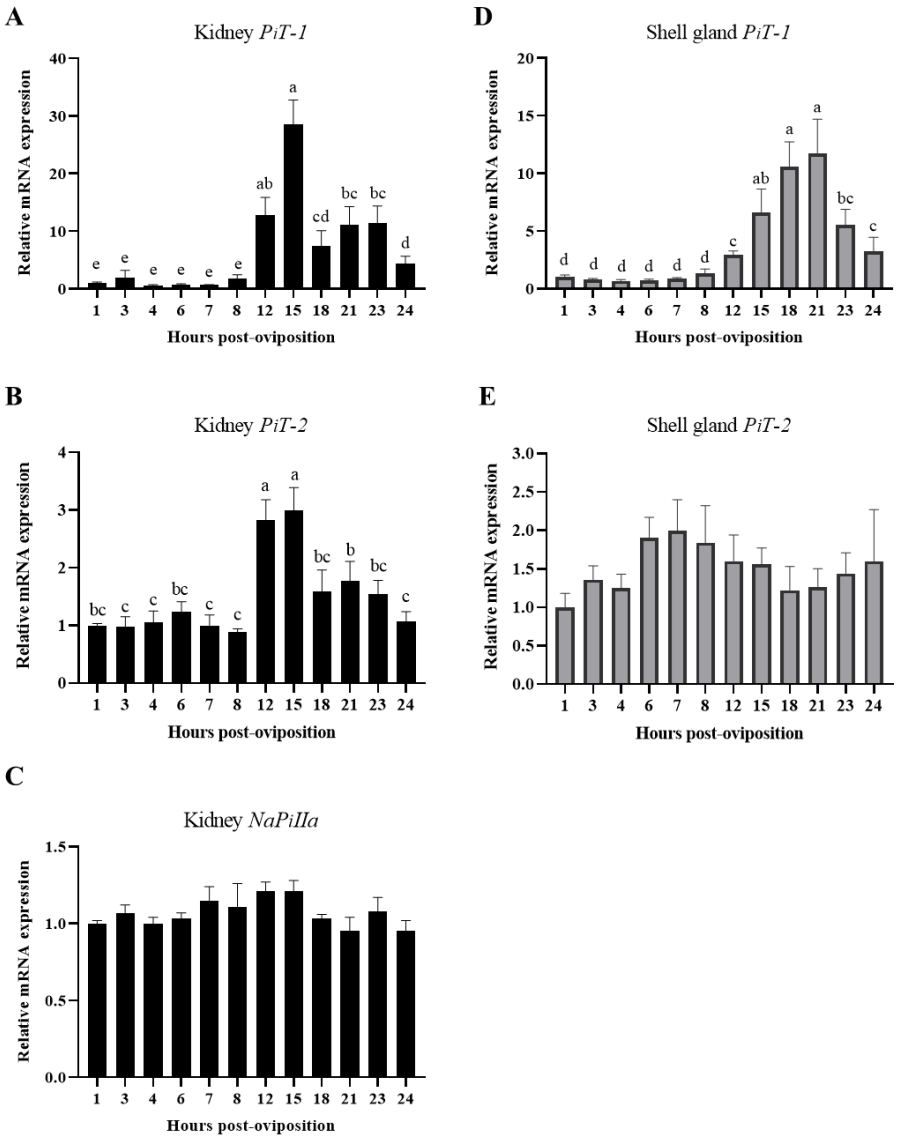

Figure 4.10. Expression of genes for phosphorus transporters in kidney and shell gland. Relative levels of mRNA were measured at indicated hours post-oviposition (HPOP) for kidney (A) *PiT-1*, (B) *PiT-2*, (C) *NaPiIIa*, and shell gland (D) *PiT-1*, (E) *PiT-2*. Expression of target genes was determined by RT-qPCR and normalized to *GAPDH* mRNA for the kidney and *18s* rRNA for shell gland. All values values (mean+SEM; n=6 hens at 3, 4, 6, 7, 23, and 24 HPOP; n=5 hens at 8, 12, and 21 HPOP; n=4 hens at 1, 15, and 18 HPOP) are expressed relative to 1 HPOP (equivalent to 1). Data were analyzed by one-way ANOVA followed by Fisher's test of least significant difference when ANOVA indicated significance, and bars not sharing a common letter differ significantly ($P \leq 0.05$).

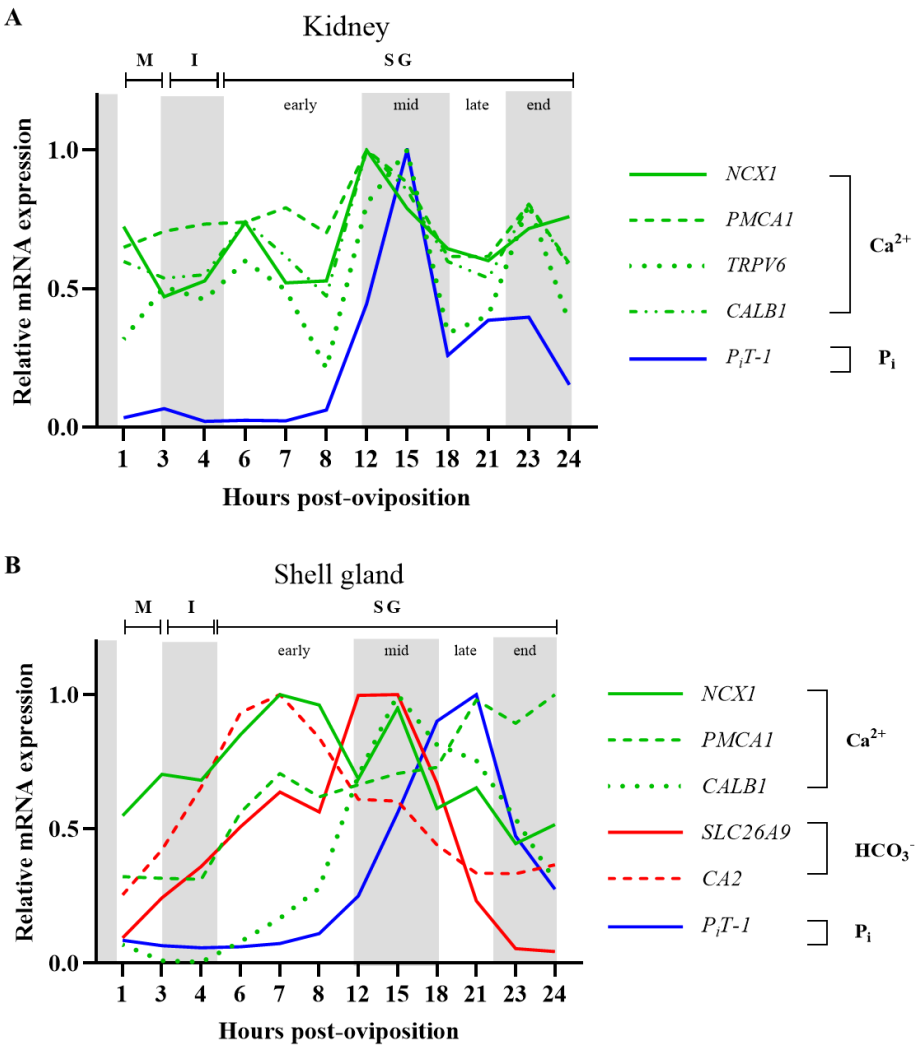

Figure 4.11. Expression profiles of key genes mediating calcium and phosphorus utilization by laying hens in the kidney and shell gland during the 24-h oviposition cycle.
(A) Relative expression of genes involved in calcium (*NCX1*, *PMCA1*, *TRPV6*, *CALB1*) and phosphorus (*PiT-1*) transport in the kidney. (B) Relative expression of genes involved in calcium transport (*NCX1*, *PMCA1*, *CALB1*), bicarbonate synthesis and transport (*CA2*, *SLC26A9*), and phosphorus transport (*PiT-1*) in the shell gland. Location of ovum within the reproductive tract [magnum (M), isthmus (I), shell gland (SG)] and stage of eggshell calcification [early, mid, late] for each time point are also shown. For each gene, expression is plotted relative to the maximum value (equivalent to 1).

CHAPTER 5

PHYSIOLOGICAL REGULATION OF CALCIUM AND PHOSPHORUS HOMEOSTASIS IN COMMERCIAL LAYING HENS DURING THE DAILY LAY CYCLE FROM EARLY THROUGH EXTENDED PRODUCTION[3]

[3]Sinclair-Black, M., Garcia, R.A., Evans, C., Angel, R., Arbe, X., Cavero, D., Ellestad L.E. 2024. To be submitted to *Poultry Science*

Abstract

In the table egg industry, production has been extended from 70 to 100 weeks of age in recent years, and older hens exhibit poor eggshell quality and weakened skeletal systems due in part to imbalances in calcium and phosphorus homeostasis. Therefore, to elucidate the physiological components regulating mineral homeostasis across an extended egg production cycle, laying hens were sampled during early, peak, late, and extended production (25, 43, 80, and 95 weeks of age) at 1:30, 6:00, 15:00, and 21:00 hours post-oviposition [HPOP]. Times were selected to represent stages of bone mineralization (1:30 HPOP), eggshell calcification (15:00 HPOP), and the transitions between bone-to-eggshell (6:00 HPOP) and eggshell-to-bone (21:00 HPOP) calcification. Eggshell characteristics, egg production parameters, circulating vitamin D_3 metabolites, expression of genes mediating uptake and utilization of calcium and phosphorus, dry matter digestibility, and blood chemistry were evaluated. Levels of $1,25(OH)_2D_3$ were reduced and those of $24,25(OH)_2D_3$ were elevated at 80 and 95 weeks of age compared to 25 weeks at 6:00 and 15:00 HPOP, likely resulting in reduced mineral transporter expression. Renal expression of 25-hydroxylase and 1α-hydroxylase was greatest at 15:00 and 21:00 HPOP, while 24-hydroxylase was lowest at these times. This suggests that the kidney may be capable of 25-hydroxylation of vitamin D_3 during eggshell calcification and that these times are when $1,25(OH)_2D_3$ is most efficiently produced. Circulating uric acid and total protein increased and pH decreased between 25 and 95 weeks, indicating a decline in renal function in older hens. Ionized calcium decreased between 1:30 and 6:00 HPOP at 25 and 43 weeks but not at 80 and 95 weeks, implying that older hens transition into eggshell calcification less efficiently. Dry matter digestibility declined with age only at 1:30 HPOP, potentially limiting nutrient availability for bone mineralization. Elevated levels of inorganic phosphorus transporter 1 at 80 weeks and at 15:00 and 21:00 HPOP and sodium-

dependent phosphorus transport protein 2b at 80 weeks, suggest that hens in late production potentially exhibit increased bone breakdown during mid and late eggshell calcification. Shell gland calcium transporter sodium-calcium exchanger 1 showed diminished expression levels at each age, which may have contributed to decreased eggshell quality at later production ages. Together, these findings highlight the physiological systems contributing to eggshell calcification and bone mineralization that become dysregulated as hens age. This fundamental information is essential to developing solutions to address declines in eggshell quality and skeletal integrity in extended production systems.

Introduction

As the global population increases, the need for affordable and sustainable protein sources continues to rise (Falcon et al., 2022). To meet this growing demand, commercial table egg producers have improved egg production efficiency through decades of selective breeding and improved husbandry. Consequently, modern laying hens often sustain longer clutch lengths with fewer pause days, resulting in over 500 eggs in a hen's lifetime (Pottguter, 2016; Preisinger, 2018). These improvements in laying persistency have allowed producers to extend egg production from 70 weeks of age to upwards of 100 weeks of age in recent years. Extended egg production systems replace hens at a slower rate, thereby reducing resource utilization on a per-bird basis (Bain et al., 2016), and have also been shown to be more economically viable than shorter production periods (Long et al., 2011; Traore et al., 2023). While the advantages of extended egg production systems are evident, it should also be noted that older hens are more likely to exhibit compromised skeletal integrity and poor eggshell quality (Al-Batshan et al., 1994; Alfonso-Carrillo et al., 2021; Benavides-Reyes et al., 2021). These challenges are likely linked to imbalances in calcium and phosphorus homeostasis as hens progress through production stages and pose significant animal welfare and economic concerns for producers.

Modern hens produce an egg approximately every 24 hours (Nys et al., 2011), and this process relies upon a cycle where dietary minerals are stored within labile skeletal reserves that are subsequently broken down to provide minerals for the developing eggshell (Dacke et al., 1993). Following oviposition, no egg is present in the shell gland for approximately 4 to 6 hours (Sinclair-Black et al., 2024). This phase occurs during the light period when feed is readily accessible, and remineralization of labile bone stores takes precedence (Wilson et al., 1990; Clunies et al., 1992; Kerschnitzki et al., 2014). Eggshell calcification initiates shortly after ovum entry into the shell

gland, and the majority of this phase occurs during the dark period when hens are unlikely to consume feed. Instead, during this period, hens rely upon the dissolution of large particle calcium sources retained in the gizzard (Zhang et al., 1997) and the breakdown of labile bone reserves (Kerschnitzki et al., 2014) to provide the minerals to the eggshell. Eggshell mineral deposition is greatest between 10 and 22 hours post-oviposition (HPOP) and terminates approximately 2 hours before the egg is laid (Nys et al., 1999), while mineral transporter expression in the shell gland peaks between 12 and 15 HPOP (Sinclair-Black et al., 2024). Maintaining this daily equilibrium requires a balance of calcium and phosphorus uptake and utilization; however, as hens age, the physiological systems that govern mineral homeostasis likely become dysregulated, resulting in insufficient calcium and phosphorus available for daily bone and eggshell mineralization (Al-Batshan et al., 1994; Bar et al., 1999).

Key tissues contributing to calcium and phosphorus homeostasis include the small intestine, liver, kidney, and shell gland. Calcium and phosphorus in the feed are absorbed through transporters and tight junctions located within and between enterocytes, respectively (Bar, 2009). The mineral absorptive capacity of the small intestine is region-dependent, and calcium and phosphorus were historically believed to be absorbed primarily in the duodenum and jejunum (Hurwitz et al., 1965). Nonetheless, unpublished findings from our lab (Sinclair-Black, M., Garcia-Mejia, R. A., Ellestad, L. E) have demonstrated heightened expression of mineral transporters, hormone receptors, and enzymes involved in vitamin D_3 metabolism in the ileum compared to the duodenum and jejunum, prompting a re-evaluation of the ileum's role as a significant regulator of calcium and phosphorus homeostasis.

Together, the liver and the kidney sequentially hydroxylate vitamin D_3 into its biologically active form, 1α,25-dihydroxycholecalciferol [$1\alpha,25(OH)_2D_3$]. Initially, vitamin D_3 absorbed from

the diet is converted to 25-hydroxycholecalciferol [25(OH)D_3] by 25-hydroxylase in the hepatocytes (Tucker et al., 1972a). The high efficacy of hepatic conversion of dietary vitamin D_3 into 25(OH)D_3 ensures sufficient substrate for the rate-limiting hydroxylation reactions of vitamin D_3 in the kidney (Heaney et al., 2008). Renal production of 1α,25$(OH)_2D_3$ is tightly regulated (Henry, 1978) and, out of all the vitamin D_3 metabolites, has the greatest impact on calcium and phosphorus homeostasis (Brommage et al., 1985). To exert its effects, 1α,25$(OH)_2D_3$ must first bind vitamin D receptor (VDR), which forms a complex with its heterodimeric partners retinoid-X-receptor alpha or gamma (RXRA, RXRG). Together, this complex binds upstream response elements on vitamin D_3-responsive genes, which in turn leads to a transcriptional response. Further regulation of 1α,25$(OH)_2D_3$ synthesis is present as a negative feedback loop, which increases the production of biologically inactive 24,25-dihydroxycholecalciferol [24,25$(OH)_2D_3$] and limits the activity of 1α-hydroxylase when 1α,25$(OH)_2D_3$ levels are elevated (Omdahl et al., 2002).

In addition to regulating active vitamin D_3 availability, the kidney is a dynamic site of mineral absorption and excretion and is, notably, the only tissue capable of independently regulating circulating calcium or phosphorus levels through differential reabsorption and excretion of each mineral. This level of control is mediated through hormonal signaling pathways that include parathyroid hormone (PTH) and calcitonin (CALC), which function to either increase or decrease levels of ionized calcium (iCa^{2+}) in circulation, respectively (Kraintz et al., 1969; Wideman, 1986). Effects of these hormones are not limited to the kidney, and their actions are also observed across other key tissues involved in mineral homeostasis, such as the small intestine, shell gland, and bone. Renal actions of PTH increase the excretion of phosphorus ions (Wideman et al., 1981) to prevent hyperphosphatemia associated with elevated bone remodeling during eggshell calcification. Furthermore, PTH increases renal expression of renal 1α-hydroxylase

(Brenza et al., 1998; Brenza et al., 2000), leading to elevated production of $1,25(OH)_2D_3$, thereby influencing calcium and phosphorus transporter expression. In these ways, the kidney tightly regulates calcium and phosphorus homeostasis, which is critical for robust bone remineralization and eggshell calcification.

During the 24-hour development of the egg, approximately 18 hours are allocated to forming the eggshell in the shell gland (Nys et al., 1999). Eggshell is primarily composed of calcium carbonate crystals sequentially deposited into distinct structural layers such as the mamillary core and palisade layers (Nys et al., 2011). Towards the end of eggshell calcification, a thin layer of hydroxyapatite crystals is deposited, followed by the cuticle (Wedral et al., 1974). The formation of each eggshell structural component requires the coordinated expression of plasma membrane and cytosolic mineral transporters, which, in turn, is orchestrated through hormonal signaling pathways involving PTH, CALC, and vitamin D_3. The hormonal control of eggshell calcification is not fully understood, and imbalances in mineral homeostasis at any level will alter eggshell structure and mineralization patterns, impacting eggshell quality (Park et al., 2018). It is, therefore, paramount to elucidate how factors such as hen age and the daily lay cycle influence the delivery of minerals to the developing egg in the shell gland.

Ultimately, as the average production age of the global laying hen population increases and genetic selection for egg production intensifies, there is an increased urgency to elucidate the physiological processes that govern calcium and phosphorus homeostasis. In doing so, the development of robust solutions geared toward maintaining eggshell quality and skeletal health can occur, ultimately improving economic outputs and animal welfare. Therefore, the objective of this study was to delineate the effects of hen age and stage within the oviposition cycle on factors influencing mineral uptake and utilization from early through extended production periods.

Materials and methods

Animal Husbandry and Experimental Design

Animals

A total of 1000 Nick Chick White pullets (H&N International, Cuxhaven Germany) were raised on the floor from day-of-hatch at the University of Georgia Poultry Research Center according to the primary breeder's guidelines (H&N International, 2020). Pullets were divided equally (500 birds/room) into two environmentally controlled rooms equipped with stir and exhaust fans and gas heaters to maintain temperature and relative humidity and fed *ad libitum* with diets described previously by Garcia-Mejia et al. (2024) and shown in Appendix B, Table B1 . During the first week after placement, pullets were exposed to 24 hours of light to encourage feed intake. During the second week, lighting was maintained at 20 hours of light and decreased by two hours each week until six weeks of age, when they were kept at 10 hours of light (0.5-foot candles) and 14 hours of darkness until transfer to individual cages at 16 weeks. Flock body weight and uniformity were assessed weekly using 100 randomly selected, individually weighed pullets from each room (20% of the total). At 16 weeks, all pullets were individually weighed, and 800 that were closest to the average pullet weight were selected for transfer into individual cages. Consequently, birds placed into cages exhibited 95% uniformity and had a body weight within 10% above or below the average. Following placement into individual cages, lighting was maintained at 10 hours of light (0.6 foot candles) and 14 hours of darkness. At 18 weeks, pullets were photostimulated by raising light intensity from 0.6 to 1.6 foot candles and increasing the hours of light by 1 hour weekly until 24 weeks to achieve 16 hours of light and 8 hours of darkness. Hens were fed corn-soybean meal-based diets according to age and stage of egg production. Initial developer and onset

diets were described previously by Garcia-Mejia et al. (2024) and are shown in Appendix B, Table B1, and diets fed at each sampling age are listed in Table 5.1.

Experimental Design

The housing unit layout consisted of 8 rows divided into four blocks of 25 cages, totaling 800 hens. A single trough feeder spanned each block of 25 hens. From the total flock, 400 were utilized in the current study. Hens from three consecutive blocks were monitored for the initial 25-week sampling (75 hens total), and thereafter, hens sampled at subsequent ages were relocated into the same cages to minimize variation due to location within the house. Relocation of hens to the three consecutive blocks was conducted eight weeks before each sampling to allow acclimation and was done using the whole block to maintain experimental units for performance parameters. Four weeks before the 25-week sampling and two weeks before each of the subsequent samplings, trough feeders were removed from the three consecutive blocks and replaced with individual feeders to monitor feed intake on an individual hen basis. The initial 4-week monitoring period was done to record the variation in feed intake, egg production, and egg size as hens transitioned into lay from 21 to 25 weeks. At later ages, feed intake, egg production, and egg size stabilized, so only two week monitoring periods were necessary. Five days before each sampling, hens were fed a diet containing 0.3% titanium dioxide as an inert marker to calculate dry matter digestibility.

A total of 240 hens were sampled across four ages throughout an extended lay period, which included early production (25 weeks), peak production (43 weeks), late production (80 weeks), and extended production (95 weeks). Additionally, at each of the four ages, hens were sampled across four time points post-oviposition (n=12 hens/age/HPOP). These time points represented periods of bone mineralization (1:30 HPOP), the transition from bone mineralization to the start of eggshell calcification (6:00 HPOP), peak eggshell calcification (15:00 HPOP), and

the transition away from shell calcification towards bone remineralization (21:00 HPOP) and were based upon results from an earlier study (Sinclair-Black et al., 2024). Hens were monitored for oviposition every 2 hours three days before sampling to estimate the number of hens available for each HPOP group. The exact oviposition time of all hens was recorded on the day preceding sampling and the day of sampling. Hens from the day preceding sampling were allocated to the 21:00 HPOP group and were the first to be sampled the following day. On the sampling day, hens were actively allocated into remaining HPOP groups and sampled at exact times after egg laying, as described in Table 5.2.

Sample Collection

Eggs were collected from individual hens 24 and 48 hours before each sampling age except for 25 weeks, at which eggs were only collected 24 hours before sampling. On the day of sampling, hens were weighed and approximately 4.5 mL of blood was collected from the brachial wing vein into a heparinized syringe and placed on ice. Hens were then euthanized by injecting 1 mL of sodium pentobarbital (390 mg/mL) and phenytoin sodium (50 mg/mL) solution (Euthasol®, Virbac, Westlake, TX) in the opposite brachial wing vein or a medial metatarsal vein. Approximately 500 mg of the right caudal liver lobe, central shell gland, right caudal kidney lobe, and 30 mg of homogenized ileal mucosal scrapings from the proximal third of the ileum were collected and snap-frozen in liquid nitrogen at all HPOP (1:30, 6:00, 15:00, and 21:00 HPOP) until further analysis for mRNA expression. Ileal digestive contents were collected from the distal two-thirds of the ileum at 1:30 and 15:00 HPOP using approximately 2 mL distilled water. Digesta samples were frozen at -20 °C until digestibility analyses were conducted.

Egg Production Parameters

Performance measurements were monitored for all potentially sampled hens for four weeks prior to the first sampling age (25 weeks) and in the two weeks preceding the later sampling periods (43, 80, 95 weeks). During this monitoring period, individual feed intake, egg number, and egg weight were recorded to calculate hen-day egg production (HDEP), egg mass, and feed conversion ratio (FCR) as follows: HDEP = [total eggs produced ÷ number of hens ÷ days measured] × 100, egg mass = [(HDEP ÷ 100) × average egg weight (g)], FCR_{kg} = [feed intake (kg)] ÷ [total weight of eggs produced (kg)], and FCR_{dozen} = [feed intake (kg)] ÷ [number of eggs ÷ 12].

Eggshell Characteristics

Eggs collected the day preceding sampling were analyzed for egg weight, eggshell breaking strength, eggshell thickness, wet eggshell weight, and wet eggshell %. Eggshell breaking strength was assessed using a static compression test utilizing a texture analyzer (TA-XTplus; Texture Technologies, Hamilton, MA) equipped with a 7.6 mm-diameter aluminum compression disc (TA-30, Texture Technologies) and a 5 kg load cell. Eggshell thickness was measured at 4 locations using a digital caliper. Eggs obtained two days prior to sampling were evaluated for egg weight, wet eggshell weight, dry eggshell weight, wet eggshell %, dry eggshell %, and eggshell mineral content. Wet and dry eggshell weights were determined after removing eggshell membranes using an adaptation of methods described by Cusack et al. (2002). Briefly, eggshells were submerged in 6% sodium hypochlorite for 60 minutes and then rinsed with distilled water. Membrane-less eggshells were then air-dried for 24 hours to measure the wet eggshell weight. Following this, the eggshells were oven-dried at 75 °C for 48 hours and then immediately weighed to evaluate the dry eggshell weight. Wet and dry eggshell percentages were calculated as follows: eggshell $percentage_{wet\ or\ dry}$ = [$eggshell\ weight_{wet\ or\ dry}$ (g) ÷ total egg weight (g)]×100. Dried eggshells were ground to 0.5 mm and evaluated for mineral content [calcium, aluminum (Al), copper (Cu), iron

(Fe), K, magnesium (Mg), manganese (Mn), Na, sulfur (S), and zinc (Zn)] using inductively coupled plasma optical emission spectroscopy (ICP-OES) at the University of Arkansas Central Analytical Laboratory (Fayetteville, AR).

RNA Extraction and Reverse Transcription Quantitative PCR (RT-qPCR)

Total RNA was isolated using QIAzol lysis reagent (Qiagen, Germantown, MD) according to the manufacturer's protocol. In short, 1 mL of QIAzol was added to each sample before homogenization with a Mini-Bead Beater (Biospec Products, Bartlesville, OK). Homogenization of samples occurred across three 45-second bursts separated by cooling on ice for 1 minute between each homogenization. Chloroform was used to extract the homogenate, followed by centrifugation at 12,000 relative centrifugal force (RCF) at 4 ºC for 15 minutes. The subsequent aqueous layer was transferred and precipitated on ice with an equal volume of isopropanol for 10 minutes. Further centrifugation of the precipitate at 12,000 RCF for 10 minutes resulted in the formation of total RNA pellets. These pellets were rinsed twice with 75% ethanol and allowed to air dry before being reconstituted with 300 µL of RNAse-free water. Total RNA was quantified using a NanoDrop-1000 (Thermo Scientific, Waltham, MA), and integrity was verified using a denaturing 1% agarose gel. Gels were imaged using a UV imaging system (Biospectrum, Upland, CA) in conjunction with Visionworks LS software (Wasserburg, Germany).

Total RNA was converted into cDNA using reverse transcription reactions with a total volume of 20 µL. Each reaction consisted of 1 µg total RNA, 5 µM random hexamers (Invitrogen, Carlsbad, CA), 5 µM anchored-dT primer (5'TTTTTTTTTTTTTTTTTTTTVN3'), Integrated DNA Technologies, Coralville, IA), 0.5 mM dNTPs (Thermo Scientific), 200 U M-MuLV reverse transcriptase (New England Biolabs, Ipswich, MA), 2 µL 10X M-MuLV buffer (New England Biolabs), and 8 U of RNaseOUT (Invitrogen). Initially, total RNA, dNTPs, and primers were

combined and heated for 5 minutes at 65 °C followed by on-ice cooling for approximately 5 minutes. Once samples were cooled, M-MuLV enzyme, M-MuLV buffer, and RNaseOUT were added, and samples were incubated under the following conditions: 25 °C for 5 minutes, 42 °C for 60 minutes, and finally 65 °C for 20 minutes. A negative control to assess genomic DNA contamination consisted of pooled RNA from all samples; however, the reverse transcriptase enzyme was not included. All reactions were diluted 1:10 with nuclease-free water before quantitative PCR (qPCR).

Primers used for qPCR analysis (Table 5.3) were designed using Primer3 Plus software (Untergasser et al., 2012) using the following parameters: amplicon length of 100 to 125 base pairs, primer length between 18 and 30 nucleotides, primer melting temperature between 58 to 60 °C, and GC content between 40 to 60%. Gene expression analysis utilized duplicate 10 µL reactions consisting of 2 µL diluted cDNA, 5 µL PowerUp™ SYBR Green Master Mix (Applied Biosystems, Foster City, CA), and 400 nM of each forward and reverse primer. Thermal cycling took place using a QuantStudio3 real-time PCR instrument (Applied Biosystems), with the following cycling conditions: 95 °C for 5 minutes, 40 cycles of 95 °C for 15 seconds, 58 °C for 30 seconds, 72 °C for 30 seconds, and a post-amplification dissociation curve to confirm that a single product was amplified.

Levels of target mRNA expression were normalized using the following genes for each tissue, which demonstrated stability across all ages and HPOP within indicated tissues: glyceraldehyde-3-phosphate dehydrogenase (*GAPDH*) [ileum and kidney], cyclophilin (*CYCLO*) [liver], or ribosomal protein L5 (*RPL5*) [shell gland]. Normalization was achieved using the equation $\Delta CT = CT_{\text{Target gene}} - (CT_{GAPDH/CYCLO/RPL5})$, followed by a transformation to $2^{-\Delta CT}$. Where significant interactive effects between age and HPOP were observed, data were expressed relative

to 1:30 HPOP at 25 weeks using the following equation [$(2^{-\Delta CT})_{sample}$]/[average $(2^{-\Delta CT})_{1:30\ HPOP\ at\ 25\ weeks}$]. When no significant interactive effects were found, main effect of HPOP or age data were expressed relative to 1:30 HPOP using the formula [$(2^{-\Delta CT})_{sample}$]/[average$(2^{-\Delta CT})_{1:30\ HPOP}$ or relative to 25 weeks using the formula [$(2^{-\Delta CT})_{sample}$]/[average $(2^{-\Delta CT})_{25\ weeks}$], respectively. Consequently, for interactive mRNA expression data, levels at 1:30 and 25 weeks will equal one; however, if no statistically significant interactive effects were observed, levels at 1:30 HPOP or 25 weeks of age will equal one.

Vitamin D_3 Metabolites

Plasma was isolated from whole blood by centrifugation at 1,500 RCF and 4 °C for 10 minutes. Plasma was analyzed for vitamin D_3 metabolites using liquid chromatography-tandem mass spectrometry (Heartland Assays, Ames, IA). Metabolites included $25(OH)D_3$, $1\alpha,25(OH)_2D_3$, and $24,25(OH)_2D_3$ with the following lower limits of detection (LLD) and lower limits of quantification (LLQ): $25(OH)_2D_3$ – 0.5 ng/mL (LLD) and 1.5 ng/mL (LLQ); $24,25(OH)_2D_3$ – 0.1 ng/mL (LLD) and 0.3 ng/mL (LLQ); and $1\alpha,25(OH)_2D_3$ – 5.0 pg/mL (LLD) and 10 pg/mL (LLQ).

Blood Chemistry

Immediately following blood collection, three 100 µL aliquots of whole blood were analyzed using an iSTAT device equipped with CG8+ or Chem 8+ cartridges, as well as a VetScan2 device equipped with Avian Reptile Plus cartridges (Zoetis, Parsippany-TroyHills, NJ). Blood chemistry parameters measured included pH, partial pressure of carbon dioxide (pCO_2), partial pressure of oxygen (pO_2), base excess, bicarbonate, (HCO_3^-), total carbon dioxide (TCO_2), sodium (Na^+), potassium (K^+), glucose (Glu), iCa^{2+}, anion gap, aspartate aminotransferase (AST), creatinine kinase (CK), uric acid (UA), total phosphorus, total protein (tProt), albumin (Alb), and globulins (Glob).

Titanium Dioxide Determination and Dry Matter Digestibility

Titanium dioxide (TiO_2) was included in diets at a level of 0.3%. Digestive contents were oven-dried at 70 ºC for 72 hours to facilitate grinding to a particle size of 0.25 mm. Feed samples containing TiO_2 were ground to 0.5 mm. Prior to the analysis of TiO_2 in ileal digesta and diet samples, the dry matter content was determined. To achieve this, ground ileal digesta (0.25 g) and feed samples (0.5 g) were weighed into ceramic crucibles in duplicate and dried at 100 ºC for 24 hours. An internal control consisting of 0.5 g of the same feed containing 0.3% TiO_2 was analyzed in duplicate for all analyses. After 24 hours, samples were immediately weighed, and dry matter content was then determined using the following formula: dry matter content (%) = [24-hour dried sample weight (g) ÷ original sample weight (g)] × 100.

Following dry matter determination, the TiO_2 concentration of the samples was immediately analyzed using an adaptation of methods described by Short et al. (1995). Briefly, duplicates of each sample and the internal control were ashed at 600 ºC for 10 hours and allowed to cool to room temperature for 3 hours. To each crucible, 10 mL H_2SO_4 (7.4 M) was added, and samples were boiled at 350 ºC for approximately 45 – 60 minutes until the solution was completely clear. Following this, 10 mL H_2O_2 was added to each sample, which was transferred into a volumetric flask and diluted with distilled water to a total volume of 100 mL. A 100 µL aliquot of each sample and standard was analyzed in triplicate using a spectrophotometer at a wavelength of 450 nm (Victor Nivo Perkin Elmer, Waltham, MA). The concentration of TiO_2 was determined by comparing the absorbance values of samples to known concentrations on the standard curve. As such, TiO_2 (%) was calculated using an equation where A is the measured absorbance of the sample, b is the Y-axis intercept of the standard curve, εm is the slope of the standard curve, and w is the weight of the sample in grams: TiO_2 (%) [As fed-basis] = [((A-b)/εm)/w]. Values were

also reported on a dry matter basis as follows: TiO2 (%) [Dry matter basis] = TiO_2 (%) [As fed-basis] / (Dry matter content (%) /100). Dry matter digestibility was then calculated in the following manner, where TF is the percent TiO_2 in the diet and TD is the percent TiO_2 in the ileal digesta: Dry matter digestibility (%) = 100 - [(TF $_{[dry\ matter\ basis]}$ / TD $_{[dry\ matter\ basis]}$)].

Statistical Analysis

Each hen was considered the experimental unit for parameters measured during sampling (eggshell quality, eggshell mineral content, vitamin D_3 metabolites, blood chemistry, and gene expression). Production performance parameters measured for the two or four weeks prior to sampling (feed intake, HDEP, egg weight, egg mass, FCR_{dozen}, and FCR_{kg}) utilized blocks of 25 hens as the experimental unit. All data were analyzed using JMP Pro 16 software (SAS Institute, Cary, NC). Performance data and eggshell characteristics were analyzed using a one-way analysis of variance (ANOVA), with hen age as the model effect. Gene expression data, vitamin D_3 metabolites, dry matter digestibility, and blood chemistry were measured using a two-way ANOVA, with HPOP-by-age as the interactive effect and hen age and HPOP as the main effects. *Post hoc* comparison of means was conducted using Fisher's test of least significant difference when ANOVA indicated significant differences. Differences were considered significant at $P \leq 0.05$.

Results

Egg Production Parameters

Egg production performance parameters are shown in Table 5.4. Feed intake per hen was lowest at 25 weeks [101.7 g] and highest at 43 weeks [121.7 g] of age ($P \leq 0.05$). A significant decline in feed intake was noted between 43 and 80 weeks of age [113.1 g], which then increased to an intermediate level at 95 weeks [116.6 g] ($P \leq 0.05$). Feed intake during this study was above the breed standards (H&N International,2020) [103-108 g]; however, diet formulations were adjusted

according to egg production and feed intake levels to ensure the nutrient requirements of hens were met throughout the study. The HDEP was comparable between 25 weeks [94.3 %] and 43 weeks [97.5%]; however, it declined significantly at 80 weeks [88.7%] and 95 weeks [80.7%] ($P \leq 0.05$). This study's HDEP values were consistently above the breed standards (H&N International, 2020) for 25 (94.3% vs. 91.6%), 43 (97.5% vs. 95.9%), 80 (88.7% vs. 84.0%), and 95 weeks (80.7% vs 70.1%). Egg weight increased steadily between 25 weeks [57.4 g] and 80 weeks [64.5 g] and was maintained through 95 weeks [64.8 g] ($P \leq 0.05$). Egg mass was significantly higher at 43 [58.1 g] and 80 [57.8 g] weeks of age than at 25 [50.7 g] and 95 weeks [53.1 g] ($P \leq 0.05$). The lowest FCR_{dozen} was noted at 25 weeks of age [1.30 kg/dozen], followed by an increase at 43 weeks [1.50 kg/dozen] that was maintained through 80 weeks [1.53 kg/dozen] ($P \leq 0.05$). The highest FCR_{dozen} occurred at 95 weeks [1.74 kg/dozen], with a 21 point increase observed between 80 and 95 weeks of age ($P \leq 0.05$). Interestingly, FCR_{kg} differed from FCR_{dozen}, wherein FCR_{kg} was lowest at 25 weeks [2.01 kg/kg] and 80 weeks [1.96 kg/kg], highest at 95 weeks [2.20 kg/kg], and intermediate at 43 weeks [2.09 kg/kg] ($P \leq 0.05$).

Eggshell Characteristics

Eggshell Quality. Analysis of eggs collected from the sampled hens on the day preceding sampling is presented in Table 5.5. Egg weights were similar to those observed while measuring egg production performance, except for 25 weeks [57.4 g], which was higher for the eggs collected the day preceding sampling, so values were not different than those at 43 weeks [59.0 g] (Table 5.5). Eggshell breaking strength was greatest at 25 [5460 g] and 43 [5329 g] weeks of age and significantly lower at 80 [3910 g] and 95 [3927 g] weeks of age ($P \leq 0.05$). Similarly, eggshell thickness was also greater at 25 [0.42 mm] and 43 [0.41 mm] weeks of age and significantly decreased at 80 [0.38 mm] and 95 [0.37 mm] weeks of age ($P \leq 0.05$). There were no significant

differences in wet eggshell weight across ages (P>0.05); however, wet eggshell % was higher at 25 [10.41%] and 43 [10.41%] weeks of age, followed by significant decreases at 80 [10.19%] and 95 [9.08%] weeks (P≤0.05).

Dry Eggshell Analysis and Mineral content. Eggs collected two days before sampling were evaluated for dry shell weight (Table 5.6) and eggshell mineral content (Table 5.7) from 43 weeks onwards. Comparisons of egg weights, wet and dry shell weights, and wet shell % were similar to those noted for other analyses (Tables 5.4 – 5.6). Similar to wet shell %, dry shell % was highest at 43 weeks [9.91 %] and significantly declined through 80 [8.78%] and 95 [8.56%] weeks (Table 5.6; P≤0.05). Interestingly, the mineral composition of the eggshells was altered across the productive lifetime of the hen (Table 5.7; P≤0.05). Eggshells had the highest concentration of calcium at 43 weeks [41.23%]; however, concentrations declined at 80 weeks [39.19%] and remained lower at 95 weeks [38.68%] (Table 5.7; P≤0.05). Levels of Al showed similar trends to calcium, such that Al was greatest at 43 weeks [128.2 PPM] and significantly lower at 80 [125.8 PPM] and 95 [125.4 PPM] weeks (Table 5.7; P≤0.05). Conversely, eggshell Cu was lowest at 43 weeks [0.9 PPM] and substantially greater at 80 [1.4 PPM] and 95 [1.6 PPM] weeks of age (Table 5.7; P≤0.05). Eggshell S was also significantly lower at 43 weeks [159.2 PPM] than at 80 [189.4 PPM] and 95 [184.7 PPM] weeks (Table 5.7; P≤0.05). Concentrations of eggshell K were similar at 43 [404.0 PPM] and 95 [424.3 PPM] weeks of age but significantly lower at 80 weeks [335.1 PPM], while Mn was greatest at 80 [2.2 PPM] and 95 [2.0 PPM] weeks and lowest at 25 weeks [1.7 PPM] (Table 5.7; P≤0.05). Levels of eggshell P, Fe, Mg, Na, and Zn were not different across ages (Table 5.7; P>0.05).

Circulating Vitamin D_3 Metabolites

Vitamin D_3 is a crucial regulator of calcium and phosphorus homeostasis; as such, plasma levels of $25(OH)_2D_3$, $1,25(OH)_2D_3$, and $24,25(OH)_2D_3$ were evaluated within the daily egg formation cycle across production stages. HPOP-by-age interactions were observed for all circulating vitamin D_3 metabolites (Figure 5.1A - 5.1C; $P \leq 0.05$). The first hydroxylation product of vitamin D_3, $25(OH)D_3$, was found to exhibit similar levels across all HPOP and ages, except for 80 weeks, which was significantly greater at 1:30, 6:00, and 21:00 HPOP (Figure 5.1A; $P \leq 0.05$). Biologically active $1,25(OH)_2D_3$ at 1:30 HPOP remained consistent at 25, 43, and 80 but significantly declined between 80 and 95 weeks (Figure 5.1B; $P \leq 0.05$). At all remaining HPOP, $1,25(OH)_2D_3$ tended to decrease as hens aged (Figure 5.1B; $P \leq 0.05$). At 1:30 and 6:00 HPOP, concentrations of inactive $24,25(OH)_2D_3$ were largely unchanged between 25 and 80 weeks of age but elevated at 95 weeks (Figure 5.1C; $P \leq 0.05$). A steady increase in $24,25(OH)_2D_3$ was noted at 15:00 HPOP for all ages, while at 21:00 HPOP, levels were comparable across ages and akin to concentrations noted at 1:30 at 25 weeks (Figure 5.1C; $P \leq 0.05$).

Vitamin D_3 Metabolism

Sequential hydroxylation of vitamin D_3 by cytochrome P450 2R1 (CYP2R1) and cytochrome P450 27B1 (CYP27B1) is required to form hormonally active $1,25(OH)_2D_3$. In contrast, cytochrome P450 24A1 (CYP24A1) is a negative regulator of vitamin D_3 availability that catalyzes the formation of biologically inactive $24,25(OH)_2D_3$. While the liver is canonically associated with CYP2R1 activity and the kidney with CYP27B1 and CYP24A1 activities, the expression of genes encoding these enzymes within other tissues may contribute to local vitamin D_3 metabolism. Expression of *CYP24A1* was not detected in liver tissue, which is in line with findings by (Garcia-Mejia et al., 2024; Sinclair-Black et al., 2024).

Ileum. As no significant HPOP-by-age interactions were observed for *CYP2R1* or *CYP27B1* in this tissue (P>0.05), data for interactive means are shown in Appendix C (Figure C1), and main effect means for hen age and HPOP are reported here (Figure 5.2A – 5.2D). Ileal *CYP2R1* expression was highest at 80 weeks of age and significantly lower at 25, 43, and 95 weeks (Figure 5.2A; P≤0.05). Expression of ileal *CYP27B1* declined steadily between 25 and 80 weeks of age and at 95 weeks, during extended egg production, levels were less than half of those observed at all earlier ages (Figure 5.2B; P≤0.05). Neither *CYP2R1* nor *CYP27B1* demonstrated significant differences within the daily egg formation cycle (Figure 5.2C, 5.2D; P>0.05). A significant HPOP-by-age interaction was observed for *CYP24A1* (Figure 5.2E; P≤0.05), with significant changes occurring at 1:30 and 15:00 HPOP between the ages (Figure 5.2E; P≤0.05). At 1:30 HPOP, levels tended to be higher at 80 and 95 weeks than at younger ages (Figure 5.2E; P≤0.05). At 15:00 HPOP, ileal *CYP24A1* was significantly lower at 95 weeks of age (Figure 5.2E; P≤0.05) but also tended to be reduced at 43 weeks of age. Other time points representing transitions from bone-to-eggshell or eggshell-to-bone calcification at 6:00 and 21:00 HPOP, respectively, exhibited consistently lower expression across all ages (Figure 5.2E; P≤0.05).

Kidney. Data for interactive means are shown in Appendix C (Figure C2), and main effect means for hen age and HPOP are reported here (Figure 5.3A – 5.3F) because no significant HPOP-by-age interactions were observed for *CYP2R1*, *CYP27B1*, or *CYP24A1* in this tissue (P>0.05). Across production stages, renal *CYP2R1* expression significantly increased between 25 and 43 weeks, followed by a steady decline through 95 weeks (Figure 5.3A; P≤0.05). Expression of renal *CYP27B1* was comparable between 25 and 43 weeks; however, at 80 weeks, levels significantly increased above all other ages before declining again at 95 weeks (Figure 5.3B; P≤0.05). In contrast, levels of *CYP24A1* exhibited an inverse pattern and remained consistent across all ages

except for 80 weeks, which was substantially lower (Figure 5.3C; P≤0.05). Within the 24 hours taken to develop the egg, renal *CYP2R1* remained consistent from 1:30 through 6:00 HPOP and was followed by elevated levels at 15:00 and 21:00 HPOP (Figure 5.3D; P≤0.05). Similarly, *CYP27B1* in the kidney was greater at 15:00 HPOP and 21:00 HPOP than earlier times within the oviposition cycle, with an almost 3-fold increase in expression occurring between 6:00 and 15:00 HPOP, and intermediate levels observed at 1:30 HPOP (Figure 5.3E; P≤0.05). Levels of the inactivating enzyme, *CYP24A1,* steadily decreased in expression from 1:30 HPOP through 21:00 HPOP (Figure 5.3F; P≤0.05).

Shell Gland. There were no significant HPOP-by-age interactions for *CYP2R1*, *CYP27B1*, or *CYP24A1* in this tissue (P>0.05), and as such, data for interactive means are shown in Appendix C (Figure C4), and main effect means for hen age and HPOP are reported here (Figure 5.4A – 5.4F). Like *CYP2R1* expression in the kidney, levels in the shell gland significantly increased between 25 and 43 weeks of age and then remained stable through 80 weeks before declining at 95 weeks to levels similar to those observed at 25 weeks (Figure 5.4A; P≤0.05). In contrast, hen age did not influence expression levels of *CYP27B1* and *CYP24A1* in the shell gland (Figure 5.4B, 5.4C; P>0.05). During the daily oviposition cycle, *CYP2R1* increased expression between 1:30 and 6:00 HPOP; however, as eggshell calcification proceeded between 15:00 and 21:00 HPOP, levels decreased (Figure 5.4D; P≤0.05). Expression of *CYP27B1* remained relatively consistent between 1:30 and 15:00 HPOP but significantly increased at 21:00 HPOP (Figure 5.4E; P≤0.05). No significant differences were observed across HPOP for *CYP24A1* (Figure 5.4F; P>0.05).

Vitamin D_3 Signaling

To evaluate the potential regulatory effects of $1,25(OH)_2D_3$ within tissues participating in calcium and phosphorus uptake and utilization, the expression of *VDR*, along with its heterodimeric partners *RXRA* and *RXRG*, was measured.

Ileum. For *VDR*, *RXRA*, and *RXRG*, the HPOP-by-age interaction was not significant (P>0.05), so data for interactive means are shown in Appendix C (Figure C1), and main effect means for hen age and HPOP are reported here (Figure 5.5A – 5.5F). Ileal *VDR* decreased between 25 and 80 weeks of age and remained low at 95 weeks (Figure 5.5A; P≤0.05). Levels of *RXRA* differed across production ages, where expression was significantly lower at 80 weeks of age compared to 25, 43, and 95 weeks (Figure 5.5B; P≤0.05). Ileal *RXRG* expression was biphasic across egg production stages, wherein levels were significantly greater at 25 and 43 weeks and lower at 80 and 95 weeks of age (Figure 5.5C; P≤0.05). Throughout the daily egg formation cycle, ileal *VDR* expression was greatest at 15:00 and 21:00 HPOP, intermediate at 1:30 HPOP, and lowest at 6:00 HPOP (Figure 5.5D; P≤0.05). In contrast, neither *RXRA* nor *RXRG* altered expression across HPOP (Figure 5.5E - 5.5F; P>0.05).

Kidney. Main effect means for hen age and HPOP are shown here (Figure 5.6A - 5.6F) because the HPOP-by-age interaction was not significant for *VDR*, *RXRA*, or *RXRG* in this tissue (P>0.05) and data for interactive means are shown in Appendix C (Figure C2). Both *VDR* and *RXRA* shared similar expression profiles across ages, where levels increased between 25 and 43 weeks and remained consistent from 43 to 95 weeks (Figure 5.6A - 5.6B; P≤0.05). Expression of *RXRG,* on the other hand, rose steadily from 25 weeks to 80 weeks but decreased slightly between 80 and 95 weeks (Figure 5.6C; P≤0.05). Within the 24-hour egg formation cycle, renal *VDR* was unaltered at all HPOP (Figure 5.6D; P>0.05). Levels of *RXRA* remained stable between 1:30 and 15:00 HPOP but was significantly reduced at 21:00 HPOP (Figure 5.6E; P≤0.05). Levels of *RXRG*

rose steadily between 1:30 and 15:00 HPOP; however, at 21:00 HPOP, expression was reduced and similar to 1:30 HPOP (Figure 5.6F; P≤0.05).

Liver. Main effect means of hen age and HPOP are reported here in Figures 5.7A – 5.7H for *CYP2R1*, *VDR*, *RXRA*, and *RXRG* for liver tissue because no significant HPOP-by-age interactions were observed (P>0.05). As a result, interactive means are shown in Appendix C (Figure C3). Throughout the egg production stages examined expression of hepatic *CYP2R1* was heightened at 43 weeks, during peak egg production, and lower at all other ages (Figure 5.7 A; P≤0.05). Levels of *VDR* declined between 25 and 43 weeks of age and remained low through 80 weeks before rising to an intermediate level at 95 weeks (Figure 5.7B; P≤0.05). Expression of *RXRA* decreased between 25 and 43 weeks of age but then increased to its greatest levels at 80 weeks and remained high at 95 weeks (Figure 5.7C; P≤0.05) Hepatic *RXRG* levels were similar across all stages of egg production (Figure 5.7D; P>0.05). During the oviposition cycle, liver *CYP2R1* decreased between 1:30 HPOP and 6:00 HPOP but increased again to similar levels as 1:30 HPOP at 15:00 and 21:00 HPOP (Figure 5.7E; P≤0.05). Expression of *VDR* was not different across HPOP in the liver (Figure 5.7F; P>0.05), while expression of a heterodimeric partner for VDR, *RXRA* was higher at 1:30 and 15:00 HPOP and lower at 6:00 HPOOP and 21:00 HPOP (Figure 5.7G; P≤0.05). Levels of *RXRG* were notably lower at 21:00 HPOP compared to all other HPOP (Figure 5.7H; P≤0.05).

Shell Gland. There were no significant HPOP-by-age interactions for *VDR*, *RXRA*, or *RXRG* in the shell gland (P>0.05), and as such, main effect means for hen age and HPOP are reported here (Figure 5.8A – 5.8F), and data for interactive means are shown in Appendix C (Figure C4). Together, *VDR* and *RXRA* increased between 25 and 43 weeks of age in the shell gland, followed by a slight decrease at 80 weeks; however, *VDR* remained low at 95 weeks while *RXRA*

rose to levels similar to those at 43 weeks (Figure 5.8A - 5.8B; P≤0.05). Levels of *RXRG* also rose between 25 and 43 weeks but continued to rise until 80 weeks and remained comparable at 95 weeks (Figure 5.8C; P≤0.05). Across the 24-hour lay cycle, shell gland expression of *VDR* doubled between bone mineralization at 1:30 HPOP and peak eggshell calcification at 15:00 HPOP, followed by a substantial reduction at 21:00 HPOP, as eggshell calcification slows (Figure 5.8D; P≤0.05). Expression of *RXRA* was slightly elevated at 1:30 HPOP compared to other HPOP, while in contrast, *RXRG* increased 3-fold between 1:30 HPOP and 6:00 HPOP and decreased to levels similar to 1:30 HPOP after that (Figure 5.8E - 5.8F; P≤0.05).

Circulating Ionized Calcium and Total Phosphorus

Circulating calcium in its ionized form is readily utilized for processes such as eggshell calcification and bone mineralization, while elevated total phosphorus levels can indicate bone breakdown. As such, evaluating these parameters is essential to understanding the dynamics of calcium and phosphorus homeostasis in laying hens.

Both iCa^{2+} and total phosphorus exhibited significant interactive HPOP-by-age effects (Figure 5.9; P≤0.05). During early egg production at 25 weeks, iCa^{2+} decreased significantly at each HPOP from 1:30 HPOP through 15:00 HPOP and remained lower at 21:00 HPOP (Figure 5.9A; P≤0.05). At peak egg production at 43 weeks, iCa^{2+} levels were significantly lower at 1:30 HPOP compared to other ages at this HPOP, remained comparatively low at 6:00 HPOP, levels then decreased slightly at 15:00 HPOP, and remained lower at 21:00 HPOP (Figure 5.9A; P≤0.05). In aged hens at 80 and 95 weeks, elevated iCa^{2+} levels were maintained between 1:30 and 6:00 HPOP and significantly reduced at 15:00 HPOP and 21:00 HPOP (Figure 5.9A; P≤0.05).Total phosphorus concentrations at 15:00 HPOP were elevated above those at 1:30, 6:00, and 21:00

HPOP at all ages except 43 weeks (Figure 5.9B; P≤0.05); however, at all other HPOP and ages, total phosphorus concentrations were comparable (Figure 5.9B; P≤0.05).

Hormone Receptors

Calcium and phosphorus homeostasis is finely tuned by hormonal signaling through parathyroid hormone receptor 1 (PTH1R), calcium-sensing receptor (CASR), and calcitonin receptor (CALCR). As such, evaluating the expression of these receptors within small intestine, kidney, and shell gland will provide valuable insight into the hormonal regulation of calcium and phosphorus uptake and utilization within these key tissues.

Ileum. Main effect means for hen age and HPOP are reported here (Figure 5.10A – 5.10F) because no significant HPOP-by-age interactions were noted for *PTH1R*, *CASR*, or *CALCR* in ileum tissue (P>0.05) and data for interactive means are shown in Appendix C (Figure C5). Ileal expression of *PTH1R* was lowest at 25 weeks and increased from 2- to 3-fold at 43, 80, and 95 weeks (Figure 5.10A; P≤0.05). Levels of *CASR* were fairly consistent between 25 and 80 weeks but decreased at 95 weeks (Figure 5.10B; P≤0.05). Expression of *CALCR* considerably increased between 25 and 43 weeks, remained steady at 80 weeks, and then increased again at 95 weeks (Figure 5.10C; P≤0.05). Ileal *PTH1R* decreased slightly but not significantly between 1:30 and 6:00 HPOP, increased 2-fold at 15:00 HPOP and remained constant at 21:00 HPOP (Figure 5.10D; P>0.05). Expression of *CASR* in the ileum decreased between 1:30 HPOP and 6:00 HPOP and then steadily increased between 6:00 HPOP and 21:00 HPOP (Figure 5.10E; P≤0.05). Levels of ileal *CALCR* were not significantly different within the daily egg formation cycle (Figure 5.10F; P>0.05).

Kidney. Data for interactive means are shown in Appendix C (Figure C6) due to no significant HPOP-by-age interactions being observed for *PTH1R*, *CASR*, or *CALCR* in kidney

tissue (P>0.05). Consequently, main effect means for hen age and HPOP are reported here (Figure 5.11A – 5.11F). All measured renal hormone receptors significantly increased between 25 and 80 weeks of age; however, *PTH1R* continued to rise at 95 weeks, while *CASR* and *CALCR* declined at this age (Figure 5.11A - 5.11C; P≤0.05). Expression of renal *PTH1R* was influenced by HPOP, such that levels remained stable between 1:30 and 6:00 HPOP; however, they steadily declined thereafter through 21:00 HPOP (Figure 5.11D; P≤0.05). Expression of *CASR* in the kidney was only elevated at 15:00 HPOP, during eggshell calcification, and similarly low at all other HPOP (Figure 5.11E; P≤0.05). No significant differences were observed across HPOP for renal *CASR* (Figure 5.11F; P>0.05).

Shell Gland. For *PTH1R*, *CASR*, and *CALCR* in the shell gland, no significant HPOP-by-age interactions were observed (P>0.05) and data for interactive means are shown in Appendix C (Figure C7). Main effect means for hen age and HPOP are reported here (Figure 5.12A – 5.12F). Neither *PTH1R* nor *CASR* in the shell gland were influenced by hen age (Figure 15.12A, 5.12B; P>0.05). In contrast, shell gland *CALCR* increased linearly from 25 through 80 weeks, decreasing at 95 weeks to levels similar to 43 weeks (Figure 5.12C; P≤0.05). During egg formation, shell gland *PTH1R* and *CALCR* shared comparable expression patterns where mRNA levels declined more than 4-fold between 1:30 and 6:00 HPOP, remained low between 6:00 and 15:00 HPOP, and then either increased 7-fold or 3-fold at 21:00 HPOP, respectively (Figure 5.12D - 5.12F; P≤0.05). Shell gland *CASR* remained low during 1:30 and 6:00 HPOP before calcification of the egg; however, at 15:00 and 21:00 HPOP, expression of *CASR* was almost double that of 1:30 HPOP (Figure 5.12E; P≤0.05).

Dry Matter Digestibility and Calcium Transport

Adequate intestinal nutrient absorption is crucial for maintaining physiological balance during bone mineralization and eggshell calcification; as such, dry matter digestibility was measured during these phases at 1:30 or 15:00 HPOP. Furthermore, the calcium transporters sodium-calcium exchanger 1 (NCX1), plasma membrane calcium transporter 1 (PMCA1), and chaperone protein calbindin (CALB1) mediate the efficient delivery of calcium for processes such as skeletal mineralization and eggshell calcification. An additional calcium transporter, transient receptor potential cation channel subfamily V6 (TRPV6), was only detected in kidney tissue, which is in line with previous findings (Proszkowiec-Weglarz et al., 2013; Rousseau et al., 2016; Proszkowiec-Weglarz et al., 2019; Hu et al., 2022; Garcia-Mejia et al., 2024; Sinclair-Black et al., 2024). As such, the expression of the genes encoding these proteins was measured in the ileum and other tissues involved in calcium and phosphorus uptake and utilization.

Dry Matter Digestibility. A significant HPOP-by-age interactive effect was observed wherein dry matter digestibility decreased linearly with age at 1:30 HPOP (Figure 5.13). In contrast, at 15:00 HPOP, digestibility values were significantly higher than at 1:30 HPOP for 43, 80, and 95 weeks of age ($P \leq 0.05$) and did not differ across the different production stages ($P > 0.05$).

Ileum. As no significant HPOP-by-age interactions were observed for *NCX1*, *PMCA1*, or *CALB1* in this tissue ($P > 0.05$), data for interactive means are shown in Appendix C (Figure C8), and main effect means for hen age and HPOP are reported here (Figure 5.14A – 5.14F). Together, ileal *NCX1* and *CALB1* demonstrated similar expression patterns across earlier ages such that their expression was steady at 25 and 43 weeks of age and decreased significantly at 80 weeks of age; however, at 95 weeks, *NCX1* maintained similar expression levels to 80 weeks while *CALB1* increased back to levels observed at earlier ages (Figure 5.14A, 5.14C; $P \leq 0.05$). The expression of ileal *PMCA1* was not altered by the stage of production (Figure 5.14B; $P > 0.05$). Similarly,

NCX1 in the ileum was not significantly influenced by HPOP (Figure 5.14D; P>0.05). Both ileal *PMCA1* and *CALB1* demonstrated almost identical expression patterns during the 24-hour oviposition cycle such that levels decreased between 1:30 and 6:00 HPOP before increasing again at 15:00 and 21:00 HPOP (Figure 5.14E - 5.14F; P≤0.05).

Kidney. Main effects of hen age and HPOP are reported in Figure 5.15A - 5.15H because the HPOP-by-age interaction was not significant (P>0.05) and data for interactive means are shown in Appendix C (Figure C9). Renal mRNA levels for *NCX1* and *CALB1* increased across production stages from 25 through 80 weeks but declined at 95 weeks (Figure 5.15A, 5.15C; P≤0.05). Expression of *PMCA1* did not differ across the different production ages (Figure 5.15B; P>0.05). The calcium transporter *TRPV6* was only detected in kidney tissue and levels more than doubled between 25 and 43 weeks but declined steadily thereafter (Figure 5.15D; P≤0.05). Within the 24 hours taken to form an egg, renal *NCX1* was significantly lower at 6:00 HPOP than at all other HPOP (Figure 5.15E; P≤0.05). Expression of *PMCA1* in the kidney was significantly greater at 15:00 HPOP than at 1:30 HPOP, with intermediate values observed at 6:00 and 21:00 HPOP; however, differences between HPOP were of a small magnitude (Figure 5.15F; P≤0.05). Levels of renal *CALB1* did not differ across HPOP (Figure 5.15G; P>0.05). Renal *TRPV6* was lowest at 1:30 and 6:00 HPOP but increased at 15:00 HPOP before declining to an intermediate level at 21:00 HPOP (Figure 5.15H; P≤0.05).

Shell Gland. Data for interactive effects for *NCX1* and *PMCA1* are shown in Appendix C (Figure C10) because no significant HPOP-by-age interactions were noted in shell gland tissue (P>0.05). Data for main effect means for hen age and HPOP are reported here in Figures 5.16A – 5.16D. As laying hens aged, expression of shell gland *NCX1* subtly diminished from 25 through 95 weeks (Figure 5.16A; P≤0.05). In contrast, *PMCA1* in the shell gland increased between 25 and

43 weeks and maintained the same expression level through 95 weeks (Figure 5.16B; P≤0.05). During individual egg formation, shell gland *NCX1* remained consistent between 1:30 and 15:00 HPOP but declined at 21:00 HPOP (Figure 5.16C; P≤0.05). Levels of *PMCA1* in the shell gland were similar at 1:30 and 6:00 HPOP; however, thereafter, expression increased at 15:00 HPOP and further at 21:00 HPOP (Figure 5.16D; P≤0.05). A significant HPOP-by-age interaction was observed for *CALB1* (Figure 5.16E; P≤0.05). The expression of shell gland *CALB1* was lowest at 1:30 and 6:00 HPOP and more than 10-fold higher at 15:00 HPOP for all ages. At 21:00 HPOP, *CALB1* expression in 25 and 43 week old hens decreased by two-fold, whereas in 80 and 95 week old hens, expression decreased by a smaller magnitude to levels that did not differ from those at 15:00 HPOP (Figure 5.16E; P≤0.05).

Phosphorus Transporters

Phosphorus transporters such as inorganic transporters 1 and 2 (P_iT-1 and P_iT-2) and sodium-dependent phosphate transporters protein 2A and 2 B (NaP_iIIa and NaP_iIIb) are responsible for maintaining the equilibrium of phosphorus movement across tissues. Therefore, their expression was evaluated in tissues participating in regulating calcium and phosphorus homeostasis in laying hens. Expression of *NaP_iIIa* was not detected in either ileum or shell gland tissues

Ileum. For ileal *P_iT-1*, *P_iT-2*, and *NaP_iIIb*, no significant HPOP-by-age interactions were found (P>0.05), and as such, data for interactive means are shown in Appendix C (Figure C11), and main effect means for hen age and HPOP are reported here (Figure 5.17A – 5.17F). Ileal *P_iT-1* increased between 25 and 43 weeks and then did not change between 43 and 95 weeks (Figure 5.17A; P≤0.05). On the other hand, *P_iT-2* levels continuously decreased as hens aged from 25 through 95 weeks (Figure 5.17B; P≤0.05). The phosphorus transporter *NaP_iIIb* increased between 25 and 43 weeks; however, it steadily declined in expression through 95 weeks to levels similar to

those at 25 weeks after that (Figure 5.17C; P≤0.05). Within the 24-hour lay cycle, *P_iT-1* in the ileum was greatest at 1:30 and 21:00 HPOP and significantly but marginally lower at 6:00 and 15:00 HPOP (Figure 5.17D; P≤0.05). Neither ileal *P_iT-2* nor *NaP_iIIb* changed expression patterns during the daily egg formation cycle (Figure 5.17E - 5.17F; P>0.05).

Kidney. Main effect means for hen age and HPOP are reported in Figures 5.18A – 5.18F for *P_iT-1*, *P_iT-2*, or *NaP_iIIb* because no significant HPOP-by-age interactions were noted in this tissue (P>0.05). As such, data for interactive means are shown in Appendix C (Figure C12). As laying hens aged, renal *P_iT-1* increased steadily between 25 weeks and 80 weeks before declining at 95 weeks to levels similar to those at 25 weeks (Figure 5.18A; P≤0.05). An additional phosphorus transporter, *P_iT-2* increased expression from 25 to 43 weeks in the kidney, followed by a steady decline through 95 weeks thereafter (Figure 5.18B; P≤0.05). Levels of *NaP_iIIb* were twice that of any other age at 80 weeks (Figure 5.18C; P≤0.05). Both renal *P_iT-1* and *P_iT-2* expression remained relatively low at 1:30 and 6:00 HPOP, increased substantially at 15:00 HPOP, and then decreased slightly at 21:00 HPOP (Figure 5.18D - 5.18E; P≤0.05). However, their expression differed in the magnitude of the increase between 6:00 and 15:00 HPOP, such that *P_iT-1* increased more than 6-fold, while *P_iT-2* increased 3-fold (Figure 5.18D - 5.18E; P≤0.05). No differences in the expression of *NaP_iIIb* were observed across HPOP (Figure 5.18F; P>0.05). A significant HPOP-by-age interaction was observed for renal *NaP_iIIa* (Figure 5.18G; P≤0.05). Expression of renal *NaP_iIIa* was substantially greater at 80 weeks during 1:30, 15:00, and 21:00 HPOP; however, at all other ages and HPOP, expression was lower and relatively consistent.

Shell Gland. A significant HPOP-by-age interaction was observed for *P_iT-1* in the shell gland (Figure 5.19A; P≤0.05). During bone mineralization at 1:30 HPOP, expression was lower for hens at 25 and 43 weeks of age compared to older hens at 80 and 95 weeks of age (Figure

5.19A; P≤0.05). At 6:00 HPOP, as hens transition from bone mineralization to eggshell calcification, *P_iT-1* levels were similar to those at 1:30 HPOP except for 80 weeks, which was more than 3-fold greater than any other age at this time (Figure 5.19A; P≤0.05). During peak eggshell calcification at 15:00 HPOP, *P_iT-1* levels increased approximately 7-fold for hens at 25, 43, and 95 weeks of age and 2-fold for 80 week old hens from those at 6:00 HPOP and did not differ across ages (Figure 5.19A; P≤0.05). Following this, as hens transition from eggshell calcification to bone mineralization at 21:00 HPOP, expression levels of *P_iT-1* tended to decrease in 25 and 43 week old hens, while 80 and 95 weeks old hens maintained similar *P_iT-1* expression to 15:00 HPOP (Figure 5.19A; P≤0.05). No significant HPOP-by-age interactions were observed for *P_iT-2* or *NaP_iIIb* in this tissue (P>0.05), so data for interactive means are shown in Appendix C (Figure C13), and main effect means for hen age and HPOP are reported here (Figure 5.19B – 5.19E). Expression of *P_iT-2* in the shell gland increased between 25 and 43 weeks, remained stable from 43 to 80 weeks, and then increased further between 80 and 95 weeks (Figure 5.19B; P≤0.05). Shell gland *NaP_iIIb* did not vary with age (Figure 5.19C; P>0.05). Levels of *P_iT-2* mRNA increased between 1:30 and 6:00 HPOP before steadily declining through 21:00 HPOP (Figure 5.19D; P≤0.05). Expression of *NaP_iIIb* in the shell gland decreased 5-fold between 1:30 and 6:00 HPOP, remained consistently low at 15:00 HPOP, and increased again at 21:00 HPOP to levels more than 29-fold greater than those noted at 15:00 HPOP (Figure 5.19E; P≤0.05).

Bicarbonate Production and Transport

Eggshell is primarily composed of calcium carbonate, which is formed from the precipitation of calcium and bicarbonate ions within the lumen of the shell gland. These bicarbonate ions are produced locally by carbonic anhydrase (CA2) in shell gland epithelial cells; however, they can also be derived from circulation. Both circulating and locally produced bicarbonate are transported

by solute carrier family 26 member 9 (SLC26A9) in the shell gland. As such, the expression of these genes was evaluated in the shell gland along with the corresponding levels of bicarbonate in circulation. No significant HPOP-by-age interactions were observed for shell gland *CA2*, *SLC26A9*, or circulating bicarbonate ($P>0.05$), so data for interactive means are shown in Appendix C (Figure C15), and main effect means for hen age and HPOP are reported here (Figure 5.20A – 5.20F).

Across production stages, both *CA2* and *SLC26A9* increased between 25 and 43 weeks and then maintained similar expression through 80 weeks; however, at 95 weeks, *CA2* remained consistent while *SLC26A9* decreased by more than 2-fold (Figure 5.20A-5.20B; $P\leq0.05$). Circulating bicarbonate also rose between 25 and 43 weeks and thereafter, levels were reduced again at 80 and 95 weeks (Figure 5.20C; $P\leq0.05$). During the daily egg formation cycle, expression of *CA2* doubled from 1:30 to 6:00 HPOP, then steadily declined again through 21:00 HPOP. Levels of *SLC26A9* sharply increased between 1:30 and 15:00 HPOP, such that at 15:00 HPOP, expression was 8-fold greater than at 1:30 HPOP (Figure 5.20E; $P\leq0.05$). Following that, *SLC26A9* levels declined to less than half of those noted at 1:30 HPOP (Figure 5.20E; $P\leq0.05$). Circulating bicarbonate levels paralleled those of *SLC26A9*, with a constant increase between 1:30 and 15:00 HPOP and a decline at 21:00 HPOP (Figure 5.20F; $P\leq0.05$).

Markers of Hepatic and Renal Function

The liver and kidney contribute to an array of metabolic processes, including the production of vitamin D_3 and the renal absorption of minerals. As such, monitoring renal and hepatic function by assessing circulating levels of select markers during the hen's productive lifetime is essential to evaluating physiological disruptions that may occur. Significant HPOP-by-age interactions were observed for circulating AST and CK (Figure 5.21A - 5.21B; $P\leq0.05$). At 1:30 HPOP, AST and

CK increased from 25 to 95 weeks of age, and at 15:00 HPOP, both metabolites tended to increase from 25 through 80 weeks but numerically decreased at 95 weeks (Figure 5.21A - 5.21B; P≤0.05). The two metabolites differed at 6:00 HPOP, where AST declined progressively from 25 to 80 weeks, and increased again at 95 weeks, while CK was elevated at 43 and 95 weeks but tended to be lower at 25 and 80 weeks (Figure 5.21A - 5.21B; P≤0.05). Lastly, at 21:00 HPOP, concentrations of AST did not differ significantly; however, CK increased more than two-fold between 25 and 80 weeks but diminished slightly at 95 weeks (Figure 5.21A-5.21B; P≤0.05). No significant HPOP-by-age interactions were observed for UA in this tissue (P>0.05), and data for interactive means are shown in Appendix C (Figure C14), while main effect means for hen age and HPOP are reported here (Figure 5.21C - 5.21D). Concentrations of UA increased between 25 and 43 weeks, maintained similar concentrations between 43 and 80 weeks, and were greatest at 95 weeks (Figure 5.21C; P≤0.05). In contrast, no differences in UA were observed within the 24-hour oviposition cycle (Figure 5.21D; P>0.05). No significant HPOP-by-age interactions were observed for circulating tProt or Alb (P>0.05), and data for interactive means are shown in Appendix C (Figure C14), while main effect means for hen age and HPOP are reported here (Figure 5.22A - 5.22D). Levels of tProt increased significantly from 25 through 95 weeks of age (Figure 5.22A; P≤0.05), while Alb concentrations were only notably elevated between 25 and 43 weeks and remained similar at older ages (Figure 5.22B; P≤0.05). Within the 24 hours taken to form an egg, both tProt and Alb were greatest at 6:00 and 15:00 and reduced at 1:30 and 21:00 HPOP (Figure 5.22C - 5.22D; P≤0.05). A significant HPOP-by-age interaction was observed for circulating Glob (Figure 5.22E; P≤0.05). At 1:30 HPOP, Glob concentrations were similar at 25 and 43 weeks and then incrementally increased at both 80 and 95 weeks (Figure 5.22E; P≤0.05). At all other HPOP, Glob

significantly increased at each age and continued to rise at 6:00 HPOP at 95 weeks but did not differ between 80 and 95 weeks at 15:00 and 21:00 HPOP (Figure 5.22E; P≤0.05).

Circulating Electrolytes

Circulating electrolytes such as Na^+ and K^+ maintain cellular osmotic balance, participate in ion transport, and contribute to the blood's acid-base balance. As such, evaluating fluctuations in Na^+ and K^+ in circulation within the daily egg formation cycle and across egg production stages is vital to elucidate factors contributing to homeostatic imbalances in mineral metabolism in hens. As no significant HPOP-by-age interactions were observed for Na^+ in this tissue (P>0.05), data for interactive means are shown in Appendix C (Figure C15), and main effect means for hen age and HPOP are reported here (Figure 5.23A , 5.23B)**.** Circulating Na^+ was elevated at 43 weeks and lower at all other ages (Figure 5.23A; P≤0.05), while during the 24-hour lay cycle, it was highest at 1:30 and 21:00 HPOP and significantly lower at 6:00 and 15:00 HPOP (Figure 5.23B; P≤0.05). A significant HPOP-by-age interaction was observed for circulating K^+ (Figure 5.23C; P>0.05). Circulating K^+ concentrations were similar across all ages at 1:30 and 15:00 HPOP, and levels at 15:00 HPOP were lower than those at 1:30 and 6:00 HPOP. At 6:00 HPOP, concentrations of K^+ tended to decrease linearly with age, except for at 43 weeks, which was notably lower and similar to concentrations observed at 95 weeks (Figure 5.23C; P≤0.05). At 1:30 and 21:00 HPOP, K^+ concentrations were similar in 25 and 43 week old hens, and concentrations significantly increased at both 80 and 95 weeks as hens aged (Figure 5.23C; P≤0.05).

Blood Acid-Base Balance

The acid-base balance of the blood significantly impacts the availability of calcium in circulation and influences the availability of bicarbonate ions for processes such as buffering and shell calcification. As such, markers of the acid-base status were measured in circulation during egg

formation and across stages of egg production. Significant HPOP-by-age interactions were observed for blood pH, anion gap, and base excess (Figure 5.24A - 5.24C; P≤0.05). Blood pH exhibited similar changes at 1:30 HPOP and 21:00 HPOP during bone mineralization and eggshell-to-bone transition periods, respectively, such that 25 and 43 weeks shared comparable pH values and pH was significantly lower at 80 and 95 weeks (Figure 5.24A; P≤0.05). At 6:00 HPOP, in the bone-to-eggshell transition period, hens at 25, 43, and 80 weeks had similar pH values; however, at 95 weeks, pH was significantly lower than 25 and 43 weeks (Figure 5.24A; P≤0.05). Lastly, during 15:00 HPOP, the period of peak eggshell calcification, blood pH declined at each age from 25 through 95 weeks (Figure 5.24A; P≤0.05). The anion gap observed closely resembled the changes in pH such that it typically diminished as hens aged at all HPOP (Figure 5.24B; P≤0.05). The most significant differences were noted at 1:30, 6:00, and 21:00 HPOP, where the anion gap significantly decreased at each age between 25 and 80 weeks (Figure 5.24B; P≤0.05). At 95 weeks, the anion gap was comparable to 80 weeks at 1:30, 6:00, and 15:00 HPOP but resembled values observed at 43 weeks at 21:00 HPOP (Figure 5.24B; P≤0.05). In contrast, at 15:00 HPOP, the only notable decrease in anion gap occurred between 25 and 43 weeks, while other ages exhibited similar values to those at 43 weeks (Figure 5.24B; P≤0.05). Circulating base excess was lowest at 1:30 HPOP, with hens either exhibiting a near-zero (25 and 43 weeks) or small negative (80 and 95 weeks) measurement (Figure 5.24C; P≤0.05). At 6:00 HPOP, base excess levels tended to be slightly greater than those observed at 1:30 HPOP and similar across ages (Figure 5.24C; P≤0.05). During peak eggshell calcification at 15:00 HPOP, younger hens (25 and 43 weeks) demonstrated the highest base excess that was more than 4-fold greater than levels observed at 1:30 HPOP; however, older hens (80 and 95 weeks) exhibited lower base excess levels that were half of those at younger ages at 15:00 HPOP (Figure 5.24C; P≤0.05). Lastly, at 21:00 HPOP, hens at 25, 80, and

95 weeks had a lower base excess akin to levels at 1:30 HPOP (Figure 5.24C; P≤0.05). Peak production hens at 43 weeks showed a lower reduction in base excess concentrations between 15:00 and 21:00 (Figure 5.24C; P≤0.05).

Blood Gases

Blood gases such as O_2 and CO_2 are a measure of respiratory activity and directly influence the acid-base balance of the blood. It is, therefore, essential to evaluate fluctuations in blood gases to delineate the factors contributing to physiological disturbances in the blood of laying hens. A significant HPOP-by-age interaction was observed for pO_2 (Figure 5.24A; P≤0.05). At 1:30 HPOP, pO_2 was comparable across ages. At 6:00 HPOP, pO_2 was lowest at 25 weeks and maintained at greater levels at older ages (Figure 5.25A; P≤0.05), while at 15:00 HPOP, increases occurred between 25 and 43 weeks, and levels decreased significantly again at 95 weeks (Figure 5.25A; P≤0.05). Lastly, at 21:00 HPOP, pO_2 levels were comparable to those observed at 1:30 and consistent from 25 through 80 weeks, although a significant decline in pO_2 was noted at 95 weeks (Figure 5.25A; P≤0.05). As no significant HPOP-by-age interactions were observed for pCO_2 or TCO_2 (P>0.05), data for interactive means are shown in Appendix C (Figure C16), and main effect means for hen age and HPOP are reported here (Figure 5.25B – 5.25E). Across the productive lifetime of the hen, pCO_2 progressively increased between each age from 25 through 95 weeks (Figure 5.25B; P≤0.05), while tCO_2 was elevated at 43 and 95 weeks of age and lower at 25 and 80 weeks of age (Figure 5.25C; P≤0.05). During the egg formation cycle, pCO2 was notably higher at 15:00 HPOP and lower at all other HPOP (Figure 5.25D; P≤0.05). Levels of TCO_2, on the other hand, steadily increased between 1:30 HPOP and 15:00 HPOP but decreased to an intermediate level at 21:00 HPOP (Figure 5.25E; P≤0.05).

Blood Glucose

Circulating Glu functions as an energy source for a multitude of cells, including those involved in eggshell mineralization and bone mineralization. Furthermore, Glu is an effective marker of nutritional status. Therefore, monitoring blood Glu during daily egg formation and across ages may provide insights into cellular energy metabolism during physiologically stressful periods. A HPOP-by-age interaction was observed for circulating Glu, wherein concentrations were consistent at 1:30 and 6:00 across all ages; however, at 15:00 and 21:00 HPOP, hens were unable to maintain blood Glu levels as they aged, with levels steadily declining from 25 through 95 weeks (Figure 5.26; $P \leq 0.05$).

Discussion

The extension of the modern hens' productive lifetime, coupled with selection for higher egg production, has been associated with poor eggshell quality and weakened skeletal integrity in older hens. The aforementioned eggshell quality and skeletal issues pose significant economic and animal welfare concerns and are likely linked to imbalances in calcium and phosphorus homeostasis that occur as hens age. As such, this study sought to investigate the physiological regulation of calcium and phosphorus uptake and utilization during the daily egg formation cycle from early through extended lay. Differences in mRNA expression were measured without additional investigation into differences in associated protein levels. Since changes in mRNA expression may not reflect functional modifications at a cellular level in all cases, caution should be used when interpreting these results. Nonetheless, these data help identify systems and processes potentially involved in regulating calcium and phosphorus homeostasis during the daily lay cycle and across production stages. Findings suggest that physiological systems supporting eggshell mineralization are not fully developed at 25 weeks of age, and substantial metabolic imbalances are notable by 80 weeks that may contribute to diminished egg production and eggshell

quality at 95 weeks. A factor likely contributing to the observed imbalances was the decreased production of biologically active $1,25(OH)_2D_3$ in older hens coupled with an indication of reduced renal function and acid-base disturbances. Dry matter digestibility decreased across ages at 1:30 HPOP, potentially reducing the availability of substrates necessary for bone mineralization that occurs at this time. Furthermore, renal phosphorus transporter expression was elevated during peak eggshell calcification at 15:00 HPOP and at 80 weeks, suggesting that these are likely periods of elevated bone breakdown. Lastly, novel expression patterns for avian *CYP27B1* were measured in the ileum, kidney, and shell gland, providing fundamental information on vitamin D_3 metabolism in laying hens.

Active vitamin D_3 is a crucial component of systems that govern calcium and phosphorus physiology through its effects on vitamin D_3-responsive genes. The initial hydroxylation of vitamin D_3 into $25(OH)D_3$ occurs in the liver and is performed by 25-hydroxylase (*CYP2R1*). Circulating $25(OH)D_3$ is taken up via endocytosis in the renal proximal renal tubules by megalin and cubilin receptors (Kuwata et al., 2024) and converted to either $1,25(OH)_2D_3$ by 1α-hydroxylase (*CYP27B1*) or $24,25(OH)_2D_3$ by 24-hydroxylase (*CYP24A1*). Circulating $25(OH)D_3$ in this study did not differ between birds at early, peak, or extended production (Figure 5.1), supporting the hypothesis that this reaction is less tightly regulated than ones producing other vitamin D_3 metabolites (Tucker et al., 1972a). However, during late production at 80 weeks, a transient 40% increase in $25(OH)D_3$ for almost all HPOP was observed (Figure 5.1). Interestingly, while hepatic *CYP2R1* was elevated at 43 weeks compared to all other ages, the same was not true at 80 weeks (Figure 5.7). Instead, renal *CYP27B1* was considerably higher at 80 weeks than at all other ages, while renal *CYP24A1* was substantially lower (Figure 5.3). This increased expression of 1α-hydroxylase and the reduction of 24-hydroxylase expression may represent a compensatory

mechanism to increase $1,25(OH)_2D_3$ formation in late production hens; however, corresponding increases in $1,25(OH)_2D_3$ were not observed (Figure 5.1), possibly due to its rapid utilization.

Further perturbations in circulating vitamin D_3 metabolites were also observed in older hens for $1,25(OH)_2D_3$ and $24,25(OH)_2D_3$ (Figure 5.1). The circulating levels of $1,25(OH)_2D_3$ typically decreased with age, with the largest reduction noted between 25 and 95 weeks during peak eggshell calcification at 15:00 HPOP. Conversely, concentrations of $24,25(OH)_2D_3$ increased between 80 and 95 weeks at most HPOP, with the greatest increase at 15:00 HPOP when $1,25(OH)_2D_3$ decreased. The reduction in the biologically active form of vitamin D_3 in aged hens is in line with previous findings (Abe et al., 1982; Joyner et al., 1986); however, the increase in $24,25(OH)_2D_3$ during egg production in aged hens has not been observed previously and provides insights into the physiological pathways that become disrupted during egg formation in aged hens. One mechanism that may contribute to the decline in circulating $1,25(OH)_2D_3$ is the reduction in cubilin expression noted in the renal tubules of aged hens (Kuwata et al., 2024). Since this receptor is responsible for the renal uptake of $25(OH)D_3$, decreased expression may limit $25(OH)D_3$ availability, consequently reducing $1,25(OH)_2D_3$ production (Nykjaer et al., 2001).

Findings from this study also provided evidence that vitamin D_3 metabolism may occur within non-canonical tissues. Typically, the liver has been categorized as the primary tissue responsible for the production of circulating $25(OH)D_3$ (Bikle, 2018); however, this study and previous studies by our lab have shown that kidney expression of *CYP2R1* significantly increases after the onset of lay (Garcia-Mejia et al., 2024) and that it is robustly expressed during peak and late eggshell calcification at 15:00 and 21:00 HPOP (Figure 5.3; Sinclair-Black et al,. 2024). Furthermore, renal *CYP27B1* was elevated during these same HPOP, while *CYP24A1* was at its lowest (Figure 5.3). Together, these findings suggest that the kidney is likely capable of performing

both hydroxylation steps involved in forming $1,25(OH)_2D_3$ during peak and late eggshell calcification, potentially increasing the efficacy of local mineral transport during these HPOP.

The ileum and shell gland, which are not traditionally associated with vitamin D_3 metabolism, also expressed *CYP2R1*, *CYP24A1*, and *CYP27B1* (Figure 5.2 and Figure 5.4), suggesting that these tissues may utilize local vitamin D_3 conversion as an additional regulatory step to control the transcription of genes associated with mineral transport. Although shell gland *CYP27B1* was not altered across ages, during the daily lay cycle it was low from 1:30 through 15:00 HPOP and significantly greater during late eggshell calcification at 21:00 HPOP (Figure 5.4). This expression pattern closely resembled the expression profile of shell gland *PMCA1* (Figure 5.16), potentially linking the regulation of this calcium transporter to local hydroxylation of vitamin D_3 within the shell gland. Ileal expression of *CYP2R1* was notably elevated at 80 weeks compared to all other ages, while ileal *CYP27B1* decreased steadily at each age (Figure 5.2). The diminishing expression of *CYP27B1* with age may also be related to the decline in ileal *NCX* expression (Figure 5.14), likely contributing to reduced intestinal calcium absorption in older hens. The dynamic expression of these enzymes during the daily egg formation may represent a mechanism by which local conversion of vitamin D_3 improves the efficiency of calcium and phosphorus regulation in independent tissues. It should also be noted that until recently, *CYP27B1* had not been correctly identified in avian species (Sinclair-Black et al., 2023). Therefore, this study is the first to evaluate *CYP27B1* expression in key tissues throughout an extended lay period during the daily egg formation cycle.

A further factor that may impact the efficiency of vitamin D_3 metabolism over time is tissue integrity of the kidney and liver. In mice, hepatic and renal function deteriorates over time (Lim et al., 2012; Hunt et al., 2019). Although kidney and liver pathologies are common in laying hens

(Mallinson et al., 1983; Shini et al., 2019), there are no published studies longitudinally evaluating indicators of renal and kidney function in layers to our knowledge and there has only been one study to date comparing markers of renal function across the productive lifetime in broiler breeder hens (Rezende et al., 2021). Circulating AST, CK, UA, tProt, and albumin can be measured to evaluate the health status of the liver and kidney. Aspartate aminotransferase is an enzyme responsible for the catabolism of amino acids and is primarily produced by the liver and skeletal muscle (Thapa et al., 2006). Cellular damage to either of these tissues results in the release of AST into circulation, resulting in elevated levels in plasma. Since the AST produced by either muscle or liver is indistinguishable, a second muscle-specific damage marker, such as CK, is measured to distinguish the likely site of tissue damage (Korones et al., 2001). Findings from our study showed a HPOP-by-age interaction for both AST and CK; however, the overall pattern across both markers was similar, such that when AST was elevated, CK generally followed the same pattern (Figure 5.21), suggesting that observed differences in AST are likely unrelated to liver damage. Maintenance of normal liver function as hens age is further supported by levels of circulating Alb, which increased slightly between 25 and 43 weeks of age and remained relatively consistent through 95 weeks (Figure 5.22). Renal function can be evaluated using circulating UA and tProt as biomarkers. Uric acid is a waste product of nitrogen metabolism excreted by the kidney; however, unlike urea excreted by mammals, UA is insoluble, and its excretion is controlled by active secretion into the proximal tubules (Braun, 1999). Uric acid production can be influenced by factors such as diet and reproductive state in avian species (Bell et al., 1958); however, elevated UA is also associated with factors such as tubular nephrosis and dysfunctional proximal convoluted tubes in birds (Scope et al., 2020). In this study, UA steadily increased as hens aged from early through extended egg production stages, with significant increases in the transitions between early

(25 weeks) and peak egg production (43 weeks) and again between late (80 weeks) and extended (95 weeks) production (Figure 5.22). Similarly, blood tProt, which can be impacted by the systemic fluid balance, also increased at each subsequent age (Figure 5.22). Together, changes in AST, CK, UA, and tProt demonstrate that, while liver function appears to be maintained in older hens, the capacity of the kidney to regulate fluid balance and excrete waste products diminishes as hens age and could alter its ability to participate in vitamin D_3 metabolism and mineral homeostasis.

The acid-base balance of the blood is maintained by pulmonary and renal function. It is interlinked with calcium and phosphorus homeostasis through its influence on calcium availability in the blood and by the production of bicarbonate ions. Circulating electrolytes such as Na^+ and K^+ are crucial in maintaining cellular osmotic balance and participating in mineral transporter activity. During the period immediately following oviposition at 1:30 HPOP, both Na^+ and K^+ were significantly greater than during peak eggshell calcification at 15:00 HPOP (Figure 5.23). This decrease in circulating Na^+ at 15:00 HPOP may be due to the increased renal resorption of calcium, whereby sodium is exchanged for calcium in renal tubules by the calcium transporter NCX1. Early studies in laying hens found no differences in pH levels as hens aged (Hamilton, 1980); however, in the current study pH and anion gap were notably lower at 80 and 95 weeks than at 25 and 43 weeks (Figure 5.24). Changes in pH and anion gap observed here can likely be attributed to the observation that renal function diminished in older hens. Nonetheless, distinguishing metabolic status requires the evaluation of additional parameters such as pCO_2 and HCO_3 (Mongin, 1968). Blood pCO_2 is an indicator of pulmonary activity and a volatile acid that can lead to respiratory acidosis when at higher levels. Reference ranges established in young Lohman hens (21-37 weeks) state that pCO_2 ranges from 13 to 38 mmHg and bicarbonate from 14 to 24 mmol/L (Ding et al., 2021). Within the daily egg formation cycle, hens had significantly elevated pCO_2 above the

reference range during rapid eggshell calcification at 15:00 HPOP compared to all other HPOP that were at the upper end of the reference range. Across ages, pCO_2 levels increased steadily from 25 through 95 weeks, with levels well above the reference range observed at 80 and 95 weeks (Figure 5.25). Bicarbonate levels also were highest during rapid eggshell calcification at 15:00 HPOP, and closely resembled the expression of bicarbonate transporter *SLC26A9* in the shell gland. The simultaneous increases in blood bicarbonate levels and elevated shell gland expression of *SLC26A9* at 15:00 HPOP in this study support the utilization of circulation-derived bicarbonate for eggshell calcification (Mongin, 1968). Across different ages, bicarbonate was also greatest during peak lay at 43 weeks (Figure 5.20). Together, it appears that circulating bicarbonate is used for eggshell calcification, and the overall elevated bicarbonate levels may also have been a compensatory measure to combat the effects of elevated pCO_2 and lower pH. However, these results should be interpreted cautiously due to the limited blood biochemistry data and reference rages available for older hens. Consequences of observed decreased blood pH with age may have included elevated renal calcium loss (Nijenhuis et al., 2006), decreased 1α-hydroxylase activity (Sauveur, 1977), and increased bone breakdown, as seen in mice (Goto, 1918; Meghji et al., 2001). Together, these metabolic changes potentially contribute to poor-quality eggshells and increased prevalence of osteoporosis in older hens. It should also be noted that environmental conditions such as ambient temperature and humidity may influence the respiratory rate of laying hens, since avian species rely on panting to dissipate excess body heat (Smit et al., 2018). In the current study, TCO_2 appears to be correlated to differences in environmental conditions, such that levels were greatest at 43 and 95 weeks and substantially lower at 25 and 80 weeks (Figure 5.25). Sampling at 43 and 95 weeks occurred during cooler periods of the year (Appendix D1) when hens would likely have a lower occurrence of panting, and consequently, a greater TCO_2 was found in circulation.

Interestingly, pCO_2 did not share similar trends, nor did pO_2, which are considered to be a more reliable index of pulmonary function since they are measured directly and are not a calculated value. Nonetheless, differences in environmental conditions may have contributed to some of the acid-base disturbances observed in this study.

Transcriptional regulation by $1,25(OH)_2D_3$ is achieved following binding to VDR and subsequent complex formation with heterodimeric partners RXRA or RXRG at vitamin D response elements on DNA (Bikle, 2014). As such, the differential expression of these proteins may influence the regulation of vitamin D_3-responsive genes such as *CALB1*, *PMCA1*, and *TRPV6* (Hall et al., 1990; Lee et al., 2015). Ileal expression of *VDR* was heightened at 15:00 and 21:00 HPOP during periods of elevated calcium demand for eggshell formation, while *RXRA* and *RXRG* levels were unaffected by HPOP (Figure 5.5). Expression of ileal calcium transporters *PMCA1* and *CALB1* paralleled *VDR*, suggesting that *VDR* may drive temporal differences in ileal vitamin D_3-dependant mineral transporter expression. Similarly, the shell gland exhibited distinct changes in *VDR* within the 24-hour egg-laying cycle. Expression of *VDR* increased steadily between bone mineralization at 1:30 HPOP and peak eggshell calcification at 15:00 HPOP but declined again by 21:00 HPOP (Figure 5.8). Interestingly, while shell gland *CALB1* showed a comparable expression profile to *VDR* (Figure 5.16), it has previously been thought that shell gland CALB1 may not be regulated by the actions of $1,25(OH)_2D_3$ (Bar et al., 1990b) but instead may be driven by estrogen (Nys et al., 1992b) due to the presence of estrogen response elements as observed in mice (Gill et al., 1995). Nonetheless, elevated expression of shell gland *VDR* at 15:00 HPOP during rapid eggshell calcification coupled with a 4-fold increase in the expression of *RXRG* at 6:00 HPOP, as the egg enters the shell gland, strongly suggests that the process of eggshell calcification is at least

in part regulated by the genomic actions of $1,25(OH)_2D_3$, potentially through other mineral transporters not measured herein.

In addition to the effects of vitamin D_3, other hormones such as PTH and CALC also contribute to the physiological regulation of calcium and phosphorus metabolism. When iCa^{2+} is low, PTH is released into circulation to re-establish circulating iCa^{2+} levels within the homeostatic range. This effect is achieved by increasing the production of $1,25(OH)_2D_3$ (Brenza et al., 2000), decreasing the formation of $24,25(OH)_2D_3$ (Tanaka et al., 1975), and facilitating bone breakdown (Taylor et al., 1969). Additionally, in broiler chicks, vitamin D_3-independent effects of PTH on intestinal calcium and phosphorus absorption have been identified (Nemere et al., 1986; Nemere, 1996). Previous studies conducted in our lab also showed a more than 50-fold increase in ileal *PTH1R* following the onset of lay (Garcia-Mejia et al., 2024), further supporting the direct effects of PTH on the intestinal mineral transport. In this study, ileal *PTH1R* declined between 1:30 and 6:00 HPOP, increased again at 15:00 HPOP, and remained elevated through 21:00 HPOP (Figure 5.10). This pattern was also noted for the ileal calcium transporters *PMCA1* and *CALB1* (Figure 5.14) but not for any phosphorus transporters measured during the daily lay cycle, suggesting that the availability of PTH1R in mature laying hens may have a greater influence on ileal calcium absorption than phosphorus absorption during the 24-hour oviposition cycle. Furthermore, the hormonal sensitivity to PTH was likely increased after early production at 25 weeks due to observed increases in *PTH1R* receptor expression in older hens (Figure 5.10).

Expression of *PTH1R* was also noted to change in a HPOP-dependent fashion in the shell gland; however, in this tissue, it may contribute to phosphorus regulation instead. Shell gland expression of *PTH1R* was substantially elevated in the hours before and after oviposition at 21:00 and 1:30 HPOP compared to 6:00 and 15:00 HPOP (Figure 5.12), once the egg has reached the

shell gland and during peak calcification. This expression pattern was comparable to the phosphorus transporter *NaP$_i$IIb* expression (Figure 5.19), potentially linking *PTH1R* to the hormonal regulation of *NaP$_i$IIb* in the shell gland during the daily lay cycle. An additional shell gland phosphorus transporter, *P$_i$T-1*, was elevated at 15:00 HPOP and 21:00 HPOP during periods of eggshell calcification; however, older hens (80 and 95 weeks) expressed twice as much *P$_i$T-1* at 21:00 HPOP than younger hens (25 and 43 weeks) (Figure 5.19). Within the eggshell, phosphorus forms part of the hydroxyapatite crystal layer directly beneath the cuticle (Cusack et al., 2003). Since phosphorus has been shown to inhibit calcite formation (Bachra et al., 1963; Simkiss, 1964), it has been speculated that the formation of these crystals or the secretion of other phosphorus-containing organic eggshell compounds may induce the termination of eggshell calcification (Nys et al., 1991; Dennis et al., 1996). In the current study, decreased expression of *SLC26A9*, a bicarbonate transporter, coupled with heightened expression of phosphorus transporters *P$_i$T-1* and *NaP$_i$IIb* in the shell gland at 21:00 HPOP (Figure 5.19) may provide evidence that phosphorus outcompetes bicarbonate to slow eggshell calcification at 21:00 HPOP. Furthermore, the elevated levels of *P$_i$T-1* towards the end of eggshell calcification observed in older hens may have led to an earlier cessation of eggshell calcification, resulting in a lower degree of mineralization reflected by the lower observed eggshell weights in older hens (Table 5.6).

Primary factors influencing eggshell integrity and breaking strength include eggshell thickness and composition (Lund et al., 1937). Findings from this study revealed an inverse relationship between eggshell thickness and breaking strength (Figure 5.5). Eggshell thickness is influenced by egg size in relation to the amount of eggshell deposited, with larger eggs having thinner eggshells given the same amount of eggshell deposited. Results herein demonstrated numerical decreases in wet and dried, demembranated eggshell weights, and the percentage

eggshell also declined with age (Tables 5.5, 5.6). Together, it appears that the decrease in breaking strength observed in aged hens in this study resulted from decreased eggshell mineralization and an increased egg size. The eggshell mineral composition may also affect structural characteristics of the eggshell directly by influencing crystal formation (Simkiss, 1964) or indirectly by acting as a cofactor for enzymes such as carbonic anhydrase (Fernandez et al., 2000; McCall et al., 2000). Approximately 95% of the eggshell is comprised of calcium carbonate, while the remainder includes Mg, P, Zn, Fe, Cu, S, and Al (Schaafsma et al., 2000). This study's findings identified a significant decrease in the percentage of calcium in the eggshell as hens aged (Table 5.7). Park et al. (2018) observed similar decreases in eggshell calcium content in older hens. Since calcium carbonate is the primary structural component of the eggshell, the measured decrease in eggshell calcium content may also contribute to the diminished breaking strength and reduced eggshell thickness in aged hens (Table 5.5). Additional factors that could have contributed to the inferior eggshell quality of older hens in this study arise from differences in iCa^{2+} at 6:00 HPOP, when the follicle has entered the shell gland and begins to calcify (Figure 5.9A). As eggshell calcification initiates, iCa^{2+} is rapidly utilized by the shell gland, resulting in decreased iCa^{2+} during periods of eggshell calcification (Luck et al., 1979). However, in this study, older hens (80 and 95 weeks) exhibited greater iCa^{2+} at 6:00 HPOP, suggesting a delayed initiation of eggshell calcification. As a result, hens in late and extended production may exhibit a shorter duration of eggshell mineralization, consequently reducing eggshell weight and thickness.

Expression of shell gland calcium transporters facilitates the delivery of iCa^{2+} to the developing eggshell. Investigations into the transporters responsible for mineral delivery to the shell gland highlighted *NCX1* and *PMCA1* as key calcium transport channels (Jonchere et al., 2012). Findings in this study showed that *NCX1* was equally expressed from the period before

ovum entry into the shell gland (1:30 HPOP) until peak eggshell calcification (15:00 HPOP) and lower at 21:00 HPOP, while *PMCA1* steadily increased from 6:00 HPOP to its highest levels at 21:00 HPOP (Figure 5.16). The dynamic alterations in gene expression of these transporters during daily egg formation support existing evidence that they are critical to eggshell mineralization and suggest that *NCX1* is likely involved in early and peak eggshell calcification, while *PMCA1* likely has a greater role in peak and late calcification of the eggshell. In addition, these transporters were also influenced by hen age, such that *NCX1* steadily decreased in expression from 43 to 95 weeks, while *PMCA1* increased between 25 and 43 weeks and remained stable thereafter. As such, the diminishing expression of *NCX1* in older hens may have limited calcium delivery to the developing eggshell and negatively impacted eggshell integrity. The chaperone protein *CALB1* is responsible for the transcellular movement of calcium ions (Bronner et al., 1988). During this study, shell gland expression of *CALB1* was low at all ages between 1:30 and 6:00 HPOP, suggesting the rate of calcium transfer to the shell gland lumen was low during these HPOP. Following this, shell gland *CALB1* expression levels increased approximately 12-fold at all ages during peak eggshell calcification at 15:00 HPOP to support rapid delivery of calcium ions to the eggshell. During late stages of eggshell calcification at 21:00 HPOP, young hens (25 and 43 weeks) decreased expression of *CALB1* from levels seen at 15:00 HPOP as expected; however, older hens (80 and 95 weeks) maintained elevated levels at 15:00 HPOP. Since calcium delivery at 21:00 HPOP would be expected to slow, elevated *CALB1* in the shell gland of older hens during this HPOP suggests that aged hens inefficiently transition out of eggshell calcification, and this may reduce circulating calcium availability for bone remineralization during this time.

In addition to calcium, the shell gland requires bicarbonate ions to form calcium carbonate (Nys et al., 1999). Bicarbonate ions needed for eggshell formation can be derived from circulation

or formed by carbonic anhydrase (CA2) in shell gland epithelial cells and transported into the shell gland lumen by SLC26A9 (Jonchere et al., 2012). Gene expression results from this study highlighted peak *CA2* expression at 6:00 HPOP, at the initiation of eggshell calcification. At the same time, levels of *SLC26A9* increased 8-fold from 1:30 to 15:00 HPOP, potentially demonstrating a mechanism whereby bicarbonate ions are produced at a greater rate during early eggshell calcification followed by efficient transport during peak eggshell calcification (Figure 5.20). During the daily lay cycle, circulating bicarbonate increased steadily from 1:30 to 15:00 HPOP and then declined at 21:00 HPOP (Figure 5.20). Although *SLC26A9* levels are not altered to the same magnitude, they closely resemble the patterns in circulating bicarbonate, suggesting that circulating bicarbonate levels may influence *SLC26A9* expression and that circulating bicarbonate likely plays a significant role in eggshell calcification. As hens entered extended egg production, expression of *SLC26A9* and circulating bicarbonate decreased, potentially reducing bicarbonate availability for calcifying the eggshell. The underlying causes of reduced mineral and ion transport to the eggshell with age likely stem from reductions in circulating $1,25(OH)_2D_3$ (Figure 5.1), reduced expression of *NCX1,* and imbalances in *CALB1* expression at 21:00 HPOP (Figure 5.16); however, there is also evidence to suggest that shell gland epithelial cells in aged hens undergo apoptosis and fibrosis, which would further impair eggshell mineralization processes (Park et al., 2018; Fu et al., 2024).

Tissue degradation in the shell gland of aged hens as observed by Park et al. (2018) likely leads to increased cellular regeneration and proliferation, which requires glucose as an energy source. In the current study, circulating glucose levels remained consistent across ages at 1:30 and 6:00 HPOP; however, at 15:00 and 21:00 HPOP, concentrations declined as hens aged from 25 through 95 weeks (Figure 5.26). As such, glucose may be removed from circulation during peak

eggshell calcification to maintain and repair shell gland tissue as hens age. Furthermore, mineral deposition onto the eggshell utilizes several ATP-dependent mineral transporters that potentially contribute to the reductions in glucose seen in this study during rapid eggshell calcification, highlighting the high energetic cost of eggshell formation (Wasserman et al., 1991). Glucose is also the primary monosacharide in the luminal fluid of the shell gland, and previous studies have shown that luminal glucose concentrations peak between 13:00 and 15:00 HPOP (Edwards, 1977; Arad et al., 1989). Therefore, in the current study, glucose may have been derived from circulation at these times to supply the luminal fluid in the shell gland. Interestingly, Watford et al. (1981) proposed that the chicken kidney may significantly contribute to glucose production via gluconeogenesis, and as such, the impaired renal function observed in older hens in this study may also contribute to the decreased circulating glucose levels.

The small intestine is an additional tissue whose function is likely negatively impacted by age. Diana et al. (2021) showed a significant decrease in calcium digestibility between 40 and 50 weeks, while another study demonstrated diminished dry matter digestibility between 19 and 75 weeks of age (Gu et al., 2021). Dry matter digestibility in chickens is influenced by intestinal integrity and feed passage rate, as reviewed by Ravindran et al. (2021). Our results observed a distinct interaction between HPOP and age for dry matter digestibility, where dry matter digestibility decreased steadily at all ages at 1:30 HPOP but remained consistent across ages at 15:00 HPOP and was generally higher than at 1:30 HPOP (Figure 5.13). During the dark phase, diet consumption is limited, thus slowing the passage rate of feed (Buyse et al., 1993), potentially allowing for greater overall dry matter digestibility at 15:00 HPOP. Contrastingly, at 1:30 HPOP immediately following oviposition, hens actively consume feed (Wood-Gush et al., 1970), possibly increasing feed passage rate and resulting in lower dry matter digestibility values. In this study,

feed intake levels (Table 5.4) generally increased across ages. Although feed intake was not measured in relation to HPOP, feed intake at 15:00 HPOP is limited and thus, increases in feed intake may have had some effect on the dry matter digestibility values at 1:30 HPOP (Figure 5.13). Nonetheless, it is possible that decreases in dry matter digestibility at 1:30 HPOP across ages may have negatively influenced the availability of dietary nutrients in aged hens, and future analysis of mineral digestibility of these samples may indicate to what extent bone and eggshell mineralization were affected.

Breakdown of labile medullary bone stores is required to provide up to 40% of the calcium required for eggshell calcification (Comar et al., 1949). Since bone is comprised of hydroxyapatite crystals [$Ca_5(PO_4)_3(OH)$], its resorption releases calcium and phosphorus into circulation. While the majority of calcium is used for eggshell calcification, phosphorus is utilized to a lesser extent and must be excreted by the kidney to prevent hyperphosphatemia (Miller et al., 1977b). As such, elevated expression of renal phosphorus transporters in conjunction with heightened circulating phosphorus is likely indicative of elevated levels of bone breakdown (Miller et al., 1977a). Results from this study showed greater expression of renal phosphorus transporters *P_iT-1,* and *NaP_iIIb* at 80 weeks of age (Figure 5.18) and a HPOP-by-age interaction for *NaP_iIIa* wherein its expression was doubled at 1:30 and 15:00 at 80 weeks compared to most other ages and HPOP (Figure 5.18). This suggests that elevated bone breakdown occurred during late production. Interestingly, circulating phosphorus was not significantly higher at 80 weeks of age, suggesting that the increased expression of renal phosphorus transporters observed in this study may have been adequate to prevent hyperphosphatemia from occurring.

Together, it is apparent that hens at 80 and 95 weeks of age experience imbalances in calcium and phosphorus homeostasis across multiple tissues, leading to poor eggshell quality and

elevated bone breakdown; however, the question remains at which point these imbalances start to take place. As a pullet matures, significant anatomical and physiological changes occur, such as the formation of labile medullary bone stores and the development of the reproductive tract (Etches et al., 1983; Whitehead, 2004). This tissue development, alongside the onset of egg production, substantially elevates the calcium and phosphorus requirements of young hens; however, to achieve this, the maturation of systems regulating mineral transport at a cellular level must also take place (Garcia-Mejia et al., 2024). Under commercial conditions, modern laying hens rapidly increase HDEP from 0% to over 90% between 19 and 25 weeks (H&N International, 2020). During this study, HDEP showed similarly swift increases aligned with or above breed standards for all ages, including 25 weeks, at which HDEP was 94.26 % (Table 5.4). However, gene expression results showed significantly lower levels during early egg production at 25 weeks compared to peak egg production at 43 weeks for the following genes: vitamin D_3 25-hydroxylase (*CYP2R1*) and genes regulating vitamin D_3 genomic responses (*VDR*, *RXRA*, and *RXRG*) in the shell gland and kidney, hormonal receptors in the kidney (*PTH1R*, *CASR*, and *CALCR*) and shell gland (*CALCR*), calcium transporters in the kidney (*NCX1*, *CALB1*, and *TRPV6*) and shell gland (*PMCA1*), and phosphorus transporters in the kidney (*P_iT-1* and *P_iT-2*) and shell gland (*P_iT-2*) (Figure 5.27). Since the availability of receptors is crucial to eliciting cellular signaling and genomic responses to circulating ligands, the lower expression of *VDR*, *PTH1R*, *CASR*, and *CALCR* during early production may have limited the capacity of the shell gland and kidney to respond to changes in hormones and minerals in the blood. Furthermore, these receptors regulate the transcription of mineral transporters, and lower expression likely limited mineral availability for processes such as eggshell calcification and bone mineralization during early production. It has been proposed by Dunn et al. (2021) that high egg production at younger ages may be negatively

correlated with bone mineralization in laying hens, particularly in the keel, and earlier studies by our lab identified keel deviations by 32 weeks of age (Garcia-Mejia et al., 2024). Therefore, these findings may demonstrate mechanisms through which high egg production, reduced hormonal responsiveness, and diminished mineral transport at an early age result in decreased bone mineralization and imbalances in calcium and phosphorus homeostasis in young hens.

In addition to differences between early (25 weeks) and peak (43 weeks) production ages, notable changes occurred between peak (43 weeks) and extended (95 weeks) production and these are summarized in Figure 5.27. Lower levels of circulating $1,25(OH)_2D_3$ in extended production hens may have altered expression of mineral transporters across tissues. Levels of *NCX1* significantly decreased in all tissues as hens aged along with renal *TRPV6* expression. Levels of *P_iT-2* were reduced between 43 and 95 weeks of age in both the ileum and kidney as well as ileal *NaP_iIIb*, suggesting that *NCX1* and *P_iT-2* may contribute to reduced mineral availability in aged hens. Shell gland phosphorus transporters *P_iT-1* and *P_iT-2* increased as hens progressed from peak through extended production, potentially increasing the rate at which eggshell calcification was terminated. Furthermore, iCa^{2+} concentration was also greater at 6:00 HPOP in aged hens compared to hens in peak production, likely as a result of delayed initiation of eggshell calcification. Together, reductions in circulating biologically active vitamin D_3 coupled with altered mineral transporter expression may contribute to dysregulated calcium and phosphorus availability for processes such as bone mineralization and eggshell calcification in extended production hens.

In conclusion, this study investigated the physiological regulation of calcium and phosphorus homeostasis at distinct stages of utilization during the 24-hour egg-laying cycle and at different ages, representing phases of production from early through extended lay. In doing so, key

transporters and regulatory pathways necessary for eggshell formation and bone mineralization were identified in the ileum, kidney, liver, and shell gland. Imbalances in mineral homeostasis and vitamin D_3 metabolism were observed from 80 weeks onwards and likely a consequence of impaired renal function and subsequently reduced circulating $1,25(OH)_2D_3$ and acid-base imbalances. Older hens also appeared to transition into and out of eggshell calcification less efficiently, potentially reducing the calcification period of the eggshell. Together, the observed physiological disturbances likely contributed to diminished eggshell quality and elevated bone breakdown observed in hens kept through extended production periods. These findings provide vital insights into the physiological processes that govern calcium and phosphorus utilization in laying hens and can be used to develop effective nutritional and genetic strategies geared toward enhancing eggshell quality and maintaining skeletal health.

Table 5.1. Ingredients and nutrient composition of diets fed during sampling for each production stage and age.

Ingredients, as-fed %	Early 25 weeks	Peak 43 weeks	Late 80 weeks	Extended 95 weeks
Corn	45.62	43.94	44.47	43.58
Soybean meal 47%	25.34	24.05	21.20	20.69
Wheat middlings	14.03	18.07	16.73	16.05
Coarse limestone	6.13	6.42	7.31	7.30
Fine limestone	3.31	2.80	1.87	1.87
Soybean oil	3.40	1.75	2.00	2.00
Alfalfa meal	-	1.00	4.87	5.98
Mono-dicalcium phosphate 21%	0.77	0.54	-	0.01
Sodium chloride	0.26	0.32	0.27	0.29
DL-Methionine	0.25	0.24	0.22	0.22
Sodium bicarbonate	0.13	0.16	0.30	0.30
Trace mineral premix[1]	0.08	0.07	0.07	0.07
L-Lysine HCL	0.03	0.03	0.03	0.04
Bacitracin methylene disalicylate	0.05	0.05	0.04	0.04
Arbocel®[2]	0.24	0.20	0.20	0.22
Choline chloride 60%	0.04	0.02	0.10	0.10
Vitamin premix[3]	0.03	0.03	0.03	0.03
L-Threonine	0.01	0.01	-	0.01
L-Tryptophan	0.01	0.01	0.01	0.01
Sand	-	-	-	0.90
Titanium dioxide[4]	0.30	0.30	0.30	0.30
Calculated nutrient content (analyzed)				
Crude protein	17.87 (18.10)	17.62 (17.70)	16.50 (16.70)	16.60 (17.20)
Crude fiber	3.91 (2.20)	3.86 (2.90)	3.33 (3.60)	3.30 (4.00)
Calcium	3.80 (3.84)	3.63 (3.30)	3.75 (3.37)	3.75 (3.66)
Total phosphorus	0.62 (0.65)	0.56 (0.50)	0.42 (0.49)	0.44 (0.47)

[1]Trace mineral premix provided the following per kilogram of diet: calcium min, 25.6 mg; calcium max, 33.6 mg; manganese min, 107.2 mg; zinc, 85.6 mg; magnesium, 19.8 mg; iron, 21 mg; copper, 3.2 mg; iodine, 0.8 mg; selenium min, 0.3 mg.

[2]JRS Pharma LP, Patterson, NY.

[3]Vitamin premix provided the following per kilogram of diet: vitamin A, 10000 IU; vitamin D3, 2000 IU; vitamin B-12, 30 mg; vitamin E, 3 IU; vitamin K (menadione), 3.5 mg; riboflavin, 10 mg; pantothenic acid, 45 mg; thiamine, 20 mg; niacin, 4 mg; pyridoxine, 0.006 mg; folic acid, 0.03 mg; biotin, 1 mg.

[4] Titanium dioxide and corn were mixed in a 35:65 ratio and ground to 0.5mm before being added to the diets to ensure an even distribution of the marker throughout the feed during mixing.

Table 5.2. An example of how hens were allocated to sampling groups at each age.

HPOP[1] group[2]	Hen oviposition time	Time of tissue collection	Stage of calcium and phosphorus utilization
21:00	8:22 AM[3]	5:22 AM	Eggshell-to-bone transition
	8:30 AM[3]	5:30 AM	
	9:41 AM[3]	6:41 AM	
01:30	7:25 AM[4]	8:55 AM	Bone remineralization
	8:18 AM[4]	9:48 AM	
	9:20 AM[4]	10:50 PM	
06:00	7:06 AM[4]	1:06 PM	Bone-to-eggshell transition
	8:35 AM[4]	2:35 PM	
	9:22 AM[4]	3:22 PM	
15:00	6:25 AM[4]	9:25 PM	Eggshell calcification
	7:11 AM[4]	10:11 PM	
	8:15 AM[4]	11:15 PM	

[1]Hours post-oviposition

[2]Not all hens allocated to each HPOP were sampled.

[3]Hypothetical oviposition time from the day immediately preceding sampling

[4]Oviposition time on the day of sampling

Table 5.3 Primers used for reverse transcription-quantitative PCR.

Target	Forward primer (5'-3')	Reverse primer (5'-3')	Transcript ID[1]
Vitamin D_3 metabolism and action			
CYP2R1	GGACAGCAATGGACAGTTTG	AGGAAAACGCAGGTGAAATC	09745
CYP24A1	TGGTGACACCTGTGGAACTT	CTCCTGAGGGTTTGCAGAGT	59161
VDR	CTGCAAAATCACCAAGGACA	CATCTCACGCTTCCTCTGC	96121
RXRA	ACTGCCGCTACCAGAAGTGT	GACTCCACCTCGTTCTCGTT	59924
RXRG	GAAGCCTACACGAAGCAGAA	CCGATCAGCTTGAAGAAGAA	49224
Calcium homeostasis and eggshell calcification			
CASR	CTGCTTCGAGTGTGTGGACT	GATGCAGGATGTGTGGTTCT	55986
PTH1R	CCAAGCTACGGGAAACAAAT	ATGGCATAGCCATGAAAACA	08796
CALCR	GCAGTTGCAAGAGCCAAATA	AGCTTTGTCACCAACACTCG	15478
CALB1	AAGCAGATTGAAGACTCAAAGC	CTGGCCAGTTCAGTAAGCTC	74265
NCX1	TCACTGCAGTCGTGTTTGTG	AAGAAAACGTTCACGGCATT	13920
PMCA1	TTAATGCCCGGAAAATTCAC	TCCACCAAACTGCACGATAA	80355
TRPV6	TATGCTGGAACGAAAACTGC	TTGTGCTTGTTGGGATCAAT	23779
CA2	CCTGACTACTCCACCACTGC	TCTCAGCACTGAAGCAAAGG	52439
SLC26A9	TCCACGATGCTGTTTTGTTT	GAGCTGCTTTCATCCACAGA	01070
Phosphorus homeostasis			
P_it-1	TATCCTCCTCATTTCGGCGG	CTCTTCTCCATCAGCGGACT	94781
P_it-2	CCATCCCCGTGTACCTTATG	AGACATGGCCATCACTCCTC	51992
NaP_iIIa	ATCGGCTTGGGGGTGATC	GAGGGCGATCTGGAAGGAG	58978
NaP_iIIb	AAAGTGACGTGGACCATG	GAGACCGATGGCAAGATCAG	23222
Housekeeping Genes			
GAPDH	AGCCATTCCTCCACCTTTGAT	AGTCCACAACACGGTTGCTGTAT	23323
CYCLO	GCTCATGAAATTGCCCCTGA	GCGTAAGCTGCCTTCTCTTTCTC	15382
RPL5	CGTTACCTGATGGAGGAGGA	CTTGACTTCTCTCTTGGGTTTCT	60043

[1]Transcript identification from Ensemble chicken genome assembly (GRCg6a; (http://www.ensembl.org/Gallus_gallus/Info/Index) preceded by ENSGALT000000

Table 5.4 Egg production parameters.[1,2]

Age (weeks)	Feed intake (g/hen/day)	Hen-day egg production (%)	Egg weight (g)	Egg mass (g/%)	FCR/ dozen	FCR/ kg feed
25	$101.7^{d} \pm 0.42$	$94.3^{ab} \pm 2.14$	$53.8^{c} \pm 0.08$	$50.7^{b} \pm 1.20$	$1.30^{c} \pm 0.03$	$2.01^{b} \pm 0.04$
43	$121.7^{a} \pm 1.65$	$97.5^{a} \pm 1.36$	$59.7^{b} \pm 0.20$	$58.2^{a} \pm 0.82$	$1.50^{b} \pm 0.02$	$2.09^{a} \pm 0.03$
80	$113.1^{c} \pm 0.78$	$88.7^{b} \pm 2.25$	$65.2^{a} \pm 0.45$	$57.8^{a} \pm 1.34$	$1.53^{b} \pm 0.04$	$1.96^{b} \pm 0.04$
95	$116.6^{b} \pm 0.92$	$80.7^{c} \pm 2.09$	$65.8^{a} \pm 0.38$	$53.1^{b} \pm 1.38$	$1.74^{a} \pm 0.05$	$2.2^{ab} \pm 0.06$
Age	P=0.0001	P=0.0010	P=0.0001	P=0.0067	P=0.0002	P=0.0293

[1]Values are expressed as mean ± SEM.

[2]Parameters were calculated using block as the experimental replicate (n=3 blocks/age [25, 43, 80 weeks] or n=4 blocks/age [95 weeks]). Each block contained 25 hens.

[abc]Means not sharing a common letter differ significantly ($P \leq 0.05$).

Table 5.5 Eggshell quality from eggs collected the day preceding sampling.[1,2]

Age (weeks)	Egg weight (g)	Breaking strength (g)	Shell thickness (mm)	Wet shell weight (g)	Wet shell %
25	$57.4^{b} \pm 0.51$	$5460^{a} \pm 109$	$0.42^{a} \pm 0.003$	5.97 ± 0.05	$10.41^{a} \pm 0.09$
43	$59.0^{b} \pm 0.59$	$5329^{a} \pm 115$	$0.41^{a} \pm 0.003$	6.13 ± 0.06	$10.41^{a} \pm 0.07$
80	$64.5^{a} \pm 0.74$	$3910^{b} \pm 91$	$0.38^{b} \pm 0.004$	6.04 ± 0.08	$10.19^{b} \pm 0.11$
95	$64.8^{a} \pm 0.78$	$3927^{b} \pm 102$	$0.37^{b} \pm 0.004$	5.88 ± 0.09	$9.08^{c} \pm 0.09$
Age	P=0.0001	P=0.0001	P=0.0002	P=0.0938	P=0.0001

[1]Values are expressed as mean ± SEM.

[2]Parameters were calculated using individual sampled hen as the experimental replicate (n=48 hens/age).

[abc]Means not sharing a common letter differ significantly ($P \leq 0.05$).

Table 5.6 Eggshell parameters for eggs collected two days before each sampling. [1,2]

Age (weeks)	Egg weight (g)	Wet shell weight (g)	Dry shell weight (g)	Wet shell %	Dry shell %
43	$59.6^{b} \pm 0.66$	5.98 ± 0.06	5.90 ± 0.07	$10.04^{a} \pm 0.08$	$9.91^{a} \pm 0.08$
80	$65.3^{a} \pm 0.72$	5.81 ± 0.08	5.72 ± 0.08	$8.92^{b} \pm 0.11$	$8.78^{b} \pm 0.11$
95	$66.6^{a} \pm 0.67$	5.75 ± 0.08	5.69 ± 0.08	$8.63^{c} \pm 0.11$	$8.56^{c} \pm 0.11$
Age	P=0.0001	P=0.0861	P=0.1158	P=0.0001	P=0.0001

[1]Values are expressed as mean ± SEM.

[2]Parameters were calculated using individual sampled hen as the experimental replicate (n=48 hens/age).

[abc]Means not sharing a common letter differ significantly ($P \leq 0.05$).

Table 5.7. Eggshell mineral content for eggs collected two days before each sampling.[1,2]

Age (weeks)	Ca %	P PPM	Al PPM	Cu PPM	Fe PPM	K PPM	Mg PPM	Mn PPM	Na PPM	S PPM	Zn PPM
43	41.23[a] ± 0.34	823.4 ± 37.04	128.21[a] ± 1.10	0.91[b] ± 0.09	3.06 ± 0.56	404.0[a] ± 14.28	3243 ± 86.84	1.69[b] ± 0.21	1136 ± 54.08	159.22[b] ± 3.16	4.79 ± 0.48
80	39.19[b] ± 0.47	747.5 ± 35.6	125.76[b] ± 0.69	1.41[a] ± 0.06	1.88 ± 0.21	335.1[b] ± 18.04	3233 ± 88.63	2.23[a] ± 0.11	1104 ± 39.57	189.44[a] ± 11.33	5.19 ± 0.29
95	38.68[b] ± 0.95	724.4 ± 26.8	125.43[b] ± 0.65	1.57[a] ± 0.20	2.07 ± 0.35	424.3[a] ± 8.41	3337 ± 86.56	2.04[ab] ± 0.11	1018 ± 20.28	184.66[a] ± 4.80	3.91 ± 0.27
Age	P=0.0183	P=0.0979	P=0.0466	P=0.0025	P=0.0981	P=0.0001	P=0.6495	P=0.0465	P=0.1098	P=0.0091	P=0.0501

[1]Values are expressed as mean ± SEM.

[2]Parameters were calculated using individual sampled hen as the experimental replicate (n=16 hens/age).

[abc]Means not sharing a common letter differ significantly (P≤0.05).

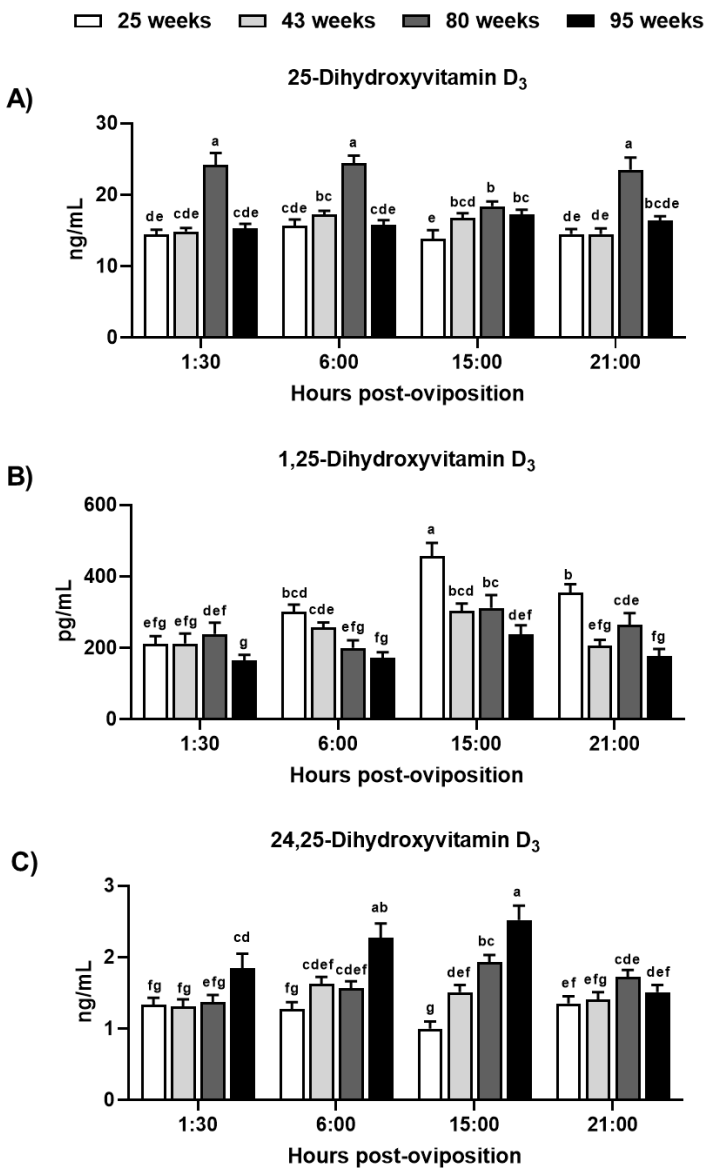

Figure 5.1. Circulating levels of vitamin D_3 metabolites.
Circulating levels of (A) $25(OH)D_3$, (B) $1\alpha,25(OH)_2D_3$, and (C) $24,25(OH)_2D_3$ at indicated hours post-oviposition (HPOP) and ages were determined by liquid chromatography-tandem mass spectrometry. Data were analyzed by two-way ANOVA followed by Fisher's test of least significant difference, and bars not sharing a common letter differ significantly ($P \leq 0.05$). Significant HPOP-by-age interactions (mean+SEM; n=12 hens/age/HPOP) were identified for (A) $25(OH)D_3$ ($P=0.0004$), (B) $1\alpha,25(OH)_2D_3$ ($P=0.0006$), and $24,25(OH)_2D_3$ ($P=0.0001$).

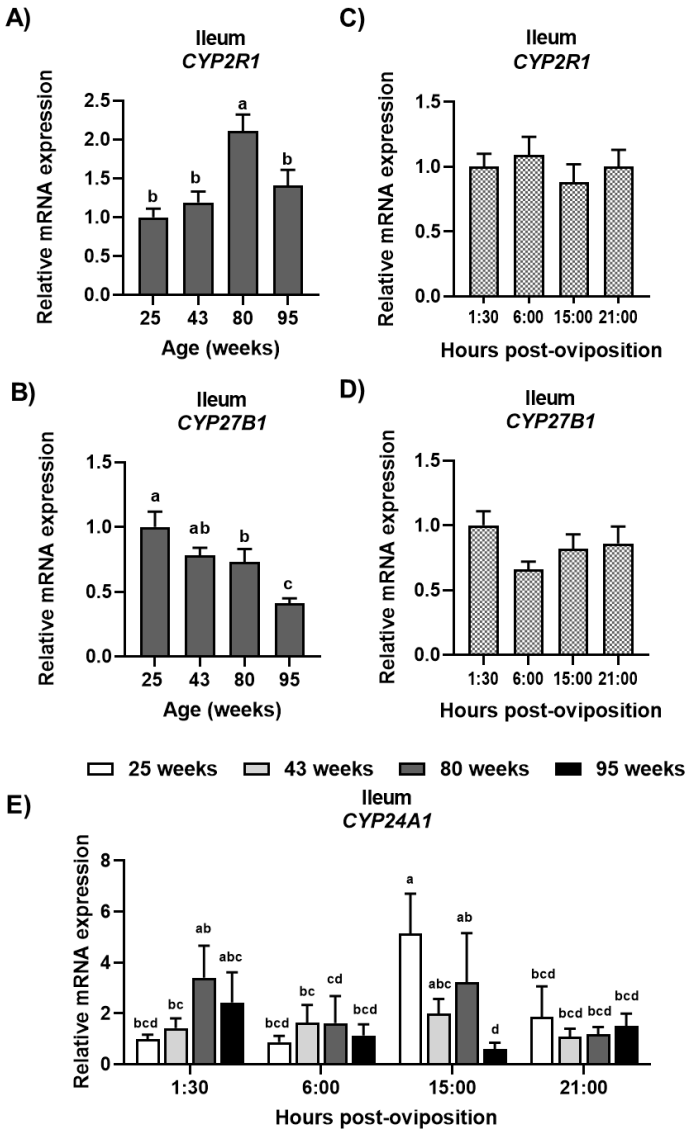

Figure 5.2. Expression of genes regulating vitamin D_3 metabolism in the ileum.
Relative levels of mRNA for (A, C) *CYP2R1*, (B, D) *CYP27B1*, and (E) *CYP24A1* in the ileum at indicated ages and hours post-oviposition (HPOP) were determined by RT-qPCR and normalized to *GAPDH* mRNA. Data were analyzed by two-way ANOVA followed by Fisher's test of least significant difference, and bars not sharing a common letter differ significantly ($P \leq 0.05$). The HPOP-by-age interaction was not significant for (A, C) *CYP2R1* (P=0.4978) or (B, D) *CYP27B1* (P=0.9013), and interactive means are shown in Appendix C, Figure C1A - C1B. Main effects of age (mean+SEM; n=32 hens/age) for (A) *CYP2R1* (P=0.0001) and (B) *CYP27B1* (P=0.0001) are expressed relative to 25 weeks. Main effects of HPOP (mean+SEM; n=32 hens/HPOP) for (C) *CYP2R1* (P=0.1549) and (D) *CYP27B1* (P=0.1924) are expressed relative to 1:30 HPOP. A significant HPOP-by-age interaction was identified for (E) *CYP24A1* (P=0.0300), and values (mean+SEM; n=8 hens/HPOP/age) are expressed relative to 1:30 HPOP at 25 weeks.

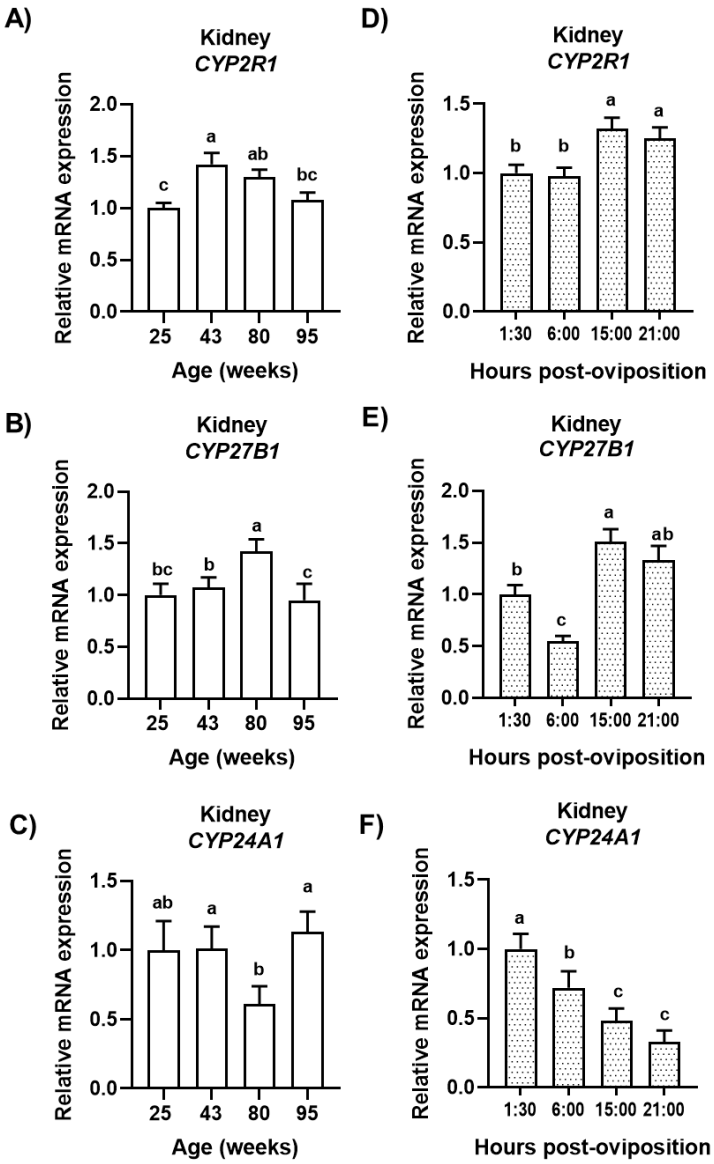

Figure 5.3. Expression of genes regulating vitamin D_3 metabolism in the kidney.
Relative levels of mRNA for (A, D) *CYP2R1*, (B, E) *CYP27B1*, and (C, F) *CYP24A1* in the ileum at indicated ages and hours post-oviposition (HPOP) were determined by RT-qPCR and normalized to *GAPDH* mRNA. Data were analyzed by two-way ANOVA followed by Fisher's test of least significant difference, and bars not sharing a common letter differ significantly ($P \leq 0.05$). The HPOP-by-age interaction was not significant for (A, D) *CYP2R1* (P=0.9084), (B, E) *CYP27B1* (P=0.9044), or (C, F) *CYP24A1* (P=0.0663) and interactive means are shown in Appendix C, Figure C2A - C2C. Main effects of age (mean+SEM; n=32 hens/age) for (A) *CYP2R1* (P=0.0001), (B) *CYP27B1* (P=0.0001), and (C) *CYP24A1* (P=0.0160) are expressed relative to 25 weeks. Main effects of HPOP (mean+SEM; n=32 hens/HPOP) for (D) *CYP2R1* (P=0.0001) and (E) *CYP27B1* (P=0.0001), and (F) *CYP24A1* (P=0.0001) are expressed relative to 1:30 HPOP.

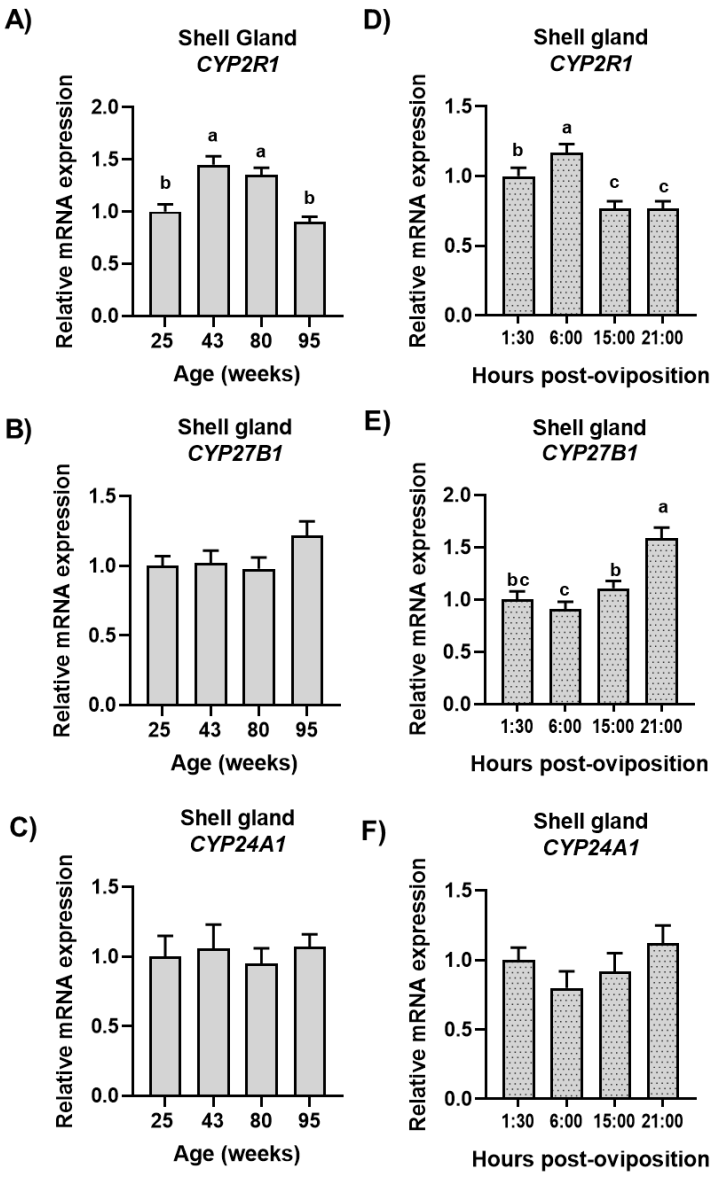

Figure 5.4. Expression of genes regulating vitamin D_3 metabolism in the shell gland.
Relative levels of mRNA for (A, D) *CYP2R1*, (B, E) *CYP27B1*, and (C, F) *CYP24A1* in the shell gland at indicated ages and hours post-oviposition (HPOP) were determined by RT-qPCR and normalized to *RPL5* mRNA. Data were analyzed by two-way ANOVA followed by Fisher's test of least significant difference, and bars not sharing a common letter differ significantly ($P \leq 0.05$). The HPOP-by-age interaction was not significant for (A, D) *CYP2R1* (P=0.5517), (B, E) *CYP27B1* (P=0.6643), or (C, F) *CYP24A1* (P=0.3699) and interactive means are shown in Appendix C, Figure C4A - C4C. Main effects of age (mean+SEM; n=32 hens/age) for (A) *CYP2R1* (P=0.0001), (B) *CYP27B1* (P=0.0906), and (C) *CYP24A1* (P=0.4675) are expressed relative to 25 weeks. Main effects of HPOP (mean+SEM; n=32 hens/HPOP) for (D) *CYP2R1* (P=0.0001) and (E) *CYP27B1* (P=0.0001), and (F) *CYP24A1* (P=0.1224) are expressed relative to 1:30 HPOP.

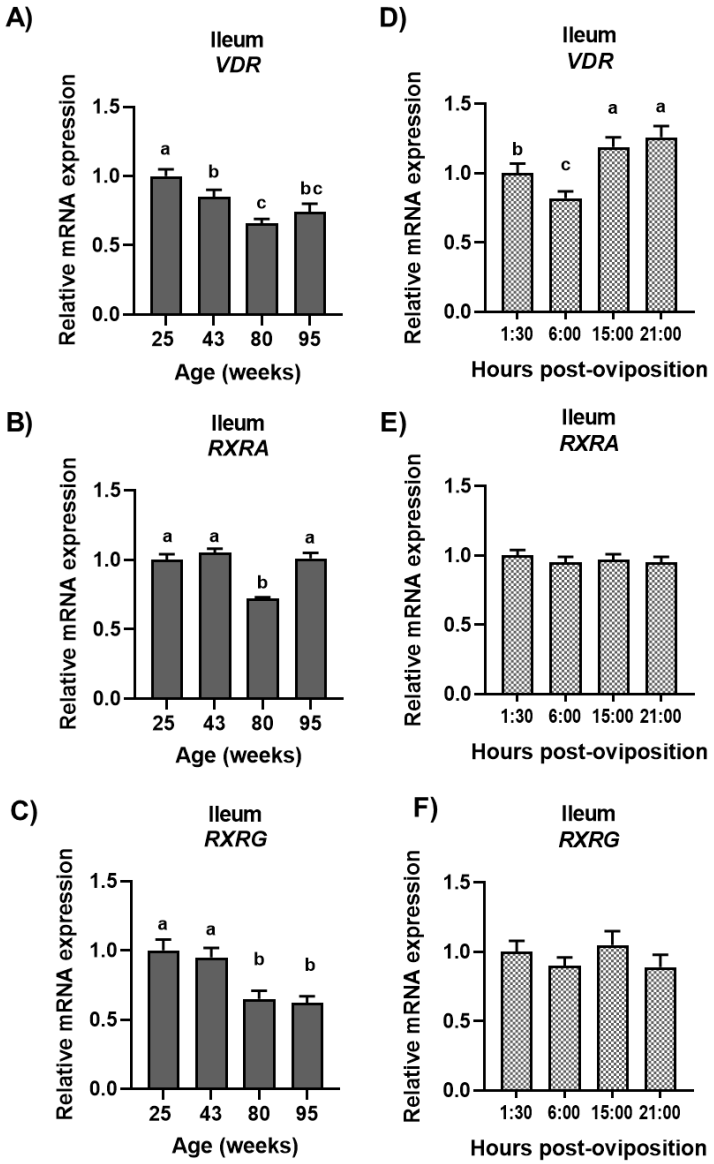

Figure 5.5. Expression of genes regulating vitamin D_3 signaling in the ileum.
Relative levels of mRNA for (A, D) *VDR*, (B, E) *RXRA*, and (C, F) *RXRG* in the ileum at indicated ages and hours post-oviposition (HPOP) were determined by RT-qPCR and normalized to *GAPDH* mRNA. Data were analyzed by two-way ANOVA followed by Fisher's test of least significant difference, and bars not sharing a common letter differ significantly ($P \leq 0.05$). The HPOP-by-age interaction was not significant for (A, D) *VDR* (P=0.0.928), (B, E) *RXRA* (P=0.9400), or (C, F) *RXRG* (P=0.5919) and interactive means are shown in Appendix C, Figure C1C - C1E. Main effects of age (mean+SEM; n=32 hens/age) for (A) *VDR* (P=0.0001), (B) *RXRA* (P=0.0001), and (C) *RXRG* (P=0.0001) are expressed relative to 25 weeks. Main effects of HPOP (mean+SEM; n=32 hens/HPOP) for (D) *VDR* (P=0.0001) and (E) *RXRA* (P=0.7679), and (F) *RXRG* (P=0.3099) are expressed relative to 1:30 HPOP.

Figure 5.6. Expression of genes regulating vitamin D_3 signaling in the kidney.
Relative levels of mRNA for (A, D) *VDR*, (B, E) *RXRA*, and (C, F) *RXRG* in the kidney at indicated ages and hours post-oviposition (HPOP) were determined by RT-qPCR and normalized to *GAPDH* mRNA. Data were analyzed by two-way ANOVA followed by Fisher's test of least significant difference, and bars not sharing a common letter differ significantly ($P \leq 0.05$). The HPOP-by-age interaction was not significant for (A, D) *VDR* (P=0.7884), (B, E) *RXRA* (P=0.8533), or (C, F) *RXRG* (P=0.4827) and interactive means are shown in Appendix C, Figure C2D - C2F. Main effects of age (mean+SEM; n=32 hens/age) for (A) *VDR* (P=0.0001), (B) *RXRA* (P=0.0001), and (C) *RXRG* (P=0.0001) are expressed relative to 25 weeks. Main effects of HPOP (mean+SEM; n=32 hens/HPOP) for (D) *VDR* (P=0.6762) and (E) *RXRA* (P=0.0040), and (F) *RXRG* (P=0.0079) are expressed relative to 1:30 HPOP.

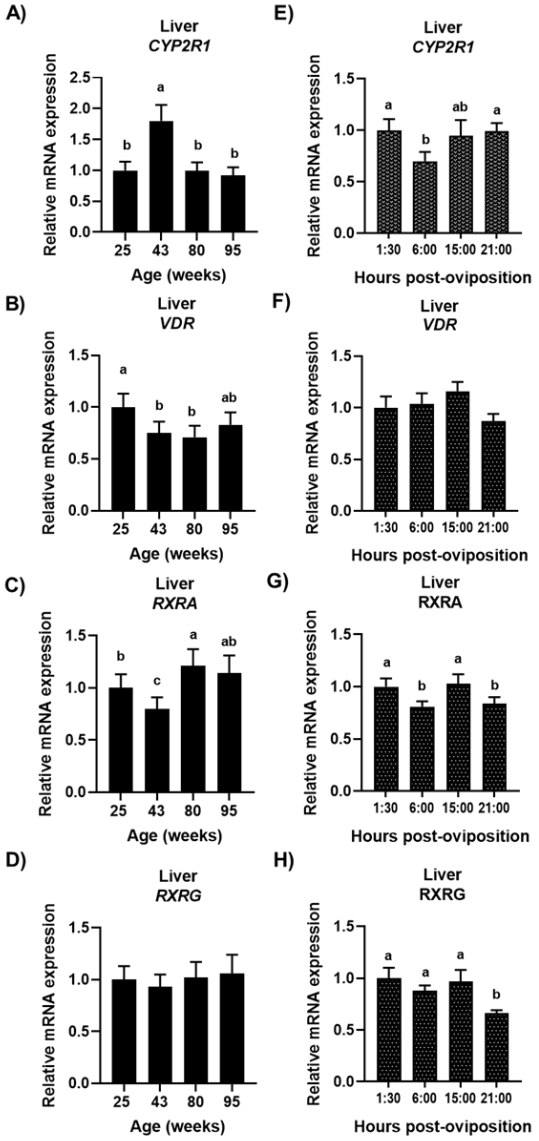

Figure 5.7. Expression of genes regulating vitamin D_3 metabolism in the liver.
Relative levels of mRNA for (A, E) *CYP2R1*, (B, F) *VDR*, (C, G) *RXRA*, and (D, H) *RXRG* in the liver at indicated ages and hours post-oviposition (HPOP) were determined by RT-qPCR and normalized to *CYCLO* mRNA. Data were analyzed by two-way ANOVA followed by Fisher's test of least significant difference, and bars not sharing a common letter differ significantly ($P \leq 0.05$). The HPOP-by-age interaction was not significant for (A, E) *CYP2R1* (P=0.2282), (B, F) *VDR* (P=0.3524), (C, G) *RXRA* (P=0.1653) or (D, H) *RXRG* (P=0.1346) and interactive means are shown in Appendix C, Figure C3A - C3D. Main effects of age (mean+SEM; n=32 hens/age) for (A) *CYP2R1* (P=0.0001), (B) *VDR* (P=0.0110), (C) *RXRA* (P=0.0001), and (D) *RXRG* (P=0.5013) are expressed relative to 25 weeks. Main effects of HPOP (mean+SEM; n=32 hens/HPOP) for (E) *CYP2R1* (P=0.0154) and (F) *VDR* (P=0.1892), (G) *RXRA* (P=0.0148), and (H) *RXRG* (P=0.0017) are expressed relative to 1:30 HPOP. Expression of *CYP24A1* was not detected in this tissue and expression of *CYP27B1* was not measured.

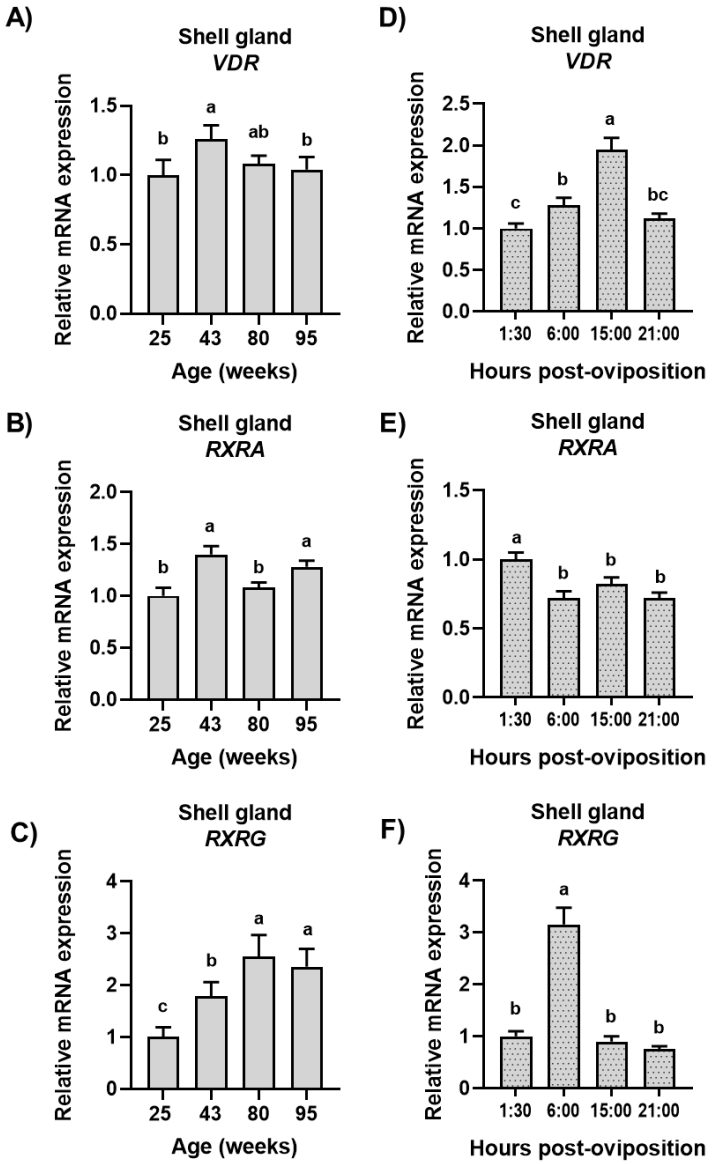

Figure 5.8. Expression of genes regulating vitamin D_3 signaling in the shell gland.
Relative levels of mRNA for (A, D) *VDR*, (B, E) *RXRA*, and (C, F) *RXRG* in the shell gland at indicated ages and hours post-oviposition (HPOP) were determined by RT-qPCR and normalized to *RPL5* mRNA. Data were analyzed by two-way ANOVA followed by Fisher's test of least significant difference, and bars not sharing a common letter differ significantly ($P \leq 0.05$). The HPOP-by-age interaction was not significant for (A, D) *VDR* (P=0.4998), (B, E) *RXRA* (P=0.3429), or (C, F) *RXRG* (P=0.4174) and interactive means are shown in Appendix C, Figure C4D - C4F. Main effects of age (mean+SEM; n=32 hens/age) for (A) *VDR* (P=0.0344), (B) *RXRA* (P=0.0001), and (C) *RXRG* (P=0.0001) are expressed relative to 25 weeks. Main effects of HPOP (mean+SEM; n=32 hens/HPOP) for (D) *VDR* (P=0.0001) and (E) *RXRA* (P=0.0001), and (F) *RXRG* (P=0.0001) are expressed relative to 1:30 HPOP.

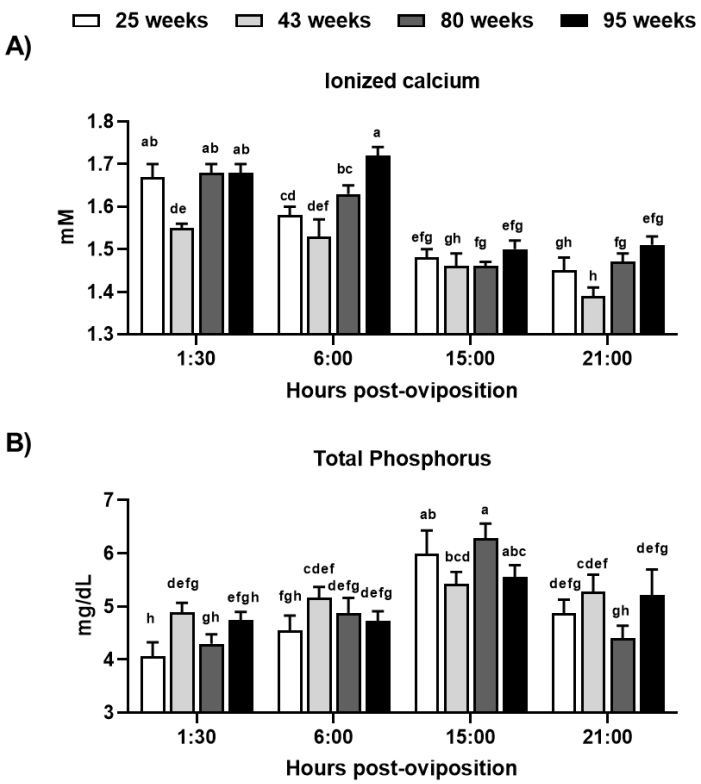

Figure 5.9. Whole blood ionized calcium and total phosphorus.
Circulating levels of (A) ionized calcium and (B) total phosphorus at indicated hours post-oviposition (HPOP) and ages were determined in whole blood using an iSTAT device and Chem8+ cartridges or a VetScan device and avian/reptile profile + cartridges, respectively. Data were analyzed by two-way ANOVA followed by Fisher's test of least significant difference, and bars not sharing a common letter differ significantly ($P \leq 0.05$). Significant HPOP-by-age interactions (mean+SEM; n=8 hens/age/HPOP) were identified for (A) ionized calcium ($P=0.0172$) and (B) total phosphorus ($P=0.0250$).

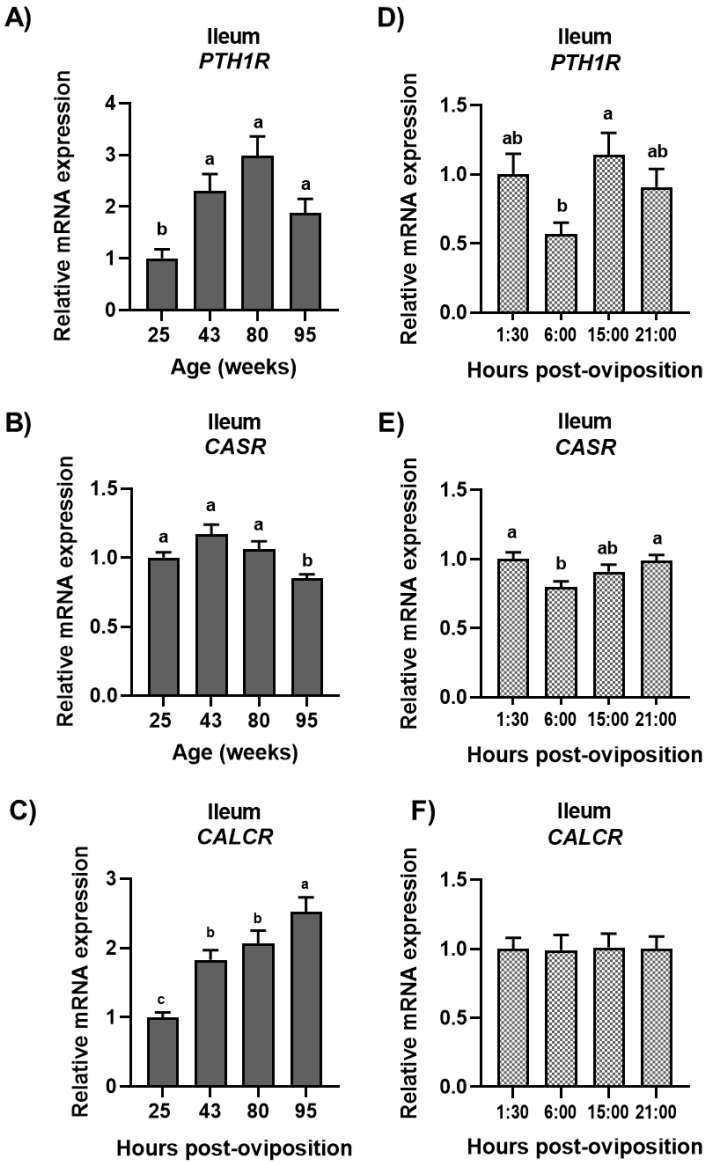

Figure 5.10. Expression of hormone receptors in the ileum.
Relative levels of mRNA for (A, D) *PTH1R*, (B, E) *CASR*, and (C, F) *CALCR* in the ileum at indicated ages and hours post-oviposition (HPOP) were determined by RT-qPCR and normalized to *GAPDH* mRNA. Data were analyzed by two-way ANOVA followed by Fisher's test of least significant difference, and bars not sharing a common letter differ significantly ($P \leq 0.05$). The HPOP-by-age interaction was not significant for (A, D) *PTH1R* (P=0.6564), (B, E) *CASR* (P=0.3890), or (C, F) *CALCR* (P=0.7984) and interactive means are shown in Appendix C, Figure C5A - C5C. Main effects of age (mean+SEM; n=32 hens/age) for (A) *PTH1R* (P=0.0001), (B) *CASR* (P=0.0001), and (C) *CALCR* (P=0.0001) are expressed relative to 25 weeks. Main effects of HPOP (mean+SEM; n=32 hens/HPOP) for (D) *PTH1R* (P=0.0205) and (E) *CASR* (P=0.0024), and (F) *CALCR* (P=0.9730) are expressed relative to 1:30 HPOP.

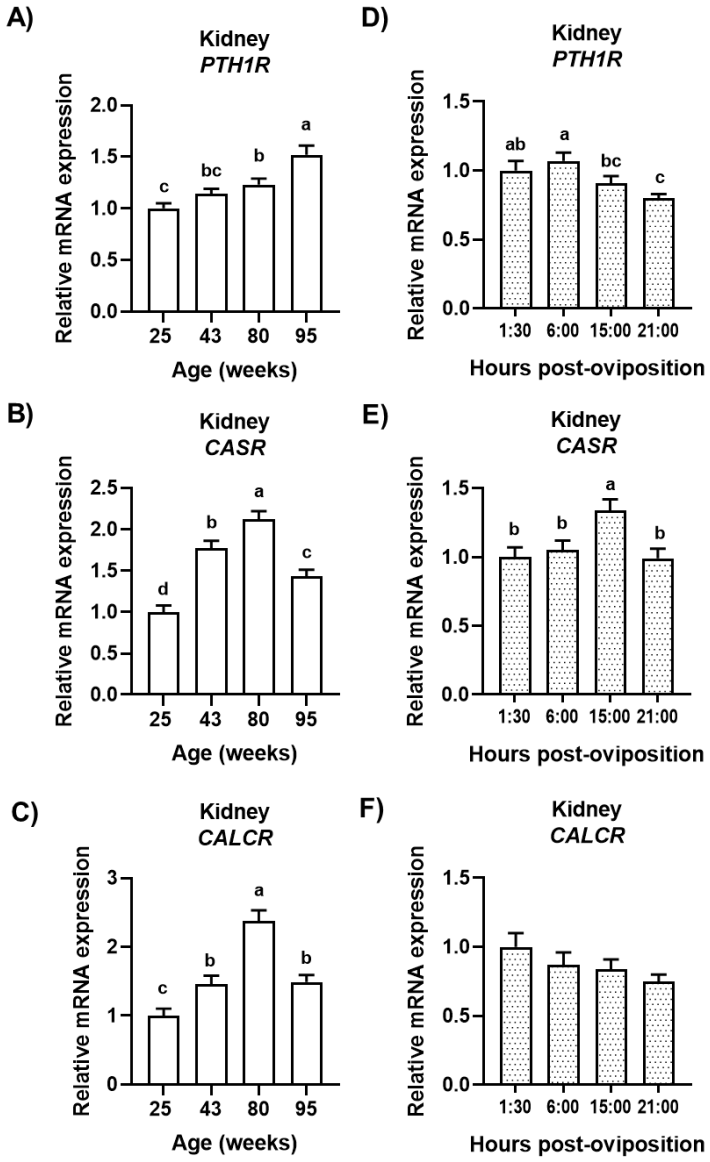

Figure 5.11. Expression of hormone receptors in the kidney.
Relative levels of mRNA for (A, D) *PTH1R*, (B, E) *CASR*, and (C, F) *CALCR* in the kidney at indicated ages and hours post-oviposition (HPOP) were determined by RT-qPCR and normalized to *GAPDH* mRNA. Data were analyzed by two-way ANOVA followed by Fisher's test of least significant difference, and bars not sharing a common letter differ significantly ($P \leq 0.05$). The HPOP-by-age interaction was not significant for (A, D) *PTH1R* (P=0.1278), (B, E) *CASR* (P=0.8552), or (C, F) *CALCR* (P=0.3542) and interactive means are shown in Appendix C, Figure C6A - C6C. Main effects of age (mean+SEM; n=32 hens/age) for (A) *PTH1R* (P=0.0001), (B) *CASR* (P=0.0001), and (C) *CALCR* (P=0.0001) are expressed relative to 25 weeks. Main effects of HPOP (mean+SEM; n=32 hens/HPOP) for (D) *PTH1R* (P=0.0012) and (E) *CASR* (P=0.0001), and (F) *CALCR* (P=0.3321) are expressed relative to 1:30 HPOP.

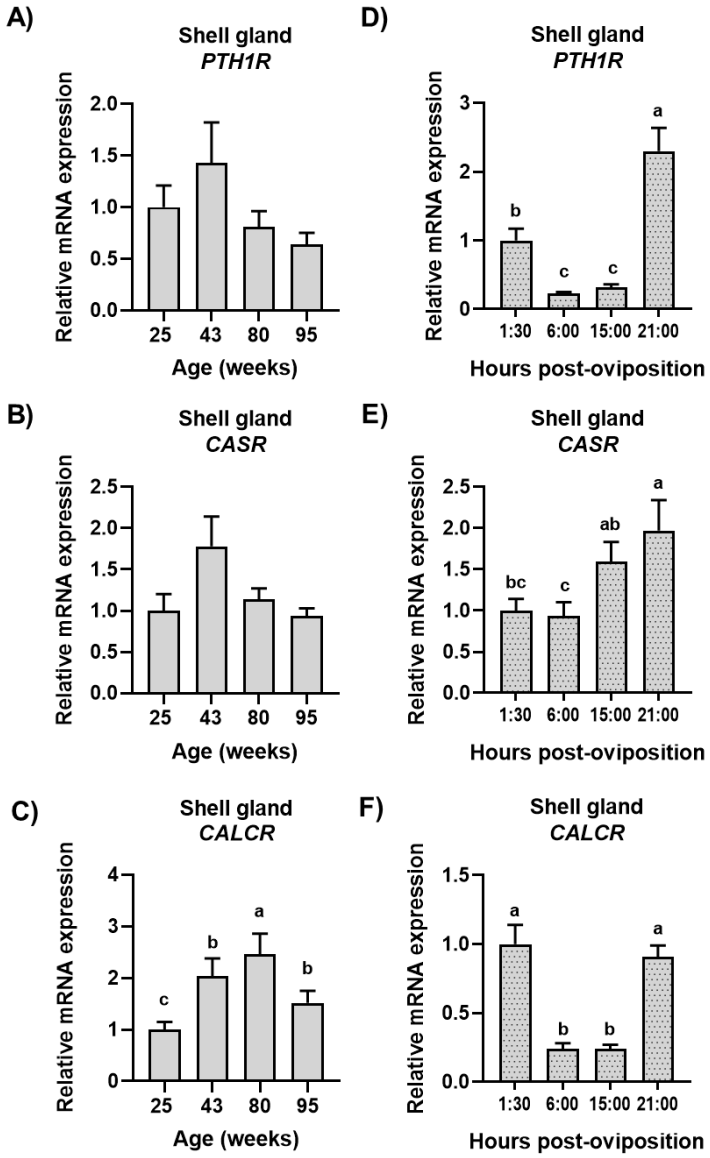

Figure 5.12. Expression of hormone receptors in the shell gland.
Relative levels of mRNA for (A, D) *PTH1R*, (B, E) *CASR*, and (C, F) *CALCR* in the shell gland at indicated ages and hours post-oviposition (HPOP) were determined by RT-qPCR and normalized to *RPL5* mRNA. Data were analyzed by two-way ANOVA followed by Fisher's test of least significant difference, and bars not sharing a common letter differ significantly ($P \leq 0.05$). The HPOP-by-age interaction was not significant for (A, D) *PTH1R* (P=0.2894), (B, E) *CASR* (P=0.7013), or (C, F) *CALCR* (P=0.3737) and interactive means are shown in Appendix C, Figure C7A - C7C. Main effects of age (mean+SEM; n=32 hens/age) for (A) *PTH1R* (P=0.0770), (B) *CASR* (P=0.1957), and (C) *CALCR* (P=0.0001) are expressed relative to 25 weeks. Main effects of HPOP (mean+SEM; n=32 hens/HPOP) for (D) *PTH1R* (P=0.0001) and (E) *CASR* (P=0.0117), and (F) *CALCR* (P=0.0001) are expressed relative to 1:30 HPOP.

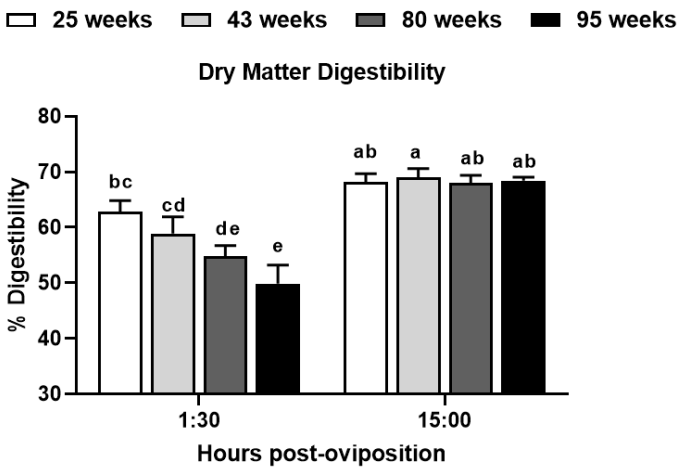

Figure 5.13. Dry matter digestibility.
Ileal dry matter digestibility at indicated hours post-oviposition (HPOP) and ages was calculated using 0.3% titanium dioxide as an inert maker. Data were analyzed by two-way ANOVA followed by Fisher's test of least significant difference, and bars not sharing a common letter differ significantly ($P \leq 0.05$). A significant HPOP-by-age interaction (mean+SEM; n=12 hens/age/HPOP) was identified ($P=0.0090$).

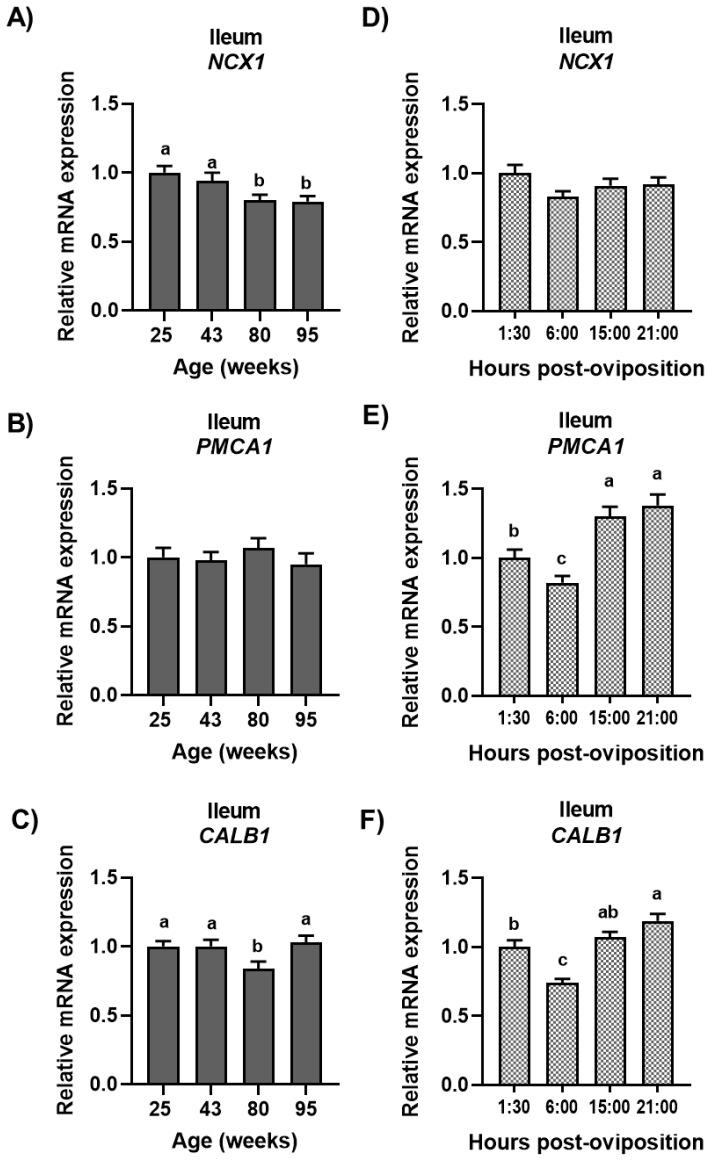

Figure 5.14. Expression of calcium transporters in the ileum.
Relative levels of mRNA for (A, D) *NCX1*, (B, E) *PMCA1*, and (C, F) *CALB1* in the ileum at indicated ages and hours post-oviposition (HPOP) were determined by RT-qPCR and normalized to *GAPDH* mRNA. Data were analyzed by two-way ANOVA followed by Fisher's test of least significant difference, and bars not sharing a common letter differ significantly ($P \leq 0.05$). The HPOP-by-age interaction was not significant for (A, D) *NCX1* (P=0.4732), (B, E) *PMCA1* (P=0.6991), or (C, F) *CALB1* (P=0.8882) and interactive means are shown in Appendix C, Figure C8A - C8C. Main effects of age (mean+SEM; n=32 hens/age) for (A) *NCX1* (P=0.0027), (B) *PMCA1* (P=0.4291), and (C) *CALB1* (P=0.0026) are expressed relative to 25 weeks. Main effects of HPOP (mean+SEM; n=32 hens/HPOP) for (D) *NCX1* (P=0.1348) and (E) *PMCA1* (P=0.0001), and (F) *CALB1* (P=0.0001) are expressed relative to 1:30 HPOP.

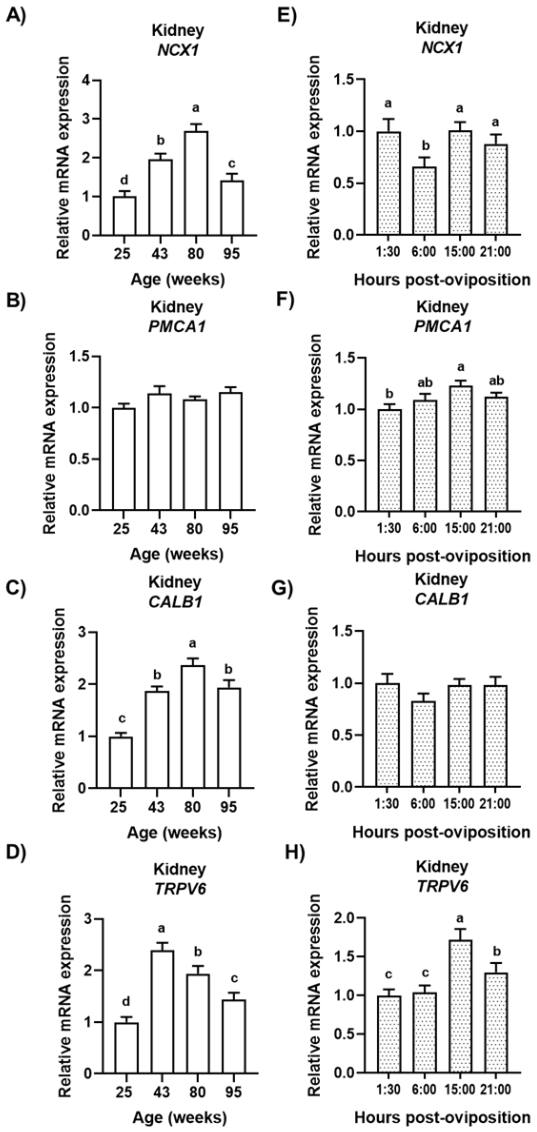

Figure 5.15. Expression of calcium transporters in the kidney.
Relative levels of mRNA for (A, E) *NCX1*, (B, F) *PMCA1*, (C, G) *CALB1*, (D, H) *TRPV6* in the kidney at indicated ages and hours post-oviposition (HPOP) were determined by RT-qPCR and normalized to *GAPDH* mRNA. Data were analyzed by two-way ANOVA followed by Fisher's test of least significant difference, and bars not sharing a common letter differ significantly ($P \leq 0.05$). The HPOP-by-age interaction was not significant for (A, E) *NCX1* (P=0.7180), (B, F) *PMCA1* (P=0.9586), (C, G) *CALB1* (P=0.9789), (D, H) *TRPV6* (P=0.5917) and interactive means are shown in Appendix C, Figure C9A - C9D. Main effects of age (mean+SEM; n=32 hens/age) for (A) *NCX1* (P=0.0001), (B) *PMCA1* (P=0.2106), (C) *CALB1* (P=0.0001), and (D) *TRPV6* (P=0.0001) are expressed relative to 25 weeks. Main effects of HPOP (mean+SEM; n=32 hens/HPOP) for (E) *NCX1* (P=0.0019) and (F) *PMCA1* (P=0.0231), (G) *CALB1* (P=0.1288), and (H) *TRPV6* (P=0.0001) are expressed relative to 1:30 HPOP.

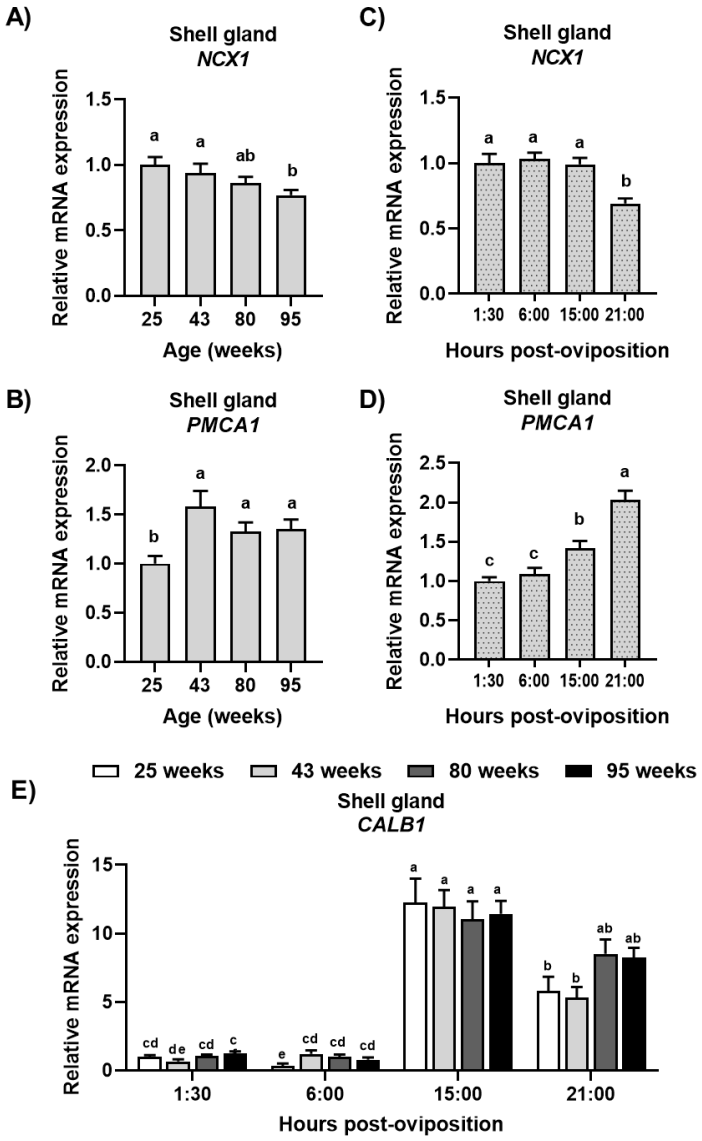

Figure 5.16. Expression of calcium transporters in the shell gland.
Relative levels of mRNA for (A, C) *NCX1*, (B, D) *PMCA1*, and (E) *CALB1* in the shell gland at indicated ages and hours post-oviposition (HPOP) were determined by RT-qPCR and normalized to *RPL5* mRNA. Data were analyzed by two-way ANOVA followed by Fisher's test of least significant difference, and bars not sharing a common letter differ significantly ($P \leq 0.05$). The HPOP-by-age interaction was not significant for (A, C) *NCX1* (P=0.4424) or (B, D) *PMCA1* (P=0.3057), and interactive means are shown in Appendix C, Figure C10A - C10B. Main effects of age (mean+SEM; n=32 hens/age) for (A) *NCX1* (P=0.0122) and (B) *PMCA1* (P=0.0001) are expressed relative to 25 weeks. Main effects of HPOP (mean+SEM; n=32 hens/HPOP) for (C) *NCX1* (P=0.0001) and (D) *PMCA1* (P=0.0001) are expressed relative to 1:30 HPOP. A significant HPOP-by-age interaction was identified for (E) *CALB1* (P=0.0012), and values (mean+SEM; n=8 hens/HPOP/age) are expressed relative to 1:30 HPOP at 25 weeks.

Figure 5.17. Expression of phosphorus transporters in the ileum.
Relative levels of mRNA for (A, D) *PiT-1*, (B, E) *PiT-2*, and (C, F) *NaPiIIb* in the ileum at indicated ages and hours post-oviposition (HPOP) were determined by RT-qPCR and normalized to *GAPDH* mRNA. Data were analyzed by two-way ANOVA followed by Fisher's test of least significant difference, and bars not sharing a common letter differ significantly ($P \leq 0.05$). The HPOP-by-age interaction was not significant for (A, D) *PiT-1* (P=0.9322), (B, E) *PiT-2* (P=0.8476), or (C, F) *NaPiIIb* (P=0.9271) and interactive means are shown in Appendix C, Figure C11A - C11C. Main effects of age (mean+SEM; n=32 hens/age) for (A) *PiT-1* (P=0.0001), (B) *PiT-2* (P=0.0001), and (C) *NaPiIIb* (P=0.0035) are expressed relative to 25 weeks. Main effects of HPOP (mean+SEM; n=32 hens/HPOP) for (D) *PiT-1* (P=0.0001) and (E) *PiT-2* (P=0.4583), and (F) *NaPiIIb* (P=0.1424) are expressed relative to 1:30 HPOP. Expression of *NaPiIIa* was not detected in this tissue.

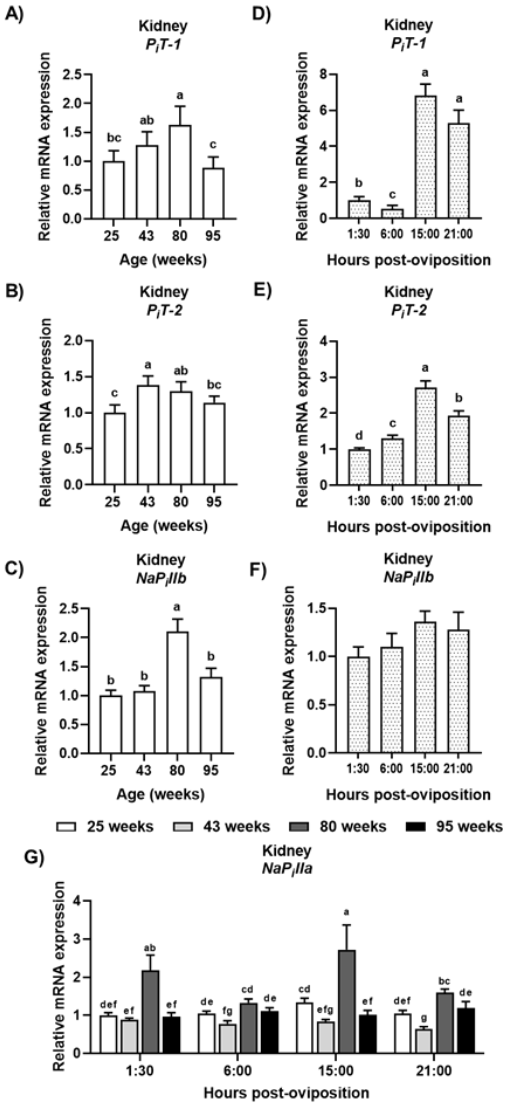

Figure 5.18. Expression of phosphorus transporters in the kidney.
Relative levels of mRNA for (A, D) *PiT-1*, (B, E) *PiT-2*, (C, F) *NaPiIIb*, and (G) *NaPiIIa* in the kidney at indicated ages and hours post-oviposition (HPOP) were determined by RT-qPCR and normalized to *GAPDH* mRNA. Data were analyzed by two-way ANOVA followed by Fisher's test of least significant difference, and bars not sharing a common letter differ significantly ($P \leq 0.05$). The HPOP-by-age interaction was not significant for (A, D) *PiT-1* (P=0.1722), (B, E) *PiT-2* (P=0.6353), or (C, F) *NaPiIIb* (P=0.2099) and interactive means are shown in Appendix C, Figure C12A - C12C. Main effects of age (mean+SEM; n=32 hens/age) for (A) *PiT-1* (P=0.0128), (B) *PiT-2* (P=0.0008), and (C) *NaPiIIb* (P=0.0027) are expressed relative to 25 weeks. Main effects of HPOP (mean+SEM; n=32 hens/HPOP) for (D) *PiT-1* (P=0.0001) and (E) *PiT-2* (P=0.0001), and (F) *NaPiIIb* (P=0.0904) are expressed relative to 1:30 HPOP. A significant HPOP-by-age interaction was identified for (G) *NaPiIIa* (P=0.0353), and values (mean+SEM; n=8 hens/HPOP/age) are expressed relative to 1:30 HPOP at 25 weeks.

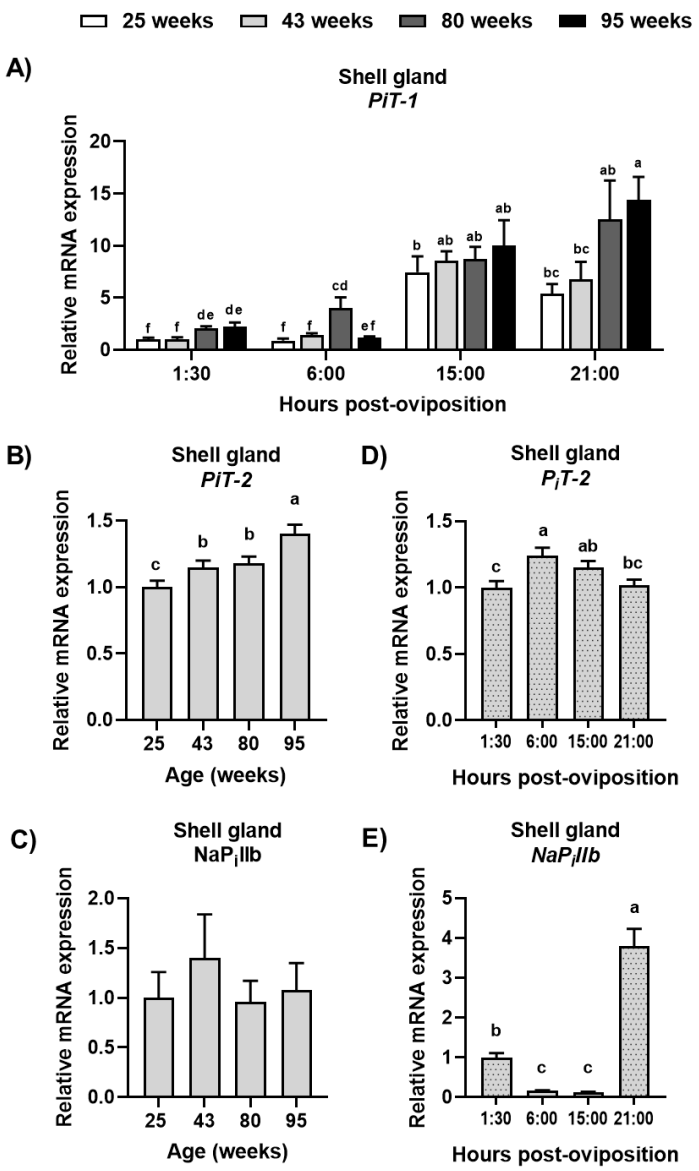

Figure 5.19. Expression of phosphorus transporters in the shell gland.
Relative levels of mRNA for (A) *P_iT-1*, (B, D) *P_iT-2*, and (C, E) *NaP_iIIb* in the shell gland at indicated ages and hours post-oviposition (HPOP) were determined by RT-qPCR and normalized to *RPL5* mRNA. Data were analyzed by two-way ANOVA followed by Fisher's test of least significant difference, and bars not sharing a common letter differ significantly ($P \leq 0.05$). A significant HPOP-by-age interaction was identified for (A) *P_iT-1* (P=0.0083), and values (mean+SEM; n=8 hens/HPOP/age) are expressed relative to 1:30 HPOP at 25 weeks. The HPOP-by-age interaction was not significant for (B, D) *P_iT-2* (P=0.9674) or (C, E) *NaP_iIIb* (P=0.0766), and interactive means are shown in Appendix C, Figure C13A - C13B. Main effects of age (mean+SEM; n=32 hens/age) for (B) *P_iT-2* (P=0.0001) and (C) *NaP_iIIb* (P=0.5052) are expressed relative to 25 weeks. Main effects of HPOP (mean+SEM; n=32 hens/HPOP) for (D) *P_iT-2* (P=0.0038) and (E) *NaP_iIIb* (P=0.0001) are expressed relative to 1:30 HPOP. Expression of *NaP_iIIa* was not detected in this tissue

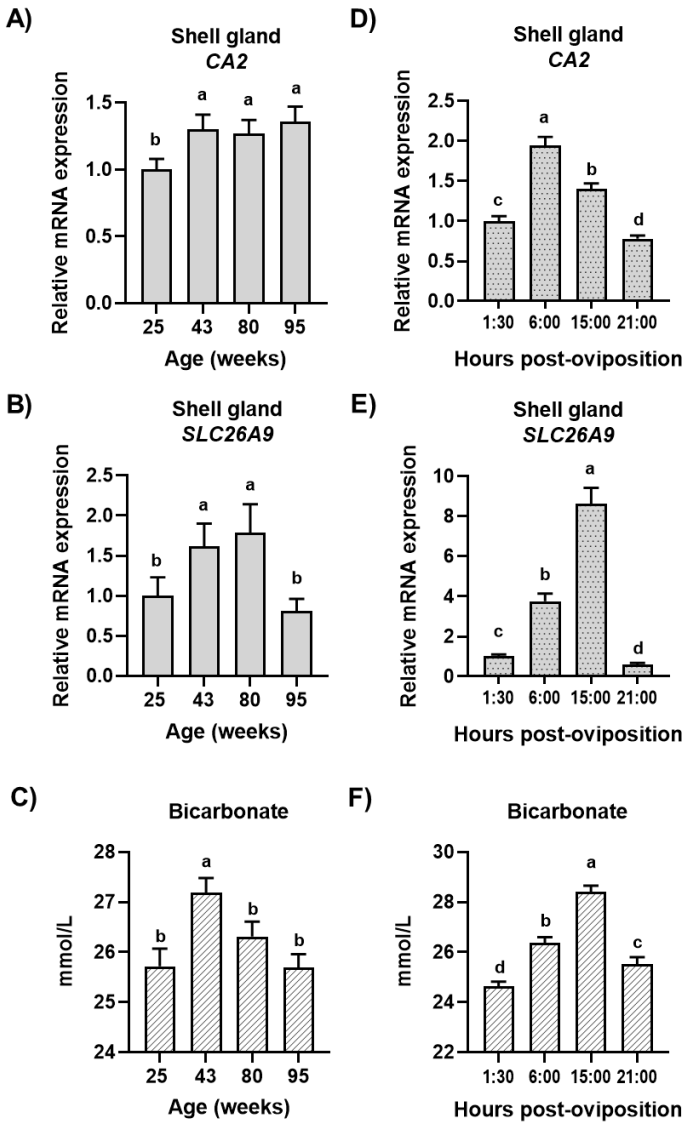

Figure 5.20. Bicarbonate production and transport.
Relative levels of mRNA for (A, D) *CA2*, (B, E) *SLC26A9*, and (C, F) bicarbonate in the shell gland at indicated ages and hours post-oviposition (HPOP) were determined by RT-qPCR and normalized to *RPL5* mRNA. Bicarbonate was measured using iSTAT CG8+ cartridges. Data were analyzed by two-way ANOVA followed by Fisher's test of least significant difference, and bars not sharing a common letter differ significantly ($P \leq 0.05$). The HPOP-by-age interaction was not significant for (A, D) *CA2* (P=0.8603), (B, E) *SLC26A9* (P=0.4104), or (C, F) Bicarbonate (P=0.1969) and interactive means are shown in Appendix C, Figure C10C - C10D. Main effects of age (mean+SEM; n=32 hens/age) for (A) *CA2* (P=0.0005) and (B) *SLC26A9* (P=0.0001) and main effects of HPOP (mean+SEM; n=32 hens/HPOP) for (D) *CA2* (P=0.0001) and (E) *SLC26A9* (P=0.0001), and (F) bicarbonate (P=0.0001) are shown.

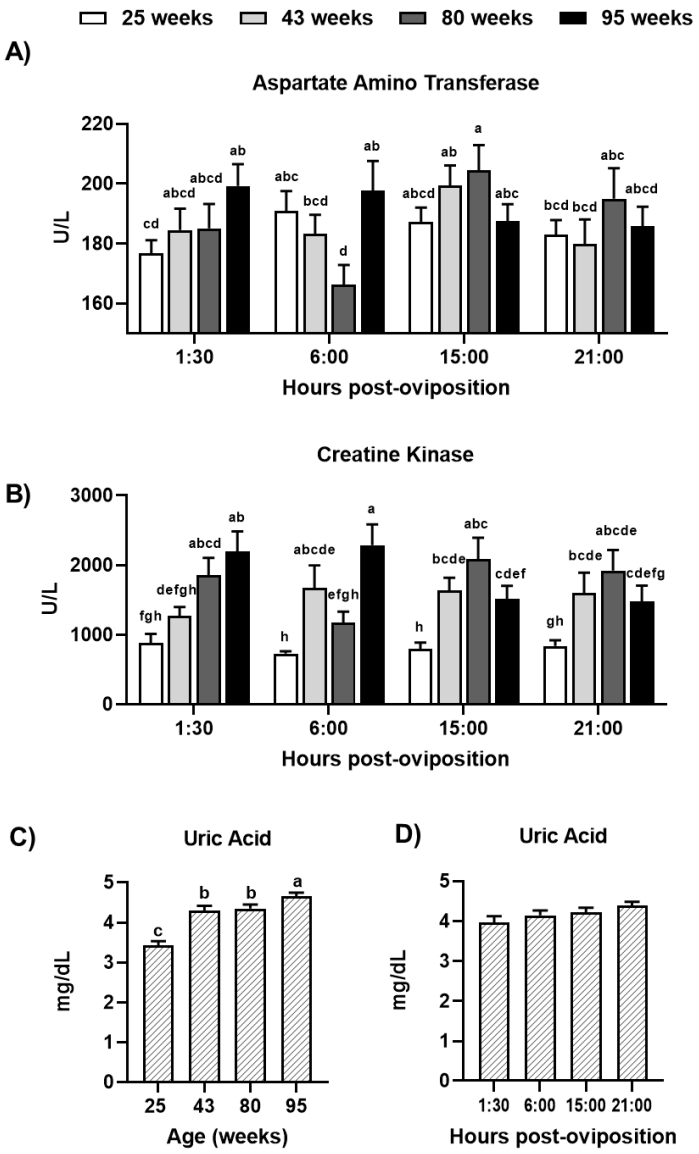

Figure 5.21. Circulating markers of renal and hepatic function.
Circulating levels of (A) aspartate aminotransferase, (B) creatine kinase, and (C, D) uric acid at indicated hours post-oviposition (HPOP) and ages were determined in whole blood using a VetScan2 device equipped with avian/reptile profile + cartridges. Data were analyzed by two-way ANOVA followed by Fisher's test of least significant difference, and bars not sharing a common letter differ significantly ($P \leq 0.05$). Significant HPOP-by-age interactions (mean+SEM; n=8 hens/age/HPOP) were identified for (A) aspartate aminotransferase ($P=0.0278$) and (B) creatine kinase ($P=0.0161$).The HPOP-by-age interaction was not significant for (C, D) UA ($P=0.5556$) and interactive means are shown in Appendix C, Figure C14A. Main effects of age (mean+SEM; n=48 hens/age) for (C) uric acid ($P=0.0001$) and main effects of HPOP (mean+SEM; n=48 hens/HPOP) for (D) uric acid ($P=0.0570$) are shown.

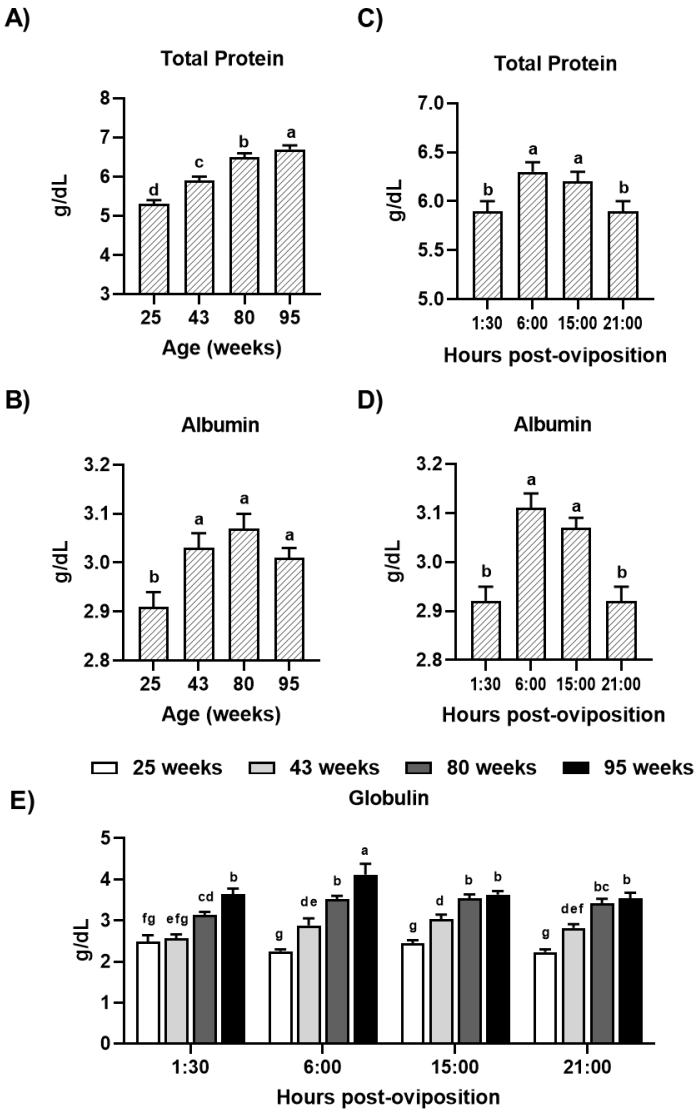

Figure 5.22. Circulating markers of renal and hepatic function.
Circulating levels of (A, C) total protein, (B, D) albumin, and (E) globulin at indicated hours post-oviposition (HPOP) and ages were determined in whole blood using a VetScan device equipped with avian/reptile profile + cartridges. Data were analyzed by two-way ANOVA followed by Fisher's test of least significant difference, and bars not sharing a common letter differ significantly ($P \leq 0.05$). The HPOP-by-age interaction was not significant for (A, C) total protein ($P=0.1000$) and (B, D) Alb ($P=0.4304$) and interactive means are shown in Appendix C, Figure C14B - C14C. Main effects of age (mean+SEM; n=48 hens/age) for (A) total protein ($P=0.0001$) and (B) albumin ($P=0.0002$) and main effects of HPOP (mean+SEM; n=48 hens/HPOP) for (C) total protein ($P=0.0001$) and (D) albumin ($P=0.0001$) are shown. A significant HPOP-by-age interaction (mean+SEM; n=8 hens/age/HPOP) was identified for (E) globulin ($P=0.0232$).

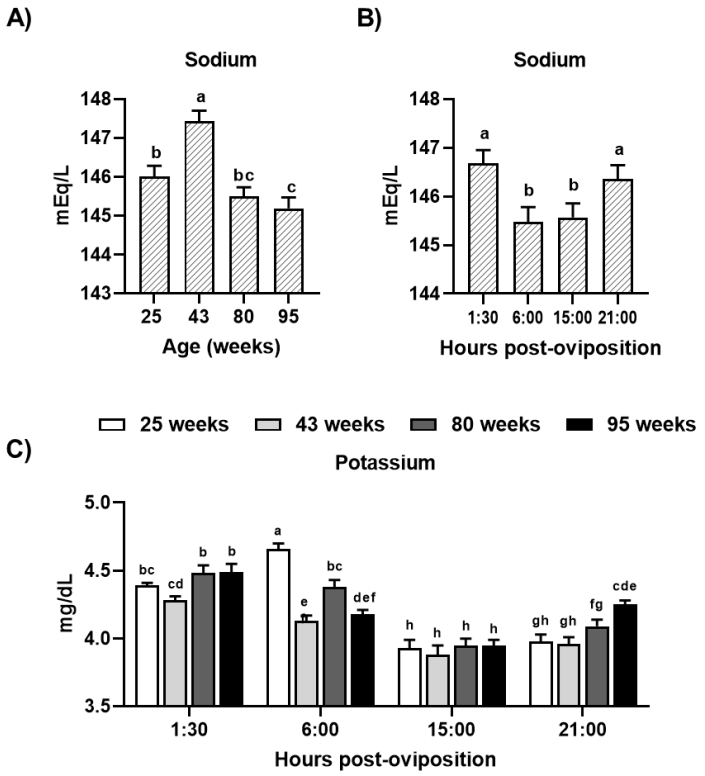

Figure 5.23. Circulating electrolytes.
Circulating levels of (A, B) sodium, and (C) potassium at indicated hours post-oviposition (HPOP) and ages were determined in whole blood using an iSTAT device equipped with CG8+ cartridges. Data were analyzed by two-way ANOVA followed by Fisher's test of least significant difference, and bars not sharing a common letter differ significantly ($P \leq 0.05$). The HPOP-by-age interaction was not significant for (A, B) sodium ($P=0.4999$) and interactive means are shown in Appendix C, Figure C15A. Main effects of age (mean+SEM; n=48 hens/age) for (A) sodium ($P=0.0001$) and main effects of HPOP (mean+SEM; n=48 hens/HPOP) for (B) sodium ($P=0.0015$) are shown. A significant HPOP-by-age interaction (mean+SEM; n=12 hens/age/HPOP) was identified for (C) potassium ($P=0.0001$).

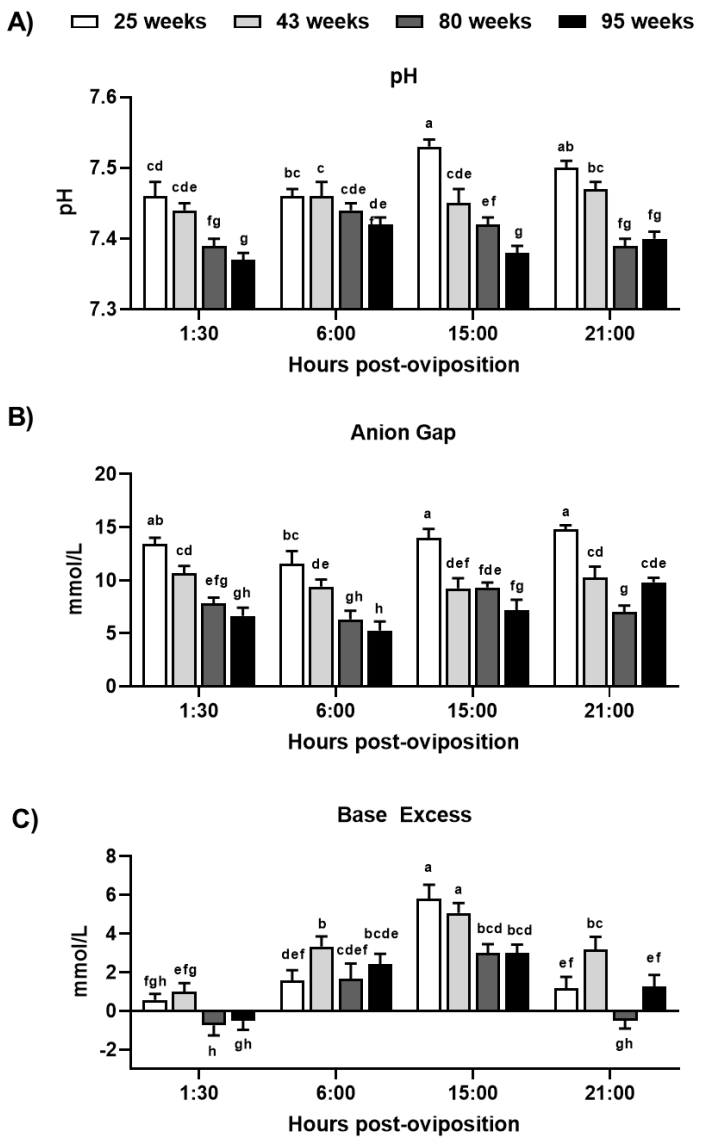

Figure 5.24. Circulating markers of acid-base balance.
Circulating (A) pH, (B) anion gap, and (C) base excess at indicated hours post-oviposition (HPOP) and ages were determined in whole blood using an iSTAT device equipped with CG8+ and Chem 8+ cartridges. Data were analyzed by two-way ANOVA followed by Fisher's test of least significant difference, and bars not sharing a common letter differ significantly ($P \leq 0.05$). Significant HPOP-by-age interactions (mean+SEM; n=12 hens/age/HPOP) were identified for (A) pH ($P=0.0028$), (B) anion gap ($P=0.0307$), and base excess ($P=0.0409$).

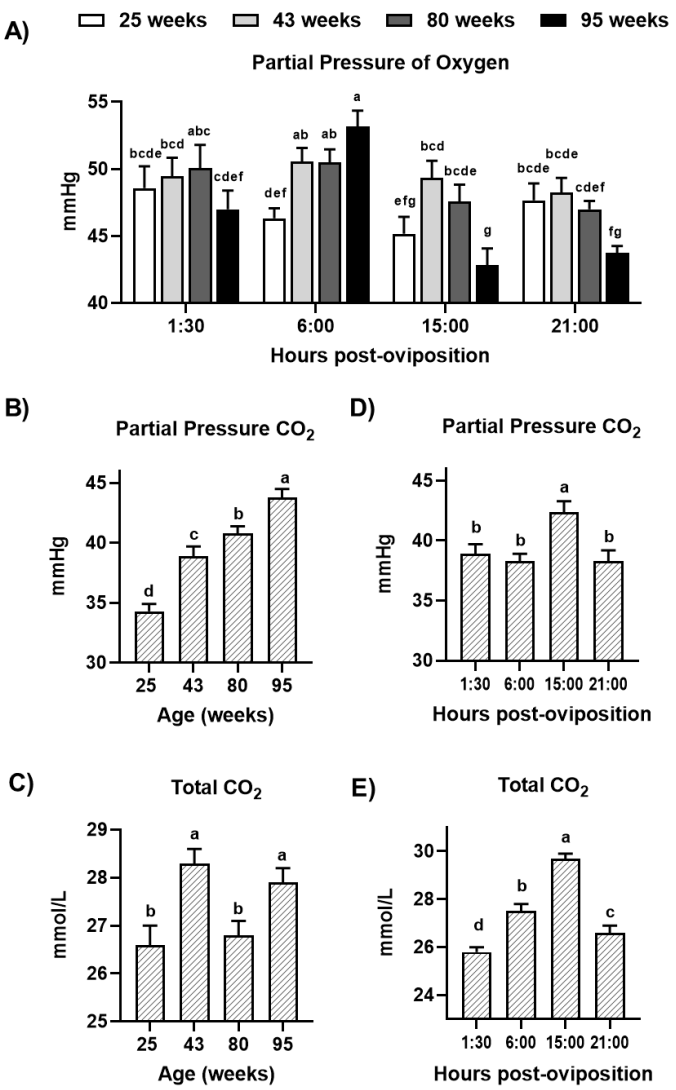

Figure 5.25. Circulating blood gases.
Circulating (A) partial pressure of oxygen (O_2), (B, D) partial pressure carbon dioxide (CO_2), and (C, E) total CO_2 at indicated hours post-oviposition (HPOP) and ages were determined in whole blood using an iSTAT device equipped with CG8+ cartridges. Data were analyzed by two-way ANOVA followed by Fisher's test of least significant difference, and bars not sharing a common letter differ significantly ($P \leq 0.05$). Significant HPOP-by-age interactions (mean+SEM; n=12 hens/age/HPOP) were identified for (A) partial pressure O_2 (P=0.0008). The HPOP-by-age interaction was not significant for (B, D) partial pressure of CO_2 (P=0.1564), and (C, E) total CO_2 (P=0.2399), and interactive means are shown in Appendix C, Figure C15 B - C15C. Main effects of age (mean+SEM; n=48 hens/age) for (B) partial pressure CO_2 (P=0.0001) and (C) total CO_2 (P=0.0001) and main effects of HPOP (mean+SEM; n=48 hens/HPOP) for (D) partial pressure CO_2 (P=0.0001) and (E) total CO_2 (P=0.0001) are shown.

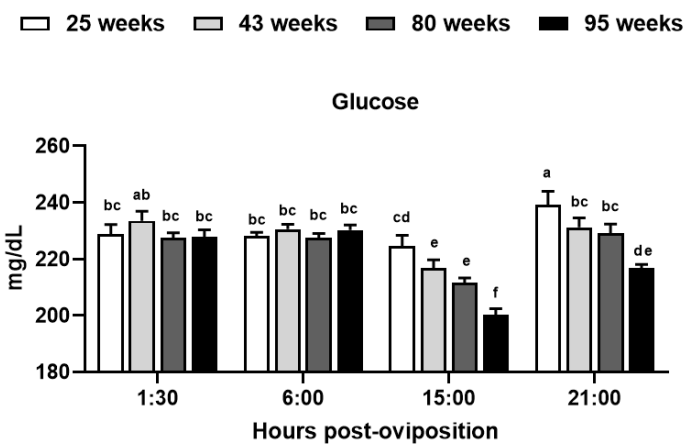

Figure 5.26. Circulating blood glucose.
Circulating glucose levels at indicated hours post-oviposition (HPOP) and ages were determined in whole blood using a VetScan2 device equipped with avian/reptile profile + cartridges. Data were analyzed by two-way ANOVA followed by Fisher's test of least significant difference, and bars not sharing a common letter differ significantly ($P \leq 0.05$). A significant HPOP-by-age interaction (mean+SEM; n=12 hens/age/HPOP) was identified for glucose ($P=0.0325$).

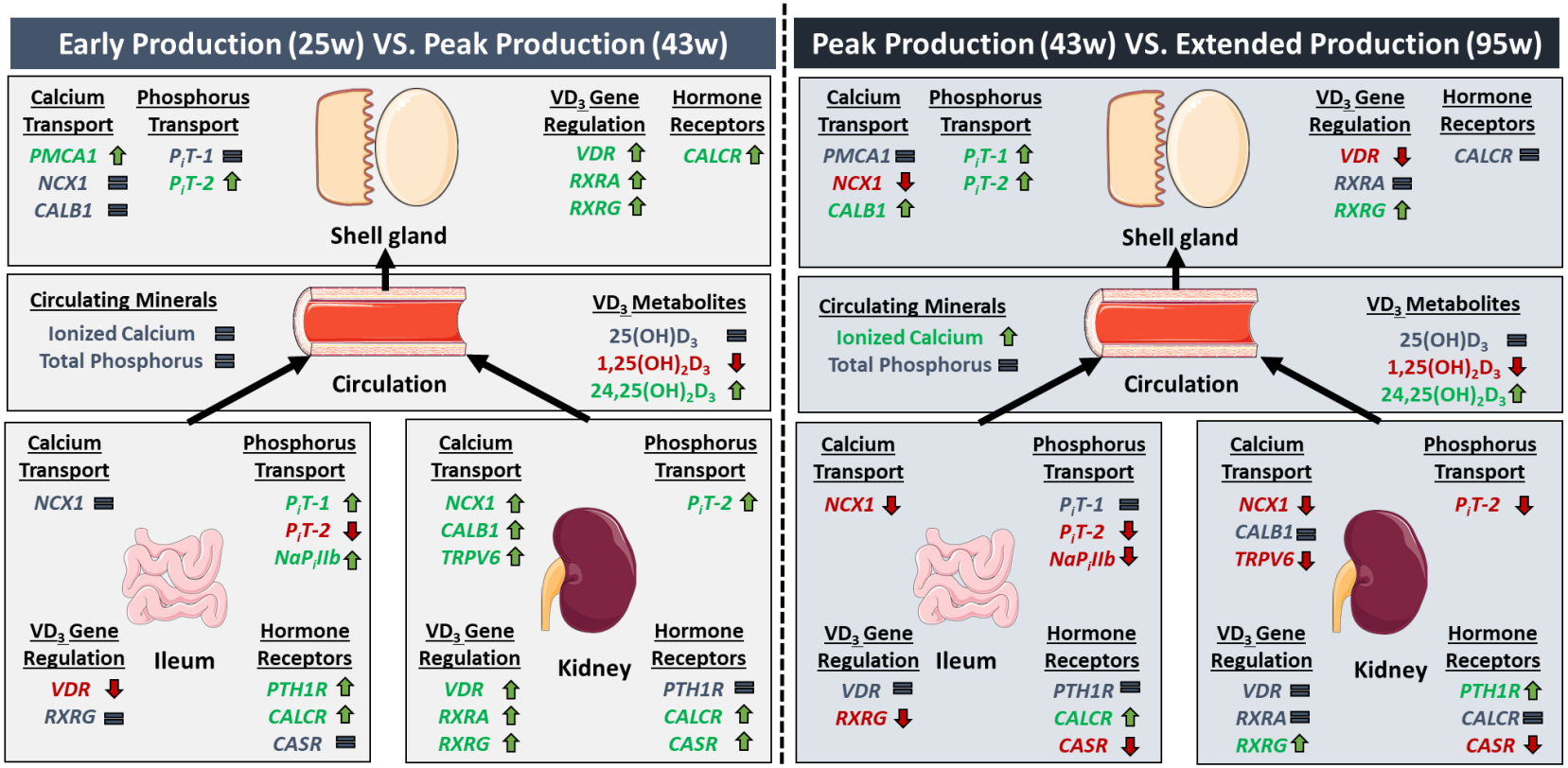

Figure 5.27 Across-age comparisons of minerals and vitamin D_3 metabolites in circulation and transcripts regulating calcium and phosphorus homeostasis between early, peak, and extended production stages.
Comparisons of circulating minerals and vitamin D_3 metabolites [$25(OH)D_3$, $1,25(OH)_2D_3$, and $24,25(OH)_2D_3$] as well as transcripts regulating calcium transport (*PMCA1*, *NCX1*, and *CALB1*), phosphorus transport (*P_iT-1*, *P_iT-2,* and *NaP_iIIb*), vitamin D_3 genomic response (*VDR*, *RXRA*, *RXRG*), and hormone receptors (*PTH1R*, *CALCR*, and *CASR*) in shell gland, ileum, and kidney tissue at 25 vs. 43 weeks of age and 43 vs. 95 weeks of age. Green arrows are indicative of a significant increase ($P \leq 0.05$) in the levels of a parameter, blue equal signs represent no significant change ($P > 0.05$), and red arrows indicate a significant decrease ($P \leq 0.05$) in the parameter.

CHAPTER 6

DISCUSSION AND CONCLUSIONS

Table eggs are affordable and an excellent source of essential amino acids and vitamins (Ruxton et al., 2010). These characteristics make eggs an ideal candidate to provide high-quality protein to the increasing global population, which is expected to grow by 2 billion individuals in the next three decades (United Nations, 2015). To meet the growing demand for eggs, the table egg industry has increased the number of eggs produced by individual laying hens through genetic selection for longer clutch lengths (Thiruvenkadan et al., 2010), and hens are being maintained in production for up to 57% longer periods of time than in previous years. It should be noted that these improvements are not without consequences. Older hens produce larger eggs with thinner eggshells (Al-Batshan et al., 1994; Tumova et al., 2014), which are more likely to break during packaging and transport, leading to economic losses and food safety concerns. Furthermore, aged hens exhibit a higher incidence of osteoporosis (Wilson et al., 1992; Whitehead et al., 2000), leading to fragile and brittle bones prone to fracture. Fractures in laying hens have been identified as a significant welfare concern by the Farm Animal Welfare Council (FAWC, 2010), and solutions must be found to limit their occurrence. Both poor-quality eggshells and osteoporosis are influenced by the regulation of calcium and phosphorus homeostasis in laying hens, and a thorough understanding of these processes is required to develop practical solutions to these challenges.

Modern hens are capable of forming an egg every 24 hours (Nys et al., 2011; Gautron et al., 2021), which requires calcium and phosphorus derived from dietary and skeletal origins (Comar et al., 1949). Shortly following oviposition, dietary minerals are utilized to mineralize labile medullary bone stores (Kerschnitzki et al., 2014). The ovum enters the shell gland around 6

hours following oviposition and remains there for 18 hours as the eggshell calcifies, with peak eggshell calcification taking place between 12 and 18 hours post-oviposition [HPOP] (Gautron et al., 2021; Sinclair-Black et al., 2024). A significant portion of the time spent calcifying the eggshell takes place during the dark phase of the lighting cycle, where hens are unlikely to consume feed. Consequently, bone resorption is elevated to release the minerals required for eggshell formation (Comar et al., 1949; Mueller et al., 1964). As such, every 24 hours, a cycle occurs where the medullary bone is broken down to provide calcium and phosphorus for eggshell calcification and then subsequently remineralized in the hours following oviposition. During this daily lay cycle, imbalances in calcium and phosphorus homeostasis have the potential to negatively impact bone integrity and eggshell quality; thus, a deeper understanding of the physiological regulation of calcium and phosphorus balance is essential to maintaining eggshell and bone integrity. Collectively, the objectives of this study were to investigate the intestinal distribution of the expression of genes regulating calcium and phosphorus uptake and evaluate the physiological regulation of calcium and phosphorus homeostasis during the daily egg-laying cycle at early, peak, late, and extended egg production.

Findings in this study identified distal increases in the expression of transcellular and paracellular calcium and phosphorus transporters across the small intestine. These results, coupled with increased expression of fibroblast growth factor 23 (*FGF23*) receptors, calcium-sensing receptor, parathyroid hormone receptor, calcitonin receptor, vitamin D receptor, and its heterodimeric partners retinoid X receptor alpha and gamma (*RXRG*), suggest that the ileum is responsive to hormonal regulation and likely an important site for calcium and phosphorus absorption in the small intestine. These findings were in contrast to previous literature in poultry, which has traditionally identified the duodenum and jejunum as the primary regions of calcium

and phosphorus absorption in birds (Hurwitz et al., 1965; Hurwitz et al., 1973). Although in dogs (Cramer, 1965) and rats (Cramer et al., 1959; Marcus et al., 1962), the ileum is considered a major site of calcium absorption. Findings also implicated ceca as a potentially novel tissue involved in mineral transport. Cecal expression of calcium transporter sodium-calcium exchanger 1 (*NCX1*) was 30-fold higher than the duodenum and 18-fold greater than the ileum. Other calcium transporters, such as plasma membrane calcium transporter four and transient receptor potential cation member 7, were also significantly higher in the ceca than in any location in the small intestine. Cecal inorganic phosphorus transporter 1 (*P_iT-1*) and sodium-dependent phosphorus transporter 2b (*NaP_iIIb*) were expressed more than 15-fold greater than any section of the small intestine. Neither the ceca nor the ileum has been traditionally associated with significant uptake of calcium and phosphorus, and, as such, elucidating the extent to which these tissues contribute to mineral homeostasis is crucial to improving our understanding of calcium and phosphorus dynamics in laying hens.

Findings herein also demonstrated that hydroxylation of vitamin D_3 potentially occurs in non-canonical tissues, serving as an additional regulatory mechanism in the local control of mineral transporter expression. The kidney, which is not typically associated with the production of circulating 25(OH)D_3, demonstrated robust expression of 25-hydroxylase during stages of peak and late eggshell calcification from 12 to 23 HPOP in conjunction with higher 1α-hydroxylase and reduced 24-hydroxylase expression. Expression of these hydroxylase enzymes was also present in the shell gland and ileum, potentially also impacting the availability of 1,25$(OH)_2D_3$ at a local level in these tissues during stages of bone mineralization and eggshell calcification.

Our results suggest that the termination of eggshell calcification is likely mediated by reduced availability of bicarbonate ions and upregulation of phosphorus transport during late

eggshell calcification. Bicarbonate utilized for eggshell calcification originates from carbonic anhydrase activity in the shell gland epithelial cells and circulation. During late calcification, expression of carbonic anhydrase significantly decreased, as did circulating bicarbonate. Furthermore, expression of the bicarbonate transporter solute carrier family 26 A9 (*SLC26A9*) decreased 8-fold between peak and late eggshell calcification, potentially leading to a considerable reduction in the amount of bicarbonate delivered into the shell gland lumen. Instead, during late calcification, FGF23 receptors 2 and 3, which are likely associated with increased phosphorus transporter expression, more than doubled in the shell gland compared to stages of peak eggshell calcification. The expression of FGF23 receptors in the shell gland has not been previously investigated, and as such, this study identified the shell gland as a novel target involved in FGF23 signaling. The elevated expression of FGF23 receptors potentially resulted in heightened expression of phosphorus transporters *P_iT-1* and *NaP_iIIb* in the shell gland during late eggshell calcification. Since the presence of phosphorus in the shell gland lumen has been shown to inhibit calcite formation (Bachra et al., 1963; Simkiss, 1964), it is possible that reductions in bicarbonate availability in conjunction with elevated phosphorus levels led to the slowing and eventual cessation of eggshell calcification at 21:00 HPOP.

Furthermore, our findings suggest that older hens may initiate eggshell calcification later and cease eggshell calcification sooner than younger hens, resulting in lower levels of calcium deposited into the eggshells and reduced eggshell weights in older hens. Circulating ionized calcium is available for processes such as bone mineralization and eggshell calcification. At 6:00 HPOP, the follicle enters the shell gland, and ionized calcium is rapidly removed from circulation to supply the calcifying eggshell. In this study, aged hens exhibited greater ionized calcium at 6:00 HPOP than younger hens, suggesting that the transition into eggshell calcification may be delayed.

Hens in extended production also expressed significantly greater levels of *P_iT-1* during late eggshell calcification at 21:00 HPOP than hens at peak production, indicating earlier termination of eggshell calcification. Together, the delayed initiation and early termination of eggshell mineralization likely contributed to reduced eggshell-breaking strength and lower eggshell calcium content in aged hens.

Findings herein also identified disturbances in vitamin D_3 hydroxylation patterns as likely contributors to inferior eggshell quality and diminished skeletal integrity observed in older hens. As hens aged, circulating levels of biologically active $1,25(OH)_2D_3$ decreased, particularly during peak eggshell calcification. Conversely, biologically inactive $24,25(OH)_2D_3$ levels increased during this period. Since $1,25(OH)_2D_3$ is necessary for the genomic regulation of mineral transporters, the diminished circulating levels of biologically active vitamin D_3 likely contributed to the altered expression of mineral transport-related genes in the ileum (*NCX1,* inorganic phosphorus transporter 2 [*P_iT-2*], and *NaP_iIIb*), kidney (*NCX1*, transient receptor potential cation channel V6 [TR*PV6*], *P_iT-1*, and *P_iT-2*) and shell gland (*NCX1*, *PiT-1*, *P_iT-2*, and *SLC26A9*) during extended production at 95 weeks in comparison to peak production at 43 weeks. Interestingly, expression of *RXRG* showed substantial increases in expression between 25 and 80 weeks in the shell gland and kidney, potentially modulating long-term effects of vitamin D_3 genomic actions in these tissues. Together, reduced mineral transport in the shell gland likely contributed to the numerically lower eggshell weights and reduced breaking strength in older hens, while in the kidney and ileum, reduced mineral transport may have affected bone mineralization and mineral availability for eggshell calcification in older hens. The reduction in 1α-hydroxylase activity in older hens may have also resulted from impaired kidney function and subsequent acid-base imbalances. Uric acid and total protein can be indicators of reduced renal function. These

markers steadily increased from early through extended production, suggesting an impaired renal capacity to excrete waste products and contribute to mineral homeostasis, as well as compromised fluid balance. Accompanying these findings were increased partial pressure of carbon dioxide well above the reference range and reduced circulating blood pH values, indicating acute respiratory acidosis in older hens. Lower blood pH values are associated with impaired 1α-hydroxylase activity (Sauveur, 1977), potentially hindering calcium availability and transport required for eggshell calcification and bone mineralization.

Collectively, this study identified key hormonal signaling pathways and associated mineral transporters involved in bone mineralization and eggshell calcification during the daily lay cycle and across extended production. Furthermore, physiological pathways that become dysregulated with age were determined, likely contributing to poor eggshell quality and compromised skeletal structure observed in older hens. Ultimately, these studies provide valuable information that can be used to develop nutritional and genetic solutions geared toward maintaining eggshell quality and skeletal integrity in extended production systems, in turn reducing economic losses and improving animal welfare.

REFERENCES

1. Abe, E., H. Horikawa, T. Masumura, M. Sugahara, M. Kubota, and T. Suda. 1982. Disorders of cholecalciferol metabolism in old egg-laying hens. Journal of Nutrition 112:436-446. doi: 10.1093/jn/112.3.436

2. Al-Batshan, H. A., S. E. Scheideler, B. L. Black, J. D. Garlich, and K. E. Anderson. 1994. Duodenal calcium uptake, femur ash, and eggshell quality decline with age and increase following molt. Poultry Science 73:1590-1596. doi: 10.3382/ps.0731590

3. Alexander, R. T., J. Rievaj, and H. Dimke. 2014. Paracellular calcium transport across renal and intestinal epithelia. Biochemistry Cell Biology 92:467-480. doi: 10.1139/bcb-2014-0061

4. Alfonso-Carrillo, C., C. Benavides-Reyes, J. de Los Mozos, N. Dominguez-Gasca, E. Sanchez-Rodriguez, A. I. Garcia-Ruiz, and A. B. Rodriguez-Navarro. 2021. Relationship between bone quality, egg production and eggshell quality in laying hens at the end of an extended production cycle (105 weeks). Animals (Basel) 11. doi: 10.3390/ani11030623

5. Arad, Z., U. Eylath, M. Ginsburg, and H. Eyal-Giladi. 1989. Changes in uterine fluid composition and acid-base status during shell formation in the chicken. American Journal of Physiology 257:R732-R737. doi: 10.1152/ajpregu.1989.257.4.R732

6. Araujo, A. C., R. D. S. Araujo, L. R. B. Dourado, J. S. Machado, G. F. V. Bayao, L. Amoroso, S. M. B. Artoni, A. C. Shimado, and K. R. Silva Sousa. 2022. Analysis of performance, bone characteristics, and expression of genes involved in the balance of ionic concentrations in broilers subjected to dietary electrolyte balance levels. British Poultry Science 63. doi: 10.1080/00071668.2021.1966754

7. Areco, V. A., R. Kohan, G. Talamoni, N. G. Tolosa de Talamoni, and M. E. Peralta Lopez. 2020. Intestinal Ca^{2+} revisited: A molecular and clinical approach. World Journal of Gastroenterology 26:3344-3364. doi: 10.3748/wjg.v26.i24.3344

8. Arias, J. L., M. S. Fernandez, J. E. Dennis, and A. I. Caplan. 1991. The fabrication and collagenous substructure of the eggshell membrane in the isthmus of the hen oviduct. Matrix 11:313-320. doi: 10.1016/S0934-8832(11)80202-7

9. Ascenzi, A., C. Francois, and S. Bocciarellli. 1963. On the bone induced by estrogens in birds. Journal of Ultrastructure Research 8:491-505. doi: 10.1016/S0022-5320(63)80051-

10. Ba, J., D. Brown, and P. A. Friedman. 2003. Calcium-sensing receptor regulation of PTH-inhibitable proximal tubule phosphate transport. Am J Physiol-Renal 285:1233-1243. doi: 10.1152/ajprenal.00249.2003

11. Bachra, B. N., O. R. Trautz, and S. Lawrence Simon. 1963. Precipitation of calcium carbonates and phosphates. I. Spontaneous precipitation of calcium carbonates and phosphates under physiological conditions. Biochemistry and Biophysics 103:124-138. doi: 10.1016/0003-9861(63)90018-3

12. Bai, X., D. Miao, D. Goltzman, and A. C. Karaplis. 2003. The autosomal dominant hypophosphatemic rickets R176Q mutation in fibroblast growth factor 23 resists proteolytic cleavage and enhances *in vivo* biological potency. J. Biol. Chem. 278:9843-9849. doi: 10.1074/jbc.M210490200

13. Bain, M. M. 1992. Eggshell strength: a relationship between the mechanism of failure and the ultrastructural organisation of the mammillary layer. British Poultry Science 33:303-319. doi: 10.1080/00071669208417469

14. Bain, M. M., Y. Nys, and I. C. Dunn. 2016. Increasing persistency in lay and stabilizing egg quality in longer laying cycles. What are the challenges? British Poultry Science 57:330-338. doi: 10.1080/00071668.2016.1161727

15. Baker, S. L., C. I. Robison, D. M. Karcher, M. J. Toscano, and M. M. Makagon. 2020. Keel impacts and associated behavior in laying hens. Applied Animal Behavior Science 222. doi: 10.1016/j.applanim.2019.104886

16. Bar, A. 2008. Calcium homeostasis and vitamin D metabolism and expression in strongly calcifying laying birds. Comparative Biochemistry and Physiology 151:477-490. doi: 10.1016/j.cbpa.2008.07.006

17. Bar, A. 2009. Calcium transport in strongly calcifying laying birds: mechanisms and regulation. Comparative Biochemistry and Physiology 152:447-469. doi: 10.1016/j.cbpa.2008.11.020

18. Bar, A., A. Cohen, U. Eisner, G. Riesenfeld, and S. Hurwitz. 1977. Differential response of calcium transport systems in laying hens to exogenous and endogenous changes in vitamin D status. Journal of Nutrition 108:1322-1328. doi: 10.1093/jn/108.8.1322

19. Bar, A., J. Rosenberg, and S. Hurwitz. 1984. The lack of relationships between vitamin D3 metabolites and calcium-binding protein in the eggshell gland of laying birds. Comparative

Biochemistry and Physiology 78B:75-79. doi: 10.1016/0305-0491(84)90148-2

20. Bar, A., M. Shani, C. S. Fullmer, M. E. Brindak, and S. Striem. 1990a. Modulation of chick intestinal and renal calbindin gene expression by dietary vitamin D_3, 1,25-dihydroxyvitamin D_3, calcium, and phosphorus. Molecular and Cellular Endocrinology 72:23-31. doi: 10.1016/0303-7207(90)90236-2

21. Bar, A., M. Sharvit, D. Noff, S. Edelstein, and S. Hurwitz. 1980. Absorption and excretion of cholecalciferol and of 25-hydroxycholecalciferol and metabolites in birds. Journal of Nutrition 110:1930-1934. doi: 10.1093/jn/110.10.1930

22. Bar, A., S. Striem, S. Mayel-Afshar, and D. E. M. Lawson. 1990b. Differential regulation of calbindin-D28k mRNA in the intestine and eggshell gland of the laying hen. J. Mol. Endocrinol. 4:93-99. doi: 10.1677/jme.0.0040093

23. Bar, A., E. Vax, and S. Striem. 1999. Relationships among age, eggshell thickness and vitamin D metabolism and its expression in the laying hen. Comparative Biochemistry and Physiology 123:147-154. doi: 10.1016/S1095-6433(99)00039-2

24. Beck, N., H. P. Kim, and K. S. Kim. 1975. Effect of metabolic acidosis on renal action of parathyroid hormone. American Journal of Physiology 5:1483-1489. doi: 10.1152/ajplegacy.1975.228.5.1483

25. Bell, D. D. 2002. Formation of the egg. Pages 59-69 in Commercial chicken meat and egg production. D. D. Bell et al. eds. Springer Science, New York, NY.

26. Bell, D. J., and W. M. McIndoe. 1958. Tissue componensts of the domestic fowl: the non-protein nitrogen of plasma and erythrocytes. J. Biol. Chem. 71:355-365. doi: 10.1042/bj0710355

27. Ben-Dov, I. Z., H. Galitzer, V. Lavi-Moshayoff, R. Goetz, M. Kuro, M. Mohammadi, R. Sirkis, T. Naveh-Many, and J. Silver. 2007. The parathyroid is a target organ for FGF23 in rats. J Clin Invest 117:4003-4008. doi: 10.1172/Jci32409

28. Benavides-Reyes, C., E. Folegatti, N. Dominguez-Gasca, G. Litta, E. Sanchez-Rodriguez, A. B. Rodriguez-Navarro, and M. Umar Faruk. 2021. Research note: Changes in eggshell quality and microstructure related to hen age during a production cycle. Poultry Science 100:101287. doi: 10.1016/j.psj.2021.101287

29. Bikle, D. D. 2014. Vitamin D metabolism, mechanism of action and clinical applications. Chemistry & Biology 21:319-329. doi: 10.1016/j.chembiol.2013.12.016

30. Bikle, D. D. 2018. Vitamin D biochemistry and physiology. Pages 1-40 in Extra-skeletal Effects of Vitamin D. E. P. Liao ed. Humana Press, New York, NY.

31. Board, R. G., and N. A. Halls. 1973. The cuticle: a barrier to liquid and particle penetration of the shell of the hen's egg. British Poultry Science 14:69-97. doi: 10.1080/00071667308415999

32. Bobeck, E. A., K. S. Burgess, T. R. Jarmes, M. L. Piccione, and M. E. Cook. 2012. Maternally-derived antibody to fibroblast growth factor-23 reduced dietary phosphate requirements in growing chicks. Biochemical and Biophysical Research Communications 420:666-670. doi: 10.1016/j.bbrc.2012.03.063

33. Bonucci, E., and G. Gherardi. 1975. Histochemical and electron microscope investigations on medullary bone. Cell and Tissue Research 163:81-97. doi: doi.org/10.1007/BF00218592

34. Bouillon, R., H. Van Baelen, and P. De Moor. 1980. Comparative study of the affinity of the serum vitamin D-binding protein. J Steroid Biochem 13:1029-1034.

35. Braun, E. J. 1999. Integration of renal and gastrointestinal function. Journal of Experimental Zoology 283:495-499.

36. Brenza, H. L., and H. F. DeLuca. 2000. Regulation of 25-Hydroxyvitamin D_3 1a-hydroxylase gene expression by parathyroid hormone and 1,25-dihydroxyvitamin D_3. Biochemistry and Biophysics 381:143-152. doi: 10.1006/abbi.2000.1970

37. Brenza, H. L., C. Kimmel-Jehan, F. Jehan, T. Shinki, S. Wakino, H. Anazawa, T. Suda, and H. F. DeLuca. 1998. Parathyroid hormone activation of the 25-hydroxyvitaminD_3-1a-hydroxylase gene promoter. Proceedings of the National Academy of Sciences of the United States of America 95:1387-1391. doi: 10.1073/pnas.95.4.138

38. Brionne, A., Y. Nys, C. Hennequet-Antier, and J. Gautron. 2014. Hen uterine gene expression profiling during eggshell formation reveals putative proteins involved in the supply of minerals or in the shell mineralization process. BMC Genomics 15:1-17. doi: 10.1186/1471-2164-15-220

39. Brommage, R., and H. F. DeLuca. 1985. Evidence that 1,25-dihydroxyvitamin D_3 is the physiologically active metabolite of vitamin D3. Endocrine Reviews 6:491-511. doi: 10.1210/edrv-6-4-491

40. Bronner, F., and W. D. Stein. 1988. CaBPr facilitates intracellular diffusion for Ca pumping in distal convoluted tubule. American Journal of Physiology 255:F558-F563. doi:

10.1152/ajprenal.1988.255.3.F558

41. Buyse, J., D. S. Adelsohn, E. Decuypere, and C. G. Scanes. 1993. Diurnal-nocturnal changes in food intake, gut storage of ingesta, food transit time, and metabolism in growing broiler chickens. British Poultry Science 34:699-709. doi: 10.1080/00071669308417628

42. Cabezas-Garcia, E. H., D. E. Rodriguez-Aguilar, and G. Afanador-Tellez. 2022. Individual egg production of Hy-Line Brown hens during the early laying phase in response to dietary CP levels. Animal 1:1-11. doi: 10.1016/j.anopes.2022.100027

43. Carlberg, C., and P. Polly. 1998. Gene regulation by vitamin D_3. Critical Reviews in Eukaryotic Gene Expression 8:19-42. doi: 10.1615/CritRevEukarGeneExpr.v8.i1.20

44. Carpenter, T. O., C. Bergwitz, and K. L. Insogna. 2020. Phosphorus homeostasis and related disorders. Pages 469-507 in Principles of Bone Biology. J. P. Bilezikian et al. eds. Academic Press, Cambridge, MA.

45. Chandra, S., C. S. Fullmer, C. A. Smith, R. H. Wasserman, and G. H. Morrison. 1990. Ion microscopic imaging of calcium transport in the intestinal tissue of vitamin D deficient and vitamin D replete chickens: A ^{44}Ca stable isotope study. Proceedings of the National Academy of Sciences of the United States of America 87:5715-5719. doi: 10.1073/pnas.87.15.5715

46. Chanpaisaeng, K., J. Teerapornpuntakit, K. Wongdee, and N. Charoenphandhu. 2021. Emerging roles of calcium-sensing in the local regulation of intestinal transport of ions and calcium. American Journal of Physiology 320:270-278. doi: 10.1152/ajpcell.00485.2020

47. Chen, X., X. Li, Y. Guo, W. Li, J. Song, G. Xu, N. Yang, and J. Zheng. 2019. Impact of cuticle quality and eggshell quality on egg antibacterial efficiency. Poultry Science 98:940-948. doi: 10.3382/ps/pey369

48. Cheng, J. B., D. L. Motola, D. J. Mangelsdorf, and D. W. Russell. 2003. De-orphanization of cytochrome P450 2R1. J. Biol. Chem. 278:38084-38093. doi: 10.1074/jbc.M307028200

49. Cheng, T. K., and C. N. Coon. 1990. Effect of calcium source, particle size, limestone solubility in vitro and calcium intake level on layer bone status and performance. Poultry Science 69:2214-2219. doi: 10.3382/ps.0692214

50. Chun, R. F., E. Blatter, S. Elliott, S. Fitz-Gibbon, S. Rieger, A. Sagasti, J. S. Adams, and M. Hewison. 2014. Cloning of a functional 25-hydroxyvitamin D-1a-hydroxylase in zebrafish (Danio rerio). Cell Biochem. Funct. 32:675-682. doi: 10.1002/cbf.3071

51. Cieplnego, W. S. 2011. Effect of heat stress on biochemical parameters of hens. Proceedings of ECOpole 5:57-60.

52. Clark, N. B., and R. F. Wideman. 1980. Calcitonin stimulation of urine flow and sodium excretion in the starling. American Journal of Physiology 238. doi: 10.1152/ajpregu.1980.238.5.R406

53. Clunies, M., J. R. Etches, C. Fair, and S. Leeson. 1992. Blood, intestinal and skeletal calcium dynamics during egg formation. Canadian Journal of Animal Science 73:517-532. doi: 10.4141/cjas93-056

54. Clunies, M., and S. Leeson. 1995. Effect of dietary calcium level on plasma proteins and calcium flux occurring during a 24 h ovulatory cycle. Canadian Journal of Animal Science 75:439-444. doi: 10.4141/cjas95-064

55. Cochran, M., M. Peacock, G. Sachs, and B. E. C. Nordini. 1970. Renal effects of calcitonin. British Medical Journal 1:135-137. doi: 10.1136/bmj.1.5689.135

56. Cohen, I., and S. Hurwitz. 1974. The response of blood ionic constituents and acid-base balance to dietary sodium, potassium, and chloride in laying fowls. Poultry Science 53:378-383. doi: 10.3382/ps.0530378

57. Cohen, I., S. Hurwitz, and A. Bar. 1971. Acid-base balance and sodium-to-chloride ratio in diets of laying hens. Journal of Nutrition 102:1-8. doi: 10.1093/jn/102.1.1

58. Comar, C. L., and J. C. Driggers. 1949. Secretion of radioactive calcium in the hen's egg. Science 109:282. doi: 10.1126/science.109.2829.282

59. Copp, D. H., D. W. Cockcroft, and Y. Kueh. 1967. Calcitonin from ultimobranchial glands of dogfish and chickens. Science 158:924-925. doi: 10.1126/science.158.3803.924

60. Corradino, R. A., C. A. Smith, L. P. Krook, and C. S. Fullmer. 1993. Tissue-specific regulation of shell gland calbindin D28K biosynthesis by estradiol in precociously matured, vitamin D-depleted chicks. Endocrinology 132:193-198. doi: 10.1210/endo.132.1.8419123

61. Craan, A. G., G. Lemieux, P. Vinay, A. Gougoux, and A. Quenneville. 1982. The kidney of the chicken adapts to chronic metabolic acidosis: in vivo and in vitro studies. Kidney International 22:103-111. doi: 10.1038/ki.1982.142

62. Cramer, C. F. 1965. Sites of calcium absorption and the calcium concentration of gut contents in the dog. Canadian Journal of Physiology and Pharmacology 43:75-78. doi:

10.1139/y65-009

63. Cramer, C. F., and D. H. Copp. 1959. Progress and rate of absorption of radiosrontium through intestinal tracts of rats. Proceedings of the Society for Experimental Biology and Medicine 102:514-517. doi: 10.3181/00379727-102-25301

64. Cusack, M., and A. C. Fraser. 2002. Eggshell membrane removal for subsequent extraction of intermineral and intramineral proteins. Cryst Growth Des 2:529-532. doi: 10.1021/cg0255624

65. Cusack, M., A. C. Fraser, and T. Stachel. 2003. Magnesium and phosphorus distribution in the avian eggshell. Comparative Biochemistry and Physiology 134:63-69. doi: 10.1016/s1096-4959(02)00185-9

66. Dacke, C. G., S. Arkle, D. J. Cook, I. M. Wormstone, S. Jones, M. Zaidi, and Z. A. Bascal. 1993. Medullary bone and avian calcium regulation. J. Exp. Biol. 184:63-88. doi: 10.1242/jeb.184.1.63

67. Dacke, C. G., T. Sugiyama, and C. V. Gay. 2015. The role of hormones in the regulation of bone turnover and eggshell calcification. Pages 549-575 in Sturkie's Avian Physiology. C. G. Scanes ed. Academic Press, Cambridge, MA.

68. Davey, R. A., A. G. Turner, J. F. McManus, W. S. Chiu, F. Tjahyono, A. J. Moore, G. J. Atkins, P. H. Anderson, C. Ma, V. Glatt, H. MacLean, C. Vincent, M. Bouxsein, H. A. Morris, D. M. Findlay, and J. Zajac. 2008. Calcitonin receptor plays a physiological role to protect against hypercalcemia in mice. Journal of Bone and Mineral Research 23:1182-1194. doi: 10.1359/jbmr.080310

69. Deng, Y., J. Bi, J. Qiao, G. He, B. Wu, M. Y. H. Zhang, and N. LV. 2010. Expression and tissue distribution of extracellular calcium-sensing receptor (CaSR) mRNA in chickens. Turk J Vet Anim Sci 34:249-254. doi: 10.3906/vet-0809-27

70. Dennis, J. E., S. Xiao, M. Agarwal, D. Fink, A. H. Heuer, and A. Caplan. 1996. Microstructure of matrix and mineral components of eggshells from White Leghorn chickens (*Gallus gallus*). J. Morph. 228:287-306. doi: 10.1002/(SICI)1097-4687(199606)228:3<287::AID-JMOR2>3.0.CO;2-%23

71. Diana, T. F., A. A. Calderano, F. d. C. Tavernari, H. S. Rostagno, A. d. O. Teixeira, and L. F. T. Albino. 2021. Age and calcium sources in laying hen feed affect calcium digestibility. Open Journal of Animal Sciences 11:501-513. doi: 10.4236/ojas.2021.113034

72. Diaz, R., S. Hurwitz, N. Chattopadhyay, M. Pines, Y. Yang, O. Kifor, M. S. Einat, R.

Butters, S. C. Herbert, and E. M. Brown. 1997. Cloning, expression and tissue localization of the calcium-sensing receptor in chicken (*gallus domesticus*). American Journal of Physiology 273:R1008-R1016. doi: 10.1152/ajpregu.1997.273.3.R1008

73. Ding, H., Q. Yue, L. Chang, J. Xi, H. Chen, F. Li, D. Wang, and R. Zhou. 2021. Whole blood gas and biochemical reference intervals for Lohman Silver layers. Poultry Science 100:1-6. doi: 10.1016/j.psj.2021.101368

74. Donate-Correa, J., M. Muros-de-Fuentes, C. Mora-Fernandez, and J. F. Navarro-Gonzalez. 2012. FGF23/Klotho axis: Phosphorus, mineral metabolism, and beyond. Cytokine Growth Factor Reviews 23:37-46. doi: 10.1016/j.cytogfr.2012.01.004

75. Dousa, T. P. 1974. Effects of hormones on cyclic AMP formation in kidneys of nonmammalian vertebrates. American Journal of Physiology 226:1193-1197. doi: 10.1152/ajplegacy.1974.226.5.1193

76. Dunn, I. C., D. J. De Koning, H. A. McCormack, R. H. Fleming, P. W. Wilson, B. Andersson, M. Schmutz, C. Benavides, N. Dominguez-Gasca, E. Sanchez-Rodriguez, and A. B. Rodriguez-Navarro. 2021. No evidence that selection for egg production persistency causes loss of bone quality in laying hens. Genetics Selection Evolution 53:1-13. doi: 10.1186/s12711-021-00603-8

77. Dunn, I. C., A. Rodriguez-Navarro, K. Mcade, M. Shmutz, R. Preisinger, D. Waddington, P. W. Wilson, and M. M. Bain. 2011. Genetic variation in eggshell crystal size and orientation is large and these traits are correlated with shell thickness and are associated with eggshell matrix protein markers. Animal Genetics 43:410-418. doi: 10.1111/j.1365-2052.2011.02280.xopen_in_newISSN0268-9146

78. Edema, M. O., and A. O. Atayese. 2006. Bacteriological Quality of Cracked Eggs Sold for Consumption in Abeokuta, Nigeria. International Journal of Poultry Science 5:772-775.

79. Edwards, N. A. 1977. The secretion of glucose into the egg of gallus gallus domesticus and observations on the uterine secretion of cations. British Poultry Science 18:641-649. doi: 10.1080/00071667708416415

80. El Hadi, H., and A. H. Sykes. 1982. Thermal panting and respiratory alkalosis in the laying hen. British Poultry Science 23:49-57. doi: 10.1080/00071688208447928

81. Eliam, M. C., M. Basle, Z. Bouizar, J. Bielakoff, M. Moukhtar, and M. C. De Vernejoul. 1988. Influence of blood calcium on calcitonin receptors in isolated chick osteoclasts. Journal of Endocrinology 199:243-248. doi: 10.1677/joe.0.1190243

82. Erben, R. G. 2018. Physiological actions of fibroblast growth factor-23. Frontiers in Endocrinology 9:1-7. doi: 10.3389/fendo.2018.00267

83. Etches, J. R. 1986. Calcium logistics in the laying hen. American Institute of Nutrition 117:619-628. doi: 10.1093/jn/117.3.619

84. Etches, R. J., H. E. MacGregor, T. F. Morris, and J. B. Williams. 1983. Follicular growth and maturation in the domestic hen. Journal of Reproduction and Fertility 67:351-358. doi: 10.1530/jrf.0.0670351

85. Ettinger, R. A., and H. F. DeLuca. 1995. The vitamin D_3 hydroxylase-associated protein is a propionamide-metabolizing amidase enzyme. Arch. Biochem. Biophys. 316:14-19. doi: 10.1006/abbi.1995.1003

86. Ettinger, R. A., R. Ismail, and H. F. DeLuca. 1994. cDNA cloning and characterization of a vitamin D_3 hydroxylase-associated protein. J. Biol. Chem. 269:176-182. doi: 10.1016/S0021-9258(17)42331-3

87. Falcon, W. P., R. L. Naylor, and S. N. D. 2022. Rethinking global food demand for 2050. Population and Development Review 48:921-957. doi: 10.1111/padr.12508

88. Farm Animal Welfare Council (FAWC) 2010. Opinion on osteoporosis and bone fractures in laying hens.

89. Feng, J., H. J. Zhang, S. G. Wu, G. H. Qi, and J. Wang. 2020. Uterine transcriptome analysis reveals mRNA expression changes associated with the ultrastructure differences of eggshell in young and aged laying hens. BMC Genomics 21:1-15. doi: 10.1186/s12864-020-07177-7

90. Fernandez, M. S., A. Moya, L. Lopez, and J. L. Arias. 2000. Secretion pattern, ultrastructural localization and function of extracellular matrix molecules involved in eggshell formation. Matrix Biology 19:793-803. doi: 10.1016/s0945-053x(00)00128-1

91. Ferrer, R., J. M. Planas, M. Durfort, and M. Moreto. 1991. Morphological study of the caecal epithelium of the chicken (*Gallus gallus domesticus L.*). British Poultry Science 32:679-691. doi: 10.1080/00071669108417394

92. Fleming, R. H., H. A. McCormack, L. McTeir, and C. C. Whitehead. 1998. Medullary bone and humeral breaking strength in laying hens. Research in Veterinary Science 64:64-67. doi: 10.1016/s0034-5288(98)90117-5

93. Fleming, R. H., H. A. McCormack, and C. C. Whitehead. 2010. Bone structure and strength

at different ages in laying hens and effects of dietary particulate limestone, vitamin K, and ascorbic acid. British Poultry Science 39:434-440. doi: 10.1080/00071669889024

94. Fraps, R. M. 1964. twenty-four-hour periodicity in the mechanism of pituitary gonadotrophin release for follicular maturation and ovulation in the chicken. Endocrinology 77:5-19. doi: 10.1210/endo-77-1-5

95. Fraser, A. C., and E. Kodicek. 1973. Regulation of 25-hydroxycholecalciferol-1-hydroxylase activity in kidney by parathyroid hormone. Nature New Biology 241:1973-1978. doi: 10.1038/newbio241163a0

96. Fraser, D. R., and E. Kodicek. 1970. Unique biosynthesis by kidney of a biologically active vitamin D metabolite. Nature 228:764-766. doi: 10.1038/228764a0

97. Frost, T. J., and D. A. Roland, Sr. 1990. The effects of various dietary phosphorus levels on the circadian patterns of plasma 1,25-dihydroxycholecalciferol, total calcium, ionized calcium and phosphorus in laying hens. Poultry Science 70:1564-1570. doi: 10.3382/ps.0701564

98. Fu, Y., J. M. Zhou, M. Schroyen, H. J. Zhang, S. G. Wu, G. H. Qi, and J. Wang. 2024. Decreased eggshell strength caused by impairment of uterine calcium transport coincide with higher bone minerals and quality in aged laying hens. Journal of Animal Science and Biotechnology 15. doi: ARTN 37

99. 10.1186/s40104-023-00986-2

100. Fullmer, C. S., M. E. Brindak, and R. H. Wasserman. 1976. The purification of calcium-binding protein from the uterus of the laying hen. Proceedings of the Society for Experimental Biology and Medicine 152:237-241. doi: 10.3181/00379727-152-39369

101. Garcia-Mejia, R. A., M. Sinclair-Black, L. R. Blair, R. Angel, B. Jaramillo, P. Regmi, N. Neupane, M. Proszkowiec-Weglarz, X. Arbe, D. Cavero, and L. E. Ellestad. 2024. Physiological changes in the regulation of calcium and phosphorus utilization at the onset of egg production in commercial laying hens. Frontiers in Physiology.

102. Garcon, C. J. J., J. L. Ellis, C. D. Powell, A. Navarro Villa, A. I. Garcia Ruiz, J. France, and S. de Vries. 2023. A dynamic model to measure retention of solid and liquid digesta fraction in chickens fed diets with differing fibre sources. Animal 17:1-11. doi: 10.1016/j.animal.2023.100867

103. Gattineni, J., C. Bates, K. Twombley, V. Dwarakanath, M. L. Robinson, R. Goetz, M. Mohammadi, and M. Baum. 2009. FGF23 decreases renal NaPi-2a and NaPi2c expression

and induces hypophosphatemia in vivo predominantly via FGF receptor 1. American Journal of Physiology 297:F282-F291. doi: 10.1152/ajprenal.90742.2008.

104. Gautron, J., M. M. Bain, S. E. Solomon, and Y. Nys. 1996. Soluble matrix of hens eggshell extracts changes *in vitro* the rate of calcium carbonate precipitation and crystal morphology. British Poultry Science 37:853-866. doi: 10.1080/00071669608417914

105. Gautron, J., M. T. Hincke, K. Mann, M. Panheleux, M. M. Bain, M. D. McKee, S. E. Solomon, and Y. Nys. 2001. Ovocalyxin-32, a novel chicken eggshell matrix protein. J. Biol. Chem. 276:39243-39252. doi: 10.1074/jbc.M104543200

106. Gautron, J., N. Le Roy, Y. Nys, A. B. Rodriguez-Navarro, and M. T. Hincke. 2021. Avian eggshell biomineralization: an update on its structure, mineralogy, and protein tool kit. BMC Molecular and Cell Biology 22:1-17. doi: 10.1186/s12860-021-00351-z

107. Gautron, J., E. Murayama, A. Vignal, M. Morisson, M. D. McKee, S. Rehault, V. Labas, M. Belghazi, M. L. Vidal, and M. T. Hincke. 2007. Cloning of ovocalyxin-36, a novel chicken eggshell protein related to lipopolysacharide-binding proteins, bactericidal permeability-increasing proteins, and plunc family proteins. J. Biol. Chem. 282:5273-5286. doi: 10.1074/jbc.M610294200

108. Gezen, S. S., M. Eren, and G. Deniz. 2005. The effect of different dietary electrolytes balances on eggshell quality in laying hens. Revue Med Vet 156:491-497.

109. Gilani, S., A. Mereu, P. W. Plumstead, R. Angel, G. Wilks, and Y. Dersjant-Li. 2022. Global survey of limestone used in poultry diets: calcium content, particle size, and solubility. Journal of Applied Animal Nutrition 10:19-30. doi: 10.3920/JAAN2021.0015

110. Gill, R. K., and S. Christakos. 1995. Regulation by estrogen through the 5' flanking region of the mouse calbindin-D28K gene. Mol Endocrinol 9:319-326. doi: DOI 10.1210/me.9.3.319

111. Gloux, A., N. Le Roy, A. Brionne, E. Bonin, A. Juanchich, G. Benzoni, M. L. Piketty, D. Prie, Y. Nys, J. Gautron, A. Narcy, and M. J. Duclos. 2019. Candidate genes of the transcellular and paracellular calcium absorption pathways in the small intestine of laying hens. Poultry Science 98:6005-6018. doi: 10.3382/ps/pez407

112. Gloux, A., N. Le Roy, J. Ezagal, N. Meme, C. Hennequet-Antier, M. L. Piketty, D. Prie, G. Benzoni, J. Gautron, Y. Nys, A. Narcy, and M. J. Duclos. 2020a. Possible roles of parathyroid hormone, $1.25(OH)_2D_3$, and fibroblast growth factor 23 on genes controlling calcium metabolism across different tissues of the laying hen. Dom. Anim. Endocrinol. 72:1-12. doi: 10.1016/j.domaniend.2019.106407

113. Gloux, A., N. Le Roy, N. Meme, M. L. Piketty, D. Prie, G. Benzoni, J. Gautron, Y. Nys, A. Narcy, and M. J. Duclos. 2020b. Increased expression of fibroblast growth factor 23 is the signature of a deteriorated Ca/P balance in ageing laying hens. Sci. Rep. 10. doi: 10.1038/s41598-020-78106-7

114. Goto, K. 1918. Mineral metabolism in experimental acidosis. J. Biol. Chem. 36:355-376. doi: 10.1016/S0021-9258(18)86403-1

115. Gow, C. B., P. J. Sharp, N. B. Carter, R. J. Scaramuzzi, B. L. Sheldon, B. H. Yoo, and R. T. Talbot. 1984. Effects of selection for reduced oviposition interval on plasma concentrations of leutinizing hormone during the ovulatory cycle in hens on a 24h lighting cycle. British Poultry Science 26:441-451. doi: 10.1080/00071668508416834

116. Gregory, N. G., L. J. Wilkins, S. D. Eleperuma, A. J. Ballantyne, and N. D. Overfield. 1989. Broken bones in domestic fowls effect of husbandry system and stunning method in end of lay hens. British Poultry Science 31. doi: 10.1080/00071669008417231

117. Grunder, A. A., C. P. Tsang, and R. Narbaitz. 1990. Effects of vitamin D_3 metabolites on physiological traits of white leghorn hens. Poultry Science 69:1204-1208. doi: 10.3382/ps.0691204

118. Gu, Y. F., Y. P. Chen, R. Jin, C. Wang, C. Wen, and Y. M. Zhou. 2021. A comparison of intestinal integrity, digestive function, and egg quality in layin ghens with different ages. Poultry Science 100:1-8. doi: 10.1016/j.psj.2020.12.046

119. Guinotte, F., J. Gautron, Y. Nys, and A. Soumarmon. 1995. Calcium solubilization and retention in the gastrointestinal tract in chicks (*Gallus domesticus*) as a function of gastric acid secretion inhibition and of calcium carbonate particle size. Brit. J. Nut. 73:125-139. doi: 10.1079/Bjn19950014

120. Guinotte, F., J. Gautron, A. Soumarmon, J. C. Robert, G. Peranzi, and Y. Nys. 1993. Gastric acid secretion in the chicken: Effect of histamine H_2 antagonists and H^+/K^+-ATPase inhibitors on gastro-intestinal pH and of sexual maturity calcium carbonate level and particle size on proventricular H^+/K^+-ATPase activity. Comparative Biochemistry and Physiology 106:319-327. doi: 10.1016/0300-9629(93)90520-E

121. Guo, F., Y. Geng, W. Abbas, W. Zhen, S. Wang, Y. Huang, Y. Guo, Q. Ma, and Z. Wang. 2022. Vitamin D_3 nutritional status affects gut health of salmonella-challenged laying hens. Frontiers in Nutrition 9:1-16. doi: 10.3389/fnut.2022.888580

122. Gutowska, M. S., and C. A. Mitchell. 1945. Carbonic anhydrase in the calcification of the egg shell. Poultry Science 24:159-167. doi: 10.3382/ps.0240159

123. Guyer, R. B., A. A. Grunder, E. G. Buss, and C. O. Clagett. 1980. Calcium-binding proteins in serum of chickens vitellogenin and albumin. Poultry Science 59:874-879. doi: 10.3382/ps.0590874

124. H&N International. 2020. Nick Chick white egg layers new management guide. Pages 1-76. H. N. I. GmbH ed. H&N International, Cuxhaven, Germany.

125. Haddad, J. G., L. Y. Matsuoka, B. W. Hollis, Y. Z. Hu , and J. Wortsman. 1993. Human plasma transport of vitamin D after its endogenous synthesis. J Clin Invest 91:2552-2555. doi: 10.1172/JCI116492

126. Hadley, J. A., M. Horvat-Gordon, W. K. Kim, C. A. Praul, D. Burns, and R. M. Leach Jr. 2016. Bone sialoprotein keratan sulfate proteoglycan (BSP-KSPG) and FGF-23 are important physiological components of medullary bone. Comparative Biochemistry and Physiology 194:1-7. doi: 10.1016/j.cbpa.2015.12.009

127. Hall, A. K., and A. W. Norman. 1990. Regulation of calbindin-D28k gene expression by 1,25-dihydroxyvitamin D3 in chick kidney. Journal of Bone and Mineral Research 5:325-330. doi: 10.1002/jbmr.5650050404

128. Hamilton, R. M. G. 1980. The effects of strain, age, time after oviposition, and egg specific gravity on acid-base balance in white leghorn hens. Poultry Science 60:1944-1950. doi: 10.3382/ps.0601944

129. Hamilton, R. M. G., K. G. Hollands, P. W. Voisey, and A. A. Grunder. 1979. Relationship between eggshell quality and shell breakage and factors that affect shell breakage in the field - a review. World Poultry Science Journal 35:177-190. doi: 10.1079/WPS19790014

130. Han, J., L. Wu, X. LV, M. Liu, Y. Zhang, L. He, J. Hao, L. Xi, H. Qu, C. Shi, Z. Li, Z. Wang, F. Tang, and Y. Qiao. 2023. Intestinal segment and vitamin D3 concentration affect gene expression levels of calcium and phosphorus transporters in broiler chickens. Journal of Animal Science and Technology 65:336-350. doi: 10.5187/jast.2022.e78

131. Haussler, M. R., P. W. Jurutka, M. Mizwicki, and A. W. Norman. 2011. Vitamin D receptor (VDR)-mediated actions of 1a,25(OH)$_2$vitamin D$_3$: Genomic and non-genomic mechanisms. Best Pract. Res. Clin. Endocrinol. Metab. 25:543-559. doi: 10.1016/j.beem.2011.05.010

132. Heald, P. J., B. E. Furnival, and K. A. Rookledge. 1967. Changes in the levels of luteinizing hormone in the pituitary of the domestic fowl during an ovulatory cycle. Journal of Endocrinology 37:73-81. doi: 10.1677/joe.0.0370073

133. Heaney, R. P., L. A. Armas, J. R. Shary, N. H. Bell, N. Binkley, and B. W. Hollis. 2008. 25-Hydroxylation of vitamin D_3: relation to circulating vitamin D_3 under various input conditions. American Journal of Clinical Nutrition 87:1738-1742. doi: 10.1093/ajcn/87.6.1738

134. Henry, H. L. 1978. Regulation of the hydroxylation of 25-hydroxyvitamin D_3 *in Vivo* and in primary cultures of chick kidney cells. J. Biol. Chem. 254:2722-2729. doi: 10.1016/S0021-9258(17)30132-1

135. Herrera, J., B. Saldana, P. Guzman, L. Camara, and G. G. Mateos. 2017. Influence of particle size of the main cereal of the diet on egg production, gastrointestinal tract traits, and body measurements of brown laying hens. Poultry Science 96:440-448. doi: 10.3382/ps/pew256

136. Hertelendy, F., and T. G. Taylor. 1960. Changes in blood calcium associated with eggshell calcification in the domestic fowl. Poultry Science 40:108-114. doi: 10.3382/ps.0400108

137. Hervo, F., A. Narcy, Y. Nys, and M. P. Letourneau-Montminy. 2022. Effect of limestone particle size on performance, eggshell quality, bone strength, and invitro/in vivo solubility in laying hens: a meta analysis approach. Poultry Science 101:1-9. doi: 10.1016/j.psj.2021.101686

138. Hincke, M. t., J. Gautron, K. Mann, M. Panheleux, M. D. McKee, M. M. Bain, S. E. Solomon, and Y. Nys. 2003. Purification of ovocalyxin-32, a novel chicken egghsell matrix protein. Connective Tissue Research 44. doi: 10.1080/03008200390152025

139. Hincke, M. T., J. Gautron, C. P. Tsang, M. D. McKee, and Y. Nys. 1999. Molecular cloning and ultrastructural localization of the core protein of an eggshell matrix proteoglycan, ovocleidin-116. J. Biol. Chem. 274:32915-32923. doi: 10.1074/jbc.274.46.32915

140. Hincke, M. T., Y. Nys, and J. Gautron. 2010. The role of matrix proteins in eggshell formation. J. Poult. Sci. 47:208-219. doi: 10.2141/jpsa.009122

141. Hincke, M. T., Y. Nys, J. Gautron, K. Mann, A. B. Rodriguez-Navarro, and M. D. McKee. 2012. The eggshell: structure, composition and mineralization. Front. Biosci. 17:1266-1280. doi: 10.2741/3985

142. Hincke, M. T., C. P. Tsang, M. Courtney, V. Hill, and R. Narbaitz. 1995. Purification and immunochemistry of a soluble matrix protein of the chicken eggshell. Calcified tissue international 56:578-583. doi: 10.1007/BF00298593

143. Hiyama, S., T. Sugiyama, S. Kusuhara, and T. Uchida. 2009. Evidence for the expression

of estrogen receptors in osteogenic cells isolated from hen medullary bone. Acta Histochemica 111:501-507. doi: 10.1016/j.acthis.2008.06.003

144. Hodges, R. D., and K. LÖRcher. 1967. Possible source of the carbonate fraction of eggshell calcium carbonate. Nature 216:609-610. doi: 10.1038/216609a0

145. Hoenderop, J. G. J., B. Nilius, and R. J. Bindels. 2005. Calcium absorption across epithelia. Physiological Reviews 85:373-422. doi: 10.1152/physrev.00003.2004

146. Hofer, A. M., and E. M. Brown. 2003. Extracellular calcium sensing and signalling. Nature Reviews Molecular Cell Biology 4:530-538. doi: 10.1038/nrm1154

147. Holick, M. F., A. Kleiner-Bossallier, H. K. Schnoes, P. M. Kasten, I. T. Boyle, and H. F. DeLuca. 1973. 1,24,25-Trihydroxyvitamin D_3. J. Biol. Chem. 248:6691-6696. doi: 10.1016/S0021-9258(19)43408-X

148. Hsiao, F. S. H., Y. H. Cheng, J. C. Han, M. H. Chang, and Y. H. Yu. 2018. Effect of different vitamin D_3 metabolites on intestinal calcium homeostasis-related gene expression in broiler chickens. R. Bras. Zootec. 47:1-8. doi: 10.1590/rbz4720170015

149. Hu, Y. X., X. D. Liao, Q. Wen, L. Lu, L. Y. Zhang, and X. G. Luo. 2018. Phosphorus absorption and gene expression levels of related transporters in the small intestine of broilers. Brit. J. Nut. 119:1346-1354. doi: 10.1017/S0007114518000934

150. Hu, Y. X., J. van Baal, W. H. Hendriks, M. Duijster, M. M. van Krimpen, and P. Bikker. 2022. Mucosal expression of Ca and P transporters and claudins in the small intestine of broilers is altered by dietary Ca:P in a limestone particle size dependent manner. PLoS One 17:1-12. doi: 10.1371/journal.pone.0273852

151. Huber, K., E. Zeller, and M. Rodehutscord. 2015. Modulation of small intestinal phosphate transporter by dietary supplements of mineral phosphorus and phytase in broilers. Poultry Science 94:1009-1017. doi: 10.3382/ps/pev065

152. Hudson, H. A., W. M. Britton, G. N. Rowland, and R. J. Buhr. 1993. Histomorphometric bone properties of sexually immature and mature white leghorn hens with evaluation of fluorochrome injection on egg production traits. Poultry Science 72:1537-1547. doi: 10.3382/ps.0721537

153. Hui, Q. R., X. Y. Zhao, P. Lu, S. X. Liu, M. Nyachoti, O. Karmin, and C. B. Yang. 2021. Molecular distribution and localization of extracellular calcium-sensing receptor (CaSR) and vitamin D receptor (VDR) at three different laying stages in laying hens (Gallus gallus domesticus). Poultry Science 100:101060. doi: 10.1016/j.psj.2021.101060

154. Hunt, N. J., S. W. Kang, G. P. Lockwood, D. G. Le Couteur, and V. C. Cogger. 2019. Hallmarks of aging in the liver. Computational and Structural Biotechnology Journal 17:1151-1161. doi: 10.1016/j.csbj.2019.07.021

155. Hurwitz, S., and A. Bar. 1965. Absorption of calcium and phosphorus along the gastrointestinal tract of the laying fowl as influenced by dietary calcium and eggshell formation. Journal of Nutrition 86. doi: 10.1093/jn/86.4.433.

156. Hurwitz, S., and A. Bar. 1968. Activity, concentration and lumen-blood electrochemical potential difference of calcium in the intestine of the laying hen. Journal of Nutrition 95:647-654. doi: 10.1093/jn/95.4.647

157. Hurwitz, S., and A. Bar. 1969. Intestinal calcium absorption in the laying fowl and its importance in calcium homeostasis. American Journal of Clinical Nutrition 22:391-395. doi: 10.1093/ajcn/22.4.391

158. Hurwitz, S., A. Bar, and I. Cohen. 1973. Regulation of calcium absorption by fowl intestine. American Journal of Physiology 225:150-154. doi: 10.1152/ajplegacy.1973.225.1.150

159. Ieda, T., T. Takahasi, N. Saito, T. Yasuoka, M. Kawashima, T. Izumi, and K. Shimada. 2001. Changes in calcitonin receptor binding in the shell gland of laying hens (*Gallus domesticus*) during the oviposition cycle. J. Poult. Sci. 38:203-212. doi: 10.2141/jpsa.38.203

160. Imamura, T., T. Sugiyama, and S. Kusuhara. 2006. Expression and localization of estrogen receptors a and b mRNA in medullary bone of laying hens. Animal Science Journal 77:223-229. doi: 10.1111/j.1740-0929.2006.00341.x

161. Jande, S. S., S. Tolnai, and D. E. M. Lawson. 1981. Immunohistochemical localization of vitamin D-dependent calcium binding protein in duodenum, kidney, uterus, and cerebellum of chickens. Histochemistry 71:99-116. doi: 10.1007/BF00592574

162. Jonchere, V., A. Brionne, J. Gautron, and Y. Nys. 2012. Identification of uterine ion transporters for mineralisation precursors of the avian eggshell. BMC Physiology 12:1-17. doi: 10.1186/1472-6793-12-10

163. Jones, G., S. A. Strungnell, and H. F. DeLuca. 1998. Current understanding of the molecular actions of vitamin D. Physiological Reviews 78:1193-1231. doi: 10.1152/physrev.1998.78.4.1193

164. Joyner, C. J., M. J. Peddie, and T. G. Taylor. 1986. The effect of age on egg production in the domestic hen. General and Comparative Endocrinology 65:331-336. doi:

10.1016/0016-6480(87)90117-1

165. Kantham, L., S. J. Quinn, O. I. Egbuna, K. Baxi, R. Butters, J. L. Pang, M. R. Pollak, D. Goltzman, and E. M. Brown. 2009. The calcium-sensing receptor (CaSR) defends against hypercalcemia independently of its regulation of parathyroid hormone secretion. American Journal of Physiology Endocrinology Metabolism 297:915-923. doi: 10.1152/ajpendo.00315.2009.

166. Kappauf, B., and A. Van Tienhoven. 1972. Progesterone concentrations in peripheral plasma of laying hens in relation to time of ovulation. Endocrinology 90:1350-1355. doi: 10.1210/endo-90-5-1350

167. Karasawa, Y. 1999. Significant role of the nitrogen recycling system through the ceca occurs in protein depleted chickens. Journal of Experimental Zoology 283:418-425. doi: 10.1002/(sici)1097-010x(19990301/01)283:4/5<418::aid-jez11>3.0.co;2-g

168. Karbach, U., and H. Feldmeier. 1993. The cecum is the site with the highest calcium absorption in rat intestine. Digestive Diseases and Sciences 38:1815-1824. doi: 10.1007/BF01296104

169. Kaseda, R., M. Hosojima, H. Sato, and A. Saito. 2011. Role of megalin and cubilin in the metabolism of vitamin D_3. Theraputic Apheresis and Dialasis 15:14-14. doi: 10.1111/j.1744-9987.2011.00920.x

170. Kebreab, E., J. France, R. P. Kwakkel, S. Leeson, H. D. Darmani Kuhi, and J. Dijkstra. 2009. Development and evaluation of a dynamic model of calcium and phosphorus flows in layers. Poultry Science 88:680-689. doi: 10.3382/ps.2008-00157

171. Kerschnitzki, M., T. Zander, P. Zaslansky, P. Fratzl, R. Shahar, and W. Wagermaier. 2014. Rapid alterations of avian medullary bone material during the daily egg-laying cycle. Bone 69:109-117. doi: 10.1016/j.bone.2014.08.019

172. Keshavarz, K., and R. E. Austic. 1990. Effects of dietary minerals on acid-base balance and eggshell quality in chickens. Journal of Nutrition 120:1360-1370. doi: /10.1093/jn/120.11.1360

173. Kim, S. W., W. Li, R. Angel, and M. Proszkowiec-Weglarz. 2018. Effects of limestone particle size and dietary Ca concentration on apparent P and Ca digestibility in the presence or absence of phytase. Poultry Science 97:4306-4315. doi: 10.3382/ps/pey304

174. King, M. W., and A. W. Norman. 1986. Analysis of the mRNA coding for the chick vitamin D-induced calbindin and its regulation by 1,25-dihydroxyvitamin D_3. Biochemistry and

Biophysics 248:612-619. doi: 10.1016/0003-9861(86)90515-1

175. Kliewer, S. A., U. Kazuhiko, D. J. Mangelsdorf, and R. M. Evans. 1992. Retinoid X receptor interacts with nuclear receptors in retinoic acid, thyroid hormone and vitamin D_3 signaling. Nature 30:446-449. doi: 10.1038/355446a0

176. Korones, D. N., M. Brown, and J. Palis. 2001. Liver function tests are not always tests of liver function. American Journal of Hematology 66:46-48. doi: 10.1002/1096-8652(200101)66:1<46::AID-AJH1007>3.0.CO;2-Oopen_in_newISSN036

177. Kraintz, L., and K. Intscher. 1969. Effect of calcitonin on the domestic fowl. Canadian Journal of Physiology and Pharmacology 47:313-315. doi: 10.1139/y69-057

178. Kraut, J. A., and N. E. Madias. 2010. Metabolic acidosis: pathophysiology, diagnosis, and management. Nature 6:274-285. doi: doi.org/10.1038/nrneph.2010.33

179. Kraut, J. A., and N. E. Madias. 2016. Metabolic acidosis of CDK: an update. American Journal of Kidney Disease 2:307-317. doi: 10.1053/j.ajkd.2015.08.028

180. Kraut, J. A., D. R. Mishler, F. R. Singer, and W. G. Goodman. 1986. The effects of metabolic acidosis on bone formation and bone resorption in the rat. Kidney International 03:694-700. doi: 10.1038/ki.1986.242

181. Kumar, R., H. K. Schnoes, and H. F. DeLuca. 1977. Rat intestinal 25-hydroxyvitamin D_3 and 1,25-dihydroxyvitamin D_3-24-hydroxylase. J. Biol. Chem. 253:3804-3809. doi: 10.1016/S0021-9258(17)34760-9

182. Kuwata, N., H. Mukohda, H. Uchida, R. Takamatsu, M. M. Binici, T. Yamada, and T. Sugiyama. 2024. Renal endocytic regulation of vitamin D metabolism during maturation and aging in laying hens. Animals 14. doi: 10.3390/ani14030502

183. Larkins, R. G., S. J. MacAuley, A. Rapoport, T. J. Martin, B. R. Tulloch, P. G. Byfield, E. W. Matthews, and I. MacIntyre. 1973. Effects of nucleotides, hormones, ions, and 1,25-dihydroxycholecalciferol on 1,25-dihydroxychoelcalciferol production in isolated chick renal tubules. Clinical Sciences and Molecular Medicine 46:569-582. doi: 10.1042/cs0460569

184. Lee, J. J., X. Liu, D. O'Neill, M. R. Beggs, R. Weissgerber, V. Flockerzi, X. C. Chen, H. Dimke, and R. T. Alexander. 2019. Activation of the calcium-sensing receptor attenuates TRPV6-dependent intestinal calcium absorption. JCI Insight 4. doi: 10.1172/jci.insight.128013.

185. Lee, S. M., E. M. Riley, M. B. Meyer, N. A. Benkusky, L. A. Plum, H. F. DeLuca, and J. W. Pike. 2015. 1,25-Dihydroxyvitamin D3 controls a cohort of vitamin D receptor target genes in the proximal intestine that is enriched for calcium-regulating components. J. Biol. Chem. 290:18199-18215. doi: 10.1074/jbc.M115.665794

186. Li, P., R. M. Wang, H. C. Jiao, X. J. Wang, J. P. Zhao, and H. Lin. 2018. Effects of dietary phosphorus level on the expression of calcium and phosphorus transport in laying hens. Frontiers in Physiology 9:1-12. doi: 10.3389/fphys.2018.00627

187. Liang, C. T., R. Balakir, J. Barnes, and B. Sacktor. 1984. Responses of chick renal cell to parathyroid hormone: effect of vitamin D. American Journal of Physiology 246:401-406. doi: 10.1152/ajpcell.1984.246.5.C401

188. Liang, C. T., J. Barnes, L. Cheng, R. Balakir, and B. Sacktor. 1982. Effects of 1,25-$(OH)_2D_3$ administered in vivo on phosphate uptake by isolated chick renal cells. American Journal of Physiology 242:312-318. doi: 10.1152/ajpcell.1982.242.5.C312

189. Liao, Q. S., Q. Du, J. Lou, J. Y. Xu, and R. Xie. 2019. Roles of Na^+/Ca^{2+} exchanger 1 in digestive system physiology and pathophysiology. World Journal of Gastroenterology 21:287-299. doi: 10.3748/wjg.v25.i3.287

190. Liao, X. D., H. Q. Suo, L. Lu, Y. X. Hu, L. Y. Zhang, and X. G. Luo. 2017. Effects of sodium, 1,25-dihydroxyvitamin D_3 and parathyroid hormone fragment on inorganic P absorption and Type IIb sodium-phosphate cotransporter expression in ligated duodenal loops of broilers. Poultry Science 96:2344-2350. doi: 10.3382/ps/pex033

191. Lim, J. H., E. N. Kim, M. Y. Kim, S. Chung, S. J. Shin, H. W. Kim, C. W. Yang, Y. S. Kim, Y. S. Chang, C. W. Park, and B. S. Choi. 2012. Age-associated molecular changes in the kidney in aged mice. Oxidative Medicine and Cellular Longevity 2012:171383. doi: 10.1155/2012/171383

192. Liu, S., W. Zhu, J. Ma, H. Zhang, Z. Li, L. Zhang, B. Zhang, Z. Li, X. Liang, and W. Shi. 2016. Bovine parathyroid hormone enhances osteoclast bone resorption by modulating V-ATPase through PTH1R. Int J Mol Med 37:284-292. doi: 10.3892/ijmm.2015.2423

193. Loken, H. F., R. J. Havel, G. S. Gordan, and S. L. whittington. 1960. Ultracentrifugal analysis of protein-bound and free calcium in human serum. J. Biol. Chem. 235:3654-3658. doi: 10.1016/S0021-9258(18)64524-7

194. Long, A., and S. Wilcox. 2011. Optimizing Egg Revenue for Poultry Farmers.

195. Loupy, A., S. K. Ramakrishnan, B. Wootla, R. Chambrey, R. de la Faille, S. Bourgeois, P.

Bruneval, C. Mandet, E. I. Christensen, H. Faure, L. Cheval, K. Laghmani, C. Collet, D. Eladari, R. H. Dodd, M. Ruat, and P. Houillier. 2012. PTH-independent regulation of blood calcium concentration by the calcium-sensing receptor. J Clin Invest 122:3355-3367. doi: 10.1172/JCI57407

196. Luck, M. R., B. A. Sommerville, and C. G. Scanes. 1979. The effect of egg-shell calcification on the response of plasma calcium activity to parathyroid hormone and calcitonin in the domestic fowl. Comparative Biochemistry and Physiology 65:151-154. doi: 10.1016/0300-9629(80)90397-7

197. Lund, W. A., V. Heiman, and L. A. Wilhelm. 1937. The relationship between eggshell thickness and strength. Poultry Science 17. doi: 10.3382/ps.0170372

198. Lyu, Z., H. Li, X. Li, H. Wang, H. C. Jiao, X. J. Wang, J. P. Zhao, and H. Lin. 2023. Fibroblast growth factor 23 inhibits osteogenic differentiation and mineralization of chicken bone marrow mesenchymal stem cells. Poultry Science 102. doi: 10.1016/j.psj.2022.102287

199. Mallinson, E. T., H. Rothenbacher, R. F. Wideman, D. B. Snyder, E. Russek, A. I. Zuckerman, and J. P. Davidson. 1983. Epizootiology, pathology, and microbiology of an outbreak of urolith in chickens. Avian Diseases 28:25-43. doi: 10.2307/1590126

200. Marcus, C. S., and F. W. Lengemann. 1962. Absorption of Ca^{45} and Sr^{85} from solid and liquid food at various levels of the alimentary tract of the rat. Journal of Nutrition 77:155-160. doi: 10.1093/jn/77.2.155

201. Marie, P., V. Labas, A. Brionne, G. Harichaux, C. Hennequet-Antier, A. Rodriguez-Navarro, Y. Nys, and J. Gautron. 2015. Quantitative proteomics provides new insights into chicken eggshell matrix protein functions during the primary events of mineralization and active calcification phase. Journal of Proteomics 126:140-154. doi: 10.1016/j.jprot.2015.05.034

202. Martin, C. J., and W. J. Evans. 1986. Phytic acid-metal ion interactions II The effect of pH on calcium binding. Journal of Inorganic Biochemistry 27:17-30. doi: 10.1016/0162-0134(86)80105-2

203. Martin, G. A. 1984. Twenthy-fifth North Carolina layer production and management test. Pages 1-20 in Layer PerformanceNorth Carolina University, NC State Extention.

204. McCall, K. A., C. C. Huang, and C. A. Fierke. 2000. Function and mechanism of zinc metalloenzymes. Journal of Nutrition 130:1437s-1446s. doi: 10.1093/jn/130.5.1437S

205. McClung, M. R., A. B. S. Wang, and W. T. Jones. 1975. Response to selection for time interval between ovipositions in the hen. Poultry Science 55:160-171. doi: 10.3382/ps.0550160

206. Meghji, S., M. S. Morrison, B. Henderson, and T. R. Arnett. 2001. pH dependence of bone resorption: mouse calvarial osteoclasts are activated by acidosis. American Journal of Physiology Endocrinology Metabolism 280:E112-E119. doi: 10.1152/ajpendo.2001.280.1.E112

207. Meyer, M. B., and J. W. Pike. 2020. Mechanistic homeostasis of vitamin D metabolism in the kidney through reciprocal modulation of *CYP27B1* and *CYP24A1* expression. J Steroid Biochem 196:1-6. doi: 10.1016/j.jsbmb.2019.105500

208. Meyer, W., A. Hellmann, and N. Kummerfeld. 2009. Demonstration of calcium transport markers in the ceca of owls (Aves: Strigiformes), with remarks on basic ceca structure. Eur J Wildlife Res 55:91-96. doi: 10.1007/s10344-008-0221-8

209. Michigami, T., M. Kawai, M. Yamazaki, and K. Ozono. 2018. Phosphate as a signaling molecule and its sensing mechanism. Physiol Rev 98:2317-2348. doi: 10.1152/physrev.00022.2017

210. Miksik, I., A. Eckhardt, P. Sedlakova, and K. Mikulikova. 2007. Proteins of insoluble matrix of avian gallus gallus eggshell. Connective Tissue Research 48:1-8. doi: 10.1080/03008200601003116

211. Miller, E. R., R. H. Harms, and H. R. Wilson. 1977a. Cyclic changes in serum phosphorus of laying hens. Poultry Science 56:586-589. doi: 10.3382/ps.0560586

212. Miller, E. R., H. R. Wilson, and R. H. Harms. 1977b. Serum calcium and phosphorus levels in hens relative to the time of oviposition. Poultry Science 56:1501-1503. doi: 10.3382/ps.0561501

213. Miller, S. C. 1978. Rapid activation of the medullary bone osteoclast cell surface by parathyroid hormone. Journal of Cell Biology 76:615-618. doi: 10.1083/jcb.76.3.615

214. Mongin, P. 1968. Role of acid-base balance in the physiology of egg shell formation. World Poultry Sci J 24:200-230. doi: 10.1079/WPS19680021

215. Mongin, P. Year. Acid-base balance during egg shell calcification. Proc. International congress of physiological sciences, Max-Planck-Institute for Experimental Medicine, Göttingen.

216. Monkawa, T., T. Yoshida, S. Wakino, T. Shinki, H. Anazawa, H. F. DeLuca, T. Suda, M. Hayashi, and T. Saruta. 1997. Molecular cloning of cDNA and genomic DNA for human 25-hydroxyvitamin D_3 1a-hydroxylase. Biochemical and Biophysical Research Communications 239:527-533. doi: 10.1006/bbrc.1997.7508

217. Mueller, W. J., R. Schraer, and H. Schraer. 1964. Calcium metabolism and skeletal dynamics of laying pullets. Journal of Nutrition 84:20-26.

218. Narbaitz, R., S. Kacew, and L. Sitwell. 1981. Carbonic anhydrase activity in the chick embryo chorioallantois: regional distribution and vitamin D regulation. Journal of Embryology and Experimental Morphology 65:127-137. doi: 10.1242/dev.65.1.127

219. Narbaitz, R., W. E. Stumpf, M. Sar, and H. F. De Luca. 1982. The distal nephron in the chick embryo as a target tissue for 1-alpha-12-duhydroxycholecalciferol. Acta Anat 112:208-216. doi: 10.1159/000145512

220. Nasr, M. A., C. J. Nicol, and J. C. Murrell. 2012. Do laying hens with keel bone fractures experience pain? PLoS One 7:e42420. doi: 10.1371/journal.pone.0042420

221. National Research Council. 1994. Nutrient Requirements of Poultry. 9 ed. The National Academies Press, Washington, DC.

222. Nemere, I. 1996. Parathyroid hormone rapidly stimulates phosphate transport in perfused duodenal loops of chicks: Lack of modulation by vitamin D metabolites. Endocrinology 137:3750-3755. doi: 10.1210/en.137.9.3750

223. Nemere, I., and A. W. Norman. 1986. Parathyroid hormone stimulates calcium transport in perfused duodena from normal chicks: comparison with the rapid (transcaltachic) effect of 1,25-dihydroxyvitamin D_3. Endocrinology 119:1406-1408. doi: 10.1210/endo-119-3-1406

224. Nicholson, G. C., J. M. Moseley, P. M. Sexton, and T. J. Martin. 1987. Chicken osteoclasts do not possess calcitonin receptors. Journal of Bone and Mineral Research 2:53-59. doi: 10.1002/jbmr.5650020109

225. Nijenhuis, T., J. G. Hoenderop, A. W. Van der Kemp, and R. J. Bindels. 2003. Localization and regulation of the epithelial Ca2+ channel TRPV6 in the kidney. Journal of the American Society of Nephrology 14:2731-2740. doi: 10.1097/01.ASN.0000094081.78893.E8

226. Norman, A. W. 1990. Intestinal calcium absorption: a vitamin D-hormone-mediated adaptive response. American journal of clinical nutrition 51:290-300. doi: 10.1093/ajcn/51.2.290

227. Nykjaer, A., J. C. Fyfe, R. Kozyraki, J. R. Leheste, C. Jacobsen, M. S. Nielsen, P. J. Verroust, M. Aminoff, A. de la Chapelle, S. K. Moestrup, R. Ray, J. Gliemann, T. E. Willnow, and E. I. Christensen. 2001. Cubulin dysfunction causes abnormal metabolism of the steroid hormone 25(OH) vitamin D_3. PNAS 98:13895-13900. doi: 10.1073/pnas.241516998

228. Nys, Y., K. Baker, H. Bouillon, H. Van Baelen, and D. E. M. Lawson. 1992a. Regulation of calbindin D28k and its mRNA in the intestine of the domestic hen. General and Comparative Endocrinology 86:460-468. doi: 10.1016/0016-6480(92)90071-Q

229. Nys, Y., K. Baker, and D. E. M. Lawson. 1992b. Estrogen and a calcium flux dependent factor modulate the calbindin gene expression in the uterus of laying hens. General and Comparative Endocrinology 87:87-94. doi: 10.1016/0016-6480(92)90153-b

230. Nys, Y., R. Bouillon, H. Van Baelen, and J. Williams. 1985. Ontogeny and oestradiol dependence of vitamin D binding protein blood levels. Journal of Endocrinology 108:81-87. doi: 10.1677/joe.0.1080081

231. Nys, Y., and N. Guyot. 2011. Egg formation and chemistry. Pages 83-132 in Improving the safety and quality of eggs and egg products. Y. Nys et al. eds. Woodhead Publishing, Sawston, Cambridge.

232. Nys, Y., M. T. Hincke, J. L. Arias, J. M. Garcia-Ruiz, and S. E. Solomon. 1999. Avian Eggshell Mineralization. Poult Avian Biol Rev 10:143-166.

233. Nys, Y., and N. Le Roy. 2018. Calcium homeostasis and eggshell biomineralization in female chicken. Pages 361-382 in Vitamin DAcademic Press, Cambridge, MA.

234. Nys, Y., T. M. N'Guyen, J. Williams, and J. R. Etches. 1986. Blood levels of ionized calcium, inorganic phosphorus, 1,25-dihydroxycholecalciferol and gonadal hormones in hens laying hard-shelled or shell-less eggs. Journal of Endocrinology 111:151-157. doi: 10.1677/joe.0.1110151

235. Nys, Y., J. Zawadzki, J. Gautron, and A. D. Mills. 1991. Whitening of brown-shelled eggs: mineral composition of uterine fluid and rate of protoporphyrin deposition. Poultry Science 70:1236-1245. doi: 10.3382/ps.0701236

236. Odom, T. W., P. C. Harrison, and W. G. Bottje. 1984. Effects of thermal-induced respiratory alkalosis on blood ionized calcium levels in the domestic hen. Poultry Science 65:570-573. doi: 10.3382/ps.0650570

237. Ogawa, H., T. Takahashi, T. Kuwayama, and M. Kawashima. 2003. Presence of calcitonin

receptors in shell gland of the guineafowl and changes in binding property during an oviposition cycle. Poultry Science 82:1302-1306. doi: 10.1093/ps/82.8.1302

238. Ohashi, T., and S. Kusuhara. 1991a. Effects of estrogen on the proliferation and differentiation of osteogenic cells during the early stage of medullary bone formation in cultured quail bones. Journal of Bone and Mineral Research 9:15-20. doi: 10.1007/BF02374901

239. Ohashi, T., S. Kusuhara, and K. Ishida. 1991b. Estrogen target cells during the early stage of medullary bone osteogenesis: Immunohistochemical detection of estrogen receptors in osteogenic cells of estrogen-treated male Japenese quail. Calcified tissue international 49:124-127. doi: 10.1007/BF02565134

240. Omdahl, J. L., H. A. Morris, and B. K. May. 2002. Hydroxylase enzymes of the vitamin D pathway: expression, function, and regulation. Annual Review Nutrition 22:139-166. doi: 10.1146/annurev.nutr.22.120501.150216

241. Padhi, M. K., R. N. Chatterjee, S. Haunshi, and U. Rajkumar. 2013. Effect of age on egg quality in chicken. Indian Journal of Poultry Science 48:122-125.

242. Pansu, D., C. Bellaton, and F. Bronner. 1981. Effect of Ca intake on saturable and nonsaturable components of duodenal transport. American Journal of Physiology 240:32-37. doi: 10.1152/ajpgi.1981.240.1.G32

243. Park, J. A., and S. H. Sohn. 2018. The influence of hen aging on eggshell ultrastructure and shell mineral components. Korean Journal for Food Science of Animal Resources 38:1080-1091. doi: 10.5851/kosfa.2018.e41

244. Parsons, A. H., and G. F. Combs, Jr. 1980. Blood ionized calcium cycles in the chicken. Poultry Science 60:1520-1524. doi: 10.3382/ps.0601520

245. Pastore, S. M., P. C. Gomes, H. S. Rostango, L. Fernando, T. Albino, A. A. Calderano, C. R. Vellasco, G. da Silva Viana, and R. L. de Almeida. 2012. Calcium levels and calcium:available phosphorus ratios in diets for white egg layers from 42 to 58 weeks of age. Revista Brasilleira de Zootecnia 41:2424-2432. doi: 10.1590/S1516-35982012001200007

246. Pelletier, N. 2018. Changes in the life cycle environmental footprint of egg production in Canada from 1962 to 2012. Journal of Cleaner Production 176:1144-1153. doi: 10.1016/j.jclepro.2017.11.212

247. Pelletier, N., M. Ibarburu, and H. Xin. 2014. Comparison of the environmental footprint of

the egg industry in the United States in 1960 and 2010. Poultry Science 93:241-255. doi: 10.3382/ps.2013-03390

248. Perwad, F., N. Azam, M. Y. H. Zhang, T. Yamashita, H. S. Tenenhouse, and A. A. Portale. 2005. Dietary and serum phosphorus regulate fibroblast growth factor 23 expression and 1,25-dihydroxyvitamin D metabolism in mice. Endocrinology 146:5358-5364. doi: 10.1210/en.2005-0777

249. Perwad, F., M. Y. H. Zhang, H. S. Tenenhouse, and A. A. Portale. 2007. Fibroblast growth factor 23 impairs phosphorus and vitamin D metabolism in vivo and suppresses 25-hydroxyvitamin D-1 -hydroxylase expression in vitro. Am J Physiol-Renal 293:1577-1583. doi: 10.1152/ajprenal.00463.2006

250. Pinheiro, P. L. C., J. C. R. Cardoso, D. M. Power, and A. V. M. Canario. 2012. Functional characterization and evolution of PTH/PTHrP receptors: insights from the chicken. BMC Evolutionary Biology 12:1-15. doi: 10.1186/1471-2148-12-110

251. Plieschnig, J. A., E. T. Gensberger, T. M. Bajari, W. J. Schneider, and M. Hermann. 2012. Renal LRP2 expression in man and chicken is estrogen responsive. Gene 508:49-59. doi: 10.1016/j.gene.2012.07.041

252. Polansky, O., Z. Sekelova, M. Faldynova, A. Sebkova, F. Sisak, and I. Rychlik. 2016. Important metabolic pathways and biological processes expressed by chicken cecal microbiota. Applied and Environmental Microbiology 82:1569-1576. doi: 10.1128/AEM.03473-15

253. Ponchon, G., and H. F. DeLuca. 1969a. The role of the liver in the metabolism of vitamin D. J Clin Invest 48:1273-1279. doi: 10.1172/JCI106093

254. Ponchon, G., A. L. Kennan, and H. F. DeLuca. 1969b. Activation of vitamin D by the liver. J Clin Invest 48:2032-2037. doi: 10.1172/JCI106168

255. Poorhemati, H., M. Ghaly, G. Sadvakassova, and S. V. Komarova. 2023. FGF23 level in poultry chicken, a systematic review and meta-analysis. Frontiers in Physiology 14:1279204. doi: 10.3389/fphys.2023.1279204

256. Pottguter, R. 2016. Feeding laying hens to 100 weeks of age. Pages 18-21 in Lohmann Information, Cuxhaven, Germany.

257. Preisinger, R. 2018. Innovative layer genetics to handle global challenges in egg production. British Poultry Science 59:1-6. doi: 10.1080/00071668.2018.1401828

258. Proszkowiec-Weglarz, M., and R. Angel. 2013. Calcium and phosphorus metabolism in broilers: Effect of homeostatic mechanism on calcium and phosphorus digestibility. J Appl Poultry Res 22:609-627. doi: 10.3382/japr.2012-00743

259. Proszkowiec-Weglarz, M., L. L. Schreier, K. B. Miska, R. Angel, S. Kahl, and B. Russell. 2019. Effect of early neonatal development and delayed feeding post-hatch on jejunal and ileal calcium and phosphorus transporter genes expression in broiler chickens. Poultry Science 98:1861-1871. doi: 10.3382/ps/pey546

260. Quelo, I., J. P. Kahlen, A. Rascle, P. Jurdic, and C. Carlberg. 1994. Identification and characterization of a vitamin D_3 response element of chicken carbonic anhydrase-II. DNA and Cell Biology 13:1181-1187. doi: 10.1089/dna.1994.13.1181

261. Quelo, I., I. Machuca, and P. Jurdic. 1998. Identification of a vitamin D response element in the proximal promoter of the chicken carbonic anhydrase II gene. J. Biol. Chem. 273:10638-10646. doi: 10.1074/jbc.273.17.10638

262. Radwan, L. M. 2015. Eggshell quality: a comparison between Fayoumi, Gimieizah, and brown Hy-Line strains for mechanical properties and ultrastructure of their eggshells. Animal Production Science 56:A-E. doi: 10.1071/AN14755

263. Randall, W. C., and W. A. Hiestand. 1939. Panting and temperature regulation in the chicken. American Journal of Physiology 127:761-768. doi: 10.1152/ajplegacy.1939.127.4.761

264. Rasmussen, H., M. Wong, D. D. Bikle, and D. B. P. Goodman. 1972. Hormonal control of the renal conversion of 25-hydroxycholecalciferol to 1,25-dihydroxychoelcalciferol. J Clin Invest 51:2502-2504. doi: 10.1172/JCI107065

265. Ravindran, V., and M. R. Abdollahi. 2021. Nutrition and digestive physiology of the broiler chick: state of the art and outlook. Animals 11:1-23. doi: 10.3390/ani11102795

266. Razzaque, M. S. 2009. The FGF23-Klotho axis: endocrine regulation of phosphate homeostasis. Nat. Rev. Endocrinol. 5:611-619. doi: 10.1038/nrendo.2009.196

267. Ren, Z., M. Ebrahimi, D. E. Butz, J. M. Sand, K. Zhang, and M. E. Cook. 2017. Antibody to fibroblast growth factor 23-peptide reduces excreta phosphorus of laying hens. Poultry Science 96:127-134. doi: 10.3382/ps/pew189

268. Ren, Z., J. Yan, Q. Hu, X. Liu, C. Pan, Y. Liu, X. Zhang, X. Yang, and X. Yang. 2020. Phosphorus restriction changes the expression of fibroblast growth factor 23 and its receptors in laying hens. Frontiers in Physiology 11:1-12. doi: 10.3389/fphys.2020.00085

269. Reynolds, C. J., N. J. Koszewski, R. L. Horst, D. C. Beitz, and J. P. Goff. 2018. Localization of the 1,25-dihydroxyvitamin D-mediated response in the intestines of mice. J Steroid Biochem 186:56-60. doi: 10.1016/j.jsbmb.2018.09.009

270. Rezende, M. S., B. B. Fonseca, P. F. de Sousa Braga, E. C. Guimaraes, and A. V. Mundim. 2021. Influence of age and sex on the blood biochemical constituent values of broiler breeders during the egg-laying stage. Tropical Animal Health and Production 53:1-8. doi: 10.1007/s11250-021-02981-z

271. Richards, S. A. 1970. Physiology of thermal panting in birds. Pages 151-168 in Annales de Biologie Animale Biochimie BiophysiqueEDP Sciences.

272. Richter, B., and C. Faul. 2018. FGF23 actions on target tissues - with and without klotho. Frontiers in Endocrinology 9:1-21. doi: 10.3389/fendo.2018.00189

273. Robinson, D. S., and N. R. King. 1963. Carbonic anhydrase and formation of the hen's egg shell. Nature 199:497-498. doi: 10.1038/199497a0

274. Rodriguez-Navarro, A. B., P. Marie, Y. Nys, M. T. Hincke, and J. Gautron. 2015. Amorphous calcium carbonate controls avian eggshell mineralization: A new paradigm for understanding rapid eggshell calcification. Journal of Structural Biology 190:291-303. doi: 10.1016/j.jsb.2015.04.014

275. Roland, D. A., Sr. 1977. The extent of uncollected eggs due to inadequate shell. Poultry Science 56:1517-1521. doi: 10.3382/ps.0561517

276. Roland, D. A., Sr. 1986. Eggshell quality IV: oystershell versus limestone and the importance of particle size or solubility of calcium source. World Poultry Science Journal 42:166-172. doi: 10.1079/WPS19860013

277. Rougiere, N., and B. Carre. 2010. Comparison of gastrointestinal transit times between chickens from D+ and D- genetic lines selected for divergent digestion efficacy. Animal 4:1861-1872. doi: 10.1017/S1751731110001266

278. Rousseau, X., A. S. Valable, M. P. Letourneau-Montminy, N. Meme, E. Godet, M. Magnin, Y. Nys, M. J. Duclos, and A. Narcy. 2016. Adaptive response of broilers to dietary phosphorus and calcium restrictions. Poultry Science 95:2849-2860. doi: 10.3382/ps/pew172

279. Ruxton, C. H. S., E. Derbyshire, and S. Gibson. 2010. The nutritional properties and health benefits of eggs. Nutrition and Food Science 40:263-280. doi: 10.1108/00346651011043961

280. Sah, N., and B. Mishra. 2018. Regulation of egg formation in the oviduct of laying hen. World Poultry Sci J 74:509-521. doi: 10.1017/S0043933918000442

281. San Martin Diaz, V. E. 2018. Effects of 1α-hydroxycholecalciferol and other vitamin D analogues on liver performance, bone development, meat yield and quality, and mineral digestibility in broilers. Master of Science. North Carolina State University, North Carolina.

282. Sandilands, V., C. Moinard, and N. H. C. Sparks. 2009. Providing laying hens with perches: fulfilling behavioral needs but causing injury? British Poultry Science 50:395-406. doi: 10.1080/00071660903110844

283. Sato, T., M. Courbebaisse, N. Ide, Y. Fan, J. I. Hanai, J. Kaludjerovic, M. J. Densmore, Q. Yuan, H. R. Toka, M. R. Pollak, J. Hou, and B. Lanske. 2017. Parathyroid hormone controls paracellular Ca^{2+} transport in the thick ascending limb by regulating the tight-junction protein Claudin 14. Proceedings of the National Academy of Sciences of the United States of America 114:3344-3353. doi: 10.1073/pnas.1616733114

284. Saunders-Blades, J. L., J. L. MacIsaac, D. R. Korver, and D. M. Anderson. 2009. The effect of calcium source and particle size on the production performance and bone quality of laying hens. Poultry Science 88:338-353. doi: 10.3382/ps.2008-00278

285. Sauveur, B. 1977. The effect of induced metabolic acidosis on vitamin D3 metabolism in rachitic chicks. Calcified Tissue Research 23:121-124. doi: 10.1007/BF02012776

286. Scanes, C. G., R. Campbell, and P. Griminger. 1987. Control of energy balance during egg production in the laying hen. Journal of Nutrition 117:605-611. doi: 10.1093/jn/117.3.605

287. Schaafsma, A., I. Pakan, G. J. H. Hofstede, F. A. J. Muskiet, E. Van Der Veer, and P. J. F. De Vries. 2000. Mineral, amino, and hormonal composition of chicken eggshell powder and the evaluation of its use in human nutrition. Poultry Science 79:1833-1838. doi: 10.1093/ps/79.12.1833

288. Scope, A., and I. Schwendenwein. 2020. Laboratory evaluation of renal function in birds. Veterinary Clinics Exotic Animal Practice 23:47-58. doi: 10.1016/j.cvex.2019.08.002

289. Senkoylu, N., H. Akyurek, E. Samli, and A. Agma. 2005. Assesment the impacts of dietary electrolyte balance levels on laying performance of commercial white layers. Pakistan Journal of Nutrition 4:423-427.

290. Sergeant, M. J., C. Constantinidou, T. A. Cogan, M. R. Bedford, C. W. Penn, and M. J. Pallen. 2014. Extensive microbial and functional diversity within the chicken cecal

microbiome. PLoS One 9:1-13. doi: 10.1371/journal.pone.0091941

291. Shang, S., Z. He, W. Hou, X. Chen, X. Zhao, H. Han, S. Chen, S. Yang, and F. Tai. 2023. Molecular cloning, expression analysis and functional characterization of chicken cytochrome P450 27A1: A novel mitochondrial vitamin D_3 25-hydroxylase. Poultry Science 102:102747. doi: 10.1016/j.psj.2023.102747

292. Shanmugasundaram, R., and R. K. Selvaraj. 2012. Vitamin D-1alpha-hydroxylase and vitamin D-24-hydroxylase mRNA studies in chickens. Poultry Science 91:1819-1824. doi: 10.3382/ps.2011-02129

293. Shi, S. M., J. P. Lin, and G. Y. Shiau. 2000. Dissolution rates of limestones of different sources. Journal of Hazardous Materials B79:159-171. doi: 10.1016/S0304-3894(00)00253-3

294. Shimada, T., M. Kakitani, Y. Yamazaki, H. Hasegawa, Y. Takeuchi, T. Fujita, S. Fukumoto, K. Tomizuka, and T. Yamashita. 2004. Targeted abalation of *FGF23* demonstrates an essential physiological role of FGF23 in phosphate and vitamin D_3 metabolism. J Clin Invest 113:561-568. doi: 10.1172/JCI200419081

295. Shimada, T., S. Mizutani, T. Muto, T. Yoneya, R. Hino, S. Takeda, Y. Takeuchi, T. Fujita, T. Fukomoto, and T. Yamashita. 2000. Cloning and characterization of FGF23 as a causative factor of tumor-induced osteomalacia. PNAS 98:6500-6505. doi: 10.1073/pnas.101545198

296. Shini, A., S. Shini, and W. L. Bryden. 2019. Fatty liver haemorrhagic syndrome occurence in laying hens: impact of production system. Avian Pathology 48:25-34. doi: 10.1080/03079457.2018.1538550

297. Shinki, T., H. Shimada, S. Wakino, H. Anazawa, M. Hayashi, T. Saruta, H. F. DeLuca, and T. Suda. 1997. Cloning and expression of rat 25-hydroxyvitamin D_3-1a-hydroxylase cDNA. Proceedings of the National Academy of Sciences of the United States of America 94:12920-12925. doi: 10.1073/pnas.94.24.1292

298. Shinki, T., Y. Ueno, H. F. DeLuca, and T. Suda. 1999. Calcitonin is a major regulator for the expression of renal 25-hydroxyvitamin D_3-1a-hydroxylase gene in normocalcemic rats. PNAS 96:8253-8258. doi: 10.1073/pnas.96.14.8253

299. Shires, A., J. R. Thompson, B. V. Turner, P. M. Kennedy, and Y. K. Goh. 1986. Rate of passage of corn-canola meal and corn-soybean diets through the gastrointestinal tract of broiler and white leghorn chickens. Poultry Science 66:289-298. doi: 10.3382/ps.0660289

300. Short, F. J., P. Gorton, J. Wiseman, and K. N. Boorman. 1995. Determination of titanium dioxide added as an inert marker in chicken digestibility studies. Animal Feed Science Technology 59:215-221.

301. Silve, C. M., G. T. Hradek, A. L. Jones, and C. D. Arnaud. 1982. Parathyroid hormone receptor in intact embryonic chicken bone: characterization and cellular localization. Journal of Cell Biology 94:379-386. doi: 10.1083/jcb.94.2.379

302. Simkiss, K. 1964. Phosphates as crystal poisons of calcification. Biol. Rev. 39:487-504. doi: 10.1111/j.1469-185X.1964.tb01166.x

303. Sinclair-Black, M., R. A. Garcia-Mejia, L. R. Blair, R. Angel, X. Arbe, D. Cevero, and L. E. Ellestad. 2024. Circadian regulation of calcium and phosphorus homeostasis during the oviposition cycle in laying hens. Poultry Science 103. doi: 10.1016/j.psj.2023.103209

304. Sinclair-Black, M., R. A. Garcia, and L. E. Ellestad. 2023. Physiological regulation of calcium and phosphorus utilization in laying hens. Frontiers in Physiology 14:1-8. doi: 10.3389/fphys.2023.1112499

305. Singh, R., C. J. Joyner, M. J. Peddie, and T. Geoffrey Taylor. 1986. Changes in the concentrations of parathyroid hormone and ionic calcium in the plasma of laying hens during the egg cycle in relation to dietary deficiencies of calcium and vitamin D. General and Comparative Endocrinology 61:20-28. doi: 10.1016/0016-6480(86)90245-5

306. Smit, B., M. C. Whitfield, W. A. Talbot, A. R. Gerson, A. E. McKechnie, and B. O. Wolf. 2018. Avian thermoregulation in the heat: phylogenetic variation among avian orders in evaporative cooling capacity and heat tolerance. J. Exp. Biol. 221:1-10. doi: 10.1242/jeb.174870

307. Smith, O. B., and E. Kabaija. 1984. Effect of high dietary calcium and wide calcium-phosphorus ratios in broiler diets. Poultry Science 64:1713-1720. doi: 10.3382/ps.0641713

308. Sommerville, B. A., and J. Fox. 1987. Changes in renal function of the chicken associated with calcitonin and parathyroid hormone. General and Comparative Endocrinology 66:381-386. doi: 10.1016/0016-6480(87)90248-6

309. Spencer, R., M. Charman, P. W. Wilson, and E. M. Lawson. 1978. The relationship between vitamin D stimulated calcium transport and intestinal calcium binding protein in the chicken. Biochemistry 170:93-101. doi: 10.1042/bj1700093

310. Stapane, L., N. Le Roy, J. Ezagal, A. B. Rodriguez-Navarro, V. Labas, L. Combes-Soia, M. T. Hincke, and J. Gautron. 2020. Avian eggshell formation reveals a new paradigm for

vertebrate mineralization via vesicular amorphous calcium carbonate. J. Biol. Chem. 295:15853-15869. doi: 10.1074/jbc.RA120.014542

311. Sturkie, P. D., and w. J. Mueller. 1976. Reproduction in the female and egg production. Pages 302-330 in Avian Physiology. C. G. Scanes ed. Springer Advanced Texts in Life Sciences, Springer, Berlin, Heidelberg.

312. Sugiyama, T., and S. Kusuhara. 1993. Ultrastructural changes of osteoclasts on hen medullary bone during the egg-laying cycle. British Poultry Science 34:471-477. doi: 10.1080/00071669308417602

313. Sun, F., P. Liang, B. Wang, and W. Liu. 2023. The fibroblast growth factor-klotho axis at molecular level. Open Life Sciences 18:20220655. doi: 10.1515/biol-2022-0655

314. Sun, M. 2018. Distribution of inositol phosphates in animal feed grains and excreta: distinctions among isomers and phosphate oxygen isotype compositions. Plant and Soil 430:291-305. doi: 10.1007/s11104-018-3723-5

315. Tanaka, Y., R. S. Lorenc, and H. F. DeLuca. 1975. The role of 1,25-dihydroxyvitamin D3 and parathyroid hormone in the regulation of chick renal 25-hydroxyvitamin D3-24-hydroxylase. Biochemistry and Biophysics 171:521-526. doi: 10.1016/0003-9861(75)90061-2

316. Taylor, T. G. 1965. The availability of calcium and phosphorus plant materials for animals. Proceedings of the Nutrition Society 24:105-112.

317. Taylor, T. G., and L. F. Belanger. 1969. The mechanism of bone resorption in laying hens. Calcified Tissue Research 4:162-173. doi: 10.1007/BF02279117

318. Taylor, T. G., and R. H. Wasserman. 1972. Vitamin D-induced calcium-binding protein: comparative aspects in kidney and intestine. American Journal of Physiology 223:110-114. doi: 10.1152/ajplegacy.1972.223.1.110

319. Thapa, B. R., and A. Walia. 2006. Liver function tests and their interpretation. Indian Journal of Pediatrics 74:663-671. doi: 10.1007/s12098-007-0118-7

320. Thiruvenkadan, A. K., S. Panneerselvam, and R. Prabakaran. 2010. Layer breeding strategies: an overview. World Poultry Science Journal 66:477-502. doi: 10.1017/S0043933910000553

321. Tomoe, Y., H. Segawa, K. Shiozawa, I. Kaneko, R. Tominaga, E. Hanabusa, F. Aranami, J. Furutani, S. Kuwahara, S. Tatsumi, M. Matsumoto, M. Ito, and K. Miyamoto. 2009.

Phosphaturic action of fibroblast growth factor 23 in Npt2 null mice. Am. J. Physiol. Renal Physiol. 298:1341-1350. doi: 10.1152/ajprenal.00375.2009

322. Toyomizu, M., M. Tokuda, A. Mujahid, and Y. Akiba. 2005. Progressive alteration to core temperature, respiration, and blood acid-base balance in broiler chickens exposed to acute heat stress. J. Poult. Sci. 42:110-1118. doi: 10.2141/jpsa.42.110

323. Traore, O. Z., and M. Doyon. 2023. Economic sustainability of extending lay cycle in the supply-managed Canadian egg industry. Front Anim Sci 4. doi: 10.3389/fanim.2023.1201771

324. Tucker, G., R. E. Gagnon, and M. R. Haussler. 1972a. Vitamin D_3-25-hydroxylase: tissue occurrence and apparent lack of regulation. Arch. Biochem. Biophy. 155:47-57. doi: 10.1016/S0003-9861(73)80008-6

325. Tucker, G., R. E. Gagnon, and M. R. Haussler. 1972b. Vitamin D_3-25 hydroxylase: Tissue occurrence and apparent lack of regulation. Arch. Biochem. Biophy. 155:47-57. doi: 10.1016/S0003-9861(73)80008-6

326. Tumova, E., and R. M. Gous. 2012. Interaction of hen production type, age, and temperature on laying pattern. Poultry Science 91:1269-1275. doi: 10.3382/ps.2011-01951

327. Tumova, E., R. M. Gous, and N. Tyler. 2014. Effect of hen age, environmental temperature,and oviposition time on egg shell quality and egg shell and serum mineral contents in laying and broiler breeder hens. Czech J. Anim. Sci. 59:435-443. doi: 10.17221/7655-Cjas

328. United Nations. 2015. World population prospects: The 2015 revision, key findings, and advance tables, New York.

329. United States Department of Agriculture. 2014. Chickens and Eggs (April 2014), Ithaca, NY.

330. United States Department of Agriculture. 2024. Chickens and Eggs. Pages 1-22 in Chickens and EggsCornell University, Ithaca, NY.

331. Untergasser, A., I. Cutcutache, T. Koressaar, J. Ye, B. C. Faircloth, M. Remm, and S. G. Rozen. 2012. Primer3--new capabilities and interfaces. Nucleic Acids Res 40:1-12. doi: 10.1093/nar/gks596

332. Uribarri, J., H. Douyon, and M. S. Oh. 1995. A re-evaluation of the urinary parameters of acid production and excretion in patients with chronic renal acidosis. Kidney International

47:624-627.

333. Van de Velde, J. P., N. Loveridge, and J. P. W. Vermieden. 1984a. Parathyroid hormone response to calcium stress during eggshell calcification. Endocrinology 115:1901-1904. doi: 10.1210/endo-115-5-1901

334. Van de Velde, J. P., J. P. W. Vermieden, J. J. A. Touw, and J. P. Veldhuizen. 1984b. Changes in activity of chicken medullary bone cell populations in relation to the egg laying cycle. Metabolic Bone Disease and Related Research 5:191-193. doi: 10.1016/0221-8747(84)90029-8

335. Van der Klis, J. D., M. W. Verstegen, and W. De Wit. 1990. Absorption of minerals and retention time of dry matter in the gastrointestinal tract of broilers. Poultry Science 69:2185-2194. doi: 10.3382/ps.0692185

336. Wang, R. M., J. P. Zhao, X. J. Wang, H. C. Jiao, J. M. Wu, and H. Lin. 2018. Fibroblast growth factor 23 mRNA expression profile in chickens and its response to dietary phosphorus. Poultry Science 97:2258-2266. doi: 10.3382/ps/pey092

337. Wang, X. J., P. Li, J. P. Zhao, H. C. Jiao, and H. Lin. 2022. The temporal gene expression profiles of calcium and phosphorus transporters in Hy-Line Brown layers. Poultry Science 101:1-11. doi: 10.1016/j.psj.2022.101736

338. Warren, D. C., and H. M. Scott. 1935. Physiological factors influencing the rate of egg formation in the domestic hen. Journal of Agricultural Research 51:565-572.

339. Wasserman, R. H., C. A. Smith, C. M. Smith, M. E. Brindak, C. S. Fullmer, L. P. Krook, and J. T. Penniston. 1991. Immunohistochemical localization of a calcium pump and calbindin D28k in the oviduct of the laying hen. Histochemistry 96:413-418. doi: 10.1007/BF00315999

340. Watanabe, K. P., Y. K. Kawai, Y. Ikenaka, M. Kawata, S. Ikushiro, T. Sakaki, and M. Ishizuka. 2013. Avian cytochrome P450 (CYP) 1-3 family genes: isoforms, evolutionary relationships, and mRNA expression in chicken liver. PLoS One 8:1-11. doi: 10.1371/journal.pone.0075689

341. Watford, M., Y. Hod, Y. B. Chiao, M. F. Utter, and R. W. Hanson. 1981. The unique role of the kidney in gluconeogenesis in the chicken. J. Biol. Chem. 256:10023-10027.

342. Wedral, E. M., D. V. Vadehra, and R. C. Baker. 1974. Chemical composition of the cuticle, and the inner and outer shell membranes from eggs of *gallus gallus*. Comparative Biochemistry and Physiology 47:631-640. doi: 10.1016/0305-0491(74)90011-x

343. Whitehead, C. C. 2004. Overview of bone biology in the egg-laying hen. Poultry Science 83:193-199. doi: 10.1093/ps/83.2.193

344. Whitehead, C. C., and R. H. Fleming. 2000. Osteoporosis in cage layers. Poultry Science 79:1033-1041. doi: 10.1093/ps/79.7.1033

345. Wideman, R. F. 1986. Renal regulation of avian calcium and phosphorus metabolism. Journal of Nutrition 117:808-815.

346. Wideman, R. F., Jr., and E. J. Braun. 1981. Stimulation of avian renal phosphate secretion by parathyroid hormone. Physiol Rev 241:263-272. doi: 10.1152/ajprenal.1981.241.3.F263

347. Wilson, S., and S. R. Duff. 1990. Morphology of medullary bone during the egg formation cycle. Research in Veterinary Science 48:216-220. doi: 10.1016/S0034-5288(18)30993-7

348. Wilson, S., S. R. I. Dugg, and C. C. Whitehead. 1992. Effects of age, sex and housing on the trabecular bone of laying strain domestic fowl. Research in Veterinary Science 53:52-58. doi: 10.1016/0034-5288(92)90084-f

349. Wongdee, K., M. Rodrat, C. Keadsai, W. Jantarajit, J. Teerapornpuntakit, J. Thongbunchoo, and N. Charoenphandhu. 2018. Activation of calcium-sensing receptor by allosteric agonists cinacalcet and AC-265347 abolishes the $1,25(OH)_2D_3$-induced Ca^{2+} transport: Evidence that explains how the intestine prevents excessive Ca^{2+} absorption. Biochemistry and Biophysics 657:15-22. doi: 10.1016/j.abb.2018.09.004

350. Wood-Gush, D. G. M., and A. R. Horne. 1970. The effect of egg formation and laying on the food and water intake of brown leghorn hens. British Poultry Science 11:459-466. doi: 10.1080/00071667008415841

351. Yamada, M., C. Chen, T. Sugiyama, and W. K. Kim. 2021. Effect of age on bone structure parameters in laying hens. Animals 11:1-8. doi: 10.3390/ani11020570

352. Yan, F., R. Angel, and C. M. Ashwell. 2007. Characterization of the chicken small intestine type IIb sodium phosphate transporter. Poultry Science 86:67-76. doi: 10.1093/ps/86.1.67

353. Yan, J., C. Pan, Y. Liu, X. Liao, J. Chen, Y. Zhu, X. Huang, X. Yang, and Z. Ren. 2022. Dietary vitamin D_3 deprivation suppresses fibroblast growth factor 23 signals by reducing serum phosphorus levels in laying hens. Anim. Nutr. 9:23-30. doi: 10.1016/j.aninu.2021.07.010

354. Yang, J. H., J. F. Hou, C. Farquharson, Z. L. Zhou, Y. F. Deng, L. Wang, and Y. Yu. 2011.

Localisation and expression of TRPV6 in all intestinal segments and kidney of laying hens. British Poultry Science 52:507-516. doi: 10.1080/00071668.2011.596994

355. Yasuoka, T., M. Kawashima, T. Takahasi, T. N., and K. Tanaka. 1998. Calcitonin receptor binding proteins in bone and kidney of the chicken during the oviposition cycle. Journal of Bone and Mineral Research 13:1412-1419. doi: 10.1359/jbmr.1998.13.9.1412

356. Yoshimura, Y., H. Ohira, and T. Tamura. 1997. Immunocytochemical localization of vitamin D receptors in the shell gland of immature, laying and molting hens. General and Comparative Endocrinology 108:282-289. doi: 10.1006/gcen.1997.6972

357. Zhang, B., and C. N. Coon. 1997. The relationship of calcium intake, source, size, solubility in vitro and in vivo, and gizzard limestone retention in laying hens. Poultry Science 76:1702-1706. doi: 10.1093/ps/76.12.1702

358. Zhao, D. R., L. B. Gao, F. Gong, J. Feng, H. J. Zhang, S. G. Wu, J. Wang, and Y. N. Min. 2024a. TMT-based quantitative proteomic analysis reveals eggshell matrix protein changes correlated with eggshell quality in Jing Tint 6 laying hens of different ages. Poultry Science 103:1-12. doi: 10.1016/j.psj.2024.103463

359. Zhao, J., H. Pan, Y. Liu, Y. He, H. Shi, and C. Ge. 2024b. Interacting networks of the hypothalamic-piuitary-ovarian axis regulate layer hens performance. Genes 14. doi: 10.3390/genes14010141

360. Zhao, Q., P. R. Brauer, L. Xiao, M. H. McGuire, and J. A. Yee. 2002. Expression of parathyroid hormone-related peptide (PTHrP) and its receptor (PTH1R) during the histogenesis of cartilage and bone in the chicken mandibular process. Journal of Anatomy 201:137-151. doi: 10.1046/j.1469-7580.2002.00078.x

361. Ziegler, R., M. Telib, and E. F. Pfeiffer. 1969. The secretion of calcitonin by the perfused ultimobranchial gland of the hen. Hormone and Metabolic Research 1:39-40. doi: 10.1055/s-0028-1096824

APPENDICES

Appendix A: Supplementary tables for Chapter 3

Table A1: Blood measurements using iSTAT CG8+ cartridges.

HPOP[1]	pH	[2]pCO_2 (mmHg)	[2]pO_2 (mmHg)	[2]BEecf (mM)	[2]HCO_3^- (mM)	[2]TCO_2 (mM)	[2]sO_2 (%)	[2]Na^+ (mM)	[2]K^+ (mM)	[2]iCa^{2+} (mM)	[2]Glu (mg/dL)	[2]Hct (%)	[2]Hb (mM)
1	7.42 ± 0.02	34.3 ± 1.7	62.5 ± 1.0	-2.50 ^{abcd} ± 0.29	22.0 ± 0.4	23.3 ± 0.5	92.0 ^{abc} ± 0.4	147.3 ^{abcd} ± 1.1	5.35 ± 0.28	1.51 ± 0.02	224.8 ± 3.0	22.0 ± 1.1	7.5 ± 0.4
3	7.49 ± 0.04	28.3 ± 3.5	61.3 ± 2.0	-2.67 ^{bcd} ± 0.92	20.7 ± 0.8	21.5 ± 0.7	93.2 ^{a} ± 0.6	146.7 ^{abcd} ± 0.5	6.20 ± 0.70	1.43 ± 0.08	201.2 ± 9.5	20.5 ± 1.9	7.0 ± 0.6
4	7.45 ± 0.02	32.1 ± 1.9	59.5 ± 1.2	-2.00 ^{abcd} ± 0.58	22.0 ± 0.5	22.8 ± 0.6	91.7 ^{abc} ± 0.4	144.8 ^{d} ± 0.8	5.70 ± 0.26	1.54 ± 0.03	218.0 ± 5.3	22.5 ± 0.8	7.7 ± 0.3
6	7.47 ± 0.04	31.3 ± 3.4	68.5 ± 8.0	-1.83 ^{abc} ± 0.60	21.8 ± 0.9	22.8 ± 0.9	93.0 ^{a} ± 1.3	148.0 ^{abc} ± 0.9	5.47 ± 0.58	1.46 ± 0.06	221.0 ± 7.7	22.8 ± 1.2	7.8 ± 0.4
Mean ± SEM 7	7.46 ± 0.02	33.0 ± 1.4	59.7 ± 0.3	-0.67 ^{ab} ± 1.12	23.2 ± 0.9	24.2 ± 0.9	92.0 ^{ab} ± 0.6	147.3 ^{abcd} ± 1.1	4.62 ± 0.19	1.48 ± 0.03	235.3 ± 3.3	23.0 ± 0.7	7.8 ± 0.3
8	7.42 ± 0.02	33.3 ± 1.6	58.8 ± 1.8	-1.80 ^{abcd} ± 0.58	22.3 ± 0.7	23.2 ± 0.8	91.0 ^{abcd} ± 0.7	145.4 ^{bcd} ± 1.7	4.92 ± 0.35	1.50 ± 0.04	229.8 ± 6.0	24.8 ± 0.4	8.4 ± 0.1
12	7.45 ± 0.01	33.7 ± 0.7	53.8 ± 1.1	-0.20 ^{a} ± 0.37	23.6 ± 0.3	24.4 ± 0.4	89.6 ^{cd} ± 0.5	144.4 ^{d} ± 0.9	4.16 ± 0.25	1.44 ± 0.07	218.4 ± 2.4	23.2 ± 1.0	7.9 ± 0.4
15	7.45 ± 0.05	33.3 ± 3.8	57.3 ± 1.7	-1.50 ^{abc} ± 1.04	22.6 ± 1.1	23.5 ± 1.2	90.3 ^{bcd} ± 1.7	148.8 ^{ab} ± 3.1	5.13 ± 0.95	1.34 ± 0.06	216.5 ± 15.0	21.5 ± 1.6	7.3 ± 0.5
18	7.38 ± 0.01	38.5 ± 1.7	56.5 ± 0.3	-2.50 ^{abcd} ± 0.87	22.8 ± 0.8	24.0 ± 0.9	88.5 ^{d} ± 0.3	144.8 ^{cd} ± 0.5	4.50 ± 0.17	1.52 ± 0.04	221.0 ± 7.2	22.5 ± 0.5	7.7 ± 0.2
21	7.41 ± 0.03	32.8 ± 2.5	57.6 ± 0.7	-4.00 ^{d} ± 0.45	20.6 ± 0.6	21.6 ± 0.7	89.8 ^{bcd} ± 0.9	146.8 ^{abcd} ± 1.4	4.78 ± 0.41	1.48 ± 0.05	217.4 ± 10.3	19.8 ± 1.4	6.7 ± 0.5
23	7.40 ± 0.02	34.1 ± 1.7	59.7 ± 2.1	-3.67 ^{cd} ± 0.61	21.2 ± 0.3	22.2 ± 0.3	90.8 ^{bcd} ± 0.8	149.2 ^{a} ± 0.7	4.83 ± 0.13	1.47 ± 0.07	217.5 ± 5.9	22.5 ± 0.8	7.7 ± 0.3
24	7.42 ± 0.02	28.4 ± 5.1	57.7 ± 2.1	-3.00 ^{cd} ± 0.89	21.5 ± 0.7	22.5 ± 0.8	90.2 ^{bcd} ± 0.7	149.5 ^{a} ± 0.6	4.73 ± 0.23	1.50 ± 0.04	225.8 ± 5.7	24.2 ± 1.0	8.2 ± 0.3
p value	0.3318	0.5879	0.1617	0.0309	0.0752	0.1248	0.0044	0.0200	0.0697	0.6461	0.1706	0.1371	0.1279

[1]Hours post-oviposition

[2]Partial pressure of carbon dioxide (pCO2), partial pressure of oxygen (pO2), base excess (BEecf), bicarbonate (HCO_3^-), total carbon dioxide (TCO_2), oxygen saturation (sO2), sodium (Na^+), potassium (K^+), ionized calcium (iCa^{2+}), glucose (Glu), hematocrit (Hct), hemoglobin (Hb) at different HPOP.

[abcd]Data were analyzed by one-way ANOVA followed by Fisher's test of least significant difference when ANOVA indicated significance, and values not sharing a common letter differ significantly ($P \leq 0.05$; n=6 hens/HPOP with the following exceptions: n=5 hens/8, 12, and 21 HPOP); n=4 hens/1, 15, and 18 HPOP).

Table A2: Plasma measurements using VetScan2 Avian/Reptile Profile Plus cartridges.

HPOP[1]		[2]AST (U/L)	[2]CK (U/L)	[2]UA (mg/dL)	[2]GLU (mg/dL)	[2]tP (mg/dL)	[2]tProt (g/dL)	[2]ALB (g/dL)	[2]GLOB (g/dL)	[2]K^+ (mM)	[2]Na^+ (mM)
Mean ± SEM	1	139 ± 13	366 ± 52	3.28 ^{abc} ± 0.38	215 ^{ab} ± 5	3.9 ^{cde} ± 0.6	4.33 ± 0.10	2.75 ± 0.10	1.58 ± 0.09	6.38 ± 0.26	148.8 ± 1.2
	3	117 ± 14	505 ± 230	3.07 ^{abcd} ± 0.41	189 ^{c} ± 16	3.2 ^{de} ± 0.9	3.83 ± 0.28	2.33 ± 0.24	1.50 ± 0.06	6.63 ± 1.16	144.0 ± 2.1
	4	138 ± 7	552 ± 95	3.93 ^{a} ± 0.24	211 ^{abc} ± 6	4.8 ^{bcde} ± 0.8	4.38 ± 0.22	2.83 ± 0.08	1.60 ± 0.16	6.58 ± 0.42	147.5 ± 3.3
	6	154 ± 22	1704 ± 817	3.37 ^{abc} ± 0.37	214 ^{abc} ± 15	4.2 ^{bcde} ± 1.6	4.07 ± 0.42	2.53 ± 0.23	1.53 ± 0.19	6.20 ± 1.11	148.0 ± 4.0
	7	154 ± 7	709 ± 123	3.58 ^{ab} ± 0.24	229 ^{a} ± 3	3.2 ^{e} ± 0.6	4.25 ± 0.12	2.52 ± 0.09	1.68 ± 0.31	5.17 ± 0.23	151.2 ± 0.9
	8	152 ± 7	1134 ± 767	3.73 ^{ab} ± 0.50	223 ^{ab} ± 8	2.8 ^{e} ± 0.5	4.38 ± 0.45	2.60 ± 0.24	1.78 ± 0.22	6.25 ± 0.37	151.3 ± 2.3
	12	138 ± 6	283 ± 33	3.14 ^{abc} ± 0.14	205 ^{bc} ± 4	7.0 ^{a} ± 0.7	4.30 ± 0.14	2.78 ± 0.15	1.52 ± 0.06	5.90 ± 0.26	144.6 ± 1.8
	15	111 ± 4	264 ± 1	2.60 ^{cd} ± 0.31	190 ^{c} ± 14	6.4 ^{ab} ± 1.7	4.13 ± 0.35	2.48 ± 0.22	1.65 ± 0.19	6.08 ± 0.85	148.5 ± 4.3
	18	143 ± 2	230 ± 60	3.13 ^{abcd} ± 0.43	218 ^{ab} ± 4	5.6 ^{abcd} ± 0.7	4.80 ± 0.12	3.07 ± 0.07	1.77 ± 0.09	5.60 ± 0.29	151.3 ± 1.9
	21	133 ± 4	421 ± 30	3.30 ^{abc} ± 0.20	221 ^{ab} ± 5	5.9 ^{abc} ± 0.4	4.15 ± 0.15	2.65 ± 0.06	1.48 ± 0.11	5.00 ± 0.17	148.0 ± 1.7
	23	142 ± 2	431 ± 38	2.97 ^{bcd} ± 0.09	212 ^{ab} ± 5	3.6 ^{de} ± 0.5	4.08 ± 0.21	2.48 ± 0.13	1.58 ± 0.08	5.82 ± 0.29	148.7 ± 2.7
	24	170 ± 23	1537 ± 1109	2.25 ^{d} ± 0.37	219 ^{ab} ± 7	3.0 ^{e} ± 0.3	3.98 ± 0.06	2.50 ± 0.05	1.88 ± 0.37	5.47 ± 0.26	151.0 ± 2.3
p value		0.0872	0.5796	0.0163	0.0217	0.0012	0.5088	0.1290	0.9176	0.2710	0.5189

[1]Hours post-oviposition

[2]Aspartate Aminotransferase (AST), uric acid (UA), glucose (GLU), total phosphorus (tP), total protein (tPr), albumin (ALB), globulin (GLOB), potassium (K+), sodium (Na+) at different HPOP. Values for bile acid and total calcium fell outside the upper detection limit of the VetScan2 and are excluded.

[abcde]Data were analyzed by one-way ANOVA followed by Fisher's test of least significant difference when ANOVA indicated significance, and values not sharing a common letter differ significantly ($P \leq 0.05$; n=6 hens/HPOP with the following exceptions: n=5 hens/8, 12, and 21 HPOP); n=4 hens/1, 15, and 18 HPOP).

Appendix B: Diets fed during rearing and onset of lay for Chapter 5.

Table B1. Ingredients and nutrient composition of the starter, grower, developer, and onset diets.[1]

Ingredients, as fed %	Starter (0-5 weeks)	Grower (6-10 weeks)	Developer (11-16 weeks)	Onset (17-22 weeks)
Corn	61.99	58.34	56.79	49.44
Soybean meal 47%	25.94	21.24	16.50	25.70
Wheat bran	-	8.50	-	-
Wheat middlings	-	-	-	9.17
Coarse limestone	-	-	-	6.53
Fish meal 60%	2.00	-	-	-
Alfalfa meal	-	2.36	4.20	2.00
Wheat middlings	5.00	5.00	16.60	-
Fine limestone	1.46	1.69	1.50	2.80
Soybean oil	1.00	1.00	0.80	2.01
Mono-dicalcium phosphate 21%	0.77	0.32	0.08	1.36
Arbocel®[2]	-	0.50	1.11	0.05
Vitamin premix	0.50[3]	0.05[4]	0.05[4]	0.03[5]
Sand	0.40	-	1.25	-
Sodium chloride	0.29	0.27	0.26	0.30
DL-Methionine	0.19	0.15	0.13	0.26
L-Lysine HCL	0.15	0.11	0.11	0.05
Coban 90	0.09	0.09	0.09	-
Trace mineral premix[6]	0.08	0.08	0.08	0.08
Sodium bicarbonate	0.08	0.16	0.31	0.12
Choline chloride 60%	-	0.07	0.04	0.04
Bacitracin methylene disalicylate	0.05	0.05	0.05	0.05
L-Threonine	0.02	0.02	0.03	0.01
L-Tryptophan	-	-	0.01	0.01
Axtra® phy gold[7]	0.005	0.005	0.005	-
Formulated nutrient composition, DM basis % (analyzed)				
Crude Protein	19.19 (17.70)	17.70 (16.60)	15.90 (16.20)	17.89 (18.40)
Crude fiber	1.94 (2.40)	3.50 (4.00)	4.22 (4.60)	2.68 (4.00)
Calcium	1.05 (0.89)	1.00 (0.84)	1.00 (0.72)	4.00 (3.60)
Phosphorus	0.60 (0.66)	0.56 (0.62)	0.48 (0.50)	0.67 (0.73)

[1]Table adapted from diets described previously (Garcia-Mejia et al., 2024)
[2]JRS Pharma LP, Patterson, NY.
[3]Vitamin premix provided the following per kilogram of diet: vitamin A, 11022 IU; vitamin D_3, 2204 IU; vitamin E, 22.05 IU; vitamin B12, 0.02 mg; Menadione, 2.21 mg; riboflavin, 8.82 mg; d-pantothenic acid, 22.05 mg; thiamine, 4.41 mg; niacin, 88.19 mg; vitamin B6, 4.41 mg; folic acid, 1.10 mg; choline, 382 mg; biotin, 0.40 mg.
[4]Vitamin premix provided the following per kilogram of diet: vitamin A, 10019 IU; vitamin D_3, 4519 IU; vitamin E, 41.34 IU; vitamin B12, 0.02 mg; Menadione, 2.48 mg; riboflavin, 13.78 mg; d-pantothenic acid, 19.29 mg; thiamine, 3.44 mg; niacin, 55.11 mg; vitamin B6, 4.82 mg; folic acid, 1.65 mg; biotin, 0.55 mg.
[5]Vitamin premix provided the following per kilogram of diet: vitamin A, 10000 IU; vitamin D_3 2000 IU, Vitamin B-12, 30 mg; vitamin E, 3 IU; vitamin K (menadione), 3.5 mg; riboflavin, 10 mg; pantothenic acid, 45 mg; thiamine, 20 mg; niacin, 4 mg; pyridoxine, 0.006 mg; folic acid, 0.03 mg; biotin, 1 mg.
[6]Trace mineral premix provided the following per kilogram of diet: Calcium min, 25.6 mg; Calcium max, 33.6 mg; Manganese min, 107.2 mg; Zinc, 85.6 mg; Magnesium, 19.8 mg; Iron, 21mg; Copper, 3.2 mg; Iodine, 0.8 mg; Selenium min, 0.3 mg.
[7]Danisco Animal Nutrition & Health (IFF), Cedar Rapids, IA.

Appendix C: Non-significant interactive means for Chapter 5

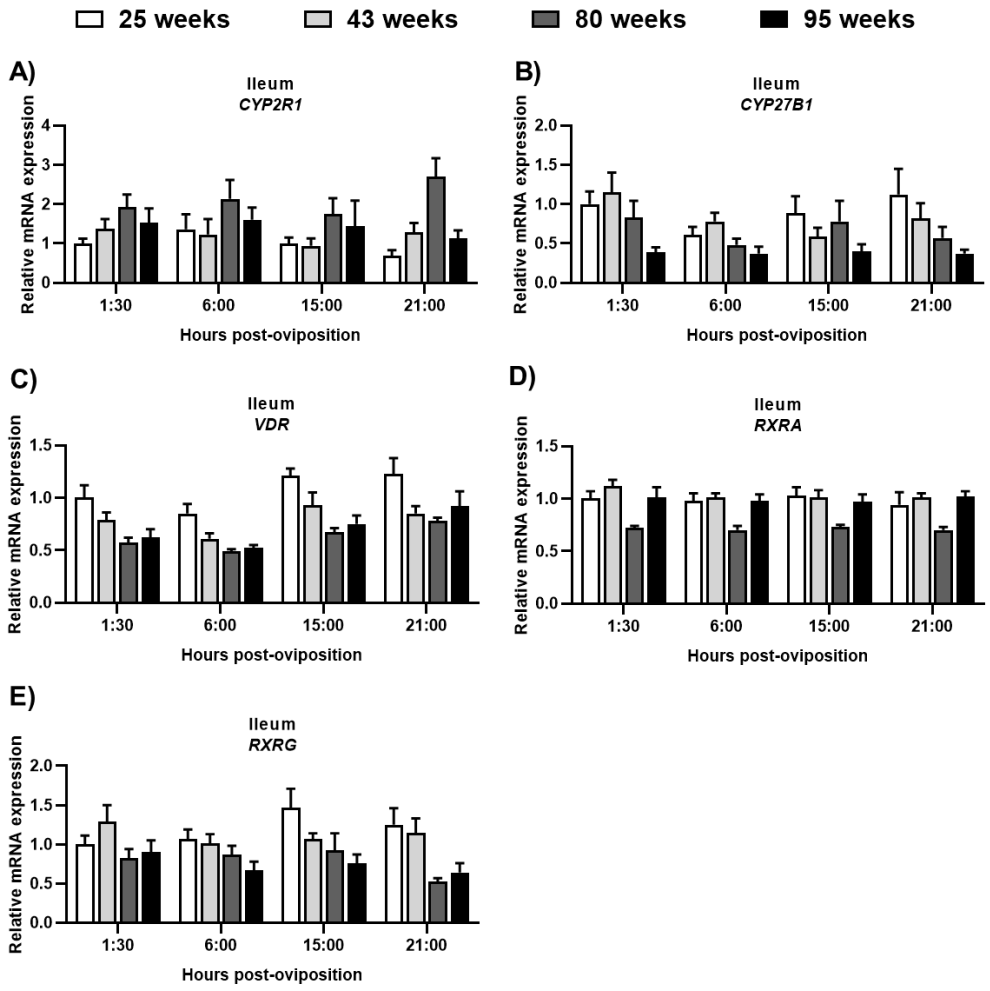

Figure C1. Expression of genes regulating vitamin D_3 metabolism in the ileum.
Relative levels of mRNA for (A) *CYP2R1*, (B) *CYP27B1*, (C) *VDR,* (D) *RXRA*, and (E) *RXRG* in the ileum at indicated ages and hours post-oviposition (HPOP) were determined by RT-qPCR and normalized to *GAPDH* mRNA. Data were analyzed by two-way ANOVA followed by Fisher's test of least significant difference, and the HPOP-by-age interaction was not significant for (A) *CYP2R1* (P=0.4978), (B) *CYP27B1* (P=0.9013), (C) *VDR* (P=0.9280), (D) *RXRA* (P=0.9400), and (E) *RXRG* (P=0.5919). Values (mean+SEM; n=8 hens/HPOP/age) are expressed relative to 1:30 HPOP at 25 weeks. Main effect means for age and HPOP are shown in Figure 5.2A - 5.2D (A, B) and Figure 5.5A - 5.5F (C - E).

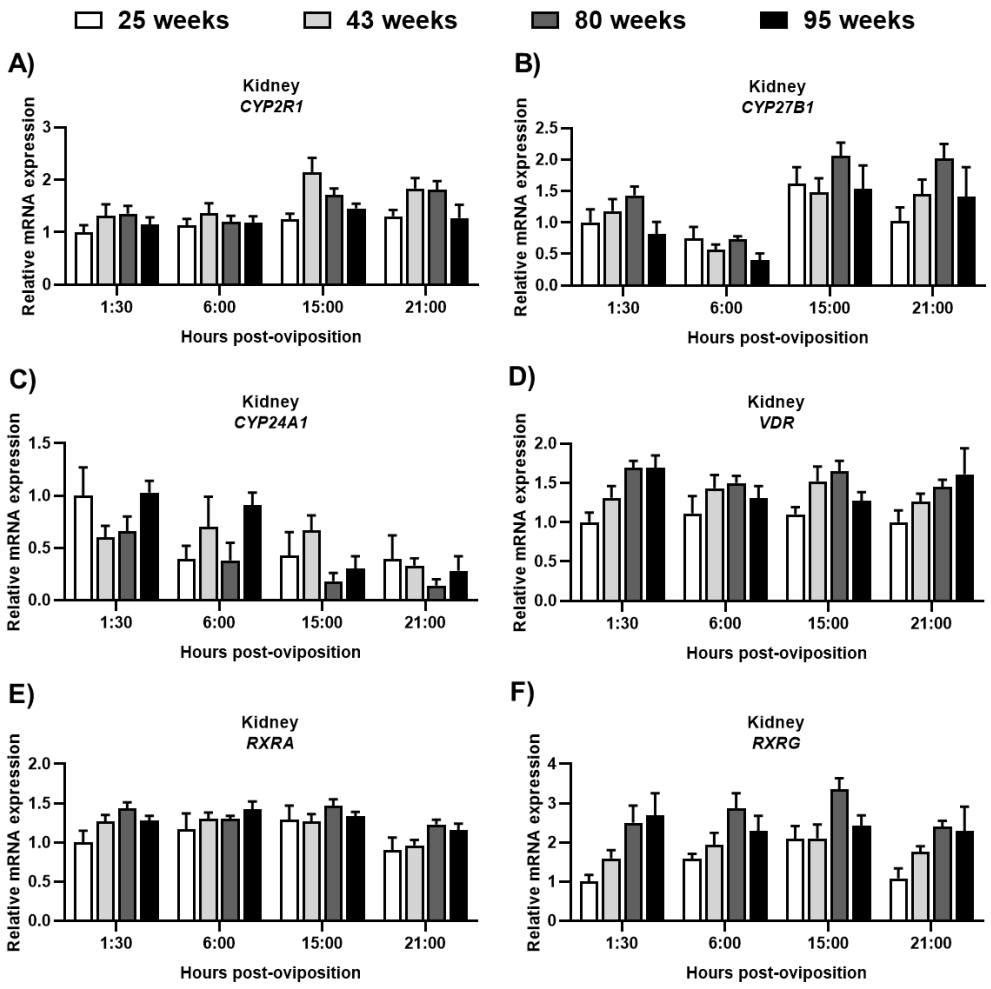

Figure C2. Expression of genes regulating vitamin D_3 metabolism in the kidney.
Relative levels of mRNA for (A) *CYP2R1*, (B) *CYP27B1*, (C) *CYP24A1,* (D) *VDR*, (E) *RXRA*, (F) *RXRG* in the kidney at indicated ages and hours post-oviposition (HPOP) were determined by RT-qPCR and normalized to *GAPDH* mRNA. Data were analyzed by two-way ANOVA followed by Fisher's test of least significant difference, and the HPOP-by-age interaction was not significant for (A) *CYP2R1* (P=0.9084), (B) *CYP27B1* (P=0.9044), (C) *CYP24A1* (P=0.0663), (D) *VDR* (P=0.7884), (E) *RXRA* (P=0.8533), and (F) *RXRG* (P=0.4827). Values (mean+SEM; n=8 hens/HPOP/age) are expressed relative to 1:30 HPOP at 25 weeks. Main effect means for age and HPOP are shown in Figure 5.3A - 5.3F (A-C) and Figure 5.6A - 5.6F (D - F).

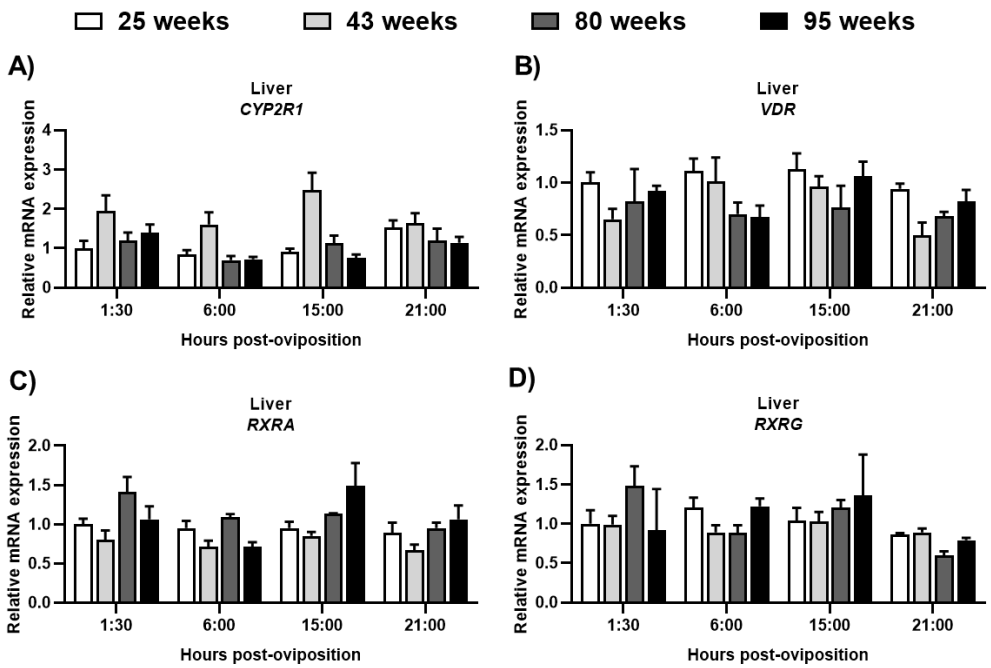

Figure C3. Expression of genes regulating vitamin D_3 metabolism in the liver.
Relative levels of mRNA for (A) *CYP2R1*, (B) *VDR*, (C) *RXRA*, and (D) *RXRG* in the liver at indicated ages and hours post-oviposition (HPOP) were determined by RT-qPCR and normalized to *CYCLO* mRNA. Data were analyzed by two-way ANOVA followed by Fisher's test of least significant difference, and the HPOP-by-age interaction was not significant for (A) *CYP2R1* (P=0.0001), (B) *VDR* (P=0.3524), (C) *RXRA* (P=0.1653), and (D) *RXRG* (P=0.1346). Values (mean+SEM; n=8 hens/HPOP/age) are expressed relative to 1:30 HPOP at 25 weeks. Main effect means for age and HPOP are shown in Figure 5.7A - 5.7H (A - D). Expression of *CYP24A1* was not detected in this tissue and *CYP27B1* was not measured.

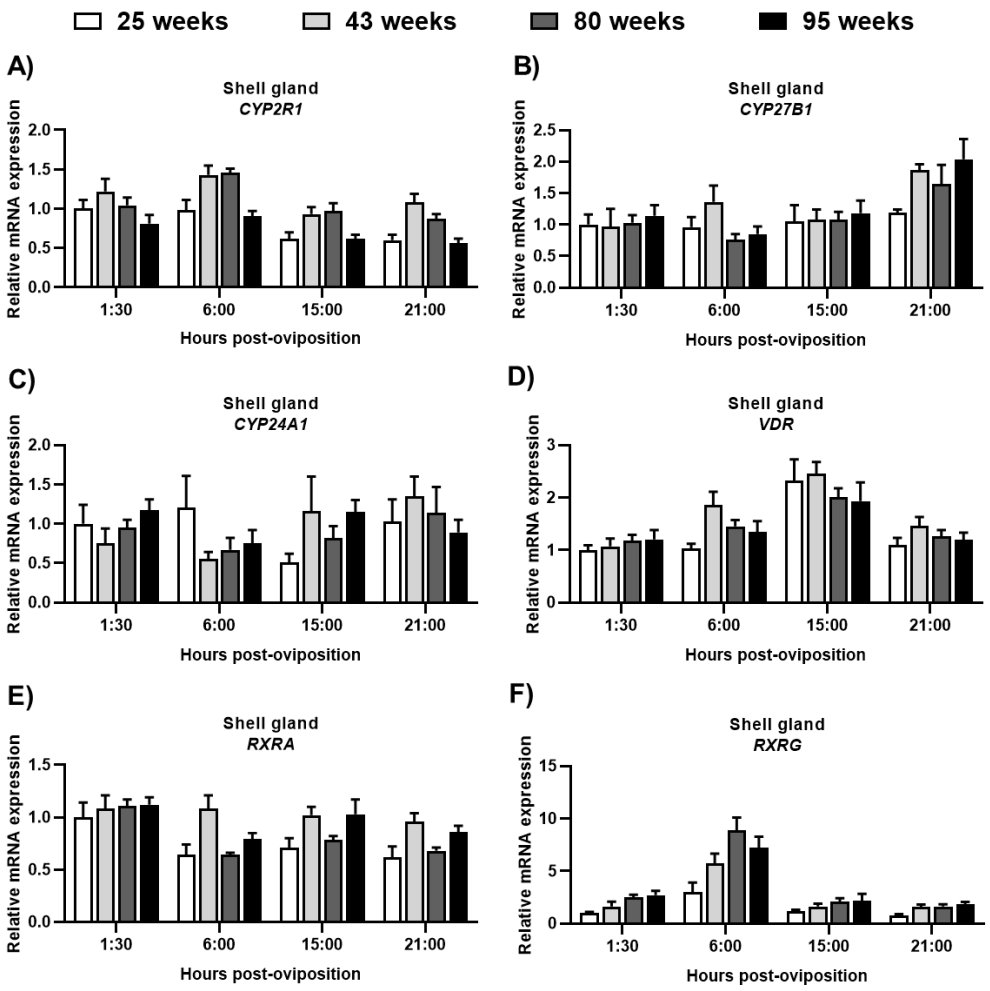

Figure C4. Expression of genes regulating vitamin D_3 metabolism in the shell gland. Relative levels of mRNA for (A) *CYP2R1*, (B) *CYP27B1*, (C) *CYP24A1,* (D) *VDR*, (E) *RXRA*, and (F) *RXRG* in the shell gland at indicated ages and hours post-oviposition (HPOP) were determined by RT-qPCR and normalized to *RPL5* mRNA. Data were analyzed by two-way ANOVA followed by Fisher's test of least significant difference, and the HPOP-by-age interaction was not significant for (A) *CYP2R1* (P=0.5517), (B) *CYP27B1* (P=0.6643), (C) *CYP24A1* (P=0.3699), (D) *VDR* (P=0.4998), (E) *RXRA* (P=0.3429), and (F) *RXRG* (P=0.4174). Values (mean+SEM; n=8 hens/HPOP/age) are expressed relative to 1:30 HPOP at 25 weeks. Main effect means for age and HPOP are shown in Figure 5.4A - 5.4F (A - C) and Figure 5.8A - 5.8F (D - F).

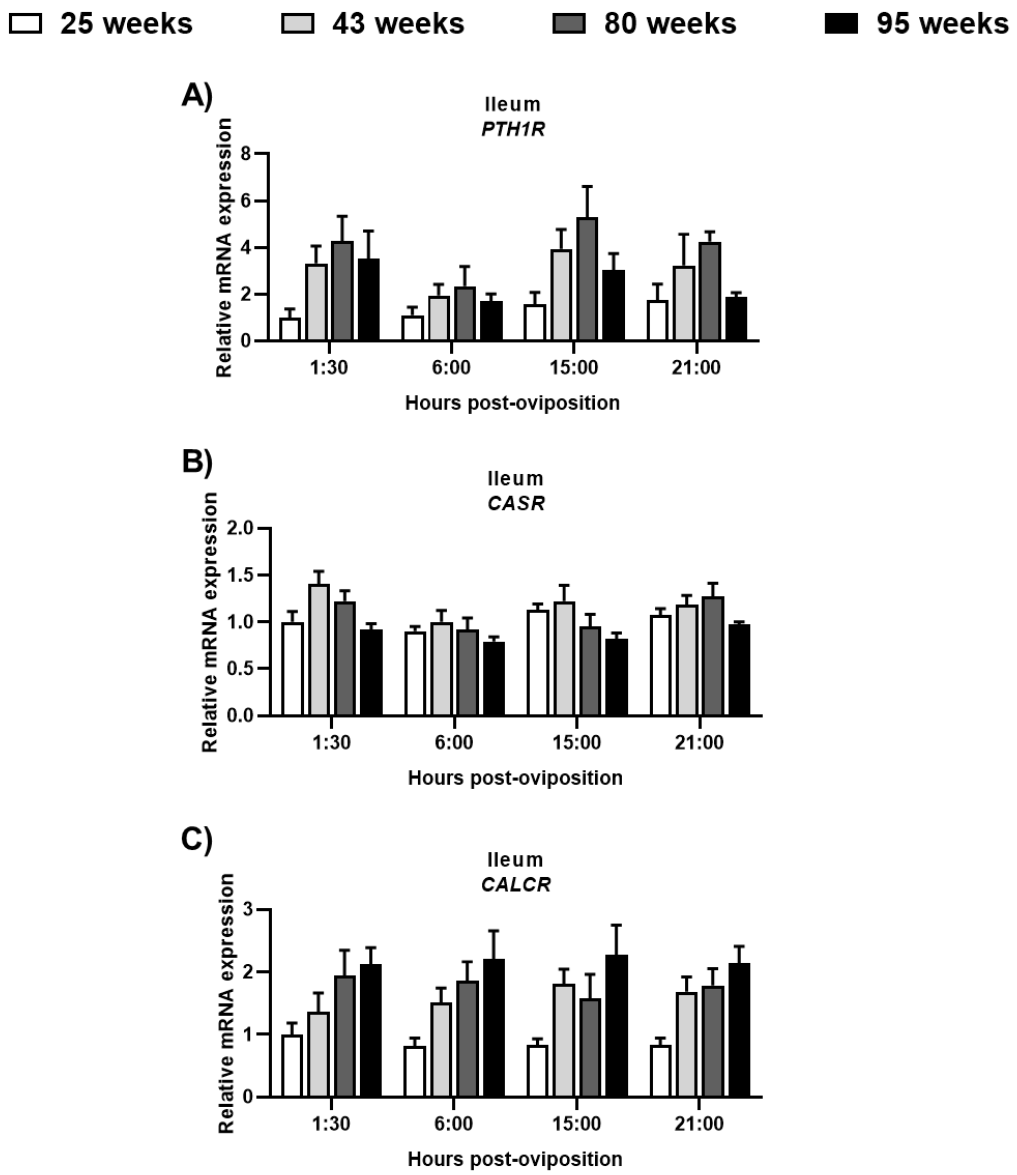

Figure C5. Expression of hormone receptors in the ileum.
Relative levels of mRNA for (A) *PTH1R*, (B) *CASR*, and (C) *CALCR* in the ileum at indicated ages and hours post-oviposition (HPOP) were determined by RT-qPCR and normalized to *GAPDH* mRNA. Data were analyzed by two-way ANOVA followed by Fisher's test of least significant difference, and the HPOP-by-age interaction was not significant for (A) *PTH1R* (P=0.6564), (B) *CASR* (P=0.3890), (C) *CALCR* (P=0.7984). Values (mean+SEM; n=8 hens/HPOP/age) are expressed relative to 1:30 HPOP at 25 weeks. Main effect means for age and HPOP are shown in Figure 5.10A - 5.10F (A - C).

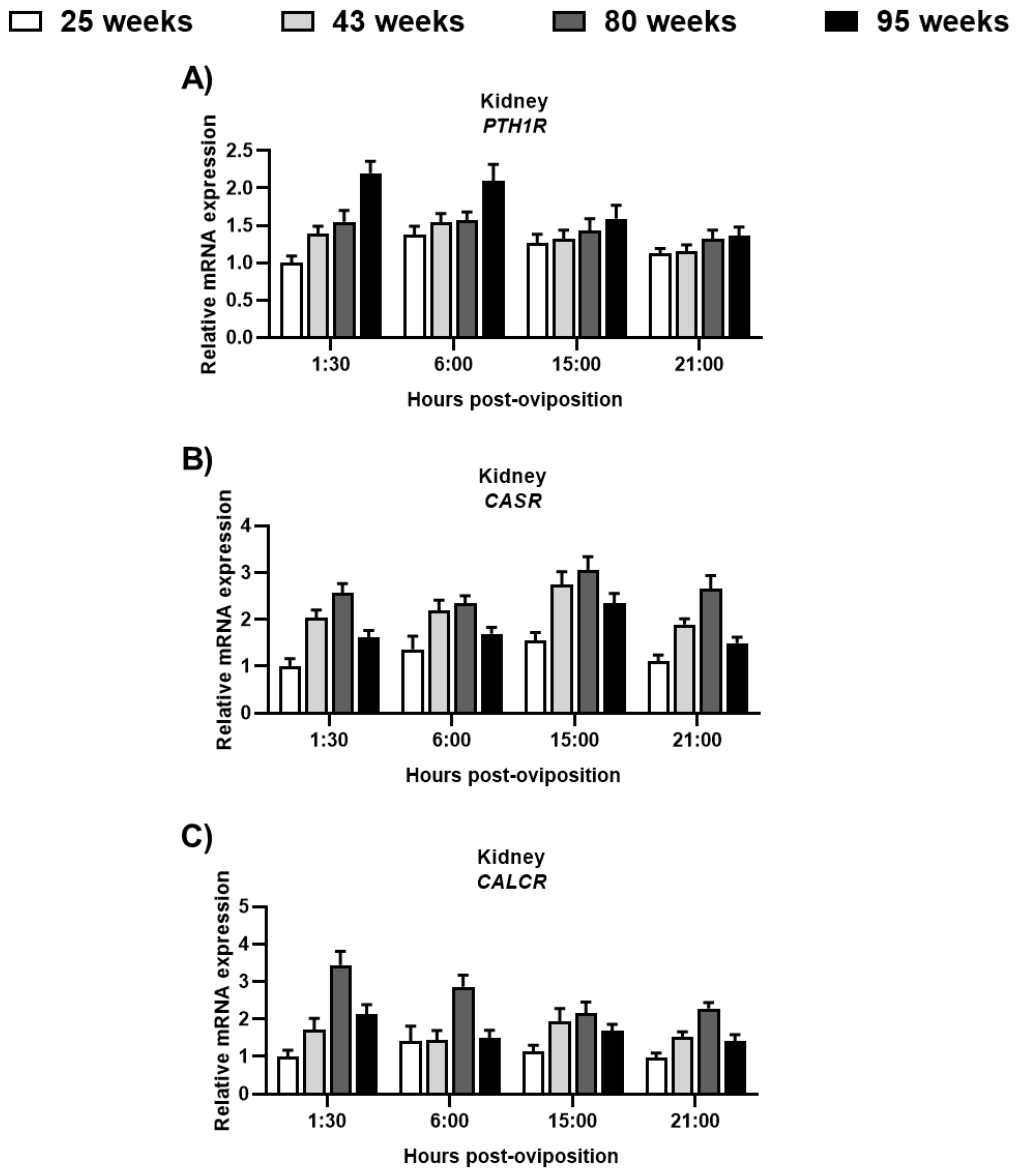

Figure C6. Expression of hormone receptors in the kidney.
Relative levels of mRNA for (A) *PTH1R*, (B) *CASR*, and (C) *CALCR* in the kidney at indicated ages and hours post-oviposition (HPOP) were determined by RT-qPCR and normalized to *GAPDH* mRNA. Data were analyzed by two-way ANOVA followed by Fisher's test of least significant difference, and the HPOP-by-age interaction was not significant for (A) *PTH1R* (P=0.1278), (B) *CASR* (P=0.8552), and (C) *CALCR* (P=0.3542). Values (mean+SEM; n=8 hens/HPOP/age) are expressed relative to 1:30 HPOP at 25 weeks. Main effect means for age and HPOP are shown in Figure 5.11A - 5.11F (A - C).

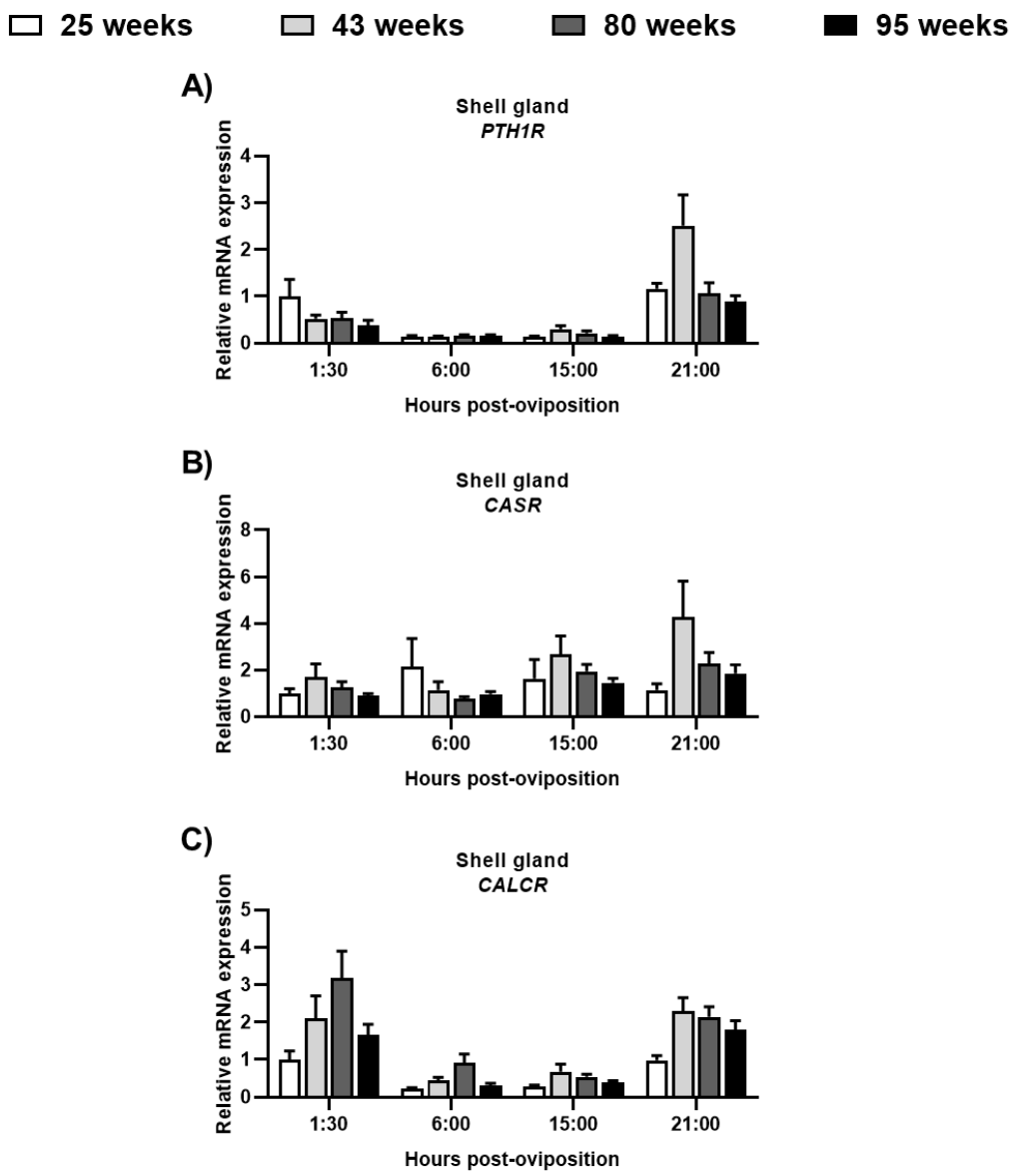

Figure C7. Expression of hormone receptors in the shell gland.
Relative levels of mRNA for (A) *PTH1R*, (B) *CASR*, and (C) *CALCR* in the shell gland at indicated ages and hours post-oviposition (HPOP) were determined by RT-qPCR and normalized to *RPL5* mRNA. Data were analyzed by two-way ANOVA followed by Fisher's test of least significant difference, and the HPOP-by-age interaction was not significant for (A) *PTH1R* (P=0.2894), (B) *CASR* (P=0.7013), and (C) *CALCR* (P=0.3737). Values (mean+SEM; n=8 hens/HPOP/age) are expressed relative to 1:30 HPOP at 25 weeks. Main effect means for age and HPOP are shown in Figure 5.12A - 5.12F (A - C).

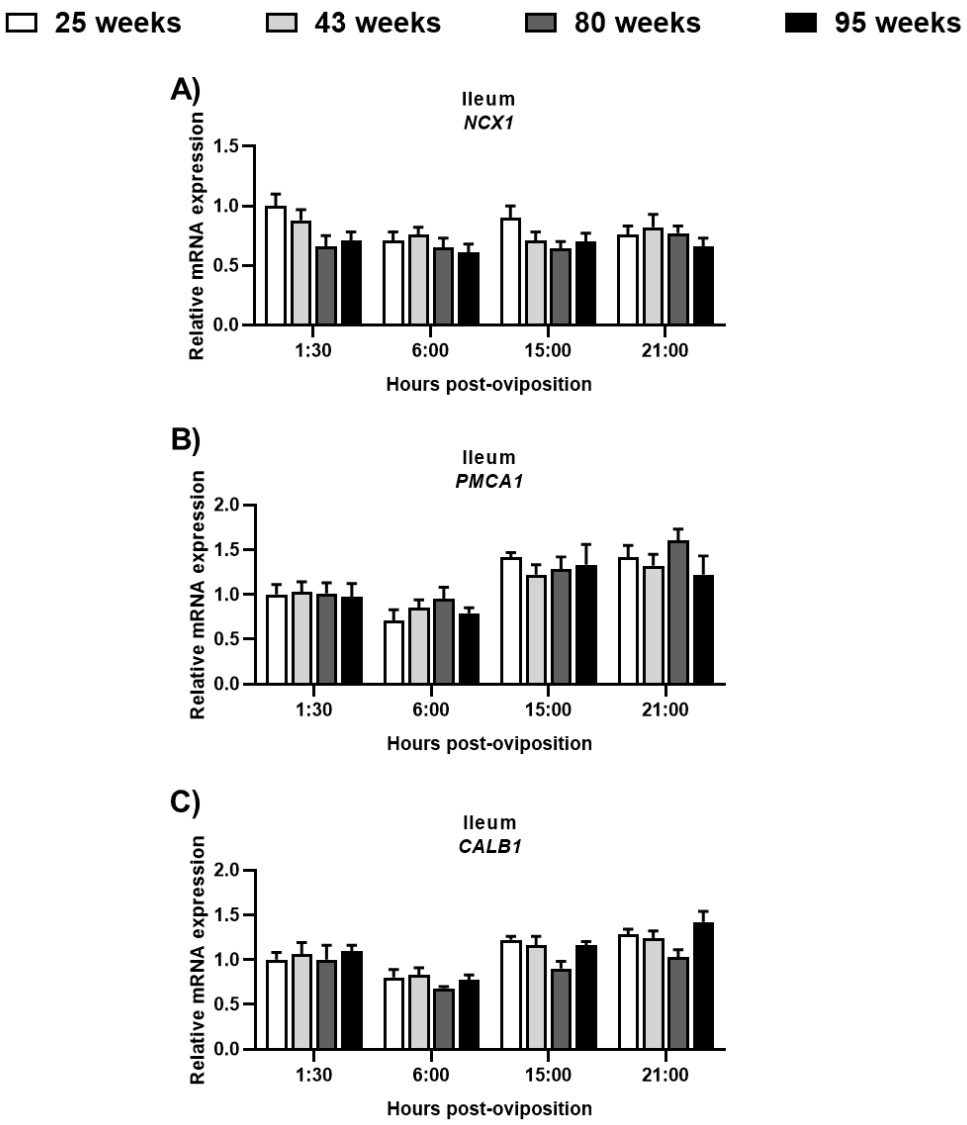

Figure C8. Expression of calcium transporters in the ileum.
Relative levels of mRNA for (A) *NCX1*, (B) *PMCA1*, and (C) *CALB1* in the ileum at indicated ages and hours post-oviposition (HPOP) were determined by RT-qPCR and normalized to *GAPDH* mRNA. Data were analyzed by two-way ANOVA followed by Fisher's test of least significant difference, and the HPOP-by-age interaction was not significant for (A) *NCX1* (P=0.4732), (B) *PMCA1* (P=0.6991), and (C) *CALB1* (P=0.8882). Values (mean+SEM; n=8 hens/HPOP/age) are expressed relative to 1:30 HPOP at 25 weeks. Main effect means for age and HPOP are shown in Figure 5.14A - 5.14F (A - C).

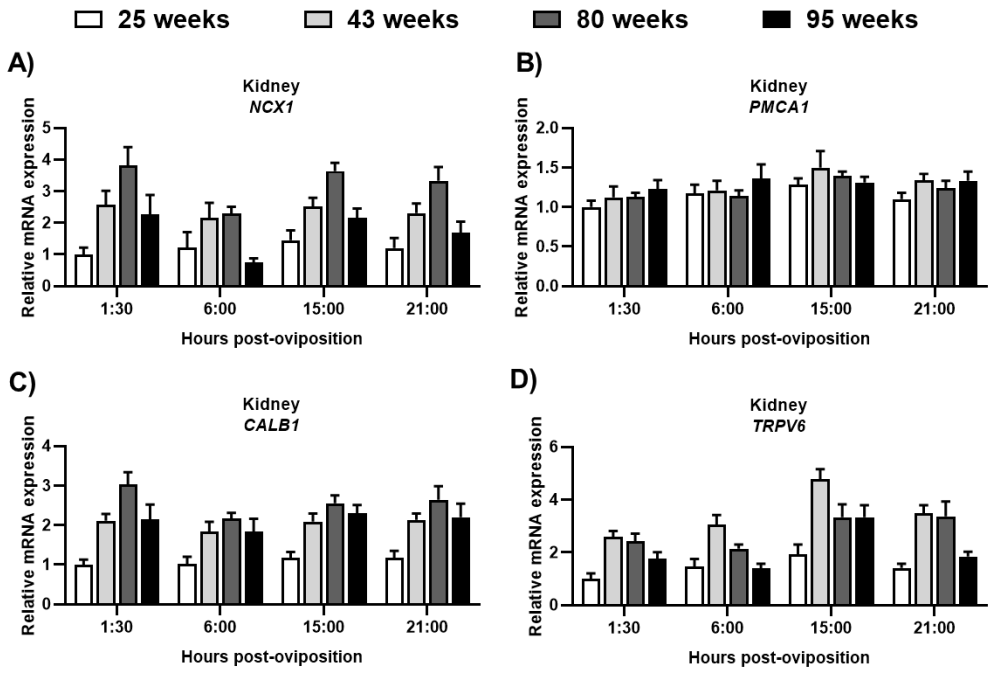

Figure C9. Expression of calcium transporters in the kidney.
Relative levels of mRNA for (A) *NCX1*, (B) *PMCA1*, (C) *CALB1*, and (D) *TRPV6* in the kidney at indicated ages and hours post-oviposition (HPOP) were determined by RT-qPCR and normalized to *GAPDH* mRNA. Data were analyzed by two-way ANOVA followed by Fisher's test of least significant difference, and the HPOP-by-age interaction was not significant for (A) *NCX1* (P=0.7180), (B) *PMCA1* (P=0.9586), (C) *CALB1* (P=0.9789), and (D) *TRPV6* (P=0.5917). Values (mean+SEM; n=8 hens/HPOP/age) are expressed relative to 1:30 HPOP at 25 weeks. Main effect means for age and HPOP are shown in Figure 5.15A - 5.15H (A - D).

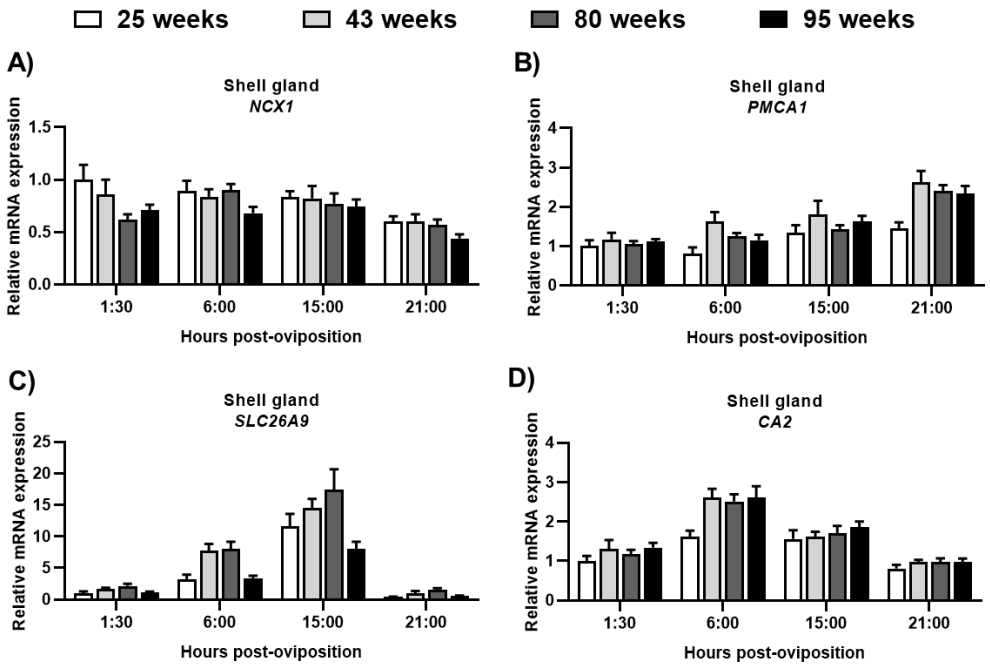

Figure C10. Expression of genes regulating bicarbonate production and transport and calcium transporters in the shell gland.
Relative levels of mRNA for (A) *NCX1*, (B) *PMCA1,* (C) *SLC26A9*, and (D) *CA2* in the shell gland at indicated ages and hours post-oviposition (HPOP) were determined by RT-qPCR and normalized to *RPL5* mRNA. Data were analyzed by two-way ANOVA followed by Fisher's test of least significant difference, and the HPOP-by-age interaction was not significant for (A) *NCX1* (P=0.4424), (B) *PMCA1* (P=0.3057), (C) *SLC26A9* (P=0.4104), and (D) *CA2* (P=0.8603). Values (mean+SEM; n=8 hens/HPOP/age) are expressed relative to 1:30 HPOP at 25 weeks. Main effect means for age and HPOP are shown in Figure 5.16A - 5.16D (A, B) and Figure 5.20A - 5.20B, 5.20D - 5.20E (C, D).

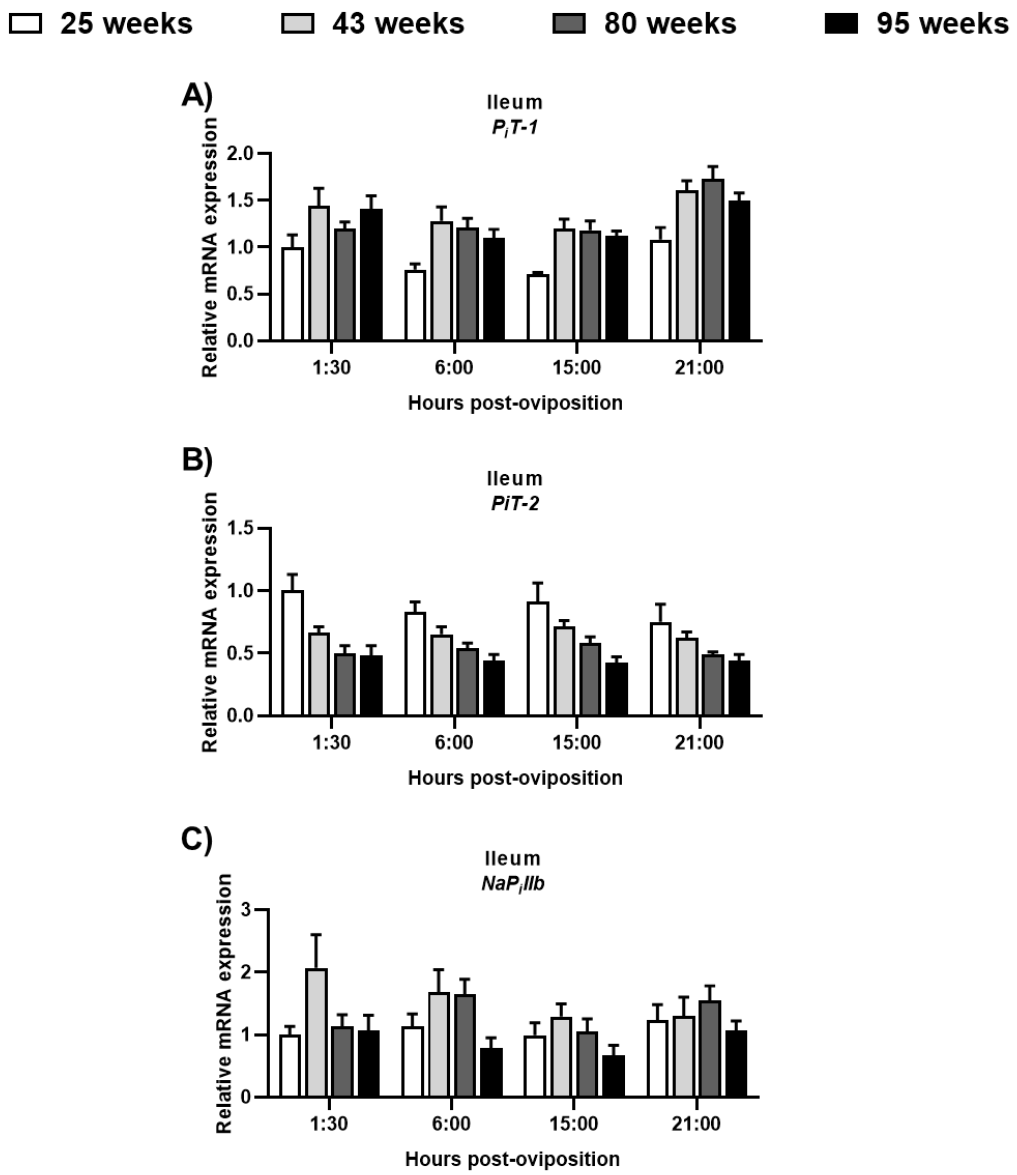

Figure C11. Expression of phosphorus transporters in the ileum.
Relative levels of mRNA for (A) *PiT-1*, (B) *PiT-2*, and (C) *NaPiIIb* in the ileum at indicated ages and hours post-oviposition (HPOP) were determined by RT-qPCR and normalized to *GAPDH* mRNA. Data were analyzed by two-way ANOVA followed by Fisher's test of least significant difference, and the HPOP-by-age interaction was not significant for (A) *PiT-1* (P=0.9322), (B) *PiT-2* (P=0.8476), and (C) *NaPiIIb* (P=0.9271). Values (mean+SEM; n=8 hens/HPOP/age) are expressed relative to 1:30 HPOP at 25 weeks. Main effect means for age and HPOP are shown in Figure 5.17A - 5.17F (A - C). Expression of *NaPiIIb* was not detected in this tissue.

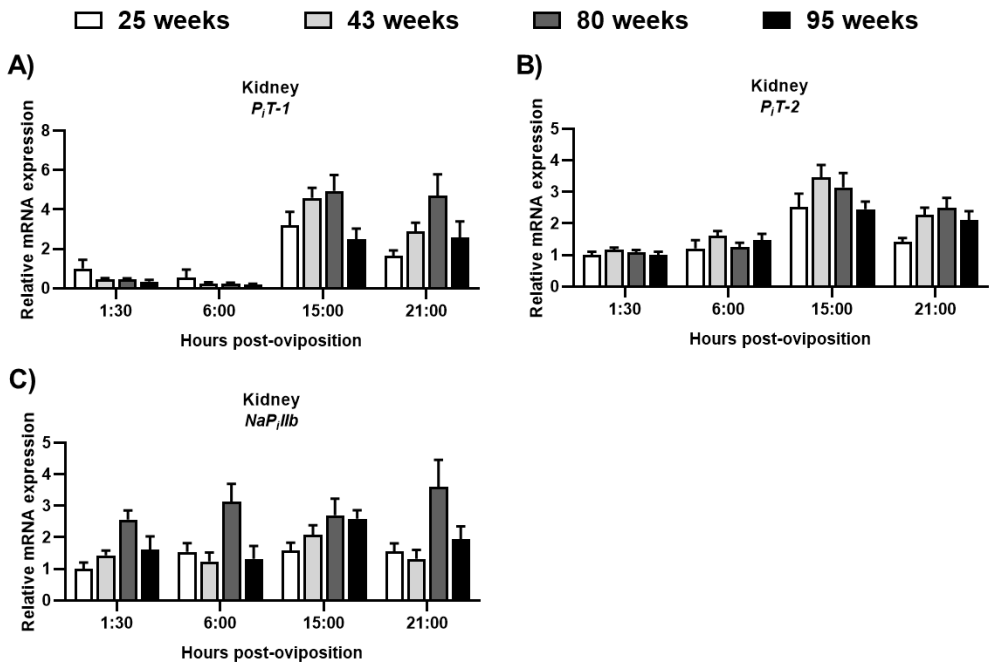

Figure C12. Expression of phosphorus transporters in the kidney.
Relative levels of mRNA for (A) *P_iT-1*, (B) *P_iT-2*, and (C) *NaP_iIIb* in the kidney at indicated ages and hours post-oviposition (HPOP) were determined by RT-qPCR and normalized to *GAPDH* mRNA. Data were analyzed by two-way ANOVA followed by Fisher's test of least significant difference, and the HPOP-by-age interaction was not significant for (A) *P_iT-1* (P=0.1722), (B) *P_iT-2* (P=0.6353), (C) *NaP_iIIb* (P=0.2099). Values (mean+SEM; n=8 hens/HPOP/age) are expressed relative to 1:30 HPOP at 25 weeks. Main effect means for age and HPOP are shown in Figure 5.18A - 5.18F (A - C).

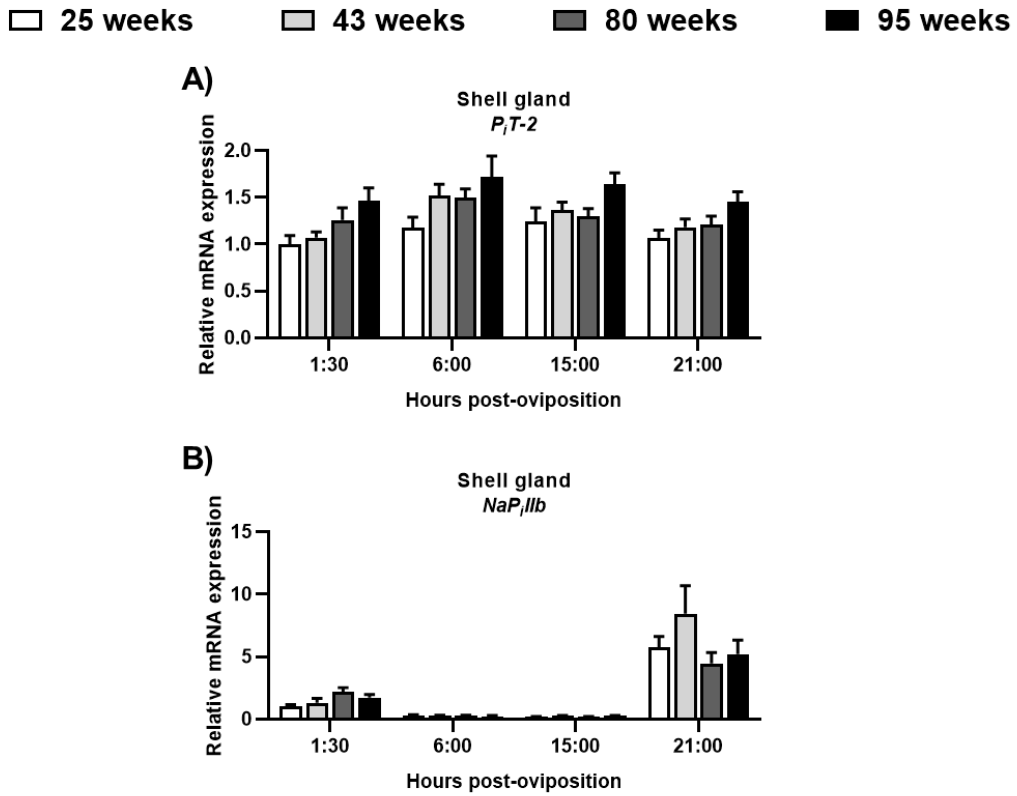

Figure C13. Expression of phosphorus transporters in the shell gland.
Relative levels of mRNA for (A) *P_iT-2* and (C) *NaP_iIIb* in the shell gland at indicated ages and hours post-oviposition (HPOP) were determined by RT-qPCR and normalized to *RPL5* mRNA. Data were analyzed by two-way ANOVA followed by Fisher's test of least significant difference, and the HPOP-by-age interaction was not significant for (A) *P_iT-2* (P=0.9674) and (C) *NaP_iIIb* (P=0.0766). Values (mean+SEM; n=8 hens/HPOP/age) are expressed relative to 1:30 HPOP at 25 weeks. Main effect means for age and HPOP are shown in Figure 5.19B - 5.19E (A, B). Expression of *NaP_iIIb* was not detected in this tissue.

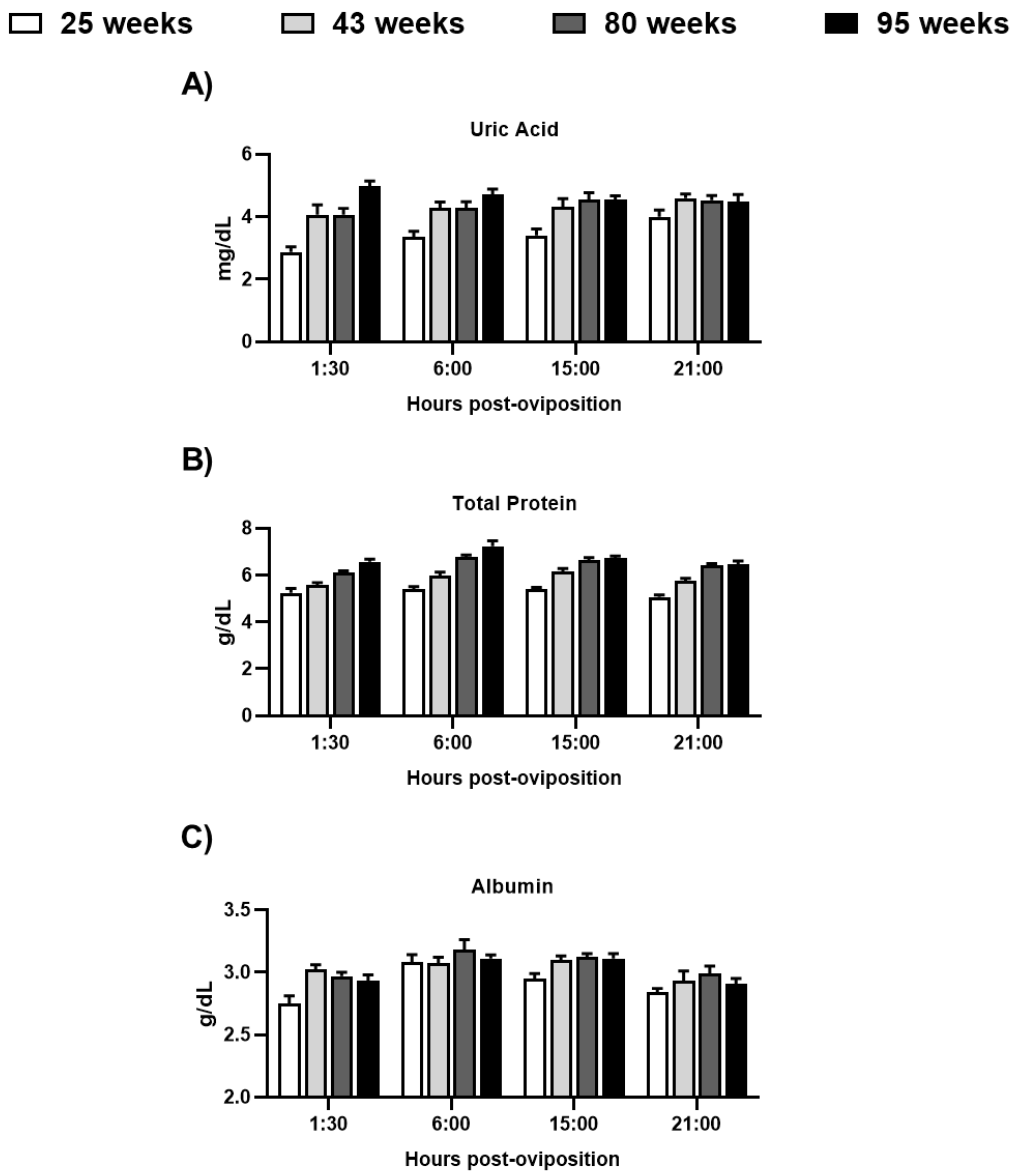

Figure C14. Circulating markers of renal and hepatic function.
Circulating levels of (A) uric acid, (B) total Protein, and (C) albumin at indicated ages and hours post-oviposition (HPOP) were determined in whole blood using a VetScan device equipped with avian/reptile profile + cartridges (mean+SEM; n=12 hens/HPOP/age) . Data were analyzed by two-way ANOVA followed by Fisher's test of least significant difference, and the HPOP-by-age interaction was not significant for (A) uric acid (P=0.5556), (B) total protein (P=0.1000), and (C) albumin (P=0.4304). Main effect means for age and HPOP are shown in Figure 5.21C, 5.21D (A) and Figure 5.22A - 5.22D (B, C).

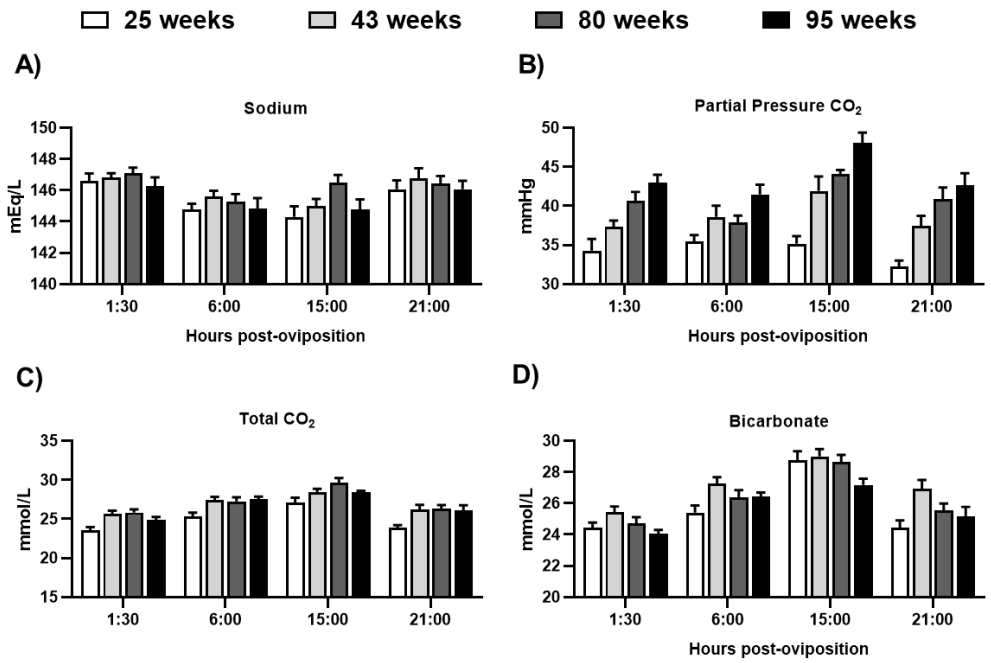

Figure C15. Circulating sodium, blood gases, and bicarbonate.
Circulating levels of (A) sodium, (B) partial pressure of carbon dioxide [CO_2], (C) total CO_2, and (D) bicarbonate at indicated ages and hours post-oviposition (HPOP) were determined in whole blood using an iSTAT device equipped with CG8+ cartridges (mean+SEM; n=12 hens/HPOP/age). Data were analyzed by two-way ANOVA followed by Fisher's test of least significant difference, and the HPOP-by-age interaction was not significant for (A) sodium (P=0.4999), (B) partial pressure CO_2 (P=0.1564), (C) total CO_2 (P=0.2399), and (D) bicarbonate (P=0.1969. Main effect means for age and HPOP are shown in Figure 5.23A-5.23B (A), Figure 5.25B - E (B, C), and Figure 5.20C, 5.20F (D).

Appendix D: Ambient conditions for Chapter 5

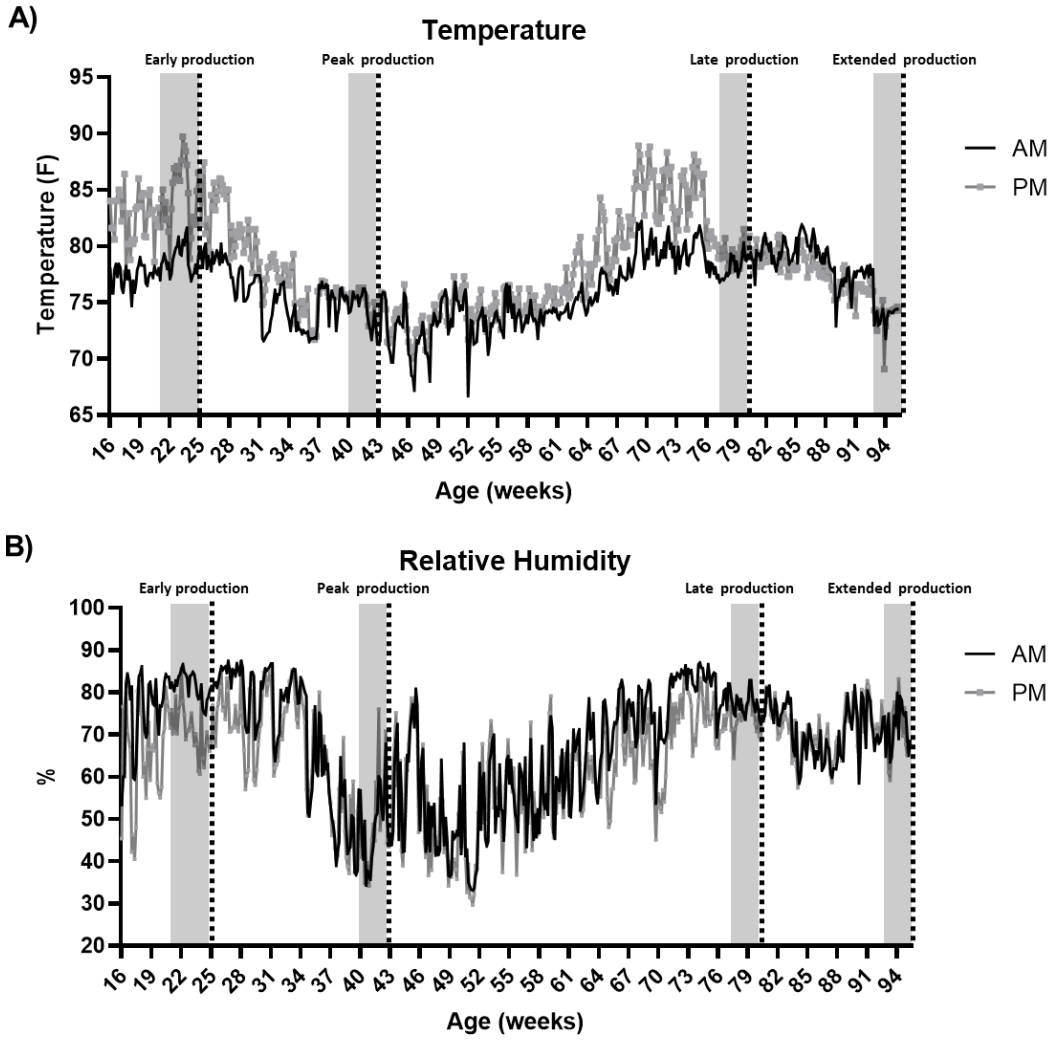

Figure D1. Housing environment.
Ambient (A) temperature and (B) relative humidity were recorded 24 hours daily in the hen housing unit across the production cycle. Data are graphed such that 12:00 AM to 11:55 AM are shown as the black line (AM) and 12:00 PM to 11:55 PM as the light grey line (PM). Data were recorded in 5-minute intervals from 6 data loggers that were evenly spaced throughout the housing unit, with at least one data logger per block. Grey regions on the graphs are representative of the period during which egg production-related performance was recorded prior to each sampling, and the dotted lines represent each sampling age and stage of production.